

SANDIA REPORT

SAND96-1368 • UC-814
Unlimited Release
Printed November 1996

Yucca Mountain Site Characterization Project

RECEIVED
JAN 13 1997
OSTI

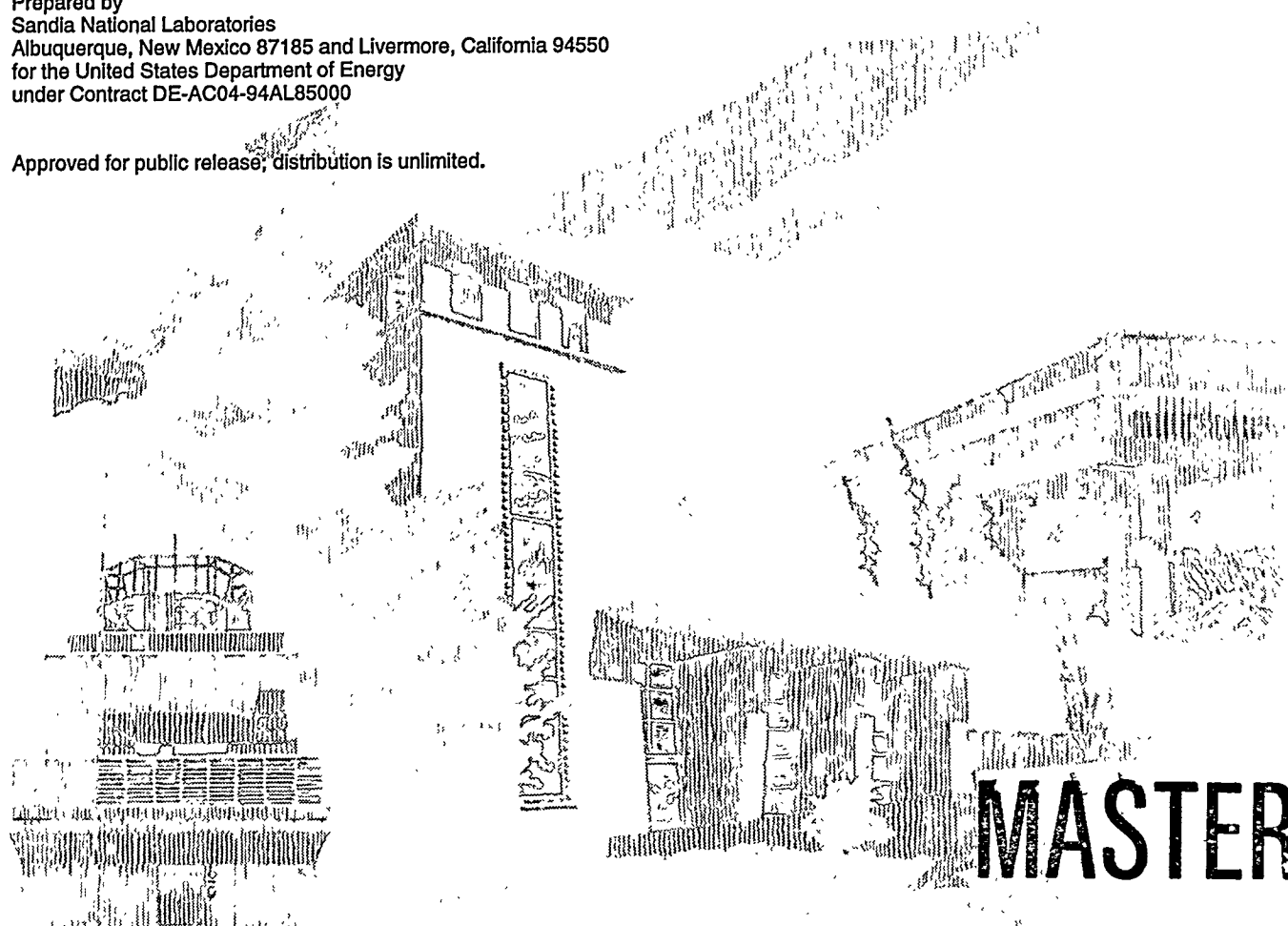
Geology of the USW SD-12 Drill Hole

Yucca Mountain, Nevada

Christopher A. Rautman, Dale A. Engstrom

Prepared by
Sandia National Laboratories
Albuquerque, New Mexico 87185 and Livermore, California 94550
for the United States Department of Energy
under Contract DE-AC04-94AL85000

Approved for public release; distribution is unlimited.



"Prepared by Yucca Mountain Site Characterization Project (YMSCP) participants as part of the Civilian Radioactive Waste Management Program (CRWM). The YMSCP is managed by the Yucca Mountain Project Office of the U.S. Department of Energy, DOE Field Office, Nevada (DOE/NV). YMSCP work is sponsored by the Office of Geologic Repositories (OGR) of the DOE Office of Civilian Radioactive Waste Management (OCRWM)."

Issued by Sandia National Laboratories, operated for the United States Department of Energy by Sandia Corporation.

NOTICE: This report was prepared as an account of work sponsored by an agency of the United States Government. Neither the United States Government nor any agency thereof, nor any of their employees, nor any of their contractors, subcontractors, or their employees, makes any warranty, express or implied, or assumes any legal liability or responsibility for the accuracy, completeness, or usefulness of any information, apparatus, product, or process disclosed, or represents that its use would not infringe privately owned rights. Reference herein to any specific commercial product, process, or service by trade name, trademark, manufacturer, or otherwise, does not necessarily constitute or imply its endorsement, recommendation, or favoring by the United States Government, any agency thereof or any of their contractors or subcontractors. The views and opinions expressed herein do not necessarily state or reflect those of the United States Government, any agency thereof or any of their contractors.

Printed in the United States of America. This report has been reproduced directly from the best available copy.

Available to DOE and DOE contractors from
Office of Scientific and Technical Information
PO Box 62
Oak Ridge, TN 37831

Prices available from (615) 576-8401, FTS 626-8401

Available to the public from
National Technical Information Service
US Department of Commerce
5285 Port Royal Rd
Springfield, VA 22161

NTIS price codes
Printed copy: A07
Microfiche copy: A01

Geology of the USW SD-12 Drill Hole Yucca Mountain, Nevada

*Christopher A. Rautman
Geohydrology Department
Sandia National Laboratories
Albuquerque, New Mexico 87185-1324*

*Dale A. Engstrom
Spectra Research Institute
Albuquerque, New Mexico 87106*

Abstract

Drill hole USW SD-12 is one of several holes drilled under Site Characterization Plan Study 8.3.1.4.3.1, also known as the "Systematic Drilling Program," as part of the U.S. Department of Energy characterization program at Yucca Mountain, Nevada, which has been proposed as the potential location of a repository for high-level nuclear waste. The SD-12 drill hole is located in the central part of the potential repository area, immediately to the west of the Main Test Level drift of the Exploratory Studies Facility and slightly south of midway between the North Ramp and planned South Ramp declines. Drill hole USW SD-12 is 2166.3 ft (660.26 m) deep, and the core recovered essentially complete sections of ash-flow tuffs belonging to the lower half of the Tiva Canyon Tuff, the Pah Canyon Tuff, and the Topopah Spring Tuff, all of which are part of the Miocene Paintbrush Group. A virtually complete section of the Calico Hills Formation was also recovered, as was core from the entire Prow Pass Tuff formation of the Crater Flat Group.

The drill hole was collared in the welded materials of the crystal-poor middle nonlithophysal zone of the Tiva Canyon Tuff; approximately 250 feet (75 m) of this formation was penetrated by the hole. The Yucca Mountain Tuff appears to be missing from the section at the SD-12 location, and the Pah Canyon Tuff is only 14.5 feet (4.5 m) thick. The Pah Canyon is completely nonwelded in the SD-12 drill core. The Topopah Spring Tuff consists of 1117.1 feet (340.48 m) of generally densely welded pyroclastic-flow deposits. Lithophysae are well developed through several thick vertical intervals within the Topopah Spring, and large lithophysal cavities up to several feet (many tenths of a meter) are present throughout these lithophysal intervals. Lithophysae and lithophysal cavities are not restricted to only the named lithophysal zones. The Calico Hills Formation in drill hole USW SD-12 consists of 237.1 feet (72.26 m) of nonwelded and mostly zeolitized tuffaceous materials. The Calico Hills has been subdivided into four units of mostly ash-flow deposits plus an underlying "bedded" interval of reworked tuffaceous material and an underlying basal tuffaceous sandstone unit. The Prow Pass Tuff at this location comprises four units dominated by ash-flow tuffs plus a basal unit of bedded and reworked materials that total 496.5 feet (151.33 m) in thickness. The hole was bottomed in the uppermost ash-flow units of the Bullfrog Tuff.

Quantitative and semiquantitative data are included in this report for core recovery, rock-quality designation (RQD), lithophysal cavity abundance, and fracturing. These data are spatially variable, both

within and among the major formation-level stratigraphic units. Nonwelded intervals in general exhibit higher core recovery and more intact (higher) RQD values than the densely welded intervals. Ten-foot (3-m) composite RQD values indicate "fair" ground conditions in the upper one-third of the Topopah Spring Tuff with "poor" to "very poor" ground conditions in the lower two-thirds. Estimation of lithophysal cavity abundances and of fracture density is complicated by the existence of cavities much larger than the core diameter; drilling through these intervals of large lithophysal cavities produced thick zones of "lost" core and rubble.

This report includes quantitative data for the "framework" material properties of porosity, bulk and particle density, and saturated hydraulic conductivity. Graphical analysis of variations in these laboratory hydrologic properties indicates first-order control of material properties by the degree of welding and presence of zeolite alteration minerals. Many of the finer-scale lithostratigraphic contacts frequently described from rocks at Yucca Mountain are not well expressed in the material-property profiles. Approximate in-situ saturation data from core samples preserved immediately upon recovery from the hole are included in the data tabulation.

Geophysical data have been obtained from approximately 1950 feet (600 m) of the USW SD-12 drill hole; only the lowermost 200 feet could not be logged geophysically because of hole-size restrictions. Geophysical logs include density, gamma-ray, epithermal-neutron porosity, electrical resistivity, and caliper profiles down to nearly the base of the Prow Pass Tuff. The bulk-density log provides the most lithologic information, and many of the lithologic subdivisions described from the core can be identified in the petrophysical profiles. Discrimination of welded from nonwelded rock type is immediately apparent in the density log, and this independent line of evidence confirms the fact that material-property units do not correspond in detail to the broader, genetic lithostratigraphic unit boundaries.

Acknowledgments

This work was performed for the U.S. Department of Energy, Office of Civilian Radioactive Waste Management, Yucca Mountain Site Characterization Project Office under contract EA9012M5X. Scientific investigations involving the Systematic Drilling Program are conducted under the descriptions of work contained in the Site Characterization Plan (DOE, 1988) and in Study Plan 8.3.1.4.3.1 (Rautman, 1993); the work-breakdown structure element is 1.2.3.2.2.2.1. The planning document that directed this work activity is WA-0301; prior to the effective date of WA-0301, work activities for this WBS element were conducted under WA-0014. The information and data documented in this report was conducted under a fully qualified quality assurance program. Full details associated with all reported data may be located in the Yucca Mountain Site Characterization Project records using the data-tracking numbers (DTNs) provided in the relevant sections of this report.

DISCLAIMER

**Portions of this document may be illegible
in electronic image products. Images are
produced from the best available original
document.**

Contents

Abstract	i
Acknowledgments	ii
Contents	iii
Figures	iv
Tables	v
Introduction	1
Purpose of the Systematic Drilling Program	1
Regional Geologic Setting	2
Volcanic Stratigraphy	3
Petrogenesis and Zonation of Paintbrush Group Tuffs	3
Subdivisions of the Calico Hills Formation and Prow Pass Tuff (Crater Flat Group)	6
The USW SD-12 Drill Hole	7
Location	7
Drilling History	7
Method of Study	8
Geologic Logging and Core Description	8
Laboratory Hydrologic Properties	9
Geology of Drill Hole USW SD-12	9
Overview	9
Thermal/Mechanical Units	13
Structural Geology of SD-12	14
Lithophysal Zones	15
Rock Quality Considerations	17
Core Recovery	17
RQD (Rock Quality Designation)	19
Measured Lithophysal Cavity Information	21
Fracture Information	22
Framework Hydrologic Properties	26
Laboratory Techniques	26
Material-Properties Data	28
Geophysical Log Data	33
Density Log Response	33
Gamma-Ray Log Response	35
Epithermal Neutron Porosity Log Response	35
Induction Log Response	37
Caliper Log Response	37
Summary	38
References	39
Appendix A: Lithologic Unit Descriptions	43
Appendix B: Geologic Core Logs	55
Appendix C: Core Recovery Data	89
Appendix D: Rock Quality Designation (RQD) Data	97
Appendix E: Lithophysal Cavity Data	109
Appendix F: Fracture Information	113
Appendix G: Laboratory Material Properties	117

Figures

1. (a) Index map showing location of the potential Yucca Mountain repository site in southern Nevada in relationship to the southwestern Nevada volcanic field. (b) Expanded map of the Yucca Mountain site showing location of drill hole USW SD-12 and selected other holes.	1
2. Gridded drilling pattern for the Systematic Drilling Program as proposed in Study Plan 8.3.1.4.3.1 (Rautman, 1993).	2
3. Location map of the potential repository region showing the USW SD-12 drill hole in relationship to nearby drill holes and the Exploratory Studies Facility	7
4. Plots showing (a) core recovery, (b) field-measured core-run RQD, (c) 10-ft averaged field-measured RQD, and (d) 10-ft averaged video-analysis RQD for the USW SD-12 drill hole as a function of depth.	18
5. Conceptual sketch for measuring the length of "intact" core segments for RQD determinations.	20
6. Graph showing (a) abundance of lithophysal cavities, (b) cumulative lengths of "lost core" and "lost core plus rubble" (table E-1), and (c) actual core recovery as function of depth for the USW SD-12 drill hole.	22
7. Graphs showing (a) measured fracture density, (b) fracture orientation, (c) mineralized fractures, (d) 10-ft video-analysis RQD, and (e) core recovery for the upper portion of the USW SD-12 drill hole.	23
8. Graphs showing fracture density adjusted for measurement effects of lost core and rubble zones.	25
10. a) Porosity, (b) bulk density, (c) particle density, (d) saturation, and (e) water-content profiles of core samples collected from the lower part of the USW SD-12 drill core.	30
9. (a) Porosity, (b) bulk density, (c) particle density, (d) saturation, and (e) water-content profiles of core samples collected from the upper part of the USW SD-12 drill core..	31
11. (a) Porosity and (b) saturated hydraulic conductivity profiles of core samples collected from the USW SD-12 drill core.	32
12. Geophysical log traces from the USW SD-12 drill hole: (a) density log; (b) gamma-ray log; (c) epithermal neutron porosity log; (d) induction log; and (e) caliper log.	34
B-1. Example geologic core log form with parallel columns for representing various geologic features and other quantitative and semiquantitative information as a function of depth.	57

Tables

1.	Comparison of several stratigraphic subdivisions of volcanic rocks at Yucca Mountain and encountered on the Yucca Mountain Site Characterization Project.	4
2.	Zonation of the Tiva Canyon and Topopah Spring Tuffs Showing Parallel Subdivisions	5
3.	Stratigraphic Unit Upper Contacts and Unit Thicknesses for the USW SD-12 Drill Hole.	10
4.	Basal Contacts and Thicknesses of Thermal/Mechanical Units for Drill Hole USW SD-12.	14
5.	RQD and Rock-Quality Descriptors.	21
C-1.	Core Recovery Data for USW SD-12	90
D-1.	Core-Run RQD Data for USW SD-12.	98
D-2.	RQD Values by 10-foot Intervals	104
E-1.	Measured Lithophysal Cavity Abundances for 10-foot Composite Intervals	110
F-1.	Measured Fracture Data for 10-foot Composite Intervals	114
G-1.	Laboratory Material Properties and Water Contents Measured on Core Samples from Drill Hole USW SD-12	118
G-2.	Porosity and Saturated Hydraulic Conductivity Values Measured on Core Samples from Drill Hole USW SD-12	131

(This page intentionally left blank.)

Geology of the USW SD-12 Drill Hole

Yucca Mountain, Nevada

Introduction

The U.S. Department of Energy is evaluating a site at Yucca Mountain, located in southern Nye County, Nevada, as the potential location for an underground high-level nuclear-waste repository (fig. 1). This report contains the results of the geologic logging and lithologic description of core from drill hole USW SD-12, which is one of a number of holes being drilled at the Yucca Moun-

tain site to characterize the subsurface geology of the proposed repository block. A suite of framework bulk and hydrologic properties are also reported in the context of the geologic description. These activities have been conducted under Site Characterization Plan (SCP; DOE, 1988) Study 8.3.1.4.3.1, "Systematic Acquisition of Site-Specific Subsurface Information," which is commonly referred to as the Systematic Drilling Program.

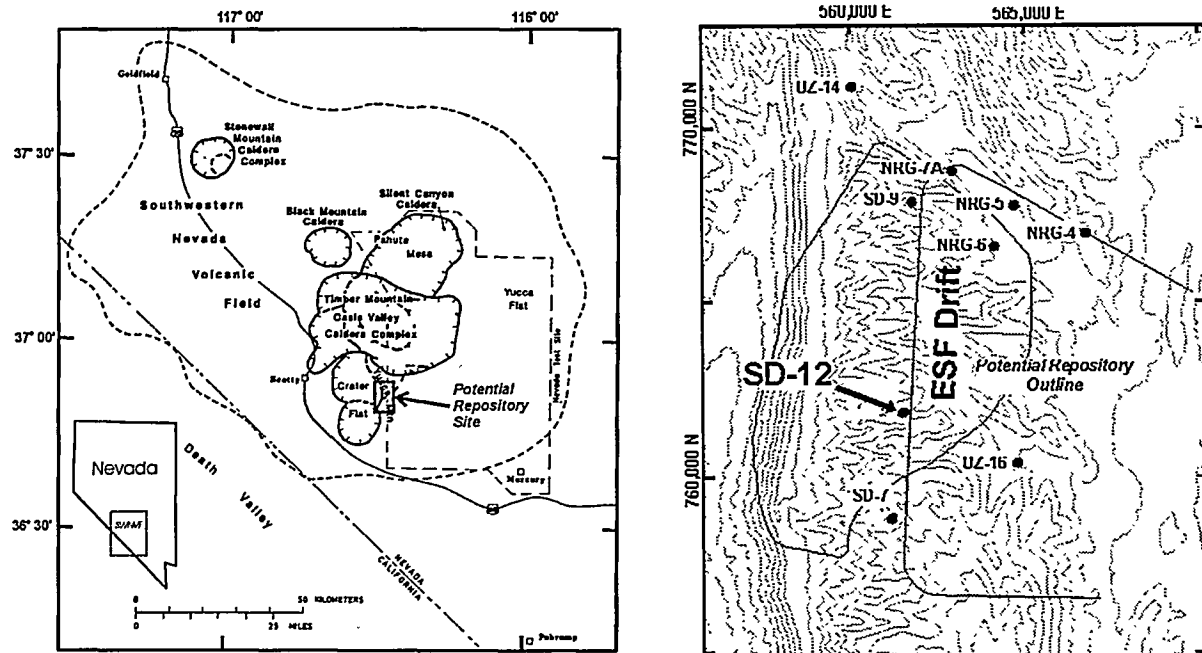


Figure 1. (a) Index map showing location of the potential Yucca Mountain repository site in southern Nevada in relationship to the southwestern Nevada volcanic field (after Byers and others, 1989). (b) Expanded map of the Yucca Mountain site showing location of drill hole USW SD-12 and selected other holes.

Purpose of the Systematic Drilling Program

The Systematic Drilling Program was proposed (Rautman, 1993) to provide critical information for repository design and performance assessment in a systematic sampling pattern (fig. 2)[†] from the volume of rock to be occupied by the

potential Yucca Mountain repository. Holes of the Systematic Drilling Program were believed particularly important in the geologic characterization of

[†]Figure 2 has been extracted directly from Study Plan 8.3.1.4.3.1 (Rautman, 1993), the bulk of which was prepared during 1992 or earlier. Hole locations shown on this figure were preliminary and final locations may be different.

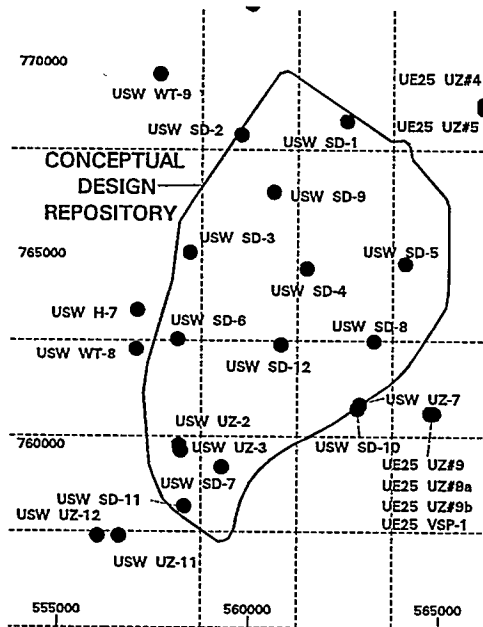


Figure 2. Gridded drilling pattern for the Systematic Drilling Program as proposed in Study Plan 8.3.1.4.3.1 (Rautman, 1993).

the Yucca Mountain site because they are located within the proposed conceptual-design perimeter drift. The drilling program is to provide descriptions and samples of the repository host rock and of rocks both above and below the repository horizon along the postulated flow path(s) of deep, unsaturated-zone ground-water percolation. The Systematic Drilling Program will also provide descriptive information and samples of rocks within the upper portion of the saturated zone, which includes zeolithically altered materials that may act to retard radionuclides migrating away from a constructed repository.

In addition to descriptive geologic information, core samples from the Systematic Drilling Program provide the raw material for quantitative measurements of thermal, mechanical, hydrologic, and geochemical material properties necessary for numerical modeling and regulatory evaluation of the waste-isolation performance of a potential nuclear-waste repository at Yucca Mountain. A basic set of framework material properties from USW SD-12 is included as part of this report. Other site-characterization studies (DOE, 1988) are

also testing samples obtained from the USW SD-12 drill hole. Pore waters extracted from appropriately preserved core specimens and drill cuttings can provide isotopic evidence relevant to the age or residence time and source of the ground water, including data on the infiltration of water containing bomb-pulse isotopes from past atmospheric testing of nuclear weapons. The drill holes themselves provide access to the interior of Yucca Mountain for geophysical logging, down-hole video examination of the borehole walls, air-permeability testing, water table monitoring and geochemical sampling, and in-situ instrumentation for monitoring temperatures, gas pressures, and changes in gas chemistry with time. Simple plots of geophysical logs from the USW SD-12 drill hole are included at a reduced scale in this report.

Regional Geologic Setting

Yucca Mountain is located within the southern portion of the southwestern Nevada volcanic field (Lipman and others, 1966; Christiansen and others, 1977; Byers and others, 1976, 1989). The southwestern Nevada volcanic field (fig. 1) consists of a thick sequence of widely distributed, 7- to 15-million-year-old silicic volcanic rocks, centered around the Timber Mountain, Oasis Valley, and Silent Canyon caldera complexes (Noble and others, 1968; Sawyer and others, 1994).

Yucca Mountain consists of a series of north-trending, eastward-dipping structural blocks that are bounded by mostly west-dipping normal faults (Carr and others, 1986). These fault blocks are composed principally of thick, welded ash-flow tuff deposits that are separated by thinner, non-welded ash-flow tuffs, silicic lavas, and tuffaceous sedimentary units, many of which were derived from caldera complexes to the north. Previous drilling at Yucca Mountain has shown that Tertiary volcanic rocks are in excess of 6000 ft (1800 m) thick in the immediate vicinity of the potential repository. Pre-Tertiary rocks underlying Yucca Mountain include thick carbonate and clastic assemblages varying in age from Precambrian to Mississippian. A Mesozoic or Tertiary pluton may lie beneath the Calico Hills to the northeast of the site (Carr, 1984).

Volcanic Stratigraphy

Yucca Mountain comprises a thick sequence of variably welded and nonwelded ash-flow tuffs intercalated with thinner intervals of bedded (reworked) and air-fall tuffs. The general sequence of stratigraphic units is illustrated in table 1. Surface exposures within the main repository block are formed by the several formations of the Miocene Paintbrush Group. In descending sequence, these are the Tiva Canyon, Yucca Mountain, Pah Canyon, and Topopah Spring Tuffs (Sawyer and others, 1994). The Tiva Canyon and Topopah Spring Tuffs occur as thick pyroclastic sheets that are regionally extensive and generally densely welded. The Yucca Mountain and Pah Canyon Tuffs are generally nonwelded to only moderately welded, and they are much less extensive in thickness and area, thinning to extinction toward the south. Each formation-level unit of the Paintbrush Group is separated from its neighbors by thin, nonwelded ash-flow tuffs, air-fall tuffs, pumice-fall beds, and reworked, bedded-tuffaceous deposits. These intervening tuffaceous materials typically are referred to collectively as "bedded tuff" without specific consideration of their actual lithologic character.

The Paintbrush Group in the general vicinity of the proposed repository typically is underlain by a heterogeneous sequence of rhyolitic rocks known as the Calico Hills Formation (Sawyer and others, 1994). Within the repository region itself, the Calico Hills consists of a downward sequence of five nonwelded ash-flow tuffs underlain by bedded tuffs and a basal tuffaceous sandstone unit (table 1; Moyer and Geslin, 1995). Elsewhere in the Yucca Mountain region, the Calico Hills Formation consists of rhyolitic lava flows, ash-flow tuffs, air-fall tuffs, and tuffaceous sediments. Much of the Calico Hills Formation has been zeolitized; vitric tuffs are preserved principally in the southwestern portion of the Yucca Mountain site.

The Calico Hills Formation is underlain by the Crater Flat Group (Sawyer and others, 1994); Moyer and Geslin, 1995), which comprises, in descending sequence, the Prow Pass, Bullfrog, and Tram Tuffs. Each of these three units represents a large-volume ash-flow eruption. The degree of

welding in these units is typically much less than that exhibited by the tuffs of the Paintbrush Group, and the welded intervals may not necessarily be continuous in the subsurface. The greater part of each ash-flow sequence is nonwelded, with welded tuffs constrained to the interior of each unit. The three formation-level units are separated from one another by thin intervals of nonwelded tuff and tuffaceous sediments ("bedded tuff") in a manner similar to that of the Paintbrush Group.

Volcanic units underlying the Crater Flat Group are somewhat poorly known by comparison. They have been encountered at Yucca Mountain only in the deeper drill holes (for example: Spangler and others, 1981; Maldonado and Koether, 1983; Scott and Castellanos, 1984; Whitfield and others, 1984). None of these units was encountered in drill hole USW SD-12.

Petrogenesis and Zonation of Paintbrush Group Tuffs

Early field and petrologic descriptions of the stratigraphic units of the southwestern Nevada volcanic field include work by Lipman and Christiansen (1964) and Lipman and others (1966). In later work more directly focused on the potential Yucca Mountain repository site, the thick, welded intervals of the Tiva Canyon and Topopah Spring Tuffs were subdivided by Scott and Bonk (1984) into a large number of informally named zones (table 1). This early zonation was based on a number of outcrop-based characteristics, including weathering character and color, in addition to more exposure-independent lithologic characteristics such as phenocryst content, alteration phenomena, and rock type.

More recently, Buesch and others (1996) have proposed a redefined zonation of the Paintbrush Group tuffs. These changes affect principally the thick, welded intervals of the Tiva Canyon and Topopah Spring Tuffs. According to the nomenclature of Buesch and others, these two major ash-flow sheets are divided informally into crystal-rich upper members and crystal-poor lower members (table 2). This fundamental change in phenocryst content, which is paralleled by a downward change in chemical composition from quartz latite to high-

Table 1: Comparison of several stratigraphic subdivisions of volcanic rocks at Yucca Mountain and encountered on the Yucca Mountain Site Characterization Project. (no scale)

Geologic Unit (from Sawyer and others, 1994)		Older hydrologic zonation (modified after Scott and Bork, 1984)			Zonation of Buesch and others (1996; also Moyer and Geslin, 1995)	Thermal/mechanical unit (Ortiz and others, 1985)
Paintbrush Group	Tiva Canyon Tuff	Tiva Canyon Member	ccr - caprock	Tpcrv	TCw	
			cuc - upper cliff	Tpcrn		
			cul - upper lithophysal	Tpcrl		
			cks - clinkstone	Tpcpm		
			cll - lower lithophysal	Tpcpl		
			ch - hackly	Tpcplh		
			cc - columnar	Tpcnc		
			ccs - shandy base	Tpcpv2		
	Yucca Mt. Tuff			Tpcpv1	PTn	
	Topopah Spring Tuff	Topopah Spring Member	upper nonwelded	Tptrv3	TSw1	
				Tptrv2		
			tc - caprock	Tptrv1		
			tr - rounded	Tptrn		
			tul - upper lithophysal	Tptrl		
				Tptrul		
			tn - nonlithophysal	Tptrnm		
			ttl - lower lithophysal	Tptrll		
			tm - mottled	Tptrln		
			tv - basal vitrophyre	Tptrv3	TSw3	
	Calico Hills Formation	Tuffaceous Beds of Calico Hills	nonwelded base	Tptrv2	CHn1	
				Tptrv1		
				Unit 5		
				Unit 4		
				Unit 3		
				Unit 2		
				Unit 1		
Crater Flat Group	Crater Flat Tuff	Prow Pass Member	Not subdivided	bedded tuff unit basal sandstone unit	CHn2	
				Unit 4	CHn3	
				Unit 3	PPw	
				Unit 2 Unit 1	CFUn	
				bedded tuff unit		
		Bullfrog Member	Not subdivided (?)		BFw	
					CFMn1	
		Tram Member	Not subdivided (?)		CFMn2	
					CFMn3	
					TRw	
					Not Recognized	

silica rhyolite, originates in the eruption of these ash-flow sequences from a compositionally zoned magma chamber underlying the source calderas (Lipman and others, 1966). More differentiated, rhyolitic magma in the upper portions of the magma chamber erupted first, followed by less-differentiated material from lower levels as the eruption progressed. Crystal settling within the magma

chamber prior to eruption produced phenocryst-rich quartz latite and phenocryst-poor rhyolite compositions corresponding to the two member subdivision. A gradational compositional-transition interval is observed in both the Tiva Canyon and the Topopah Spring Tuffs that exhibits attributes of both rock types.

Table 2: Zonation of the Tiva Canyon and Topopah Spring Tuffs Showing Parallel Subdivisions (simplified after Buesch and others, 1996)
[Lithophysal intervals are shaded]

Tiva Canyon Tuff (Tpc)	Topopah Spring Tuff (Tpt)
crystal-rich member (Tpcr)	crystal-rich member (Tptr)
vitric zone (Tpcrv)	vitric zone (Tptrv)
non- to partially welded subzone (Tpcrv3)	non- to partially welded subzone (Tptrv3)
moderately welded subzone (Tpcrv2)	moderately welded subzone (Tptrv2)
vitrophyre subzone (Tpcrv1)	vitrophyre subzone (Tptrv1)
nonlithophysal zone (Tpcrn)	nonlithophysal zone (Tptrn)
subvitrophyre transition subzone (Tpcrn4)	crystal transition subzone (Tptrn1)
pumice-poor subzone (Tpcrn3)	lithophysal zone
mixed pumice subzone (Tpcrn2)	crystal transition subzone (Tptrl1)
crystal transition subzone (Tpcrn1)	crystal-poor member
lithophysal zone	upper lithophysal zone
crystal transition subzone (Tpcrl1)	cavernous lithophysae subzone (Tptpl2)
crystal-poor member	small lithophysae subzone (Tptpl1)
upper lithophysal zone	middle nonlithophysal zone (Tptpmn)
spherulite-rich subzone (Tpcpl1)	upper subzone (Tptpmn3)
middle nonlithophysal zone (Tpcpmn)	lithophysae-bearing subzone (Tptpmn2)
upper subzone (Tpcpmn3)	lower subzone (Tptpmn1)
lithophysae-bearing subzone (Tpcpmn2)	lower lithophysal zone (Tptpll)
lower subzone (Tpcpmn1)	lower nonlithophysal zone (Tptpln)
lower lithophysal zone (Tpcpll)	hackly subzone (Tptplnh)
lower nonlithophysal zone (Tpcpln)	columnar subzone (Tptplnc)
hackly subzone (Tpcplnh)	spherulitic pumice interval (Tptplnc3)
columnar subzone (Tpcplnc)	argillic pumice interval (Tptplnc2)
spherulitic pumice interval (Tpcplnc3)	vitric pumice interval (Tptplnc1)
argillic pumice interval (Tpcplnc2)	vitric zone (Tptpv)
vitric pumice interval (Tpcplnc1)	vitrophyre subzone (Tptpv3)
vitric zone (Tpcpv)	moderately welded subzone (Tptpv2)
vitrophyre subzone (Tpcpv3)	non-to partially welded subzone (Tptpv1)
moderately welded subzone (Tpcpv2)	
non-to partially welded subzone (Tpcpv1)	
Pre-Tiva Canyon Tuff bedded tuff (Tpbt4)	Pre-Topopah Spring Tuff bedded tuff (Tpbt1)

Buesch and others further subdivide the crystal-rich and crystal poor members into a number of informal smaller zones and subzones (tables 1, 2). Some of these zones are based on widespread petrogenetic phenomena, principally cooling processes, that affected the ash-flow tuffs during and shortly after deposition. Both the Tiva Canyon and Topopah Spring Tuffs exhibit a quenched, non-welded, vitric zone at the upper and lower margins, where the hot mass of glassy pyroclastic shards and other debris cooled rapidly from exposure to ambient air or to the relatively cold pre-existing topography. Welded vitric zones, usually expressed as vitrophyres that compacted, fused, and cooled before devitrification could begin, are found inside the nonwelded vitric zones. The vitrophyre zones are thicker and more laterally extensive at the base of each ash-flow sequence than at the top because of the weight of the overlying, progressively accumulating pyroclastic deposit. The major part of both the Tiva Canyon and Topopah Spring Tuffs compacted and cooled slowly because of the insulating effect provided by the quenched and largely nonwelded upper and lower margins of the deposits. The interior parts of each ash-flow sheet thus consist of moderately to densely welded, devitrified tuff.

Buesch and others also define other zones and subzones (tables 1, 2) that are related more to later-stage alteration phenomena. Residual magmatic gasses exsolved from the compacting and devitrifying mass of glassy shards and these gasses produced vapor-phase alteration consisting principally of microcrystalline, open-space growths of high-temperature silica and feldspar minerals. These phases are distinct from the more "primary" assemblages of minerals resulting from devitrification. Locally, the vapor pressure of the exsolving gas was sufficient to inflate secondary "bubbles," known as lithophysal cavities, along crudely horizontal horizons where the internal pressure exceeded the weight of the overlying column of compacting tuff. These lithophysal cavities are themselves rimmed by vapor-phase alteration minerals, and the alteration may extend some distance into the groundmass surrounding the cavity as rims and borders. The resulting, alternating lithophysae-bearing and non-lithophysae-bearing intervals figure prominently into the zonation of Buesch and

others (table 2, shaded intervals). Additional factors, such as presence, quantity, and composition of pumice and foreign lithic clasts, presence of spherulites, and fracturing habit, also have been used to define some of the subzones shown in table 2.

The tabular nature of a cooling and compacting ash-flow sheet causes most of the thermal and pressure gradients that control alteration to be oriented essentially normal to the long dimensions of the deposit. Thus, the alteration phenomena of vapor-phase alteration zones, intervals of lithophysal cavity development, and zones of strong, near-vertical cooling joint development tend to be subhorizontal and roughly stratiform. However, because these features are the result of secondary, alteration phenomena, they can—and do—cross-cut "primary" stratification features such as the crystal-rich/crystal-poor transition.

Subdivisions of the Calico Hills Formation and Prow Pass Tuff (Crater Flat Group)

Recent review by Moyer and Geslin (1995) of older samples, data, and published lithologic descriptions of rocks underlying the Paintbrush Group tuffs has led to a refined subdivision of both the Calico Hills Formation and the Prow Pass Tuff, as these units were redefined by Sawyer and others (1994). The names and sequence of the informal units described by Moyer and Geslin from the Calico Hills Formation and the Prow Pass Tuff are illustrated in table 1.

Moyer and Geslin (1995) indicate that the Calico Hills Formation in the vicinity of Yucca Mountain comprises five pyroclastic units, a dominantly reworked "bedded-tuff" unit, and a basal volcanoclastic sandstone. Some of these units appear regionally discontinuous. The pyroclastic intervals are generally ash-flow tuffs separated by locally preserved air-fall tuff horizons; the content and composition of pumice clasts and lithic fragments are diagnostic of the different ash-flow groupings. The Calico Hills Formation, in notable contrast to the tuffs of the entire Paintbrush Group, contains volumetrically significant quantities of quartz phenocrysts, whereas the Paintbrush Group Tuffs are virtually quartz-free. There are indications that the

basal sandstone may represent material reworked from the Wahmonie Formation, a distinctive, more mafic volcanic assemblage (Sawyer and others, 1994) not generally present in the immediate Yucca Mountain region.

Moyer and Geslin have concluded that the Prow Pass Tuff (Crater Flat Group) consists of four regionally correlative pyroclastic tuff units plus an underlying interval of bedded tuff. Separation of the different ash flows is based in part on differences in welding and in the proportions and types of phenocrysts, pumices, and lithic fragments. The Prow Pass Tuff is crystal rich in comparison with the volumetrically dominant crystal-poor lower members of the Topopah Spring and Tiva Canyon Tuffs. Also in contrast with the Paintbrush units, the Crater Flat Group tuffs are quartz-bearing. In contrast with the various subunits of the Calico Hills Formation, the rocks of the Prow Pass Tuff contain pyroxene and/or pyroxene pseudomorphs.

The USW SD-12 Drill Hole

Location

Drill hole USW SD-12 is located at Nevada state plane coordinates (North American Datum of 1927) 761,956.6 ft North, 561,605.6 ft East[†] [fig. 1(b)]. The collar of the hole is at an elevation of 4342.8 ft (1323.7 m). The hole is located in a wash to the north of Whaleback Ridge, and is approximately 3100 ft (945 m) to the east of the crest of Yucca Mountain. The hole was collared approximately 700 ft (210 m) west of the surface trace of the Ghost Dance Fault, as mapped by Scott and Bonk (1984), and is located some 150 ft (45 m) to the west of the proposed ESF Main Test Level drift, as that drift was shown on design documents current when the hole was sited (fig. 3). Drill hole SD-12 was intended to penetrate the repository

[†]Note: Nevada State Plane coordinates in feet are widely used on the Yucca Mountain Project. These coordinates are for the central zone of Nevada and are based on a Transverse Mercator projection. The origin of this projection for the central zone of Nevada is latitude 34°45'N., and the central meridian is at longitude 116°40'W. Metric conversions of Nevada State Plane Coordinates are distinctly separate from metric coordinates obtained using the 10,000 metre Universal Transverse Mercator grid, Zone II.

horizon near the mid-point of the north-south Main Test Level drift, it is actually located some 3000 ft (900 m) north of SD-7 near the south corner of the ESF and 6000 ft (1830 m) south of SD-9 near the north corner.

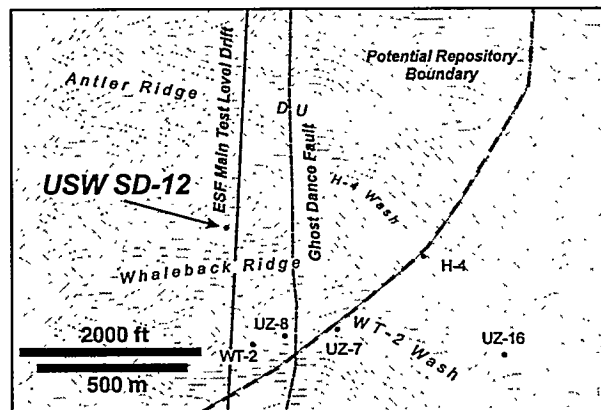


Figure 3. Location map of the potential repository region showing the USW SD-12 drill hole in relationship to nearby drill holes and the Exploratory Studies Facility

Drilling History

Drilling of hole USW SD-12 started on January 28, 1994, when the top of the borehole was drilled to bedrock at a depth of 5.3 ft (1.62 m). Continuous coring operations in welded tuff commenced on February 1, using the Yucca Mountain Project's LM-300 drilling rig equipped with HQ-sized tools (~2.5-inch core) and air only as the circulating medium. The LM-300 rig uses reverse circulation and a dual-wall primary drill-string that serves as temporary casing while coring ahead with conventional circulation. The hole is advanced using alternating coring and reaming cycles.

Surface casing (16-inch; 40-cm) was set to a depth of 50 ft (15.24 m) on February 9. Significant free perched water was not observed in SD-12 near the base of the Tiva Canyon Tuff. However, a water-bearing fracture was encountered at a depth of approximately 251.0 to 253.0 ft (76.5–77.1 m), which is within the nonwelded, crystal-poor vitric subzone of the Tiva Canyon. Water was also encountered associated with core run 80 from 387.97–393.34 ft (118.25–119.88 m) (crystal-rich

nonlithophysal Topopah Spring Tuff); however, this moisture appeared to represent only condensation on the core barrel and the core itself appeared dry.

Core recovery from the upper lithophysal zone of the Topopah Spring Tuff was exceptionally poor because of the presence of the large, closely-spaced lithophysae. The base of the upper lithophysal zone (corresponding approximately to the TSw1/TSw2 thermal/mechanical unit contact) was penetrated at a depth of 661.5 ft (201.62 m) on May 10. Wet core was encountered in core runs 183 and 184 (1059.61–1062.17 ft and 1062.17–1065.74 ft; 322.95–323.73 and 323.73–324.82 m, respectively). These two intervals both are within the crystal-poor lower nonlithophysal zone of the Topopah Spring Tuff. No free fluid was detected in the borehole following core run 184. Geophysical logs were run from 1100 ft (335 m) (middle of the lower nonlithophysal zone of the Topopah Spring Tuff) to the surface on July 11 and 12. Drilling of USW SD-12 was suspended on August 17, 1994 at a depth of 1361.04 ft (414.8 m), just above the base of the Topopah Spring Tuff, but below the lower vitrophyre subzone.

A second round of geophysical logging for the deeper portion of the SD-12 hole below approximately 1100 ft (335 m) was conducted beginning January 23, 1995, in association with logging activities at another location at Yucca Mountain. The drill rig was also moved off the hole and third-party testing was conducted in the drill hole.

Operations resumed at USW SD-12 on July 5, 1995 when the borehole was cleaned of accumulated fill and actual coring using the same HQ-sized drilling tools recommenced on July 6. Wet core was encountered in core run 277 from 1492.58 to 1501.40 ft (454.92–457.60 m) on July 13, but no free water could be detected in the borehole following completion of the core run. Wet core was again encountered in core runs 278 (1501.58–1510.77 ft; 457.60–460.46 m) and 279 (1510.77–1520.78 ft; 460.46–463.51 m). Free water was not identified in the drill hole following either of these latter two runs. Core samples between 1528.32 and 1590.60 ft (465.81–484.79 m; core runs 281–287) appeared continuously

damp when recovered from the bore hole; again, no free-standing water was measured in the hole. On August 7, the drilling tools were wet when removed from the hole at a depth of 1890.72 ft (576.26 m) and the lower 3.5 ft (about 1 m) of the core barrel was coated by mud.

Core exhibiting free water was recovered from a depth of 2004.0 to 2010.6 ft (610.79–612.8 m) on August 11, 1995. Drilling was halted and the water level was observed in the hole at a depth of 1949.65 ft (594.22 m), corresponding to a standing water column of 60.92 ft (118.57 m). Water levels were monitored episodically, and the water level appeared to stabilize at a depth of about 1948 ft (593.7 m). Coring was resumed on August 14 after collection of water samples for laboratory analysis. SD-12 reached a final depth at 2166.3 ft (660.3 m) on August 16, 1995 (in 225 drilling shifts). Drilling was terminated 133.7 ft (40.75 m) short of the intended depth of 2300 ft (701 m) on August 17, 1995 because it was not possible to remove drill cuttings adequately from the saturated-zone part of the drill hole using only air as the drilling fluid. Geophysical logs were run in the bottom portion of SD-12 beginning on September 7, 1995.

Method of Study

Geologic Logging and Core Description

Geologic logging and description of drill core is principally an interpretive activity. The resulting geologic log is dependent upon the skill and experience of the individual performing the examination. The logging procedure used to describe core from drill hole USW SD-12 and other holes of the Systematic Drilling Program emphasizes physical description in an attempt to eliminate partially dependence on stratigraphic nomenclature that may change over time (compare Scott and Bonk, 1984; Buesch and others, 1996). A standardized geologic log form is used to record observations of lithology, composition, alteration, structure, and similar features, and of changes in those multiple characteristics with depth. The observations are thus effectively independent of the names applied to units of similar or contrasting character.

Interpretative geologic logging and core description consists of observing the rock in its intact, relatively undisturbed state. Core was laid out in continuous profile on examination tables at the Yucca Mountain Project Sample Management Facility. A graphical geologic log was prepared at a scale of 1:120 (one inch equals 10 feet) after macroscopic visual examination using a hand lens, binocular microscope, videotaped images and photographs of cored intervals. Photographic records are particularly important for intervals from which core samples had previously been removed for preservation and laboratory measurement of selected material properties. The geologic log includes description of:

- contacts between geologic units
- degree of welding
- degree of devitrification
- size, type, and abundance of pumice
- size, type, and abundance of lithic clasts
- size, type, and abundance of phenocrysts
- size, type, and abundance of lithophysal cavities
- type, nature, and degree of alteration
- presence or absence of bedding or other depositional features
- fault zones or shear zones
- joints or fractures and fracture frequency
- percent core recovery
- RQD (rock quality designation).

Rock color descriptions follow the naming conventions prescribed in the rock-color chart published by the Geological Society of America (1991).

Laboratory Hydrologic Properties

A limited suite of framework material properties were measured in the laboratory for core samples taken from the USW SD-12 drill hole. Adjoining core samples were preserved at the drill-

ing rig in sealed steel cans and in plastic Lexan tubing. In-situ water contents were determined by gravimetry from the canned samples. Porosity, bulk density and particle density also were determined by gravimetry for the canned samples using Archimedes' principle. Initial water content and porosity were used to determine approximate in-situ saturations and volumetric water contents. Machined core plugs were cut from selected larger samples preserved in Lexan and used to determine saturated hydraulic conductivity using Darcy's law relating water flow and pressure drop; the corresponding porosity values for these plugs were also determined. The laboratory property determinations were a collaborative effort of Sandia National Laboratories and the U.S. Geological Survey, Hydrologic Research Facility (USGS, 1991a).

Geology of Drill Hole USW SD-12

Overview

Drill hole USW SD-12 is located immediately to the north of Whaleback Ridge in a small wash draining the eastern slope of Yucca Mountain, approximately 700 ft (210 m) west of the Ghost Dance fault, which is upthrown to the east (fig. 3). This topographic and structural position places the collar of the hole within the middle portion of the Tiva Canyon Tuff. The drill hole also penetrated several nonwelded Paintbrush units underlying the Tiva Canyon Tuff, the entire Topopah Spring Tuff, the Calico Hills Formation and all of the Prow Pass Tuff. The hole was terminated in the upper ash-flow units of the Bullfrog Tuff. A summary of geologic unit contacts is presented in table 3. Lithologic descriptions for the rocks encountered in drill hole USW SD-12 are presented Appendix A, and the corresponding detailed geologic log sheets are in Appendix B.

Table 3: Stratigraphic Unit Upper Contacts and Unit Thicknesses for the USW SD-12 Drill Hole
[--: not present in this hole. Stratigraphic Compendium tops derived from DTN GS940908314211.045]

Lithostratigraphic Unit	Unit Abbreviation	This Report		Stratigraphic Compendium
		Depth to Upper contact (ft)	Apparent thickness (ft)	
Tiva Canyon Tuff (Tpc) — 237.0 ft				
Crystal-poor middle nonlithophysal zone	Tpcpmn	--	55.3 [†]	--
upper nonlithophysal subzone	Tpcpmn3	--	--	--
lithophysae-bearing subzone	Tpcpmn2	26.7	17.4 [†]	27.0
lower nonlithophysal subzone	Tpcpmn1	44.7	37.9	44.5
Crystal-poor lower lithophysal zone	Tpcpll	82.0	52.6	93.4
Crystal-poor lower nonlithophysal zone	Tpcpln	134.6	105.5	129.5±1.0
hackly subzone	Tpcplnh	134.6	41.4	129.5
columnar subzone	Tpcplnc	176.0	64.1	176.0
Crystal-poor vitric zone (“shardy base”)	Tpcpv	240.1	23.6	239.1±1.0
moderately welded subzone	Tpcpv2	240.1	15.4	239.1
nonwelded subzone	Tpcpv1	255.5	8.2	256
Pre-Tiva Canyon Tuff bedded tuff — 8.3 ft	Tpcbt4	263.7	8.3	263.7
Yucca Mountain Tuff (Tpy) — not present				
Pre-Yucca Mountain Tuff bedded tuff — 5.0 ft	Tpbt3	272.0	5.0	268.3
Pah Canyon Tuff (Tpp) — 14.5 ft				
Pre-Pah Canyon Tuff bedded tuff — 2.7 ft	Tpbt2	291.5	2.7	291.2
Topopah Spring Tuff (Tpt) — 1117.1 ft				
Crystal-rich vitric zone	Tptrv	294.2	36.6	314.1
nonwelded subzone	Tptrv1	294.2	26.7	314.1
moderately welded subzone	Tptrv2	320.9	3.7	320.8
densely welded subzone	Tptrv3	324.6	6.2	324.6±0.6
Crystal-rich nonlithophysal zone	Tptrn	330.8	101.2	330.7
Crystal-rich lithophysal zone	Tptrl	432.0	44.5	436.4
Crystal transition interval	--	439.0–476.5	37.5	439.0–476.5
Compositional transition	--	428.3–480.7	52.4	-- [‡]
Crystal-poor upper lithophysal zone	Tptpul	476.5	185.0	476.5
Crystal-poor middle nonlithophysal zone	Tptpmn	661.5	123.5	663.7
Crystal-poor lower lithophysal zone	Tptpll	785.0	257.2	788.7
Crystal-poor lower nonlithophysal zone	Tptpln	1042.2	235.9	1041
Crystal-poor vitric zone	Tptpv	1278.1	133.2	1278.1±0.4
densely welded subzone	Tptpv3	1278.1	24.3	1278.1
moderately welded subzone	Tptpv2	1302.4	36.6	1308.0
nonwelded subzone	Tptpv1	1339.0	72.3	1337.5±0.4
Pre-Topopah Spring Tuff bedded tuff — not present	Tpbt1	--	0.0	1408.0

Table 3: Stratigraphic Unit Upper Contacts and Unit Thicknesses for the USW SD-12 Drill Hole

(Continued)

[--: not present in this hole. Stratigraphic Compendium tops derived from DTN GS940908314211.045]

Lithostratigraphic Unit	Unit Abbreviation	This Report		Stratigraphic Compendium
		Depth to Upper contact (ft)	Apparent thickness (ft)	
Calico Hills Formation (Tac) — 237.1 ft				
unit 4	Tac4	1411.3	63.7	--
unit 3	Tac3	1475.0	79.0	1411.5±1.0
unit 2	Tac2	1554.0	46.6	--††
unit 1	Tac1	1600.6	11.0	--
bedded tuff unit	Tacbt	1611.6	29.7	--
basal sandstone unit	Tacbs	1641.3	7.1	--
Prow Pass tuff (Tcp) — 496.5 ft				
unit 4	Tcp4	1648.4	8.2	--
unit 3	Tcp3	1656.6	215.1	--
unit 2	Tcp2	1872.1	74.9	--
unit 1	Tcp1	1947.0	186.0	--
bedded tuff unit	Tcpbt	2133.0	11.9	--
Bullfrog Tuff (Tpb)		2144.9	21.4†	--

† Entire unit not penetrated, partial thickness only

‡ Not recognized as part of nomenclature of Buesch and others (1996)

†† DTN GS940908314211.045 does not extend below 1435.3 ft

The 258.4 ft of the lower Tiva Canyon Tuff encountered in drill hole SD-12 consist of (in descending sequence) the majority of the crystal-poor middle nonlithophysal zone, the lower lithophysal, lower nonlithophysal and lower vitric zones (table 3). The middle nonlithophysal zone of the Tiva Canyon Tuff contains a middle “lithophysae-bearing subzone” at this location. Below the middle nonlithophysal zone, a gradational increase in the number of lithophysae and in the intensity of associated vapor-phase alteration marks the top of the lower lithophysal zone; a “contact” is defined at a depth of 82.0 ft (25.0 m). Very large diameter lithophysae (larger than the core diameter) have been observed in parts of the lower lithophysal zone using down-hole video imagery. Vapor-phase alteration decreases downward through the interval. However, both lithophysae and the intensity of vapor-phase alteration end abruptly forming a distinct lower contact with the lower nonlithophysal

zone at 134.6 ft (41.0 m). Two subzones (table 3) can be distinguished within the lower nonlithophysal zone based on characteristic styles of fracturing; additional minor subdivisions can be distinguished based on the alteration of contained pumice clasts (Buesch and others, 1996). Devitrification and welding decrease progressively between depths of 240.1 to 255.5 ft (72.9–77.9 m), marking the lower vitric zone of the Tiva Canyon Tuff. A nonwelded interval forms the lowermost part of the lower vitric zone, ending at a basal contact at 263.7 ft (80.37 m).

The sequence of nonwelded units below the Tiva Canyon Tuff generally follows in normal succession: the pre-Tiva Canyon Tuff bedded tuff (Tpbt4) is defined between 263.7 and 272.0 ft (80.4–82.9 m), the pre-Yucca Mountain Tuff bedded tuff (Tpbt3) from 272.0 to 277.0 ft (8.29–84.4 m), and the Pah Canyon Tuff from 277.0 to 291.5

ft (84.4–88.8 m). Pre-Pah Canyon Tuff bedded tuff (Tpbt2) is present from 291.5 to 294.2 ft (88.8–89.7 m). The Yucca Mountain Tuff is missing in drill hole SD-12.

The Topopah Spring Tuff was encountered beginning at a depth of 294.2 ft (89.7 m), and the unit exhibits a total apparent thickness of 1117.1 ft (340.5 m). The Topopah Spring is nonwelded at the upper contact, but welding increases abruptly at the upper contact of the “caprock” vitrophyre at 324.6 ft (98.9 m), and the rock becomes devitrified below 330.8 ft (100.8 m), marking the contact between the crystal-rich vitric zone and the underlying crystal-rich nonlithophysal zone (also known as the “rounded” zone of Scott and Bonk, 1984). The “nonlithophysal” unit becomes weakly lithophysal down to approximately 432.0 ft (131.7 m), at which depth an increase in the frequency and size of lithophysae marks the top of the crystal-rich lithophysal zone. A compositional transition interval from quartz latite to rhyolite 52.4 ft (16.0 m) thick leads to distinction of the crystal-poor upper lithophysal zone (Buesch and others, 1996) beginning at a depth of 476.5 ft (145.2 m). The intensity (frequency and size) of both lithophysal-style alteration and associated vapor-phase alteration is somewhat variably, but it is essentially continuous throughout both crystal-rich and crystal-poor lithophysal zones. Very large lithophysae are visible in down-hole video imagery beginning at depth of approximately 555.2 ft (169.2 m); these large-than-core-sized cavities and their altered margins are represented in the core as highly broken zones or intervals of no recovery. A zone of very intense lithophysal cavity development containing both large and small closely-spaced lithophysae extends from 555.2 to 661.1 ft (169.2–201.5 m).

Lithophysae in the core end abruptly at the contact with the middle nonlithophysal zone at 663.5 ft (202.2 m). The lithophysal-bearing subzone of the middle nonlithophysal zone is not identified in core from SD-12, however, intensively broken and unrecovered intervals between 699.1 and 729.9 ft (213.0–222.46 m) may represent very large lithophysal cavity development in this interval.

The top of the lower lithophysal zone is defined at 785.0 ft (239.3 m) by the presence of small, oval-shaped lithophysal cavities and alteration-spot development. Evidence of large lithophysal cavities is present in the core as thick broken and unrecovered intervals below approximately 798.4 ft (243.4 m); the presence of large lithophysal cavities is confirmed by down-hole video imagery. These very large lithophysae are widely spaced, and they appear to continue downward to a depth of at least 1098.7 ft (334.9 m). This depth is well below the base of the crystal-poor lower lithophysal zone, although the frequency of large cavities in borehole video images decreases noticeably below approximately 1045 ft (318.5 m). A subtle change in alteration of the groundmass of the core and a general decrease in the content of mesoscopic lithophysae at about 1042.2 has been taken as the “contact” between the crystal-poor lower lithophysal and lower nonlithophysal zones. Large lithophysal cavities can still be observed in down-hole video images below this depth, however. Large, angular, rhyolite lithic fragments up to 60.0 mm in diameter are present beginning at a depth of about 1060.0 ft (323.1 m) and continue to the bottom of the Topopah Spring welded section. These types of inclusions are typical of the lower nonlithophysal zone (formerly the “mottled” zone; Scott and Bonk, 1984) in some outcrop exposures of the Topopah Spring Tuff elsewhere at Yucca Mountain. A sharp contact at a depth of 1278.1 ft (389.6 m) separates devitrified tuff from the underlying crystal-poor vitric zone, and specifically from the characteristic lower (or “basal”) vitrophyre unit of the Topopah Spring Tuff. The densely welded (vitrophyre) subzone (Tptpv3) is 24.3 ft (7.4 m) thick at SD-12. Welding decreases gradationally through the crystal-poor vitric zone beginning at about 1278 ft (389.5 m), and the basal nonwelded subzone of the Topopah Spring Tuff extends from 1339.0 to 1411.3 ft (408.1 to 430.2 m). Incipient zeolitization begins within the lowest part of the Topopah Spring Tuff at about 1381.1 ft (420.9 m) and affects principally pumice clasts and shard boundaries. The pre-Topopah Spring Tuff bedded tuff (Tpbt1) is missing from the SD-12 section.

The Calico Hills Formation was encountered at a depth of 1411.3 ft (430.2 m) and the unit is 237.1

ft (72.3 m) thick. The Calico Hills in SD-12 has been subdivided into four nonwelded ash-flow tuff units, a reworked bedded tuff unit, and a basal tuffaceous sandstone. The uppermost Calico Hills ash-flow unit (unit 5 of Moyer and Geslin, 1995) either was not deposited in the vicinity of drill hole SD-12 or was subsequently removed before deposition of the Topopah Spring Tuff. The Calico Hills formation is essentially entirely zeolitic. Numerous intervals of prominent red-brown rhyolitic lithic fragments form swarms throughout the ash-flow deposits of Calico Hills in the SD-12 drill core.

The Prow Pass Tuff was encountered beginning at a depth of 1648.4 ft (502.4 m); this uppermost formation of the Crater Flat Group is 496.5 ft (151.3 m) thick at SD-12. The Prow Pass Tuff has been subdivided into four ash flows and a basal bedded tuff unit by Moyer and Geslin (1995). Ash-flow deposits of the Prow Pass Tuff in the core from SD-12 are generally zeolitized and fairly uniform in appearance. Ash-flow unit 3 is variably but weakly to moderately welded and vapor-phase altered in the SD-12 drill core. Zeolitic alteration is less intense in ash-flow unit 3. Swarms of fine-grained lithic fragments occur at numerous vertical positions within the Prow Pass Tuff. An immature tuffaceous, iron-stained sandstone ("bedded tuff") underlies the ash-flow deposits.

The Bullfrog Tuff underlies the Prow Pass Tuff beginning at a depth of 2144.9 ft (653.7 m); only the top 21.4 ft (6.5 m) of the Bullfrog was cored. The uppermost Bullfrog Tuff is nonwelded, zeolitized, and pumiceous. Drilling at USW SD-12 was terminated at a depth of 2166.29 ft (660.3 m) in what is termed Bullfrog unit 4 of Rautman and Engstrom (1996).

Thermal/Mechanical Units

A somewhat formalized thermal, mechanical, and hydrologic stratigraphy was defined originally by Ortiz and others (1985), based upon preliminary concepts put forward by Lappin and others (1982). The concept was to define coherent rock units for performance analyses based on rock properties, rather than on more classical geologic criteria. According to the original citation, "Two properties used to differentiate units are porosity and grain

density" (p. 8). Further reading of the Ortiz and others reference indicates that this subdivision based on porosity and grain density translates to a first-order subdivision between welded and non-welded materials, with additional subdivisions determined by whether the rocks are still vitric, or whether they have been altered either to a devitrification (high-temperature "crystallization") mineral assemblage or to zeolites. The so-called thermal/mechanical units were correlated with the more conventional geologic stratigraphy in use at the time in table 1 of Ortiz and others; this correlation is reproduced essentially intact in table 1 of this report. The thermal/mechanical stratigraphy, as originally described, also subdivided the Topopah Spring welded interval into a lithophysae-rich upper portion in contrast with the lower part, which was presumed to be relatively poor in lithophysae (p. 11). In fact, the distribution of lithophysal-style alteration and of lithophysal cavities is significantly more complex than was recognized by Ortiz and her coworkers.

It is important to note that the major changes in material properties recognized as the basis for subdividing the volcanic section at Yucca Mountain by Ortiz and others do not correspond to the boundary of the formal geologic units, which are identified principally by major breaks and changes in the genetic processes that produced the southwestern Nevada volcanic field. The descriptive but unfortunate use by Ortiz and her coworkers of the conventional geologic names as the "base" for the thermal/mechanical unit names can cause confusion if the critical distinction between property-based and process-based nomenclature is not fully understood. Nevertheless, this physical-property subdivision, which aggregates materials that behave in a similar manner, has proven to be an enduring feature of the Yucca Mountain Project.

Table 4 presents the thermal/mechanical units identified from the SD-12 drill core. In keeping with Ortiz and others (1985), who presented a series of surfaces representing the *bottom* of each thermal/mechanical unit, table 4 gives the depths to each basal contact as well as the apparent thickness of each unit

Table 4: Basal Contacts and Thicknesses of Thermal/Mechanical Units for For Drill Hole USW SD-12
 [Definitions of thermal/mechanical units from Ortiz and others (1985), p. 11–12]

Thermal/Mechanical Unit	Lower Contact (ft)	Apparent Thickness (ft)
TCw: Tiva Canyon welded	240.1	213.4 [†]
PTn: Paintbrush nonwelded	324.6	84.5
TSw1: Topopah Spring welded, "lithophysae rich"	661.5	336.9
TSw2: Topopah Spring welded, "lithophysae poor"	1278.1	616.6
TSw3: Topopah Spring welded, vitrophyre	1302.4	24.3
CHn1: Calico Hills nonwelded—lower nonwelded part of Topopah Spring Tuff plus ash-flow tuffs of Calico Hills Formation	1641.3	338.9
CHn2: Calico Hills nonwelded—basal reworked zone and "bedded tuffs" of the Calico Hills Formation	1648.4	7.1
CHn3: "Calico Hills" nonwelded—upper nonwelded ash-flow tuffs of the Prow Pass Tuff	1656.6	8.2
PPw: Prow Pass welded—welded ash-flow tuffs of the Prow Pass Tuff	1790.0?	133.4
CFUn: Upper Crater Flat nonwelded—nonwelded ash-flow tuffs of the lower Prow Pass Tuff and upper Bullfrog Tuff	TD	354.9 [†]

[†] Entire unit not penetrated, partial thickness only.

Structural Geology of SD-12

No faults were recognized in the USW SD-12 drill core that exhibit displacement large enough to cut-out completely or to replicate identifiable stratigraphic intervals. Small faults may be difficult to distinguish from more generally rubblized core. Thus, even though a large fraction of the rubble intervals logged from the SD-12 drill hole may be attributed confidently to breakage of rock associated with lithophysal cavities, it is possible that other rubble zones—and some intervals of nonrecovery—may represent unrecognized faults or fault zones. This interpretive difficulty notwithstanding, a number of specific indicators of faulting were identified in the core, as described in this section and as indicated on the geologic log sheets of Appendix B. An additional complicating factor is that a significant cumulative length of the recovered core was removed to preserve the in-situ hydrologic properties of core samples for laboratory testing; these intervals were not available for detailed study during creation of the geologic log

for this report. Some information regarding indicators of faulting thus has been extracted from the drill-site preliminary logs and been included on the geologic log sheets in the appendix.

Brecciated core was identified at two separate depths: at 234.1–234.3 ft and at 330.7–331.1 ft (approx. 71.3 and 100.8 m, respectively). The former breccia occurs within the moderately welded subzone of the Tiva Canyon crystal-poor vitric zone (also known as the shandy base interval), whereas the latter appears to be near the base of the densely welded subzone of the Topopah Spring crystal-rich vitric zone (the caprock vitrophyre). In both instances, the breccia is directly associated with calcite in-filling.

Slickensides occur at a number of depths. Poorly defined slickensides are described in the drilling-support log at 253.3 ft (77.20 m). Better defined slickensides occur at 261.4 ft (79.67 m) with measurable striations at approximately 5° to the core axis and at 276.2 ft (84.18 m) at about 10°

to the core axis. Both of these occurrences are within the bedded tuff interval underlying the Tiva Canyon Tuff and overlying the Pah Canyon Tuff. Unmeasurable slickenlines are also reported at a depth of 1744.1 ft (531.58 m) within the welded part of ash-flow unit 3 of the Prow Pass Tuff.

Identifiable, soft, clay(?)-rich fault gouge 0.3-ft (9-cm)-thick was encountered at a depth of 814.3–814.6 ft (248.19–248.28 m) along a plane dipping approximately 30° to the core axis. It is not possible to determine a sense of displacement on this fault, which occurs near the top of the crystal-poor lower lithophysal zone of the Topopah Spring Tuff. A second zone of clay-rich(?) gouge material is present along a plane dipping at roughly 50° to the core axis at a depth of 875.9 ft (266.96 m); this occurrence is also within the lower lithophysal zone of the Topopah Spring. A fault at 50° to the core axis implies a dip from horizontal of about 40°. This is a relatively low angle fault that might involve significant horizontal displacement. Note that there are a great many intervals within the lithophysal intervals of the Topopah Spring Tuff that recovered only rubble or that were completely lost during the drilling process. Many of these intervals could also represent small-displacement faults.

Lithophysal Zones

The definition of lithophysal zones within the welded tuffs at Yucca Mountain is a complex problem that has a long history of confusion within the Yucca Mountain Project. The issue involves distinguishing (informally) named “lithophysal zones” from other intervals that may contain lithophysae. In logging and describing other recent core obtained from Yucca Mountain, T. C. Moyer (Science Applications International Corporation/U.S. Geological Survey, personal communication, 1994) originally indicated that lithophysal zones were to be defined simply based on “the presence of lithophysae.” Ortiz and others (1985, p. 11) gave a threshold value of “approximately 10% by volume lithophysal cavities” as the criterion for separating their “lithophysae-rich” (TSw1) and “lithophysae-poor” (TSw2) subunits of the Topopah Spring welded tuff. Buesch and others (1996) present a more specific description of crite-

ria for the identification of specifically named lithophysal zones (page 18; quoted almost in its entirety):

Lithophysal zones occur where vapor concentrates in the densely welded parts of ignimbrites [ash-flow tuffs] to form lithophysal cavities (Ross and Smith, 1961).... Lithophysae consist of a cavity, which is commonly coated with vapor-phase minerals on the inner wall of the cavity, a fine-grained rim surrounding the cavity wall, and a thin very fine-grained border.... Many lithophysae in the Tiva Canyon and Topopah Spring Tuffs have light-gray (N8) to grayish-orange pink (10R8/2) rims of microscopic to barely macroscopic elongate crystals that radiate from the walls of the lithophysae into the surrounding groundmass. These rims are up to 3-cm wide. Locally, rims have 1- to 3-mm-wide, grayish red-purple (5YR4/2) borders. Associated with the lithophysae are light-gray (N8) to grayish-orange pink (10R8/2) spots 1- to 5-cm in diameter. Some spots may represent the cross sections of rims on lithophysae, whereas others have a crystal or lithic clast in the core that could have acted as a nucleation site. There is no genetic interpretation for the spots; however, they are characteristic for some lithophysal zones. Lithophysal zones in the Tiva Canyon and Topopah Spring Tuffs are identified by a combined occurrence of lithophysae and spots [emphasis added]. The shape of the lithophysae and spots and width of the rims on the lithophysae can also be diagnostic of specific zones. Locally surface exposures contain lithophysae with diameters of up to 1 m; thus regions of poor core recovery might indicate large lithophysae [emphasis added].

Vapor-phase altered rocks containing abundant (greater than 10 percent) lithophysae, with or without significant open-space cavities, are readily recognized and are easily assigned to discrete lithophysal zones. One real complication appears to be the recognition and treatment of lithophysal-style alteration associated with cavities that are too large to be recognized *directly* in the core (and by extension, recognition of the mere presence of lithophysae). Where very large lithophysae are penetrated by the drill string, the thin, brittle septae of rock dividing the cavities typically are shattered by the force of the rotating drill bit; this logically results in intervals of rubble and unrecovered core (cavity plus rubble blown away from the bit face

into other parts of the cavity). Diagnostic, remnant vapor-phase alteration rims and distinctive cavity-coating minerals frequently can be identified in the recovered rubble fragments. The question essentially reduces to whether or not an interval exhibiting these very large lithophysal cavities, but *without* significant quantities of the small-scale lithophysae or vapor-phase-altered spots, can be classified as a “lithophysal zone.”

Descriptions of the SD-12 drill core for this report use multiple criteria derived from the description of lithophysal zones presented by Buesch and others (quotation above). In keeping with the logging philosophy presented in the section on core description beginning on page 8, the *principal emphasis* of the Systematic Drilling Program *has been placed on objective description of the core and associated down-hole video imagery* (particularly that presented in the foot-by-foot geologic log sheets presented in Appendix B). Association of unit names with these descriptions is distinctly secondary. Generally, named “lithophysal zones” identified in this report contain rocks exhibiting small- to medium-sized lithophysae and/or “spots” whose matrix is grayish red-purple in color, as recommended by Buesch and others (1996, p. 18). This type of material typically is associated with vapor-phase alteration of varying, but relatively strong, intensity immediately adjacent to observable lithophysae. The matrix of rocks from named *nonlithophysal* zones is typically more brownish or orangish in color; note that description of rock colors is somewhat subjective, even when using standard rock-color charts (Geological Society of America, 1991). The finer-scale texture of the rock between lithophysal cavities in lithophysal zones is typically stretched and foliated, as if distorted by the inflating lithophysal cavities. Fracturing within named lithophysal zones is generally distinctive as well; fractures tend to be shorter and more irregular in form, and to exhibit rougher surfaces than those encountered outside the named lithophysal zones. Unquestionably, some of the names assigned in this report are somewhat in conflict with the description of the corresponding interval. The descriptions should take precedence, as these do reflect local heterogeneities in the tuff mass.

Drill hole USW SD-12 was collared in the crystal-poor middle nonlithophysal zone of the Tiva Canyon Tuff, which extends from the top of bedrock at 12.91 ft (3.94 m) to 82.0 ft (25.0 m). This middle “nonlithophysal” interval includes a “lithophysae-bearing subzone” from approximately 26.7 to 44.7 ft (8.1–13.6 m) that contains relatively crowded small- to medium-sized lithophysae associated with open cavities. However, as indicated by geologic log sheet 1 of Appendix B, more sparse lithophysae, both with and without cavities, occur throughout the nominally nonlithophysal zone. The transition from the middle nonlithophysal zone to the underlying crystal-poor lower lithophysal zone is marked simply by an increase in the density of lithophysae and in the intensity of the associated vapor-phase alteration. The lower contact of lithophysae-bearing rocks with truly nonlithophysal materials belonging to the crystal-poor lower nonlithophysal zone is sharp and distinct at 134.6 ft (41.0 m). Yet here too, the issue of the “contact” is not simple, because short, closely spaced, flat-lying, “hackly” fractures that are characteristic of the hackly subzone of the lower nonlithophysal interval (Buesch and others, 1996) are encountered nearly 5 ft (1.5 m) above the abrupt termination of lithophysae within the Tiva Canyon Tuff.

Within the Topopah Spring Tuff, lithophysal alteration associated with the crystal-rich and crystal-poor upper lithophysal zones begins at approximately 432 ft (131.7 m), approximately 100 ft (31 m) below the caprock vitrophyre (see log sheet 7, Appendix B). Lithophysae increase rapidly in both abundance and size by a depth of 448.0 ft (136.54 m), as does the incidence of intervals of broken and unrecovered core. Many intervals of “lost” core are attributed to void space representing large lithophysae that appear to be several core-diameters across in down-hole video images. The highly broken nature of much “core” recovered from lithophysal zones is attributed to disintegration of the vuggy tuff during drilling.

Lithophysal cavity development decreases quite sharply at a depth of approximately 661.5 ft (201.6 m; log sheet 10, Appendix B), marking the contact of the crystal-poor upper lithophysal zone with the underlying middle nonlithophysal zone. A

few sparse flattened lithophysae and numerous vapor-phase alteration streaks and speckles continue below the contact to a depth of about 675 ft (206 m). A well-defined “lithophysae-bearing subzone” (table 2; Buesch and others, 1996) cannot be identified in the core or down-hole video images from the SD-12 drill hole, although core recovery and rock quality (see “Rock Quality Considerations” beginning on page 17) decrease noticeably from about 712 to 727 ft (217–222.5 m). Evidence from petrophysical logs (see “Geophysical Log Data” beginning on page 33) also supports the presence of a poorly developed lithophysae-bearing subzone at about this depth.

The lower lithophysal zone of the Topopah Spring Tuff was encountered at a depth of 785.0 ft (239.26 m; log sheet 12). In addition to sparse lithophysae visible in the core, the material recovered from this relatively thick unit also includes broken and “lost-core” zones that appear to correspond to large (many centimeter) lithophysal cavities visible in down-hole video logs. Interestingly, mesoscale lithophysae are *not* prominent in the recovered core material throughout this interval (log sheets 12–15). Small- to medium-sized lithophysae, in fact, are most obvious only in the uppermost and lowermost 20 to 30 ft (6–9 m) of the named crystal-poor lower lithophysal zone. Fragments of altered lithophysal rims, broken zones, unrecovered intervals and large lithophysae visible in the borehole video attest to their presence within the rock mass. Down-hole images of large lithophysae are common between roughly 800 and 908 ft (245–277 m).

Core recovery increased markedly below a zone of inferred very large lithophysal-cavity development that ends at 1022.4 ft (311.3 m), and medium-sized lithophysae diminish below this depth. By a depth of 1042.4 ft (317.7 m), the style of alteration affecting the groundmass of the rock changes distinctly, and this change, together with a general lack of mesoscopic lithophysae, is interpreted to represent the contact of the crystal-poor lower lithophysal zone with the lower nonlithophysal zone (or “mottled” zone of Scott and Bonk, 1984) of the Topopah Spring Tuff. Large lithophysal cavities are observed in down-hole video imagery to a depth of approximately 1098.7 ft

(334.9 m) (log sheets 15–16), more than 50 ft (15 m) into the lower “nonlithophysal” zone.

Rock Quality Considerations

Core Recovery

Percent core recovery was determined at the drill rig by Yucca Mountain Project drilling support staff during the coring of hole USW SD-12. Recording core recovery information is a relatively mechanical process and it follows a set procedure. Core recovery data are presented in Appendix C, Table C-1; this information is also presented graphically in summary form in figure 4. Core recovery information is presented in more detail on the geologic log sheets of Appendix B, which allows inference of possible lithologic controls of lost core and as means of qualifying the reliability of the associated lithologic descriptions. Description of intervals with exceptionally poor core recovery requires a subjective “reading” of multiple lines of indirect evidence.

A generalized summary of the procedure used to determine core recovery is as follows.

- 1) The core is laid out in an appropriate manner. Broken segments are fitted back together as best possible to represent *in-situ* dimensions. Rubble is reaggregated to continuous piles of approximately the core diameter.
- 2) The start and stop depths of the core run are identified from information provided by the driller and the length of the core run is determined.
- 3) The total length of core recovered from a given run is measured using a steel tape measure and the footage is recorded.
- 4) Recovery is computed as the percentage of material actually recovered from that drilling interval.

Core recovery data are only estimates. The accuracy of these estimates in reflecting the actual recovery for a core run can be quite precise for intervals of generally good recovery of essentially intact core. Accuracy diminishes markedly as the integrity of the core decreases, because loose rubble recovered in the core barrel must be approxi-

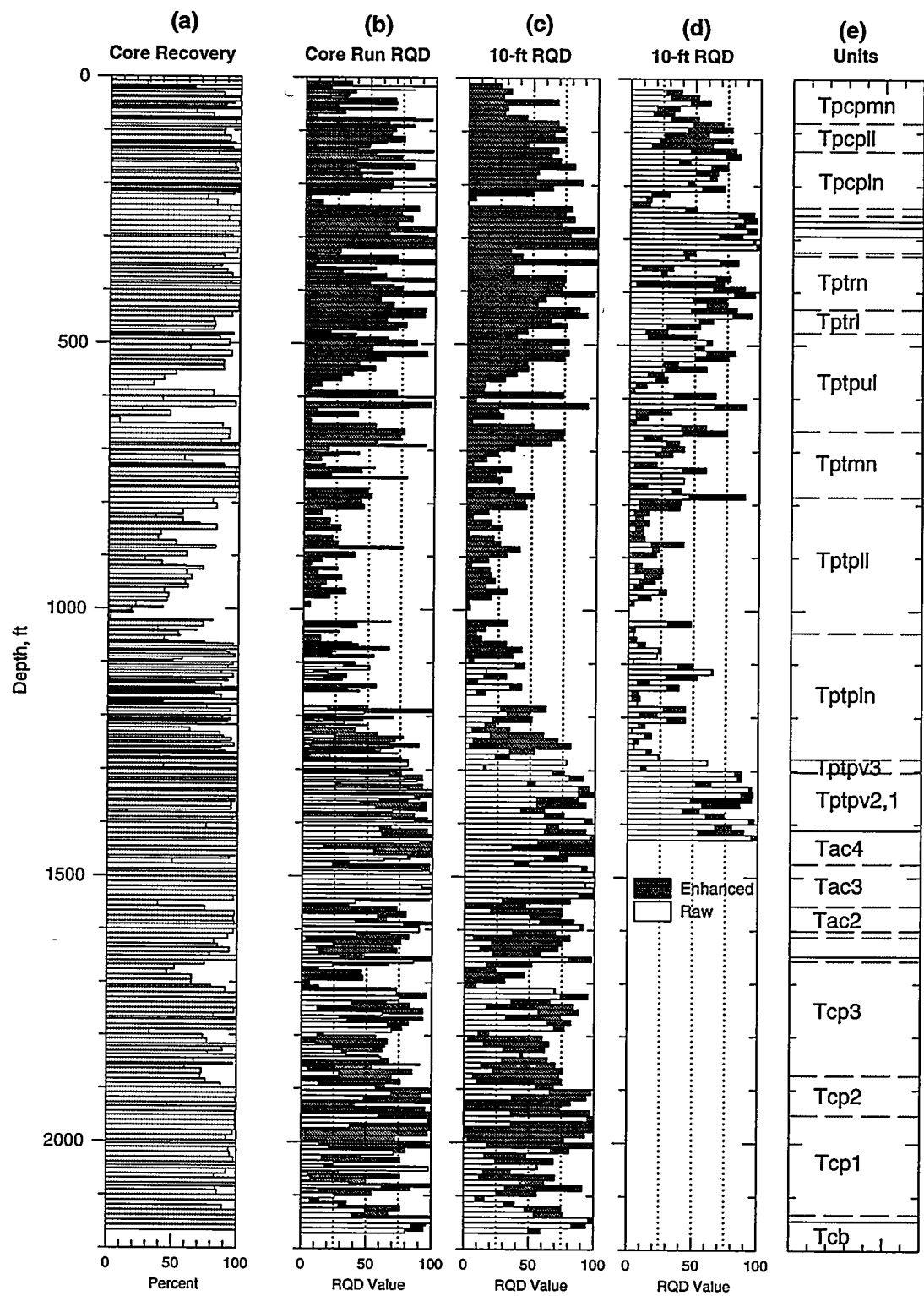


Figure 4. Plots showing (a) core recovery, (b) field-measured core-run RQD, (c) 10-ft averaged field-measured RQD, and (d) 10-ft averaged video-analysis RQD for the USW SD-12 drill hole as a function of depth. Dark grey bars are “enhanced” or original RQD values of Deere and Deere (1989); white bars are raw RQD values uncorrected for coring-induced fractures. Dotted vertical lines are RQD classes from table 5. Thinner geologic units are not labeled.

mated back to in-situ dimensions prior to measurement.

A summary of the core-recovery information is presented graphically in figure 4(a). Detailed core-recovery information is shown on the individual geologic log sheets of Appendix B. Core recovery averaged 81 percent across the entire SD-12 drill hole. However, this average figure belies the fact that thick intervals were recovered with nearly 100-percent recovery whereas other, equally thick intervals were cored with substantially less recovery—in places less than 50 percent. Examination of figure 4(a) clearly indicates that the named lithophysal zones within the Topopah Spring Tuff are associated with much-below-average core recoveries. Interestingly, despite the common occurrence of very large lithophysal cavities in the crystal-poor upper lithophysal zone, the fraction of material recovered from this zone generally exceeds the fractional recovery from the lower part of the crystal-poor lower lithophysal zone. In both lithophysal intervals, recovery from the bottom half of the zone was lower than that from the top half. The cause of this internal zonation is not clear. Core recovery from the very top of the lower nonlithophysal zone of the Topopah Spring Tuff resembles that of the overlying lower lithophysal zone, which is consistent with independent observations that large lithophysal cavities continue for some tens of feet below the last prominent mesoscale lithophysae and the more pronounced change in intensity of vapor-phase alteration (log sheets 15–16, Appendix B). Intervals of poor recovery totalling several tens of feet were encountered at the top and at the bottom of Prow Pass ash-flow unit 3 (extending into the top of ash-flow unit 2).

RQD (Rock Quality Designation)

Measurement of RQD is also a relative mechanical process, and it is usually performed as an adjunct to measurement of core recovery. Like core recovery, RQD has been defined on a per-run basis for each drilling interval (Deere and Deere, 1989). RQD is generally also reported on the basis of a standardized interval, typically 10 feet (approximately 3 m). The use of a standard-length measurement interval reduces the occurrence of interspersed, wildly erratic RQD values that may

be associated with numerous very short core runs (particularly in broken rock).

The procedure for determining RQD data is as follows.

- 1) The core is laid out in an appropriate manner as for core-recovery measurements.
- 2) The length of the core run is determined as for core-recovery measurements.
- 3) The cumulative footage of intact, whole core segments of sound rock longer than 4 inches (100 mm) as measured along the centerline of the core is measured using a steel tape measure. Ends that result from diagonal fracturing of the rock mass are excluded from the measurement (fig. 5). There are two alternatives for the treatment of fractures:
 - (a) all extant fractures are considered as breaks in the core, regardless of whether or not the fractures appear to be natural or drilling induced; or
 - (b) only natural fractures are considered to be breaks in the core.
- 4) The cumulative footage thus measured is converted to a percentage of the drilling interval and recorded to the nearest percent.

The originator of the RQD measurement system (Deere, 1963; see also Deere and Deere, 1989, p. 15, 43) recommended that only natural breaks in the core be considered. Deere and Deere explicitly state that breaks that are obviously an artificial result of the drilling and/or core-handling process are to be discounted in the determination of “broken” core. Criteria for identifying natural fractures may include: fracture in-filling or mineralization; obvious non-matching sides; the presence of gouge, slickensides, or other structures suggestive of relative movement; and potentially other site-specific features. Criteria for induced fractures include: actual observation of core breakage during handling; absence of any fracture-filling material other than drilling mud (which was not used in site-characterization drill holes at Yucca Mountain); clean, sharp edges that fit tightly together; and breaks at 90° to the core axis. If the origin of a particular break is in doubt (indeterminate), their procedure is to count it as a natural break, which would produce an RQD value that is conservative from a rock-stability standpoint. If all fractures are

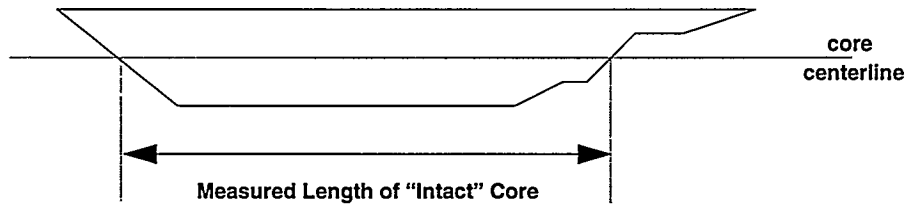


Figure 5. Conceptual sketch for measuring the length of "intact" core segments for RQD determinations. Ends, "ears," and other segments are not included in the length measurement. Segments must be longer than 4 inches (100 mm) to count toward RQD.

considered breaks in the core, value that results is referred to in this report as "raw RQD." If induced fractures are discounted, the value is referred to as "enhanced RQD" or "Deere RQD."

The requirement for "sound rock" is also subjective, but it is intended (Deere and Deere, 1989, p. 16) to exclude intervals of altered, weathered, or otherwise unstable material that might conceivably be recovered "intact" (not fractured or broken). If the soundness of a particular core segment that would otherwise qualify is in doubt, it is excluded from the cumulative piece-length measurement for RQD determination. The intent is to be conservative from a design standpoint of estimating ground stability. In practice, such subjective decisions involving Yucca Mountain core are not an issue, as the type of alteration that typically produces "soft," intact core is virtually unknown from the upper portion of the volcanic section.

Measured RQD data for the individual core runs of drill hole USW SD-12 are given in Appendix D, table D-1. The 10-ft composite (averaged) RQD values are in table D-2. RQD values for the SD-9 drill hole are presented in graphical form in figure 4, parts (b), (c), and (d). RQD values are also included graphically on the detailed geologic log sheets in Appendix B.

Note that there two sources of RQD data and RQD composites. The data in table D-1 and the columns in table D-2 that are headed "Drilling Support" are based on actual physical measurement of the core by drilling support staff at the time of recovery of the core from the hole. The values in

the columns of table D-2 that are headed "Study 8.3.1.14.2" are based on offsite interpretation of video images of the core that were filmed immediately upon opening of the core barrel in the field. The field-measured values benefit from direct physical observation of the core, including the ability to examine actual fracture surfaces for the presence of mineralization and other phenomena that may bear on the issue of natural versus induced. However, the logistics of sampling the core at the rig site and preserving those samples in near-in-situ hydrologic conditions limits the time that can be spent examining a core run to a few minutes. The video-based RQD measurements, which were actually obtained as part of SCP Study 8.3.1.14.2 (Soil and Rock Properties of Potential Locations of Surface Facilities; USGS, 1991b), are not subject to this time limitation; however, these data are limited by the inability to examine the core itself physically. The values portrayed on the detailed geologic log sheets of drill hole SD-12 (Appendix B) are the 10-foot composite, field-measured, enhanced RQD values from table D-2 (column 3).

A confounding factor for the SD-12 drill hole is that the same types of measurements (raw, enhanced) from the two different sources (drilling support, Study 8.3.1.14.2) are not available uniformly for the same broad intervals. The drilling support staff did not record raw piece-length measurements for the upper part of the hole. The procedure controlling this work at that time provided only for recording of adjusted piece lengths, corresponding to enhanced or original RQD as defined by Deere and Deere (1989). A revised procedure for recording both types of measurements became

effective with core run number 186 (table D-1), beginning at a depth of 1070.7 ft (326.33 m). The video-analysis-derived RQD values measured by Study 8.3.1.14.2 were not obtained below 1430.0 ft (435.84 m) because these values were developed specifically for use in design of the Exploratory Studies Facility. The deeper portion of the SD-12 drill hole is below this zone of short-term engineering interest.

Examination of figure 4 [compare columns (c) and (d)] indicates that the differences among the RQD values derived from the two different sources are relatively insignificant in light of the fact that RQD is a rough, preliminary estimate of rock mass integrity. Design decisions for ground support of underground openings, such as the Exploratory Studies Facility or a potential repository, are generally based on large categorical groupings of RQD values (table 5), or on the basis of more sophisticated indicators of rock mass stability, such as those provided by the "RMR" or "Q" rating systems (Barton and others, 1974; Bieniawski, 1989).

Table 5: RQD and Rock-Quality Descriptors [after Deere and Deere (1989)]

RQD	Description
90–100	Excellent
75–90	Good
50–75	Fair
25–50	Poor
0–25	Very poor

As anticipated, the core-run RQD values are more variable than the ten-foot composites [fig. 4, compare column (b) with (c) or (d)]. For the available enhanced RQD data, $\sigma_{\text{run}} = 38$ whereas $\sigma_{10\text{-ft}} = 30$. For the composite 10-ft values, the enhanced or Deere RQD values are logically higher ($\bar{X} = 56$, drilling support; $\bar{X} = 45$, Study 8.3.1.14.2) than the raw values ($\bar{X} = 39$; $\bar{X} = 32$), for which the impact of drilling and sample handling have not been discounted. Note that in some intervals, the effect of presumed coring-induced fracturing may be fairly substantial: compare figure 4(d), 80–140 ft, 380–390 ft, 780–810 ft, 1600–1710 ft, and 1800–2100 ft (24.38–42.67, 115.82–118.87, 237.73–246.88,

487.66–521.18, and 579.09–640.05 m, respectively).

Generally, the integrity of the thick welded sections of both the Tiva Canyon and Topopah spring Tuffs is relatively poor by any measure (RQDs less than 50 are "poor" or "very poor;" table 5). RQD is distinctly lower in the lithophysae-bearing zones than in the nonlithophysal intervals that over- and underlie the two major lithophysal portions of the Topopah Spring Tuff. The crystal-poor lower lithophysal zone of the Topopah Spring exhibits markedly lower RQD values (virtually all indicate "very poor" ground conditions) compared with the aggregated "upper" lithophysal intervals. The highest RQD values measured in the Paintbrush Group tuffs are associated with the PTn nonwelded interval from 240 to 325 ft (73–99 m), the lower crystal-rich nonlithophysal zone of the Topopah Spring (370–440 ft, 110–135 m), and the moderately and nonwelded portions of the crystal-poor vitric zone of the Topopah (1300–1410 ft, 396–430 m). High RQD values continue below the Topopah Spring Tuff into underlying upper Calico Hills Formation from 1410 to 1540 ft (430–469 m). Thick intervals of "good" to "excellent" rock are present at several locations within the Prow Pass Tuff as well. The lowest RQD values in the Prow Pass units are associated with the upper part of the welded subzone of ash-flow unit 3.

Measured Lithophysal Cavity Information

Quantitative information regarding the abundance of lithophysal *cavities* (as distinct from the abundance of lithophysae) is reported in Appendix E, table E-1. These data is also summarized graphically in figure 6. Core-recovery information from figure 4(a) is repeated in figure 6 for comparison purposes.

The data of table E-1 were obtained by comparing the surface area of the core and core-video images occupied by actual cavities with standard charts for estimating mineral percentages in thin sections (for example, Compton, 1962, p. 332–333). Lithophysal cavities larger than the core diameter, or which were sufficiently large that the core was rubblized during the drilling process *are*

not included in these estimates. Note that the down-hole video images suggest that such large lithophysal cavities may be quite abundant locally: compare for example the core recovery data or RQD data (from fig. 4) with the down-hole distribution of lithophysal cavities in figure 6. A separate graphical representation of the quantity of "lost core" and of "lost core plus rubble" (table E-1) is presented in figure 6 for comparison with the with the lithophysal cavity abundances.

Fracture Information

Fracture information has been measured during logging of the core from drill hole USW SD-12. Fractures are represented schematically on the geologic log sheets in Appendix B. This representation is qualitative; however, it does capture much of the general style of fracturing. Fracture density is shown approximately, and fracture orientations are shown with respect to the core axis (effectively vertical at SD-12). The simultaneous presentation of fracture style with the other geologic indicators allows some understanding of controls on fracture density, orientation, and mineralization. This qualitative fracture description is available for the entire drill core. More quantitative fracture information has been acquired from detailed counting and measurement of individual fractures for the upper portion of the SD-12 drill core (to a depth of 1430 ft or 435.8 m). These data have been summarized into 10-foot depth increments, and the numerical values are presented in Appendix F, table F-1.

The fracture density log shown in part (a) of figure 7 distinguishes coring- and handling-induced fractures from natural fractures. The "natural" category actually includes both natural fractures and fractures of "indeterminate" origin, per the recommendation of Deere and Deere (1989). The figure indicates that a very large portion of the total number of fractures appear to be coring induced, particularly in the upper part of the hole (above the middle nonlithophysal zone of the Topopah Spring Tuff). Part (b) of figure 7 portrays fracture orientations by 30-degree increment; a somewhat expanded frequency scale has been used to allow better visualization of the different orientation classes. The appendix contains a more detailed 10-degree categorization of fractures. Nei-

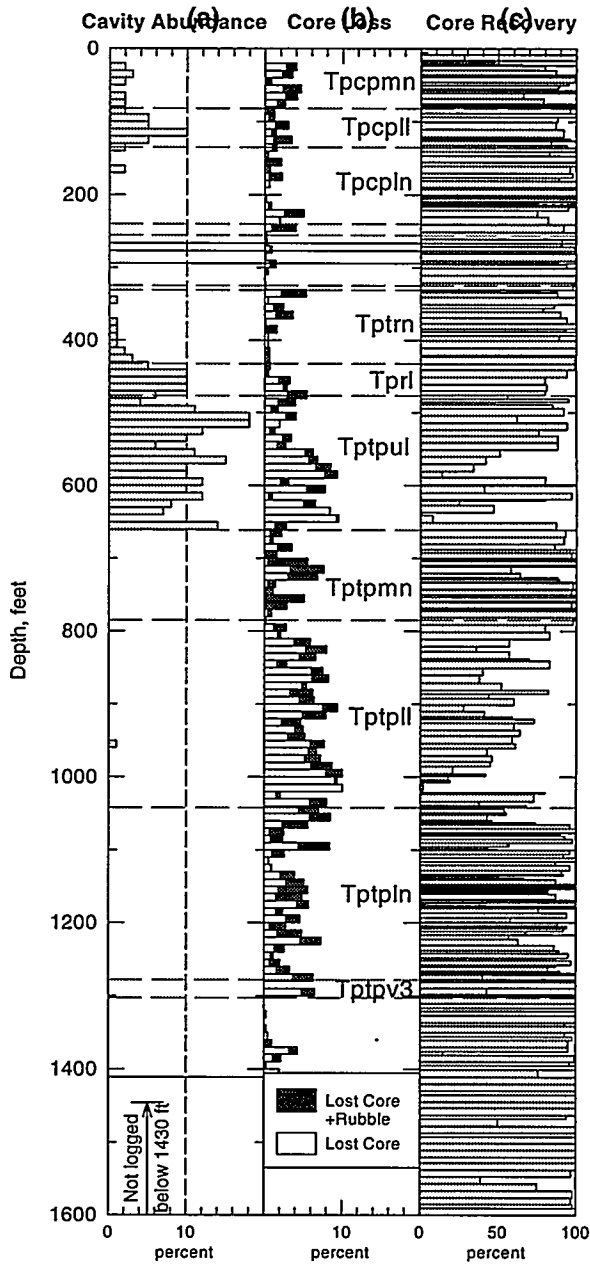


Figure 6. Graph showing (a) abundance of lithophysal cavities, (b) cumulative lengths of "lost core" and "lost core plus rubble" (table E-1), and (c) actual core recovery as a function of depth for the USW SD-12 drill hole. Selected major stratigraphic units and subdivisions of the Topopah Spring Tuff are indicated by horizontal lines (solid and dashed, respectively).

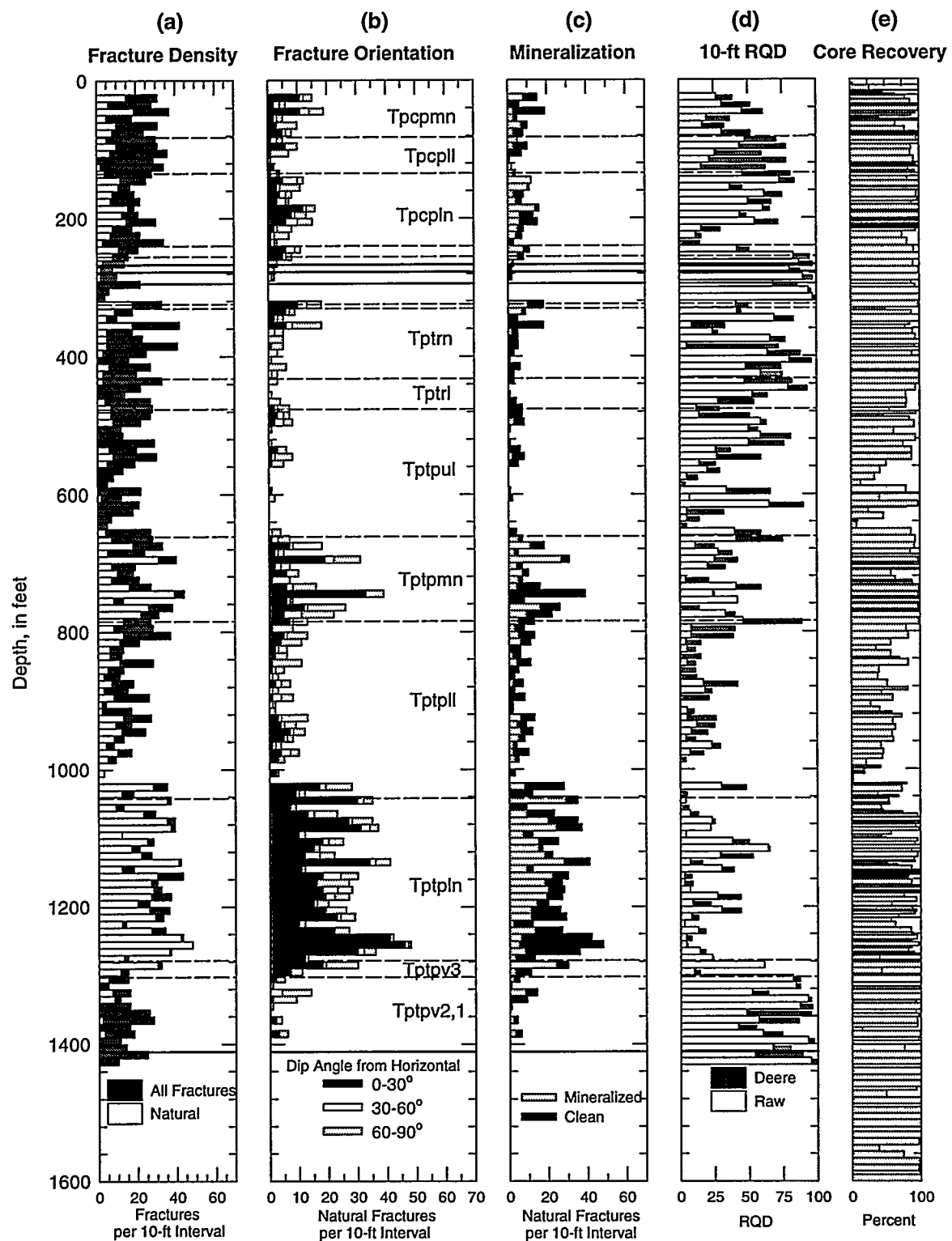


Figure 7. Graphs showing (a) measured fracture density, (b) fracture orientation, (c) mineralized fractures, (d) 10-ft video-analysis RQD, and (e) core recovery for the upper portion of the USW SD-12 drill hole. Solid horizontal lines indicate top and bottom contacts of the Tiva Canyon and Topopah Spring Tuffs and the top of the Calico Hills Formation. Dashed horizontal lines are contacts of selected Topopah Spring zonal units.

ther the fracture data nor the illustrations in this report has been corrected for the well-known effect of fracture dip on the numbers of fractures observed in a vertical borehole (Scott and others, 1983):

$$F_c = \frac{F_m}{\cos \alpha} , \quad (1)$$

where F_c is the fracture frequency corrected for fracture dip, α , and F_m is the measured fracture density. The impact of this cosine-correction factor can be relatively large in selected intervals.

Part (c) of figure 7 provides a breakdown of "clean" fractures in contrast to fractures that contain some degree of mineralization or veining (table F-1). Mineralization is common in the uppermost part of the drill hole, principally associated with the crystal-poor middle nonlithophysal and lower nonlithophysal zones of the Tiva Canyon Tuff. Mineralized fractures are distinctly fewer in the crystal-poor lower lithophysal zone of the Tiva Canyon. Mineralized fractures are relatively common in the Topopah Spring Tuff immediately below the uppermost nonwelded units at about 320 ft (100 m), and then mineralized fractures are virtually absent down to the top of the crystal-poor middle nonlithophysal zone. The crystal-poor lower nonlithophysal zone of the Topopah Spring Tuff is clearly the most extensively fractured part of this geologic unit; a large number of these fractures are mineralized, particularly above a depth of about 1200 ft (366 m).

RQD values and core recovery information are also shown in figure 7 for comparison. Rock quality and RQD values should be *inversely* related to the overall intensity of fracturing, and to a first-order approximation, RQD values are high in the less-fractured nonwelded units of the PTn between the Tiva Canyon and Topopah Spring Tuffs and in the crystal-rich nonlithophysal (Tp_{rn}) portion of the Topopah Spring, as well as in the crystal-poor vitric units of the Topopah (Tp_{tpv}) where there are few interpreted natural fractures. Conversely, RQD values are distinctly lower in the lower crystal-poor nonlithophysal part (Tp_{tpln}) of the Topopah Spring tuff where the number of natural fractures is relatively high. However, there also appear to be smaller-scale *direct* relationships between fracture

density and the RQD profiles, with lower RQD values [profile (d)] in those zones with the fewest natural fractures [profile (a)]. Compare, for example, the number of natural fractures and the RQD values in the lower parts of both the upper and lower crystal-poor lithophysal zones with the relationships exhibited by the upper parts of these same units. Examination of figure 7 [columns (a), (d) and (e)] also suggests that there is a positive correlation between core recovery and both fracture density and RQD. The cause of this correlation is that fractures cannot be physically observed and counted for core that is not recovered. Measurement of RQD is affected in a similar manner in that missing core adds zero footage to the cumulative footage of core segments greater than four inches.

Figure 8 presents the results of several different attempts to adjust the measured fracture density data for the impacts of "unobservable" core. Table E-1 contains a summary of "lost core" for each 10-foot composite interval; these values were determined through analysis of the video images of the recovered core, and thus they are not directly comparable to the core recovery data measured by drilling support staff (table C-1). Additionally, table E-1 contains the cumulative footage for each depth increment that was logged as "rubble zone".

The question of the number of actual, in-situ fractures represented by an interval of "core loss" or "rubble" is problematic. Certainly some disaggregation of rock is associated with the drilling process. However, it is possible to place some limits on the number of real fractures that may be represented by logged lost core and rubble zones using the following adjustments.

Part (a) of figure 8 presents both the number of "natural" (natural plus indeterminate) fractures logged from the core video tapes and the likely number of fractures that would have been logged had there been 100 percent core recovery. The formula for this adjustment is as follows:

$$N_{cl} = \frac{N + I}{(10 - CL)/10} , \quad (2)$$

where N_{cl} is the number of fractures per 10-ft interval adjusted for core loss, $N + I$ is the number of natural and indeterminate fractures, and CL is the

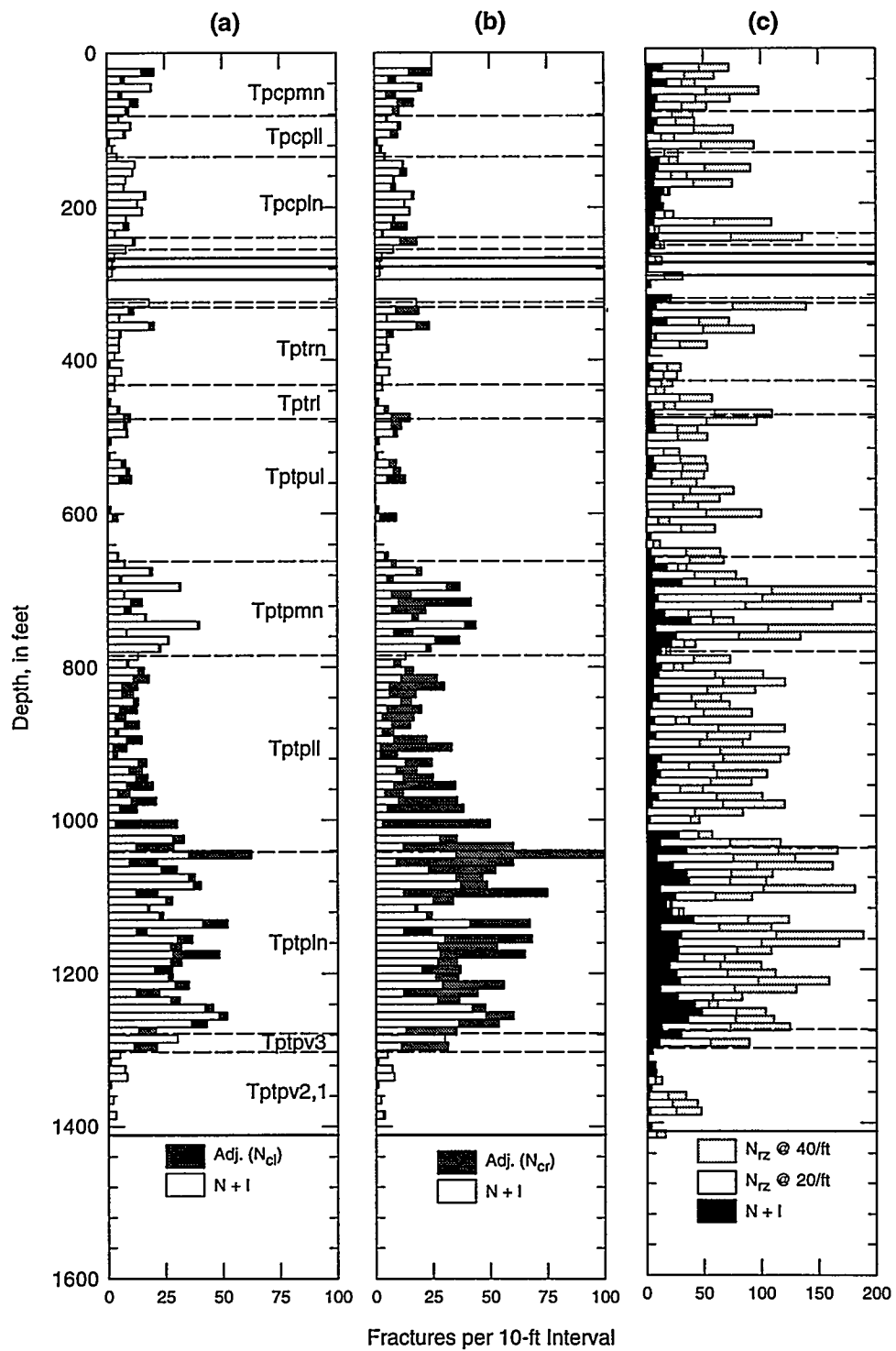


Figure 8. Graphs showing fracture density adjusted for measurement effects of lost core and rubble zones. (a) Adjusted for core recovery only. (b) Adjusted for core recovery and length of rubble zones. (c) Adjusted for core recovery and for intensity of fracturing in rubble zones. See text for method of calculation. Note expanded (2x) frequency scale in (c).

cumulative footage of lost core in the 10-ft interval.

Equation (2) adjusts only for unrecovered intervals. Part (b) of figure 8 attempts an additional first-order correction for the effect of fractures that could not be logged because the core was rubblized. This correction is:

$$N_{cr} = \frac{N + I}{(10 - (CL + RZ))/10} , \quad (3)$$

where N_{cr} is now the number of fractures adjusted for both core loss and rubble zones and RZ is the cumulative footage of those rubble zones in the relevant 10-ft depth interval.

Both equations (2) and (3) amount to an assumption that the density of fracturing present in situ for those parts of the core that were either lost or rubblized is the same as the density of fracturing present in the core that was recovered. This assumption of equal fracture densities in both lost and recovered core probably is somewhat conservative. One might anticipate lost (or rubblized) intervals to have been more densely fractured initially than material that maintained its integrity to some extent during the mechanical agitation of drilling and core retrieval.

A more hypothetical and less-conservative adjustment of the measured fracture densities has been attempted in part (c) of figure 8. For this adjustment, a rubble zone is considered to consist of an arbitrary number of fractures per foot of rubble. The total number of fractures per 10-ft depth increment is then simply the core-recovery-adjusted fracture density, N_{cl} , plus the footage of rubble times this assumed fracture density:

$$N_{rz} = N_{cl} + D_{rz} \times L_{rz} . \quad (4)$$

Here, N_{rz} is the desired total number of fractures, adjusted for rubble-zone fracture density, and D_{rz} is either 20 or 40 fractures per foot of rubble. L_{rz} is simply the cumulative length of rubble zones within the relevant computational interval. The values of 20 and 40 fractures per foot originate from the criteria that drilling support staff used to distinguish the intervals that would be classified as rubble zones. A value of 40 fractures per foot was used initially, but was reduced to 20 per foot after it became

evident that much of the rock at Yucca Mountain was highly fractured. Note that neither value for D_{rz} may be necessarily correct for any particular interval of core. Mechanical disaggregation of some otherwise-intact core is anticipated during the course of drilling. Additionally, the presence of large lithophysal cavities in parts of the welded-tuff sequences (captured in down-hole video imagery) means that some intervals of lost core may, in fact, represent actual void space in the rock; such void space is not "fractured," per se. Note, for example, the very low core recoveries indicated in figure 7(e) that correspond to virtually unfractured (natural fractures) intervals at 580–590, 640–650, and 1010–1020 ft (176.78–179.82, 195.06–198.11, and 307.83–310.88 m, respectively). Unsupported (but unfractured) rock, particularly near the upper margins of large lithophysal cavities, may be mechanically broken by pressure of the advancing drill string and dropped into the cavity to be recovered as "rubble" when the coring assembly advances to the bottom of the cavity. For intervals from which very little rubble was recovered, it may be possible to infer that actual void space constituted a major fraction of the drilled interval. Log sheets 9, 10, and 15 (Appendix B) describe the presence of large lithophysal cavities on down-hole video imagery covering these (and other) intervals.

Framework Hydrologic Properties

Laboratory Techniques

Core samples were obtained from SD-12 at approximately regular intervals for laboratory measurements of framework material properties. "Framework materials properties" are defined in Study Plan 8.3.1.4.3.1 (Rautman, 1993) as porosity, bulk and particle density, and saturated hydraulic conductivity. Water contents were also determined and used to compute approximate in-situ saturations.

Approximately 570 eight-inch long core samples were collected for hydrologic analyses on a nominal 3-foot, regular sampling interval. Each core sample was subdivided into two subsamples. A 2-inch long core fragment was placed in a metal container and sealed within minutes of core retrieval from the hole. An immediately adjacent 6-

inch subsample was preserved in a Lexan tube that was capped and sealed with duct tape. The intent was to preserve in-situ moisture contents as closely as possible, and especially to prevent dry-out of the core and subsequent changes in pore geometry caused by desiccation of clays and zeolites. Such changes have been demonstrated to affect permeability measurements irreversibly.

Porosity, bulk density, particle density, and water content were determined in the laboratory for the hermetically sealed 2-inch core fragments. Separately, a subset of the 6-inch core samples were subcored to produce specimens suitable for measurement of saturated hydraulic conductivity. Core plugs were trimmed using a small diamond saw to approximate right-circular cylinders approximately 2.5 cm in diameter and 3–10 cm long prior to testing. Porosity, bulk density, and particle density were also measured for these prepared specimens.

Water content was determined by gravimetry and is reported as volumetric water content in cubic centimeters per cubic centimeter. Porosity (ϕ , in cubic centimeters per cubic centimeter and expressed as a decimal fraction for simplicity), bulk density (ρ_b , in grams per cubic centimeter), and particle density (ρ_p , in grams per cubic centimeter) were determined using gravimetry and Archimedes' principle to determine sample volume. There were two departures from the classical application of this technique. First, the samples were initially saturated with carbon dioxide gas by introducing the gas into an evacuated bell jar containing the samples; this process, repeated three times, prevents air entrapment in small internal pores within the low-permeability, densely welded tuff samples because the CO_2 is water-soluble. The samples were then saturated with degassed distilled water under a vacuum. Scoping studies have indicated that saturated weights did not change meaningfully following a single iteration of this vacuum-saturation process, even with the addition of a pressure-saturation step. Second, the samples were dried in a relative-humidity (RH)-controlled oven at 60°C and 65-percent RH (following concepts of Bush and Jenkins, 1970), rather than at 105°C and associated ambient RH. Soeder and others (1991) advocated the use of a lower-temperature, humidified technique, not only to preserve

water present in the crystal structure of any clays or hydrated minerals (such as zeolites), but also to retain water loosely bound to grain surfaces which is otherwise unavailable for unsaturated flow. The selected RH of 65 percent translates to an estimated residual-saturation pressure for Yucca Mountain samples of approximately –700 bars (L.E. Flint, U.S. Geological Survey, written communication, 1996).

Particle density, as used in this report, is similar to the more commonly reported grain density. However, because particle density is a property computationally derived from intact core samples, totally encapsulated void space (which thus is inaccessible to water flow) is not considered. Particle density is almost invariably lower than a grain density determination obtained by crushing the rock and measuring the change in total volume. Particle density will approach grain density for rocks that have little totally encapsulated pore space. Bulk-property measurements were repeated after more conventional sample drying at 105°C to allow for comparison with other reported data (ASTM, 1994). Sample weights (masses) were reduced to the desired bulk properties as follows:

$$\rho_b = \frac{\text{dry weight}}{\text{bulk volume}} , \quad (5)$$

$$\phi = \frac{\text{pore volume}}{\text{bulk volume}} , \text{ and} \quad (6)$$

$$\rho_p = \frac{\text{dry weight}}{\text{bulk volume} - \text{pore volume}} , \text{ where} \quad (7)$$

pore volume =

$$\frac{(\text{saturated weight} - \text{dry weight})}{\rho_w} , \text{ and} \quad (8)$$

ρ_w is the temperature-adjusted density of water (in grams per cubic centimeter). Bulk volume is simply the mass of the fully saturated sample submerged in water (by Archimedes' principle). "Dry" weight is the weight (mass) of the sample for either the RH- or 105°C -dried samples. Volumetric water content (VWC) is determined as:

VWC =

$$\left(\frac{\text{saturated weight} - \text{dry weight}}{\text{dry weight}} \right) \cdot \rho_b . \quad (9)$$

Saturated hydraulic conductivity, K_s , in meters per second and usually presented as $\log_{10} K_s$ throughout this report, was measured using a constant-head method. The core plugs were saturated with tap water using the vacuum evacuation/CO₂ flooding technique. Each sample was encased in heavy vinyl tubing and placed in a chamber (Hassler permeameter) that produced a hydraulic confining pressure (~0.41–0.55 MPa), slightly exceeding the gradient across the sample, to prevent escape flow around the sides of the sample. Confining pressures of this magnitude do not affect the permeability of the rock, especially since welded samples have compressive strengths on the order of 100 MPa (Nimick and Schwartz, 1987). A separate system provided J-13 tap water under pressure for flow through the sample. Effluent was weighed on a top-loading balance and the mass was recorded as a function of time as the water left the sample. Saturated hydraulic conductivity was computed from Darcy's law:

$$K_s = \frac{Q}{A} \cdot \frac{L}{\Delta H} \quad (10)$$

where Q is the quantity of water flowing through the sample (cm³/sec), A is the cross-sectional area of the sample core plug (cm²), ΔH is the change in total head (cm) across the sample, and L is the length (cm) of the core plug. Note that K_s has been converted to units of meters per second in all tables and figures in this report.

Material-Properties Data

The results of the laboratory materials properties determinations are presented in Appendix G. Table G-1 contains bulk properties (porosity, bulk density, particle density) and initial water contents for both relative-humidity oven-dried and 105°C-dried samples. Saturated hydraulic conductivity measurements are presented in table G-2. Separate porosity measurements were also obtained from the permeability plug samples. These data are given in the table of conductivity values.

Data from table G-1 are presented graphically in log format in figure 9. The figure includes both the relative-humidity and 105°C data, which are represented by different symbols. Note that the two values for each sample are essentially identical

throughout most of the upper portion of the SD-12 drill hole. Major differences in the properties measured by these two techniques generally occur only in the presence of hydrated minerals, such as clays and particularly, at Yucca Mountain, zeolites. Generally, the picture that emerges from the materials-properties data is reflective of the thermal/mechanical units identified in table 4. The saturated hydraulic conductivity data from table G-2 are presented in graphical format in figure 11, together with the corresponding porosity measurements from these subcored sample plugs. Porosity and bulk density values from table G-1 are also illustrated on the log sheets of Appendix B, as are values for approximate in-situ saturations.

The major lithologic subdivisions of the rock column penetrated by drill hole USW SD-12 can be identified in the materials-property profiles shown in figure 9. This is particularly true for the thermal/mechanical stratigraphic units, which were effectively defined on the basis of material properties by Ortiz and others (1985). The welded portion of Tiva Canyon Tuff (thermal/mechanical unit TCw) is represented by measured porosity values of approximately 0.10, down to a depth of 240.1 ft (73.2 m). Below this depth, porosity values increase progressively through the lower vitric zone of the Tiva Canyon Tuff (the shandy base interval of Istok and others, 1994), and they remain high (0.30–0.60) through the interval comprising the base of the Tiva Canyon Tuff, the Pah Canyon Tuff (and associated bedded tuffs), and the nonwelded and moderately welded subzones of the upper, crystal-rich vitric zone of the Topopah Spring Tuff. The bottom of this latter subzone is at 324.6 ft (98.9 m). This mostly nonwelded interval constitutes the PTn thermal/mechanical unit. Welded materials with moderately high porosities of around 0.15 are characteristic of the more intensely vapor-phase-altered, crystal-rich nonlithophysal and upper lithophysal zones (TSw1). Porosities generally less than 0.10–0.12 form the bulk of the remainder of the Topopah Spring Tuff (TSw2), extending through the base of the "basal" vitrophyre (densely welded) subzone of the crystal-poor lower vitric zone (Tptpv3) at 1302.4 ft (379.0 m) (TSw3).

A few of the internal zones of the Topopah Spring Tuff can be identified within the thick welded portion of this unit. Notably, the thin caprock vitrophyre (densely welded subzone) of the upper vitric zone (Tpdrv1 is easily identifiable at a depth of approximately 325 ft (99 m) by its particularly low porosity values (0.05 or less) and equivalent high bulk density values. The much thicker lower vitrophyre subzone of the lower vitric zone (Tpdrv3) is also easily identified as the 25-foot (7.6 m) interval ending at around 1300 ft (396 m) of uniformly low (less than 0.05) porosity values. The prominent high porosity-low bulk density spike at 1284.9 ft (391.62 m) within the lower vitrophyre subzone accompanied by marked separation of the relative-humidity and 105°C values is attributed to the inclusion of a presumably argillized (possibly zeolitized) fracture coating in this one sample (L.E. Flint, U.S. Geological Survey, personal communication, 1996). The geologic log for this interval notes the presence of argillic alteration along fractures in the immediately overlying and underlying units. Note also that the basal vitrophyre subzone also exhibits uniform and distinctly lower values of particle density. A suggestion of lower particle densities is associated with the caprock vitrophyre as well.

The lowermost portion of the Topopah Spring Tuff exhibits a progressive increase in porosity underlain by a largely nonwelded interval of nearly 30-percent porosity (0.30) that extends to approximately 1330 ft (405 m). The two porosity values (RH- and 105°C-dried) begin to diverge markedly at approximately 1380 ft (420 m), representing the presence of zeolitized materials in the underlying Calico Hills Formation (thermal/mechanical unit CHn). The dichotomy between relative-humidity dried samples and their 105°C counterparts is particularly well displayed by the particle density data (center profile in fig. 9). The base of the Calico Hills Formation occurs at 1648.4 ft (502.41 m), although the most prominent change in porosity is associated with the top of the bedded tuff and basal tuffaceous sandstone units of the Calico Hills at 1611.6 ft (491.2 m). The remainder of the hole consists principally of ash-flow units within the Prow Pass Tuff. These units are generally zeolitized, as indicated by the separation of the relative-humidity and 105°C data, with the exception of an

interval from approximately 1680–1800 ft (512–549 m). This interval corresponds approximately to welded subzone (thermal/mechanical unit PPw) of ash-flow unit 3 (Tcp3), from 1656.6 to about 1790 ft (504.91–546 m). The geologic description of this interval notes the presence of vapor-phase mineralization and slight welding. The classic \subset -shaped porosity profile of a welded tuff is not associated with this welded subzone. Rather, porosity increases steadily upward through the welded subzone of ash-flow unit 3 from about 1830 ft to a maximum value near 1700 ft (557.8–518.1 m). Examination of geologic log sheets 25–27 suggests that this prominent trend in porosity can be related directly to the intensity of vapor-phase alteration associated with the weak to moderate welding in ash-flow unit 3. Marked separation of the RH and 105°C data in Prow Pass ash-flow unit 2 and below indicate intense zeolitization in this lowest part of the USW SD-12 drill hole. This latter interval plus the nonwelded subzone of ash-flow unit 3, below about 1830 ft (557.8 m), constitutes the upper part of thermal/mechanical unit CFUn.

Saturation and initial water content data are also presented in figure 9. Volumetric water contents (right-hand column) invariable are higher in the nonwelded intervals above about 325 ft (100 m) and below 1500 ft (460 m). There is simply more void space in these materials to contain moisture. Note that a non-negligible fraction of the total water content of the zeolitic samples, those obtained from 1600 to 1650 ft (490–500 m) and below about 1875 ft (570 m), consists of weakly molecular-bound water that is driven off with heating above 105°C.

Saturations are generally high throughout the welded Tiva Canyon Tuff interval. Saturations continue to increase through the progressively less welded, upper part of the “shady base” interval of the crystal-poor vitric zone, and measured values effectively reach 90 percent and greater (table G-1) at the point where the shady base becomes non-welded (approximately 245–255 ft, 75–78 m). This near-saturated condition within what is otherwise a continuously permeable, high porosity horizon may indicate that a capillary barrier can exist at this stratigraphic level, caused by the increase in pore size caused by jointly changing degree of welding

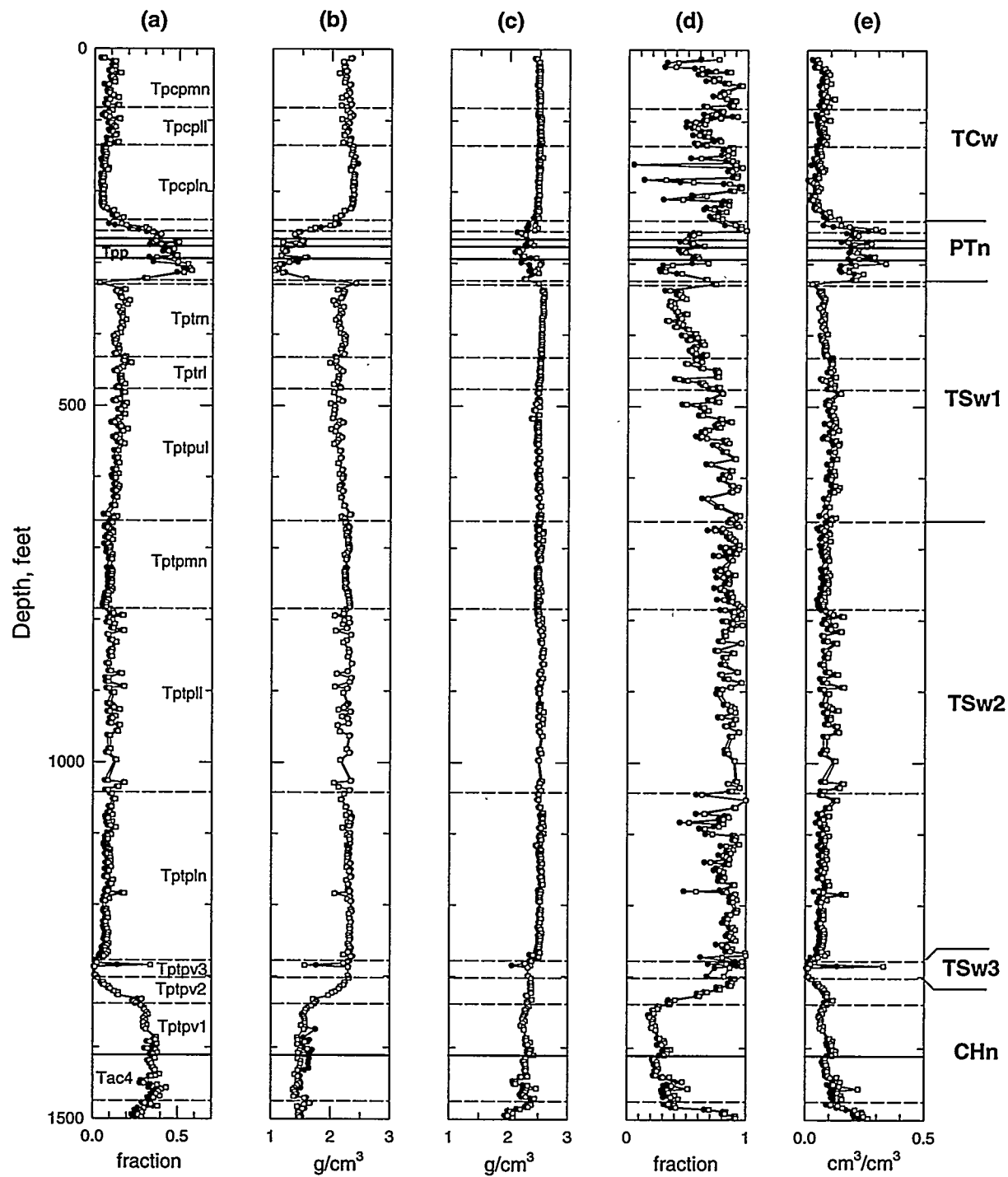


Figure 9. (a) Porosity, (b) bulk density, (c) particle density, (d) saturation, and (e) water-content profiles of core samples collected from the upper part of the USW SD-12 drill core. Solid circles—relative-humidity oven-dried samples; open squares—105°C-dried samples. Solid horizontal lines indicate top and bottom contacts of the Tiva Canyon and Topopah Spring Tuffs, and the Calico Hills Formation. Dashed horizontal lines are contacts of Topopah Spring zonal units.

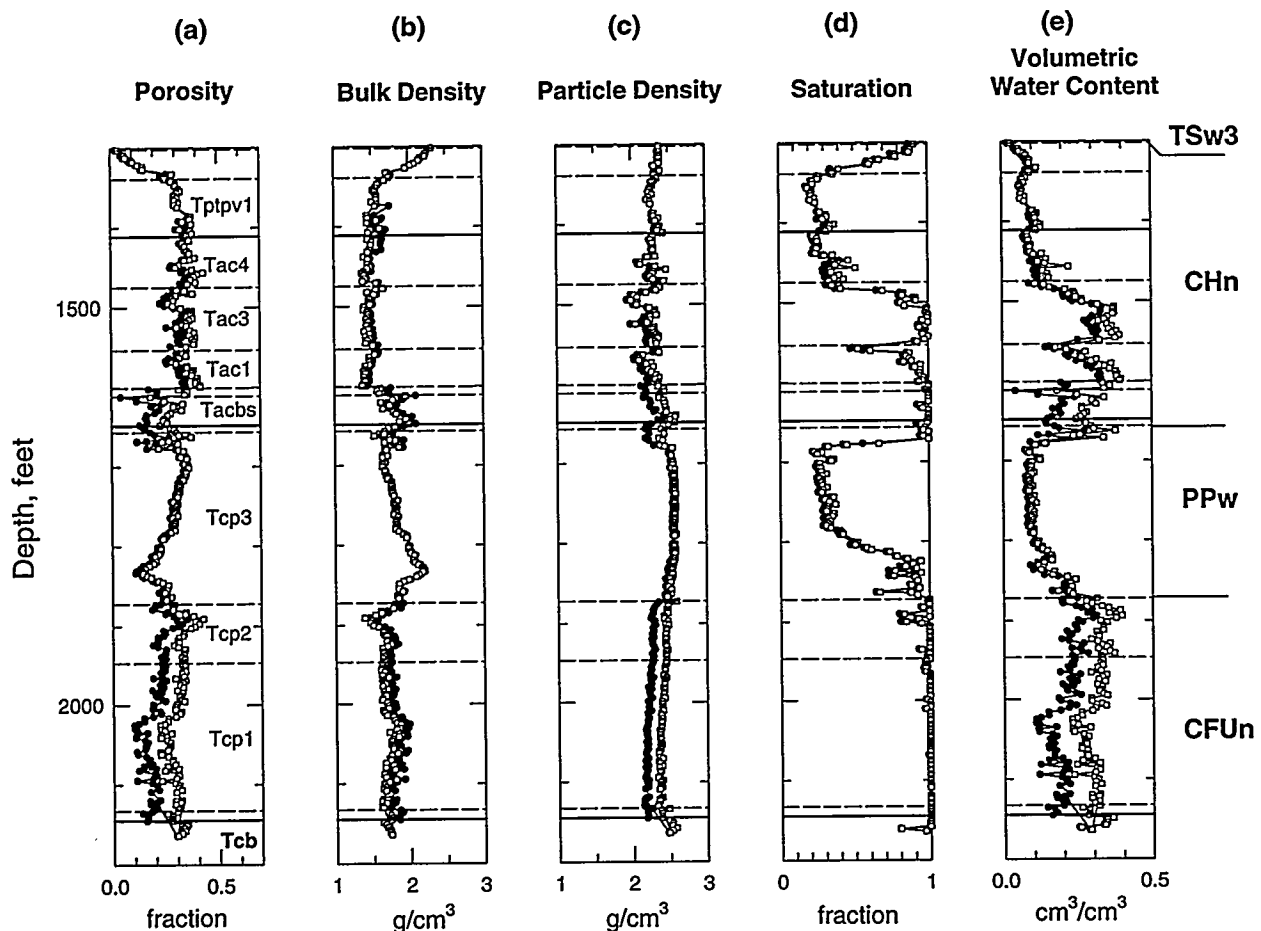


Figure 10. (a) Porosity, (b) bulk density, (c) particle density, (d) saturation, and (e) water-content profiles of core samples collected from the lower part of the USW SD-12 drill core. Solid circles—relative-humidity oven-dried samples; open squares—105°C-dried samples. Solid horizontal lines indicate top and bottom contacts of the Topopah Spring Tuffs, the Calico Hills Formation and the Prow Pass Tuff. Dashed horizontal lines are contacts of selected zonal units.

(compaction), devitrification, and vapor-phase alteration (see log sheet 4, Appendix B). A water-filled fracture was encountered in the core at 251.0 to 253.0 ft (76.5–77.1 m) in core run number 62. Saturations below 255 ft (78 m) drop immediately to approximately 40–60 percent and remain at this level through the remainder of the nonwelded PTn interval.

Saturations within the welded Topopah Spring Tuff generally increase down hole. Exceptions to this general trend can be related directly to the abrupt decrease in porosity associated with the caprock vitrophyre of the Topopah Spring Tuff at approximately 325 ft (99 m). Saturations exceed 90

percent at a number of depths beginning at slightly more than 570 ft (173 m), including a notable cluster of values immediately above and below the lower contact of the crystal-poor middle nonlithophysal zone. The cause of numerous mostly single-point low-saturation measurements closely associated spatially with the crystal-poor lower nonlithophysal zone is uncertain; however the general trend is for increasing saturations within this latter unit by itself.

Core saturations decrease progressively in samples taken from below the lower vitrophyre subzone, and they reach values as low as 20 percent in the lowermost nonwelded part of the

Topopah Spring and ash-flow unit 4 of the Calico Hills Formation. Saturation increase markedly immediately above a depth of 1500 ft (about 450 m), and the first indications of "damp" core are noted on the geologic log at a depth of 1488 ft (343.5 m). Core samples are nearly fully saturated below this depth, with the exception of an interval at 1550–1575 ft (472.4–480.0 m) directly associated with the upper contact of Calico Hills ash-flow unit 2.

At a depth of about 1675 ft (510 m), the saturation profile reverses with a sharp decrease in saturations to 20–25 percent; this relatively dry interval extends to approximately 1830 ft (558 m) and it corresponds almost exactly with the welded sub-zone of Prow Pass ash-flow unit 3. Saturations return to values of one (plus or minus small sample-handling and measurement errors) below a depth of about 1870 ft (570 m). Standing water was observed in the hole following the overnight shutdown on August 7–8 at a depth of 1897.7 ft (576.3 m). The regional water table rose to a depth of 1948 ft (593.7 m) on August 11, 1995 once water-bearing fractures were encountered at a depth of 2010.6 ft (612.8 m).

Samples for saturated hydraulic conductivity measurements were not selected systematically from the SD-12 core, as were the samples for measurement of the bulk properties. This decision was a matter of pragmatism related to the facts that (a) the permeability of densely welded samples of the Tiva Canyon and Topopah Spring Tuffs is very low to begin with, thus limiting interest in these relatively impermeable rocks, and (b) resources available to perform the laboratory measurement of these low permeability—and thus time-consuming—samples simply were not available. Engstrom and Rautman (1996) have presented more comprehensive saturated hydraulic conductivity data for the Tiva Canyon and Topopah Spring welded units from drill hole USW SD-9.

The available saturated hydraulic conductivity data from SD-12 (table G-2) are presented in figure 11. High hydraulic conductivity values are associated with the nonwelded tuffs and reworked materials between the welded phases of the Tiva Canyon and Topopah Spring Tuffs; these values

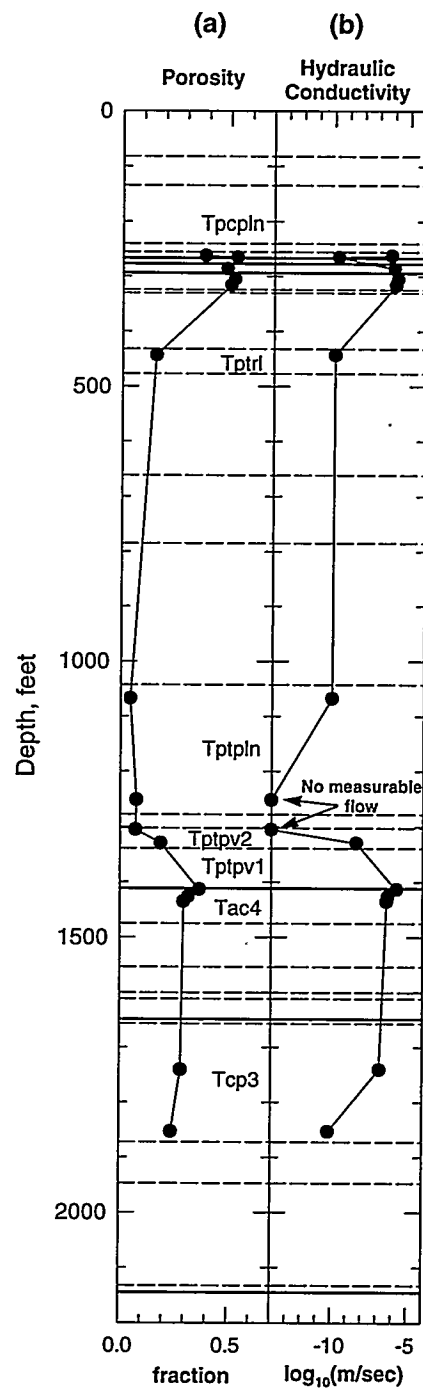


Figure 11. (a) Porosity and (b) saturated hydraulic conductivity profiles of core samples collected from the USW SD-12 drill core.

may be as high as 10^{-6} meters per second. Two of the three samples selected from the main, welded portion of the Topopah Spring Tuff exhibit fairly low conductivities of 10^{-10} m/sec. No measurable flow was obtained for the lowest of the three sam-

ples (from the Tptpln unit), and measurable flow was not observed for a similar sample selected from the gradationally less welded lower part of the Topopah Spring below the lower vitrophyre. Samples selected from lower in the basal vitric zone of the Topopah Spring and from the upper part of the Calico Hills Formation exhibited higher K_s values (10^{-7} – 10^{-6} m/sec), as expected for relatively nonwelded materials. The two samples that were selected from Prow Pass ash-flow unit 3 exhibit markedly different hydraulic conductivities. Interestingly, the higher of these two K_s values, that from a depth of about 1740 ft (530 m) is from just below the most densely welded part of this ash-flow tuff, whereas the deeper value (1853 ft; 564.8 m) is from the essentially nonwelded part of the same unit. The explanation for this counter-intuitive permeability behavior is that the lower, less conductive sample has been zeolitized, whereas the higher, more conductive sample is intensely vapor-phase altered in addition simply to being welded. The changes to the pore throats that result from zeolitization can create hydraulic conductivity values as low as those associated with the very densely welded parts of the Topopah Spring Tuff (see also fig. 10 of Engstrom and Rautman, 1996).

Geophysical Log Data

Down-hole geophysical logging runs were conducted by Schlumberger Well Services on three separate occasions beginning July 12, 1994; January 12, 1995; and September 7, 1995. The complete, composite suite of acquired logs consists of a bulk density log, an epithermal neutron log, two induction-conductivity logs (medium and deep) from which resistivity logs were computed, a spectral gamma-ray log (K, U, Th, plus total γ , and a set of 4-arm caliper traces. The composite set of logs extends from near the ground surface to a depth of approximately 1950 ft (600 m). This logged interval comprises rock units from the crystal-poor middle nonlithophysal unit of the Tiva Canyon Tuff through ash-flow unit 2 of the Prow Pass Tuff. The lowermost 200 ft (60 m) of the hole was not logged because of mechanical restrictions. Selected log traces are presented in figure 12.

Density Log Response

The bulk density log [fig. 12(a)] displays the expected geophysical trace reactions to welding and lithophysae development. Petrophysical bulk densities typically are greater than about 2.0 g/cm³ in welded tuffs and less than about 1.8 g/cm³ in nonwelded units. Note that the highest observed bulk density values are present in the crystal-poor lower nonlithophysal (Tp_pln) zones of both the Tiva Canyon and Topopah Spring Tuffs, and that densities are generally lower at higher stratigraphic levels within each ash-flow sheet. This progressive increase in density with stratigraphic depth probably reflects both increased welding and compaction at lower levels and an increase in secondary vapor-phase alteration higher in the section. Large positive density-correction factors [dotted curve in fig. 12(a)] appear to reflect washed-out intervals indicated by the 4-arm caliper survey [fig. 12(e)]. Wash-outs affect principally the highly fractured welded tuffs and they are particularly severe in the lithophysal zones. The nonwelded PTn thermal/mechanical unit is also severely washed out in the lower part of this generally unconsolidated interval.

Lithophysal intervals in both the Tiva Canyon and Topopah Spring logically exhibit lower bulk densities than do nonlithophysal intervals that lack the macroporosity of lithophysal cavities. Bulk density values approach near-nonwelded values of 1.8 g/cm³ in the upper lithophysal zones (Tp_{tr} and Tp_{pul}) of the Topopah Spring Tuff. This observation is interpreted to indicate that the fraction of lithophysal void space is markedly higher in these zones than in the crystal-poor lower lithophysal zone; density values in the Tptpl unit generally are higher than 2.0 g/cm³.

There is a relatively prominent density low within the crystal-poor middle nonlithophysal zone of the Topopah Spring Tuff at approximately 705 to 720 ft (214.9–219.4 m). This density low may indicate the “lithophysae-bearing subzone,” a feature for which there is only indirect evidence in the geologic log (log sheet 11 of Appendix B). This interval is a zone of decreased core recovery and extensive broken core (log sheet 11), and the geologic log does note the existence of large voids of

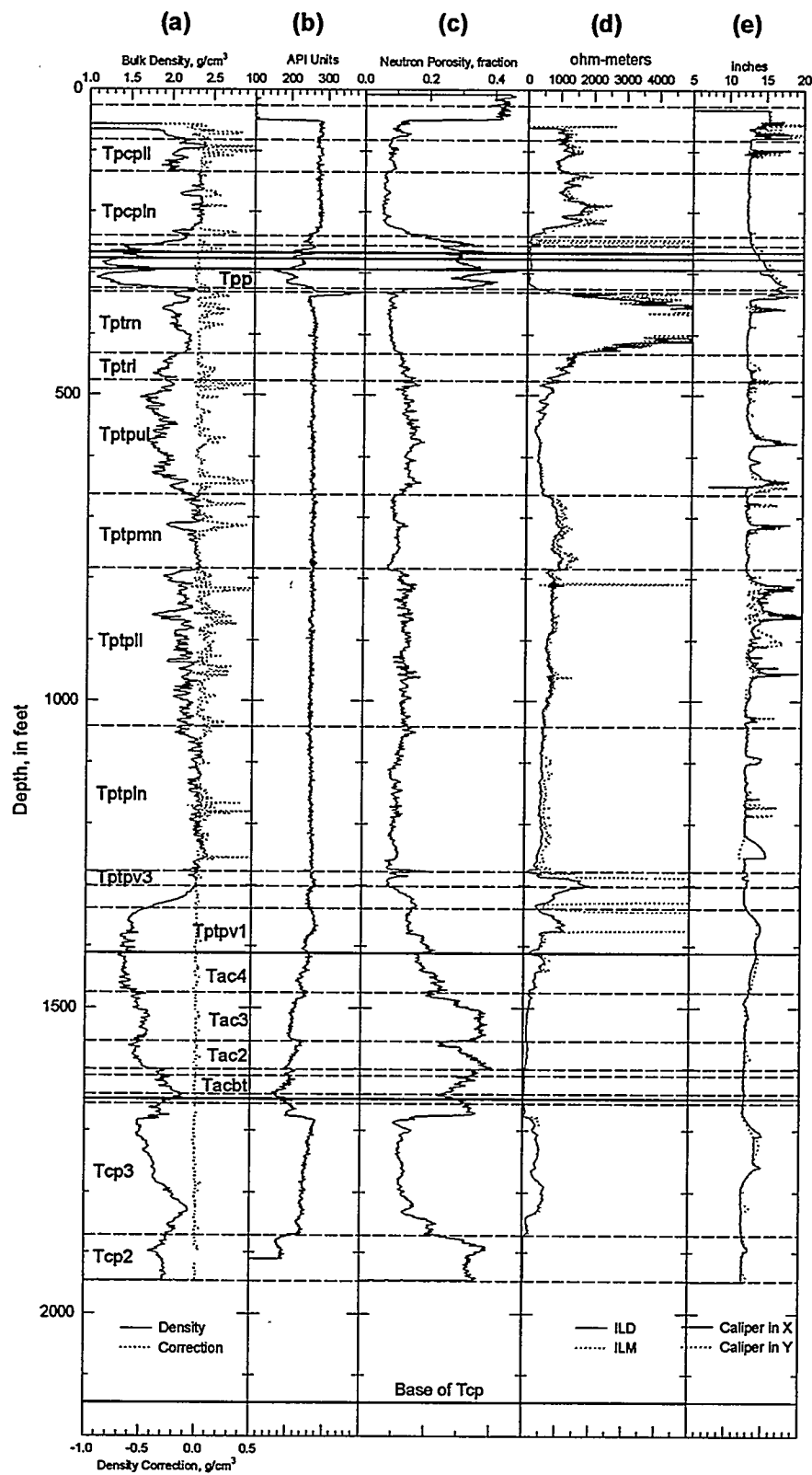


Figure 12. Geophysical log traces from the USW SD-12 drill hole: (a) density log; (b) gamma-ray log; (c) epithermal neutron porosity log; (d) induction log; and (e) caliper log.

indeterminate origin in the down-hole video from 709.6 to 723.8 ft (216.3–220.6 m).

The 10- to 15-foot (3–5 m) mismatch of the lower contact of the Topopah Spring crystal-poor lithophysal zone and the relatively abrupt change in average bulk density level is interesting in light of other information available on the detailed geologic logs of Appendix B (log sheets 15 and 16). The geophysical log of figure 12(a) suggests that lithophysal cavity development extends to a depth closer to 1060 ft (323.1 m) than the indicated contact in Appendix B of 1042.2 ft (317.6 m). The 1060-foot depth corresponds more closely to the marked increase in general core recovery indicated on log sheet 16. The geologic-log contact was selected largely on the basis of the change in alteration of the groundmass and the fact that small- to medium-sized lithophysae are markedly less common below roughly 1042 ft. The geologic log does suggest that there is some uncertainty regarding the exact definition of the lower lithophysal zone in this interval.

The gradational transition from welded to non-welded tuff at the base of both the Tiva Canyon and Topopah Spring Tuffs is strongly reflected by the transitional bulk density traces in these intervals. This transition compares well with the progressive increase in porosity observed in laboratory measurements from core samples in these intervals [compare to fig. 9(a)].

The individual ash-flow units of the Calico Hills Formation are relatively identifiable in the petrophysical bulk density traces of figure 12(a). Density generally increases with depth through the formation, and the “bedded tuff” intervals present at the base of ash-flow unit 4 and at the top of ash-flow unit 1 are marked by thin intervals of distinctly higher density. Similar high-density spikes also mark the bedded tuffs between the Tiva Canyon and the Topopah Spring Tuffs.

The density response of the tuffs of the Prow Pass Tuff is somewhat more complex. The prominent decrease in density at about 1680 ft (510 m) appears to be associated with the onset of vapor-phase alteration below this approximate depth in the core. Density continues to increase through the

moderately welded portion of ash-flow unit 3. However, density continues to increase below the lower limit of the welded subzone, and the density trace reaches a maximum of nearly 2.2 g/cm^3 at a depth of about 1830 ft (558 m), well within the nonwelded subzone of ash-flow unit 3. This depth is also associated with the presence of zeolitic alteration as stabilization of former volcanic glass by vapor-phase alteration dies out downward.

Gamma-Ray Log Response

The gamma-ray logging tool responds principally to radioactive potassium (^{40}K) in the whole rock; the total-gamma trace is presented in column (b) of figure 12. The gamma-ray log is essentially flat throughout the welded intervals of both the Tiva Canyon and Topopah Spring Tuffs. Total gamma values (API units) are markedly lower in the several “bedded tuff” intervals that are present between about 260 and 300 ft (60–91 m). These decreased gamma counts may reflect weathering and leaching of potassium from feldspar phenocrysts in these intervals. Iron-staining and probable paleosols are described from this interval in the geologic logs (sheets 4–5) of Appendix B.

The gamma-ray log response within the Calico Hills Formation and the Prow Pass Tuff consists of a repetitive sequence of increasing-upward profiles, each roughly corresponding to the individual ash-flow units described from the core. A genetic interpretation of these prominent features of the total-gamma trace is not immediately apparent. The lowest observed gamma count in this general interval is associated with the basal sandstone unit of the Calico Hills Formation. This low-count interval presumably is related to leaching of radioactive potassium-40 (and nonradioactive potassium as well) from the weathered and argillized reworked sediments of this geologic unit.

Epithermal Neutron Porosity Log Response

The neutron-porosity log responds principally to the presence of water (hydrogen atoms) in the rock. Higher “porosity” values indicate greater absorption of neutrons by moisture. This log trace [fig. 12(c)] indicates very high values (> 0.40) down to a depth of approximately 50 ft (15.25 m), suggesting that water contents are quite high in this

portion of the near-surface tuff environment. The neutron log response drops markedly at 50 ft, and the values of 0.05–0.12 encountered below this depth are roughly typical of the neutron porosity throughout the remainder of the welded section in both the Tiva Canyon and the Topopah Spring Tuffs. The crystal-poor lower lithophysal zone of the Tiva Canyon exhibits somewhat higher neutron porosity values than the lower nonlithophysal zone. This correlation with the presence of significant lithophysal-style alteration appears general throughout the drill hole, and it may be related to increased total porosity caused by spatially associated vapor-phase alteration of the groundmass.

Epithermal neutron porosity values increase markedly and progressively near the base of the Tiva Canyon Tuff corresponding the progressive decrease in welding observed in the “shady base” interval of the crystal-poor vitric zone. Neutron porosities generally exceed 20 to 30 percent (0.20–0.30 throughout the nonwelded PTn thermal/mechanical unit interval from 240 to 325 ft (73–99 m). Volumetric water contents measured on core samples (fig. 9) through this PTn interval are quite high, and saturations in parts of this nonwelded zone are near 100 percent.

The neutron porosity trace exhibits a very rapid decrease to values of approximately 0.10 directly associated with the densely welded and fused caprock vitrophyre (unit Tptrv1) of the crystal-rich vitric zone of the Topopah Spring Tuff. Neutron porosity values are distinctly higher (0.10–0.15) in the two “upper” lithophysal zones (Tptrl and Tptpul) and in the crystal-poor lower lithophysal zone. These same values are typically less than 0.10 in the three nonlithophysal intervals of the Topopah Spring Tuff.

As described in the latter part of the section entitled “Density Log Response” on page 33, there is evidence in the neutron-porosity log response that the crystal-poor lower lithophysal zone extends to depths of at least 1060 ft and perhaps to nearly 1100 ft (323–335 m). Geologic log sheet 16 (Appendix B) indicates that the intensity of vapor-phase alteration decreases noticeably at a depth of 1103.0 ft (336.2 m). A similar decrease in logged vapor-phase alteration from about 662 ft to about

800 ft (202–244 m) is associated spatially with the lower neutron porosity values of the crystal-poor middle nonlithophysal zone. This spatial association suggests that secondary porosity induced by this style of alteration may be important in holding moisture within welded devitrified sequences, such as the main phase of the Topopah Spring Tuff.

Neutron porosity values increase sharply near the contact of the devitrified Topopah Spring Tuff with the lower vitrophyre subzone. The geologic log (sheet 19, Appendix B) indicates argillic alteration at this depth. More generally, Buesch and others (1996) have described argillically altered pumice clasts from the base of the crystal-poor nonlithophysal zone. Clay minerals may contain significant quantities of bound water (water within the mineral structure itself), and the neutron response at this depth may be reflecting such structural water.

Water contents (as indicated by the neutron porosity trace) increase progressively below the lower vitrophyre subzone as the degree of welding decreases progressively to nonwelded at the base of the Topopah Spring Tuff. Neutron porosity values generally exceed 0.20 throughout the tuffs and reworked materials of the Calico Hills Formation with the exception of ash-flow unit 4. Each ash-flow with the exception of unit 1 is characterized by lower neutron porosity values at the top underlain by progressively increasing values toward the bottom. The Calico Hills bedded tuff unit and the basal sandstone units exhibit decreased neutron porosity values.

Within the Prow Pass Tuff, the epithermal neutron log indicates high bound-water contents associated with zeolitization above roughly 1680 ft (510 m) and below 1830 ft (560 m). The presence of structurally bound water contained in zeolite minerals is also indicated by separation of the RH-oven and 105°C-oven-dried laboratory property measurements shown in figure 9. The intervening interval corresponds approximately to the welded subzone of Prow Pass ash-flow unit 3. The neutron log near the bottom of the logged interval returns to very high values associated with zeolitization of ash-flow unit 4.

Induction Log Response

The log traces shown in figure 12(d) represent the apparent resistivity of the rocks surrounding the bore hole, and they are computed from data obtained by a induction-conductivity tool. Both the induction log-deep (ILD) and -medium (ILM) traces are portrayed on the figure.

Resistivity values are moderately high and quite variable within the near-surface welded portion of the Tiva Canyon Tuff. There is some correlation of the prominent resistivity low (~1000 $\Omega\text{-m}$) from about 100 to 134.6 ft (30–41 m) with the most crowded and open lithophysae of the crystal-poor lower lithophysal zone; another resistivity low is present at about 160 ft (50 m) that corresponds approximately to an interval of moderately spaced lithophysae within the crystal-poor lower nonlithophysal zone shown on geologic log sheet 3 (Appendix B).

Resistivity values decrease concomitantly with the increase in porosity (fig. 9) and the decrease in the bulk density log [fig. 12(a)] associated with the progressive decrease in welding at the base of the Tiva Canyon Tuff. Resistivity values remain very low throughout the nonwelded interval between the Tiva Canyon and the Topopah Spring Tuffs. A notable exception to this last statement is observed within the shandy base interval of the crystal-poor vitric zone immediately below 250 ft (75 m). At this depth, the induction log-medium trace (dashed) goes off-scale to extremely high resistivity values, whereas the induction log-deep trace (solid) appears relatively unaffected. The cause of this resistivity anomaly is unclear, although the geologic log (log sheet 4, Appendix B) does make reference to fracturing at these depths.

The Topopah Spring Tuff is characterized by very high resistivity values (some exceeding 10,000–15,000 $\Omega\text{-m}$) in the upper portion (crystal-rich nonlithophysal zone), that decrease with depth to values slightly lower (generally $< 1000 \Omega\text{-m}$) than those observed from the welded portion of the Tiva Canyon Tuff. Most of the major zones of the Topopah Spring Tuff below the crystal-rich lithophysal zone are identifiable in the resistivity traces, although whether the crystal-poor middle nonlitho-

physal and lower lithophysal zones could be distinguished solely on the basis of the resistivity log is uncertain. Resistivity values exhibit a marked increase within the lower vitrophyre of the crystal-poor vitric zone, and are distinctly more variable within the underlying progressively less-welded rocks near the base of the Topopah Spring Tuff. Major (off-scale) separation of the deep and medium resistivity traces is present at two depth intervals at about 1280–1330 ft, and 1350–1375 ft (390–405 and 411.5–419 m, respectively) within this lower vitric zone. The two traces also separate to a much more modest extent in the middle nonlithophysal and lower nonlithophysal zones of the Topopah Spring Tuff.

The Calico Hills Formation is characterized generally by low apparent resistivity values and relatively low variability. This subdued response may be related to the presence of zeolitic alteration, particularly below a depth of roughly 1470 ft (448 m). Resistivity values within the Prow Pass Tuff are noticeably higher than those associated with the Calico Hills units. Higher resistivity readings appear to be associated with welding and vapor-phase alteration within Prow Pass ash-flow unit 3 from approximately 1680 to 1830 ft (510–555 m). Quite low apparent resistivities are associated with the interval of zeolitic alteration present beginning at a depth of 1830 ft (557.8 m).

Caliper Log Response

Drill hole USW SD-12 was drilled using down-hole tools that produce a nominal 12-1/4-inch (31-cm) diameter drill hole. The 4-arm caliper tool produces two mutually perpendicular measurements of the borehole diameter at each depth; these traces are presented in figure 12(e). Although much of the SD-12 drill hole is relatively in-gauge, there are numerous out-of-gauge intervals throughout the hole. Major wash-out zones of increased hole diameter are associated with the lithophysal intervals at around 100 ft (30 m), 450–660 ft (137–201 m), and 800–1040 ft (244–317 m). A severely washed out interval extends over nearly 100 ft (30 m) and is associated with the nonwelded and poorly consolidated materials of the PTn thermal/mechanical unit between 240 and 325 ft (73–99 m). Additional significant intervals of increased

hole diameter are associated with the lowermost nonwelded zone of the Topopah Spring Tuff below 1339 ft (408 m), and this zone of wash-out extends through nonwelded ash-flow unit 4 of the Calico Hills Formation to a depth of about 1480 ft (450 m). Another major interval of hole enlargement is associated with the upper part of Prow Pass ash-flow unit 3, extending roughly from a depth of 1700 to 1800 ft (520–550 m). Interestingly, this latter interval corresponds to the more welded portion of Prow Pass ash-flow unit 3.

Summary

Drill hole USW SD-12 is one of several holes drilled under Site Characterization Plan Study 8.3.1.4.3.1, also known as the Systematic Drilling Program, to provide geologic characterization of the potential Yucca Mountain nuclear-waste repository site. The SD-12 drill hole is located slightly more than half way between the North Ramp and the proposed South Ramp declines, immediately to the west of the Main Test Level drift of the Exploratory Studies Facility. The drill hole, which is located in a small wash immediately to the north of Whaleback Ridge, was positioned west of the Ghost Dance Fault, and this structural and topographic position allowed penetration of about the lower one-half of the Tiva Canyon Tuff. Essentially complete sections of the Pah Canyon Tuff, the Topopah Spring Tuff, the Calico Hills Formation, and the Prow Pass Tuff were recovered by the SD-12 drill core. The Yucca Mountain Tuff, which lies between the Tiva Canyon and Pah Canyon Tuffs, appears to be absent at this location.

The USW SD-12 drill hole was collared in the crystal-poor middle nonlithophysal zone of the Tiva Canyon Tuff. The hole also penetrated the underlying crystal-poor lower lithophysal and lower nonlithophysal vitric zones of the Tiva Canyon Tuff. Approximately 250 ft (75 m) of this formation was penetrated by the hole. The Yucca Mountain Tuff appears to be missing from the section at the SD-12 location, and the Pah Canyon Tuff is only 14.5 ft (4.5 m) thick. The Pah Canyon is completely nonwelded in the SD-12 drill core. The Topopah Spring Tuff consists of nearly 1117.5 ft (340.6 m) of generally densely welded pyroclastic-flow deposits. Lithophysae are well developed

through two major intervals within the Topopah Spring Tuff. The upper lithophysal interval, a combination of the crystal-rich lithophysal and crystal-poor upper lithophysal zones, is 229.5 ft (69.95 m) thick and the lower lithophysal interval is 257.2 ft (78.39 m) thick. Large lithophysal cavities more than a foot (many tenths of a meter) across are present throughout these lithophysal intervals and have been observed in down-hole video imagery from the SD-12 drill hole. Lithophysae and lithophysal cavities are not restricted to the named “lithophysal” lithostratigraphic units, and the larger-than-core cavities in particular extend downward as much as 60 ft (18 m) into the lower “nonlithophysal” zone as defined by Buesch and others (1996). The lower vitrophyre (densely welded vitric subzone) of the Topopah Spring Tuff is 24.3 ft (7.41 m) thick in the SD-12 core. The Calico Hills Formation in drill hole USW SD-12 consists of 237.1 ft (72.26 m) of nonwelded and mostly zeolitized tuffaceous materials. The Calico Hills has been subdivided into four units of mostly ash-flow deposits plus an underlying “bedded” interval of reworked tuffaceous material and a basal tuffaceous sandstone unit. The Prow Pass Tuff at this location comprises four units dominated by ash-flow tuffs plus a basal unit of bedded and reworked materials that total 496.5 ft (151.33 m) in thickness. The hole was bottomed in the uppermost ash-flow units of the Bullfrog Tuff.

Quantitative and semiquantitative data are included in this report for core recovery, rock-quality designation (RQD), lithophysal cavity abundance, and fracturing. These data are spatially variable, both within and among the major formation-level stratigraphic units. Nonwelded intervals in general exhibit higher core recovery and more intact (higher) RQD values than the densely welded intervals. Core recovery was a significant problem in a number of lithostratigraphic units, principally those involving extensive development of lithophysal-style alteration. Ten-foot (3-m) composite RQD values indicate “fair” ground conditions in the upper one-third of the Topopah Spring Tuff with “poor” to “very poor” ground conditions in the lower two-thirds. Estimation of lithophysal cavity abundances and of fracture density is complicated by the existence of cavities much larger than the core diameter; drilling

through these intervals of large lithophysal cavities produced thick zones of "lost" core and rubble.

This report includes quantitative data for the "framework" material properties of porosity, bulk and particle density, and saturated hydraulic conductivity. Graphical analysis of variations in these laboratory hydrologic properties confirm previously reported first-order control of material properties by the degree of welding and presence of zeolite alteration minerals. Many of the finer-scale lithostratigraphic contacts frequently described from rocks at Yucca Mountain are not well expressed in the material-property profiles. Approximate in-situ saturation and volumetric water content data for core samples preserved immediately upon recovery from the hole are included in the data tabulation.

Geophysical well-log data have been obtained from approximately 1950 ft (600 m) of the USW SD-12 drill hole; the lowermost 200 ft could not be logged geophysically because of hole-size restrictions. The suite of petrophysical log traces recorded during three separate periods of logging include density, gamma-ray, epithermal-neutron porosity, electrical resistivity, and caliper profiles. These logs are available down to the base of ash-flow unit 2 of the Prow Pass Tuff. The density log provides the most lithologic information. Many of the major lithologic subdivisions described from the core can be identified in the petrophysical profiles. Discrimination of welded from nonwelded rock type is immediately apparent in the density log, and this independent line of evidence confirms the fact that material-property units do not correspond in detail to the broader, genetic lithostratigraphic unit boundaries. The other log traces reflect some of the lithologic subdivisions to greater or lesser degrees; however, their principal purpose is for use in quantitative calculations of material properties that are beyond the scope of this Study.

References

ASTM (American Society for Testing and Materials), 1994, Standard test methods for absorption and bulk-specific gravity of dimension

stone: 1995 Annual Book of ASTM Standards, C97-90(1994), 04.07.

Barton, N.R., Lien, R., and Lunde, J., 1974, Engineering classification of rock masses for the design of tunnel support: *Rock Mechanics*, v. 6, p. 189-236.

Bierniawski, Z.T., 1989, *Engineering rock mass classifications, A complete manual for engineers and geologists in mining, civil, and petroleum engineering*: New York: John Wiley & Sons, 251 p.

Buesch, D.C., Spengler, R.W., Moyer, T.C., and Geslin, J.K., 1996, Proposed stratigraphic nomenclature and macroscopic identification of lithostratigraphic units of the Paintbrush Group exposed at Yucca Mountain, Nevada: *U.S. Geological Survey Open-File Report 94-469*, 47 p.

Bush, D.C., and Jenkins, R.E., 1970, Proper hydration of clays for rock property determinations: *Journal of Petroleum Technology*, v. 22, p. 800-804.

Byers, F.M., Jr., Carr, W.J., Orkild, P.P., Quinlivan, W.D., and Sargent, K.A., 1976, Volcanic suites and related cauldrons of Timber Mountain-Oasis Valley caldera complex, southern Nevada: *U.S. Geological Survey Professional Paper 919*, 70 p.

Byers, F.M., Jr., Carr, W.J., and Orkild, P.P., 1989, Volcanic centers of southwestern Nevada: Evolution of understanding, 1960-1988: *Journal of Geophysical Research*, v. 94, p. 5908-5924.

Carr, W.J., 1984, Regional structural setting of Yucca Mountain, southwestern Nevada, and late Cenozoic rates of tectonic activity in part of the southwestern Great Basin, Nevada and California: *U.S. Geological Survey Open-File Report 84-854*, 109 p.

Carr, W.J., Byers, F.M., Jr., and Orkild, P.P., 1986, Stratigraphic and volcano-tectonic relations of the Crater Flat tuff and some older volcanic units: *U.S. Geological Survey Professional Paper 1323*, 28 p.

Christiansen, R.L., Lipman, P.W., Carr, W.J., Byers, F.M., Jr., Orkild, P.P., and Sargent, K.A., 1977, The Timber Mountain-Oasis Valley caldera complex of southern Nevada: *Geological Society of America Bulletin*, v. 88, p. 943–959.

Compton, R.R., 1962, *Manual of field geology*, New York: John Wiley & Sons, Inc., 378 p.

Deere, D.U., 1963, Technical description of rock cores for engineering purposes: *Felsmechanik und Ingenieurgeologie* (Rock Mechanics and Engineering Geology), v. 1, p. 16–22.

Deere, D.U., and Deere, D.W., 1989, *Rock quality designation (RQD) after twenty years*: U.S. Army Corps of Engineers, Waterways Experiment Station Contract Report GL-89-1, 100 p.

DOE (U.S. Department of Energy), 1988, *Site characterization plan, Yucca Mountain site, Nevada Research and Development Area, Nevada*: Report DOE/RW-0198, U.S. Department of Energy, Office of Civilian Radioactive Waste Management, Washington, D.C.

Engstrom, D.A., and Rautman, C.A., 1996, Geology of the USW SD-9 Drill Hole, Yucca Mountain, Nevada: *Sandia Report SAND96-2030*, Sandia National Laboratories, Albuquerque, N. Mex., 128 p.

Geological Society of America, 1991, *Rock-color chart*: Boulder, Colorado: Geological Society of America.

Istok, J.D., Rautman, C.A., Flint, L.E., and Flint, A.L., 1994, Spatial variability of hydrologic properties of a volcanic tuff: *Ground Water*, v. 32, p. 751–760.

Lappin, A.R., VanBuskirk, R.G., Enniss, D.O., Butters, S.W., Prater, F.M., Muller, C.B., and Bergosh, J.L., 1982, Thermal conductivity, bulk properties, and thermal stratigraphy of silicic tuffs from the upper portion of hole USW G-1, Yucca Mountain, Nye County, Nevada: *Sandia Report SAND81-1873*, Sandia National Laboratories, Albuquerque, N. Mex., 48 p.

Lipman, P.W., and Christiansen, R.L., 1964, Zonal features of an ash-flow sheet in the Piapi Canyon Formation, southern Nevada, in *Geological Survey Research 1964: U.S. Geological Survey Professional Paper 501-B*, p. B74–B78.

Lipman, P.W., Christiansen, R.L., and O'Connor, J.T., 1966, A compositionally zoned ash-flow sheet in southern Nevada: *U.S. Geological Survey Professional Paper 524-F*, p. F1–F47.

Maldonado, F., and Koether, S.L., 1983, Stratigraphy, structure and some petrographic features of Tertiary volcanic rocks at the USW G-2 drill hole, Yucca Mountain, Nye County, Nevada: *U.S. Geological Survey Open-File Report 83-732*, 83 p.

Moyer, T.C. and Geslin, J.K., 1995, Lithostratigraphy of the Calico Hills Formation and Prow Pass Tuff (Crater Flat Group) at Yucca Mountain, Nevada: *U.S. Geological Survey Open-File Report 94-460*, 59 p.

Nimick, F.B., and Schwartz, B.M., 1987, Bulk, thermal, and mechanical properties of the Topopah Spring Member of the Paintbrush Tuff, Yucca Mountain, Nevada: *Sandia Report SAND85-0762*, Sandia National Laboratories, Albuquerque, N. Mex., 180 p.

Noble, D.C., Sargent, K.A., Mehnert, H.H., Ekren, E.B., and Byers, F.M., Jr., 1968, Silent Canyon volcanic center, Nye County, Nevada, in *Nevada Test Site: Geological Society of America Memoir 110*, p. 65–75.

Ortiz, T.S., Williams, R.L., Nimick, F.B., Whittet, B.C. and South, D.L., 1985, A three-dimensional model of reference thermal/mechanical and hydrological stratigraphy at Yucca Mountain, southern Nevada: *Sandia Report SAND84-1076*, Sandia National Laboratories, Albuquerque, N. Mex., 76 p.

Rautman, C.A., 1993, Study plan for the systematic acquisition of site-specific subsurface information, site characterization plan study 8.3.1.4.3.1, *YMP-SNL-SP-8.3.1.4.3.1, R1*, U.S. Department of Energy, Office of Civilian

Radioactive Waste Management, Washington, D.C., 61 p.

Rautman, C.A., and Engstrom, D.A., 1996, Geology of the USW SD-7 drill hole, Yucca Mountain, Nevada: *Sandia Report SAND96-1474*, Sandia National Laboratories, Albuquerque, N. Mex., 164 p.

Rautman, C.A., Istok, J.D., Flint, A.L., Flint, L.E., and Chornack, M.P., 1993, Influence of deterministic geologic trends on spatial variability of hydrologic properties in volcanic tuff, in *High-level Radioactive Waste Management, Proceedings of the Fourth Annual International Conference*: La Grange Park, Ill., American Nuclear Society, p. 921-929.

Rautman, C.A., Flint, L.E., Flint A.L., and Istok, J.D., 1995, Physical and hydrologic properties of outcrop samples from a nonwelded to welded tuff transition, Yucca Mountain, Nevada: U.S. Geological Survey *Water-Resources Investigations Report 95-4061*, 28 p.

Ross, C.S., and Smith, R.L., 1961, Ash-flow tuffs: their origin, geological relations, and identification: *U.S. Geological Survey Professional Paper 366*, 81 p.

Sawyer, D.A., Fleck, R.J., Lanphere, M.A., Warren, R.G., Broxton, D.E., and Hudson, M.R., 1994, Episodic caldera volcanism in the Miocene southwestern Nevada volcanic field: Revised stratigraphic framework, $^{40}\text{Ar}/^{39}\text{Ar}$ geochronology, and implications for magmatism and extension: *Geological Society of America Bulletin*, v. 106, p. 1304-1318, October 1994.

Scott, R.B. and Bonk, J., 1984, Preliminary geologic map of Yucca Mountain with geologic sections, Nye County, Nevada: *U.S. Geological Survey Open-File Report 84-494*, 10 p., 3 sheets.

Scott, R.B., and Castellanos, M., 1984, Stratigraphic and structural relations of volcanic rocks in drill holes USW GU-3 and USW G-3, Yucca Mountain, Nye County, Nevada: *U.S. Geological Survey Open-File Report 84-491*, 127 p.

Scott, R.B., Spengler, R.W., Diehl, S., Lappin, A.R., and Chornack, M.P., 1983, Geologic character of tuffs in the unsaturated zone at Yucca Mountain, southern Nevada, in *Role of the unsaturated zone in radioactive and hazardous waste disposal*, J. Mercer, P.S.C. Rao, and I.W. Marine, eds., Ann Arbor Science, Ann Arbor, Mich., p. 289-335.

Soeder, D.J., Flint, L.E., and Flint, A.L., 1991, Effects of sample handling and measurement methodology on the determination of porosity in volcanic rock samples (abs): *Agronomy Abstracts*, 1991 Annual Meeting, p. 232.

Spengler, R.W., Byers, F.M., Jr., and Warner, J.B., 1981, Stratigraphy and structure of volcanic rocks in drill hole USW G-1, Yucca Mountain, Nye County, Nevada: *U.S. Geological Survey Open-File Report 81-1349*, 51 p.

USGS (U.S. Geological Survey), 1991a, Characterization of the Yucca Mountain unsaturated-zone percolation, site characterization plan study 8.3.1.2.2.3, *YMP-USGS-SP 8.3.1.2.2.3*, R0, U.S. Department of Energy, Office of Civilian Radioactive Waste Management, Washington, D.C.

USGS, 1991b, Studies to provide soil and rock properties of potential locations of surface and subsurface access facilities, site characterization plan study 8.3.1.14.2, *YMP-USGS/USBR-SP 8.3.1.14.2*, R0, U.S. Department of Energy, Office of Civilian Radioactive Waste Management, Washington, D.C.

Whitfield, M.S., Jr., Thordarson, W., and Eshom, E.P., 1984, Geohydrologic and drill-hole data for test well USW H-4, Yucca Mountain, Nye County, Nevada: *U.S. Geological Survey Open-File Report 84-449*, 64 p.

(This page intentionally left blank.)

Appendix A: Lithologic Unit Descriptions

Lithologic Unit Descriptions

The following are unit-by-unit descriptions of the USW SD-12 core. The SD-12 borehole was drilled through pad-fill materials to a depth of 5.3 ft (1.62 m), after which depth coring was attempted. Initial coring recovered fragments of Tiva Canyon Tuff that in retrospect appear to represent large boulders or slightly displaced blocks in colluvial deposits. These materials continued downward until inferred in-place bedrock was encountered at about 12.9 ft (3.93 m). These descriptions attempt to use stratigraphic nomenclature proposed by Buesch and others (1996) for the various units of the Paintbrush Group. Unit descriptions are also cross-referenced where feasible to the older zonation of the Paintbrush Group tuffs used by Scott and Bonk (1984). The older names and some of their historical modifications are frequently encountered in earlier Yucca Mountain Project publications. Nomenclature and descriptions for subunits of the Calico Hills Formation and the Prow Pass Tuff (Crater Flat Group) follow those of Moyer and Geslin (1995). The lithologic descriptions are presented graphically on the detailed core-log sheets in Appendix B.

Tiva Canyon Tuff (Tpc)

Crystal-poor middle nonlithophysal zone (Tpcpmn) 12.9–82.0 ft (3.9–25.0 m)

The crystal-poor middle nonlithophysal zone of the Tiva Canyon section, formerly known variously as the “clinkstone” or “rounded step” zones (Scott and Bonk, 1984) in the immediate vicinity of the potential repository, is divided into upper and lower nonlithophysal subzones separated by a lithophysae-bearing subzone. SD-12 encountered the lower 13.8 ft (4.2 m) of the upper nonlithophysal subzone. This subzone does not contain well developed lithophysae, but approximately one-third of the pumice are weakly (incipiently) lithophysal. The lithophysae-bearing subzone is 22-ft (6.7 m) thick and is present from 26.7 to 44.7 ft (8.1–13.6 m) in depth. The lithophysae-bearing subzone contains moderately spaced, small- to medium-sized, well opened lithophysae. Small lithophysae are also present below 44.7 ft (13.6 m), although they are much more widely

spaced below this depth, which is taken as the top of the lower nonlithophysal subzone. Vapor-phase alteration of the groundmass accompanies lithophysae throughout the lower two subunits.

Crystal-poor lower lithophysal zone (Tpcpll) 82.0–134.6 (25.0–41.0 m)

Small, flattened lithophysae increase in number at a depth of about 82.0 ft (25.0 m), marking the upper gradational contact of the lower lithophysal zone (lower lithophysal zone of Scott and Bonk, 1984). The volume fraction of lithophysae is estimated at more than 10 percent. A sharp increase in the intensity of number and general intensity of lithophysae is observed at 93.4 ft (28.5 m); with large, ragged lithophysae are interspersed with small, closely-spaced lithophysae. Large lithophysal cavities up to twelve inches (0.3 m) in diameter are visible on the borehole video log between 94.9 and 107.8 ft (28.9–32.9 m). Lithophysae generally increase in size and intensity down to approximately 125 ft (38 m), and then diminish to a well defined contact with nonlithophysal rock at a depth of 134.6 ft (41.0 m). The increased development of lithophysae is associated with a parallel increase in the intensity of medium-purple-gray vapor-phase alteration.

Crystal-poor lower nonlithophysal zone (Tpcpln) 134.6–240.1 ft (41.0–73.2 m)

The crystal-poor lower nonlithophysal zone of the Tiva Canyon Tuff historically has been subdivided into to principal units: the “hackly” and the “columnar” zones of Scott and Bonk (1984). This subdivision structure has been maintained by Buesch and others (1996), with the exception that these two units have been downgraded to subzone status.

Hackly subzone (Tpcplnh) 134.6–176.0 ft (41.0–53.6 m)

Hackly (closely spaced, subhorizontal) fractures are first encountered at a depth of 129.5 ft (39.5 m), approximately five feet above the last closely spaced lithophysae, which extend continuously to a depth of 134.6 ft (41.0 m). Buesch and others (1996) cite the first appearance of hackly fracture as defining the upper contact of the hackly

subzone. However, the prominent and continuous presence of lithophysae below this change in fracture habit appears in conflict with a designation of "nonlithophysal." The contact between lithophysal and nonlithophysal tuff is quite distinct. Weak but pervasive vapor-phase alteration of the groundmass is characteristic of this unit. Thin (2–3-mm wide) white, vapor-phase veinlets are present at crudely five-foot (1.5-m) intervals throughout the unit. A prominent interval of small, flattened, moderately spaced lithophysae is present at the bottom of the hackly subzone from 165.0 to 176.0 ft (50.3–53.6 m).

Columnar subzone (Tpcplnc) 176.0–240.1 ft (53.6–72.9 m)

High-angle, columnar-style joints are present from about a depth of about 158 to 241 ft (48.2–73.5 m). The contact between the hackly subzone and the underlying columnar subzone is indistinct, and is taken at approximately 176.0 ft (53.6 m) where near-vertical joints begin to dominate the subhorizontal hackly-style fracturing. Buesch and others (1996) subdivide the columnar subzone into three smaller intervals based on the alteration of the larger pumice clasts. The upper subzone of the columnar subzone contains dark, vapor-phase altered, spherulitic and flattened pumice clasts that are set in dense compact-textured groundmass. The pumice of the middle interval have been argillized to pink clay between about 177.5 and 232.7 ft (54.1–70.9 m). The lower interval of the columnar subzone, that below 232.7 ft, is characterized by light tan-gray colored, welded, devitrified groundmass punctuated by dark, vitric, flattened, rectangular pumice clasts with feathery ends. Sparse larger pumice clasts that have been totally altered to pink clay continue to the bottom contact of the columnar subzone. The upper part of the columnar subzone is vapor-phase altered. The intensity of alteration decreases markedly below at a depth of 192.2 ft (58.6 m).

Crystal-poor vitric zone (Tpcpv) 240.1–263.7 ft (72.9–80.4 m)

The crystal-poor vitric zone of Buesch and others (1996) was aggregated by Scott and Bonk (1984) into their columnar zone. This single older unit thus comprised lithologies varying from

densely welded (even vitrophyric) to nonwelded. Many Yucca Mountain Project workers adopted a convention whereby the non-densely welded parts of the Scott and Bonk columnar zone were identified separately as the "shardy base" unit (Rautman and others 1993, 1995; Istok and others, 1994), in recognition of the presence of diagnostic glass shards throughout the less welded portion of the crystal-poor vitric zone.

The densely welded subzone (Tpcpv3) of the crystal-poor vitric zone described by Buesch and others (1996) consists of a black vitrophyre in outcrops along the west face of Yucca Mountain in Solitario Canyon. This vitrophyric unit appears to be absent in the SD-12 drill hole.

*Moderately welded subzone (Tpcpv2)
240.1–255.5 ft (72.9–77.9 m)*

Vitric materials lying below devitrified welded tuff or below a local vitrophyre of dense black glass and exhibiting a progressive downward decrease in welding were described as the "shardy base" of the Tiva Canyon Tuff by Istok and others (1994) in recognition of an essentially continuous, gradational increase in porosity toward the base of the formation, and in recognition of the prominent presence of vitric shards throughout the unit. The same interval was recognized by Scott and Bonk (1984), although they aggregated these rocks as part of their columnar zone (dominantly welded and devitrified materials). Buesch and others (1996) subdivide the crystal-poor vitric interval into two laterally extensive subzones (a third subzone corresponding to the black vitrophyre is laterally restricted). This partially to moderately welded subzone of the lower vitric zone consists of a matrix of moderately deformed, orange-brown bubble-wall shards; the unit contains approximately 30 percent black glassy shards from 240.1 to about 243.1 ft (72.9–74.1 m), where the black-shard content decreases to virtually zero. Dark gray pumice fragments make up about a quarter of the rock volume; these clasts are weakly vapor-phase altered.

Non- to partially welded subzone, (Tpccpv1)
255.5–263.7 ft (77.9–80.4 m)

The lower nonwelded vitric subzone of Buesch and others (1996) was aggregated as part of the “shardy base” interval Istok and others. Their gradational increase in porosity at the base of the Tiva Canyon Tuff tended to stabilize at high values typical of nonwelded ash in what now is known as the nonwelded subzone. The nonwelded subzone is separated from the overlying moderately welded subzone by a gradational contact at a depth of about 255.5 ft (77.9 m). The matrix in this interval is vitric, nonwelded, and comprised of partially-argillized, orange-brown bubble-wall shards. Approximately 3–4 percent of the shards are black and vitric. Fractures in this zone are generally smooth and commonly are coated by a black material.

Pre-Tiva Canyon Tuff bedded tuff (Tpbt4)
263.7–272.0 ft (80.4–82.9 m)

Volcanic rocks lying between the ash-flow deposits of the Tiva Canyon and the Pah Canyon Tuffs at USW SD-12 consist of a sequence of tuffaceous materials that exhibit some evidence of reworking, and which generally in the past have been aggregated simply as “bedded tuff” (Scott and Bonk, 1984). A number of separate units can be identified; these are described here using the conventions of Buesch and others (1996).

The pre-Tiva Canyon Tuff bedded tuff consists of an upper, nonwelded unit beginning at a depth of 263.7 ft (80.4 m). The rock is a bedded tuff exhibiting a sandy, reworked, clast-supported matrix that contains 20 percent small, gray, pumice clasts. A 1.4-foot thick pumice fall forms a second unit extending to a depth of 266.4 ft (81.2 m). This pumice fall is medium grained and composed of partially altered pumice and 3–4 percent black obsidian clasts. The upper units are underlain by a fallout deposit that may be only slightly reworked; this unit coarsens downward into a three-foot-thick lithic-rich pumice fall. The abundance of lithic fragments in this unit marks it as part of the pre-Tiva Canyon bedded tuff sequence.

Yucca Mountain Tuff (Tpy)

Rocks identifiable as the Yucca Mountain Tuff were not encountered in drill hole USW SD-12.

Pre-Yucca Mountain Tuff bedded tuff (Tpbt3)
272.0–277.0 ft (82.9–84.4 m)

The pre-Yucca Mountain Tuff bedded tuff unit has been characterized as a sequence of reworked, fallout, and pyroclastic flow deposits overlying a nonwelded pumice-fall deposit (Buesch and others, 1996). The upper part of the pre-Yucca Mountain Tuff bedded tuff exhibits a sandy, clast-supported, moderately reworked matrix containing nearly no lithic fragments. This material rests on a 4-inch (1.6 cm) coarse-grained, white pumice fall. The lowest unit of the pre-Yucca Mountain Tuff sequence, directly overlying the Pah Canyon Tuff, is composed of a 3.4-foot- (1.0 m-) thick ash-flow deposit that includes a 6-inch coarse, white pumice fall at its base.

Pah Canyon Tuff (Tpp) 277.0–291.5 ft (84.4–88.8 m)

The Pah Canyon Tuff is relatively thin, 14.5 ft (4.4 m) at the USW SD-12 location. The tuff, which was encountered at a depth of 277.0 ft (84.4 m), contains 30–40 percent pastel-colored pumice clasts set in an weakly altered, mostly vitric, nonwelded matrix. Pumice clasts are bimodal in appearance, split between a light gray, densely-textured, vitric variety and a finely-laminated vesicular type ranging in size from 0.5–1.75 inch (12–45 mm). The Pah Canyon Tuff contains 1 percent dark, small, vitric lithic fragments. A characteristic, vaguely-pumiceous basal “white zone” is present from 288.4 to 291.5 ft (87.9 to 88.8 m).

Pre-Pah Canyon Tuff bedded tuff (Tpbt2)
291.5–294.2 ft (88.8–89.7 m)

The pre-Pah Canyon Tuff bedded tuff is vitric, reworked, sandy-textured, and nonwelded. This bedded tuff contains 8–10 percent small, light-gray, laminated pumice clasts, 2–4 percent dark vitric lithic clasts, 3–5 percent feldspar phenocrysts and 2 percent biotite flakes in an altered matrix.

Topopah Spring tuff (Tpt)

Crystal-rich vitric zone (Tptrv) 294.2–330.8 ft (89.7–100.8 m)

Crystal-rich vitric zone, nonwelded subzone (Tptrv3) 294.2–324.6 ft (89.7–98.9 m)

The Topopah Spring Tuff upper vitric zone is subdivided by Buesch and others (1996) into a downward sequence consisting of nonwelded, moderately welded, and vitrophyre subzones. The upper contact of the Topopah Spring Tuff is placed in this report at a depth of 294.2 ft (89.7 m) in this report. This contact is represented by a prominent hematite-stained interval, an inferred paleosol or weathering horizon, that stands in marked contrast to the overlying “bedded tuff” (especially the immediately overlying, non-iron-stained pumiceous “white zone”). Buesch and others (1996, p. 7) propose locating the upper contact of the Topopah Spring Tuff at the top of a 2-cm-thick, pink, very fine-grained ash layer that is located in the SD-12 drill core nearly 20 ft (6 m) below the prominent iron-stained horizon at 294.2 ft. According to this criterion, the top of the Topopah Spring Tuff would be located at a depth of 314.1 ft (95.7 m). However, because the texture and composition of the rock above and below this pink marker bed are essentially identical, and because the hematite-stained interval at 294.2 ft presumably represents a significant period of exposure and weathering following eruption of the Topopah Spring Tuff, we believe that the higher location is the more logical geologic break. If the 2-cm pink ash layer at 314.1 ft in the SD-12 core is as uniform in thickness and as laterally extensive as implied by Buesch and others (1996, p. 7), it is unlikely that the ash layer’s upper contact represents any significant time break in eruptive activity.

The upper nonwelded subzone of Topopah Spring Tuff is crystal-rich, containing 10–20 percent feldspar and biotite phenocrysts. Approximately 1–2 percent small, angular quartz latite lithics are common. The upper vitric zone contains 15–20 percent pumice, with a pumice content of up to 25–30 percent between depths of 294.3 and 302.0 ft (89.7–92.0 m). A prominent thin pumice-rich layer occurs between 307.2 and 308.2 ft (93.6–93.9 m). The pumice content increases sharply at a

depth of 318.6 ft (97.8 m), associated with what commonly has been referred to as a “sintered” interval, in which the rock appears to have been partially welded by thermal effects even though there is no meaningful degree of compaction of individual pumice clasts.

Moderately welded subzone (Tptrv2)

320.9–324.6 ft (97.1–98.9 m)

The upper contact of the moderately welded subzone is placed at the uppermost limit of deformation of large gray pumice clasts that constitute 80–90 percent of the rock within the so-called “sintered” interval that was encountered at a depth of about 318.6 ft (97.8 m). As is typical of the ash-flow deposits at Yucca Mountain, this contact is, in fact, gradational and, to some extent, arbitrary. The unit also contains approximately 10 percent devitrified and vitric lithic clasts and 3–5 percent phenocrysts of feldspar and oxybiotite in a vitric, clast-supported pumiceous matrix.

Densely welded (“caprock vitrophyre”) subzone (Tptrv1) 324.6–330.8 ft (98.9–100.8 m)

The crystal-rich densely welded vitric subzone (commonly referred to as the “caprock” vitrophyre based on terminology of Scott and Bonk, 1984) was encountered between depths of 324.6 and 330.8 ft (98.9–100.8 m) and is composed of dark-colored, densely fused, crystal-rich glass. Two phases are easily distinguished in core: an upper “red vitrophyre” containing prominent black fiamme, and a lower “black vitrophyre” containing roughly 20 to 30 percent stretched red vitric lithics. Phenocrysts (15–20 percent of the rock) are predominantly of feldspar with traces of oxybiotite and rare pyroxene. Thin, pale-blue, weakly opaque, vapor-phase silica coatings are preferentially found on open joints.

Crystal-rich nonlithophysal zone (Tptrnl) 330.8–432.0 ft (100.8–131.7 m)

The crystal-rich nonlithophysal zone (“rounded” zone of Scott and Bonk, 1984) is distinguished from the overlying caprock vitrophyre by the presence of devitrification, or crystallization of the initially glassy tuff to a microcrystalline groundmass. This unit in the SD-12 drill hole is

composed of 15–17 percent phenocrysts, 10–30 percent pumice clasts, and 2–3 percent small, dark lithic fragments, all set in densely welded, devitrified matrix. Stretched, altered, and zoned rhyolitic “soft” (deformed) lithics constitute approximately 10 percent of the rock volume. Vapor-phase alteration of pumice fragments increases gradually downward. Fine-grained aphyric and porphyritic volcanic “hard” lithic fragments occur throughout the unit. The unit is weakly lithophysal, increasing in intensity from weakly opened small vugs within pumice clasts near the upper boundary to widely-spaced, small, flattened lithophysae near the lower contact at 432.0 ft (131.7 m). Vapor-phase alteration of the matrix is pronounced, although relict shard textures are preserved locally.

Crystal-rich lithophysal zone (Tptrl)

432.0–476.5 ft (131.7–145.2 m) and

Crystal-poor upper lithophysal zone (Tptpul)

476.5–661.5 ft (145.2–201.6 m)

As the intensity of vapor-phase alteration increases progressively with depth, the densely-welded and devitrified matrix of the core changes to lighter shades of pale red-purple. Small, ovate lithophysae that deform the flattened, welding texture of the rock increase abruptly to more than 10 percent of the rock volume at a depth of 432.0 ft (131.7 m); this depth is taken as the upper contact of the crystal-rich lithophysal zone (upper lithophysal zone of Scott and Bonk, 1984). Lithophysae increase in size and frequency downward, together with the intensity of associated vapor-phase alteration. Weak vapor-phase alteration rims on lithophysae are first encountered at a depth of 448.0 ft (136.5 m), and lining of the lithophysal cavities by vapor-phase minerals is present at a depth of around 476.5 ft (145.2 m). Below this depth, the matrix of the tuff is highly altered, and the sizes of lithophysae are distinctly bimodal. The intensity of lithophysae development and vapor-phase alteration increases toward a strongly developed lithophysal interval from 555.2 to 661.1 ft in depth (169.2–201.5 m). Extensive broken core or unrecovered intervals below 555.2 ft (169.2 m) are interpreted as indicating presence of lithophysal cavities that are several times larger than the core diameter. The actual presence of large cavities is confirmed by observation of the down-hole video

log. Nonlithophysal pumice clasts constitute approximately 25 percent of the rock mass at the top and bottom of this interval but are absent in the middle portion.

Compositional transition interval – 428.3–480.7 ft (130.5–146.5 m): This roughly 52.4-foot (16-m) interval is characterized by a downward change in the overall composition of the Topopah Spring Tuff from quartz latite into rhyolite. Crystal-rich quartz latite containing deformed clasts of crystal-poor rhyolite dominates the top of the transition interval, and the relative proportions of the two rock types progressively change downward to crystal-poor rhyolite containing deformed clasts of crystal-rich quartz latite. The relationship of the two clast lithologies indicates that the different rock types are comagmatic (cognate lithic clasts). The rock throughout this compositional transition interval becomes progressively more lithophysal downward.

Crystal transition interval – 439.0–476.5 ft (133.8–145.2 m): The phenocryst content of the tuff matrix (excluding that of the “soft” deformed cognate lithic clasts) changes progressively downward through a crystal-transition interval from 10–12 percent in crystal-rich quartz latite at 439.0 ft (133.8 m) to 3–5 percent in crystal-poor rhyolite at 476.5 ft (145.2 m). Although Buesch and others (1996, p. 7) define the crystal-poor lower member of the Topopah Spring Tuff as containing “less than 3 percent felsic phenocrysts,” it is clear that the change in crystal content occurs over an approximately 37.5-foot (11.4 m) interval and that the distinction between the crystal-rich lithophysal zone (Tptrl) and the crystal-poor upper lithophysal zone (Tptpul) does not represent a sharp contact.

Crystal-poor middle nonlithophysal zone (Tptpmn) 661.5–785.0 ft (201.6–239.3 m)

Lithophysal cavities and lithophysal-style alteration (including intense vapor-phase alteration end abruptly at a depth of 661.5 ft (201.6 m). Below this depth, the rock is densely welded and devitrified, exhibiting a more compact, less grainy texture than above. The matrix appears moderately but pervasively altered. The rock is speckled and streaked by subhorizontal white alteration veinlets

along pumice sites and bedding partings; this veining affects 15–20 percent of the rock. An interval of small, light-gray and red-brown lithic fragments is present between depths of 734.5 and 755.8 ft (223.9–230.4 m). A lithophysae-bearing subzone is not mesoscopically evident in the SD-12 core. However, core recovered between depths of 699.1 and 726.4 ft (213.0–221.4 m) is intensely broken, and there were numerous unrecovered intervals (log sheet 11, Appendix B). Examination of down-hole video images in this interval indicate the presence of large lithophysal voids in this middle portion of the middle nonlithophysal zone. Welding foliation is uncommon in the nonlithophysal zone except where the core appears been distorted by development of the lithophysal-bearing subzone inferred from down-hole videos. Jointing and fracturing in recovered core is smooth and mostly vertical.

**Crystal-poor lower lithophysal zone (TptplII)
785.0–1042.2 ft (239.3–317.7 m)**

The crystal-poor lower lithophysal zone in SD-12 is defined below approximately 785.0 ft (239.3 m) by the presence of vapor-phase alteration spots and of small, oval-shaped lithophysae that occur within spots of pink-tan vapor phase alteration. The spacing of these lithophysae is much wider than that in the lithophysal zones higher in the section. Much of the core is badly fractured below 798.4 ft (243.4 m) and there are many, thick unrecovered intervals caused by the presence of lithophysae and lithophysal cavities several times larger than the core diameter, in addition to the small- to medium-sized lithophysae visible in the core fragments. These large lithophysae are quite evident in the down-hole video survey. The intensity of mixed-size lithophysal cavity development and associated strong vapor-phase alteration appears fairly constant below this depth. Foliation is weakly to moderately developed in the lower two-thirds of the unit. Fractures are irregular with rough surfaces.

**Crystal-poor lower nonlithophysal zone (TptplIn)
1042.2–1278.1 ft (317.7–389.6 m)**

The crystal-poor lower lithophysal zone of Buesch and others (1996) was also known as the “mottled” zone according to the older nomencla-

ture of Scott and Bonk (1984). Identification of the distinction between the lower lithophysal and lower nonlithophysal intervals of the Topopah Spring Tuff is complicated in that the “contact” cannot be determined simply on the presence or absence of lithophysae.

For purposes of this report, the upper contact of the crystal-poor lower nonlithophysal zone was assigned at approximately 1042.2 ft (317.7 m) based on a decrease in the quantity of mesoscopic lithophysal cavities and lithophysal-style vapor-phase alteration spots plus subtle changes in alteration of the tuff matrix. The abundance of large-diameter lithophysae visible in core video images decreases abruptly at this depth, although more isolated, and perhaps somewhat smaller large lithophysal cavities and some vapor-phase alteration spots continue down-hole to a depth of 1098.7 ft (334.9 m). Such larger-than-core-diameter lithophysae are presumed related to rubblized intervals and intervals of no core recovery.

Vapor-phase alteration decreases near the top of the unit (above a depth of approximately 1042.2 ft), and again below about 1100 ft (335.3 m), corresponding to the last large cavities apparent in down-hole video images. This change in alteration produces a rock matrix that is somewhat less granular; the rock takes on a “mottled” appearance. Below 1100 ft, about 40 percent of the matrix unaltered from its original high-temperature devitrified mineralogy. Vapor-phase alteration becomes restricted downward to light-pink alteration halos and wisps plus a pervasive blue alteration closely associated with relict flattened pumice clasts, lithic fragments, and phenocrysts. The vapor-phase event appears to have healed numerous distinctive microfractures throughout the rock with thin (millimeter-width) selvages and deposited hairline coatings of silica and accessory minerals in the healed fractures.

The rock contains 1–3 percent total phenocrysts and 2–3 percent small, white altered rhyolite lithics. Large (to 50 mm) rhyolitic lithic fragments that are relatively diagnostic of the “mottled” zone are encountered at a depth of 1060.0 ft (323.1 m) and are present to the bottom of the Topopah Spring Tuff. A dense swarm of mixed-composition

lithic fragments is present from 1114.5 to 1116.5 ft (339.7–340.3 m). Below this depth, the both the size and quantity of lithic fragments decrease sharply and then continue to decrease gradually. Foliation is weakly developed, and near-vertical and subhorizontal fracturing predominate throughout the unit. High-angle, planar, smooth fractures are more prevalent in the zone's lower portion. Buesch and others (1996) have distinguished a columnar subzone in the lower part of the crystal-poor lower nonlithophysal zone.

**Crystal-poor lower vitric zone (Tptpv)
1278.1–1411.3 ft (389.6–430.1 m)**

*Densely welded ("basal vitrophyre") subzone
(Tptpv3) 1278.1–1302.4 ft (389.6–396.9 m)*

The crystal-poor lower vitric zone (lower or "basal" vitrophyre of Scott and Bonk, 1984) of the Topopah Spring Tuff was encountered at a depth of 1278.1 ft (389.6 m). The rock is vitric, dark colored, and densely welded (or fused?), and it contains 3–4 percent sanidine phenocrysts and approximately 5 to 8 percent coarse, black vitric spots up to 15 mm across that appear to represent cognate pumice clasts. Small rhyolite and quartz-latite lithics fragments are scattered through the vitrophyre and may form 2 to 5 percent of the rock. The lithic fragments are associated with alteration rims and generally average 5 mm (0.2 inch) in diameter. An intense rectilinear and conchoidal fracturing habit reflects the glassy composition. Pale-blue vapor-phase silica forms crusts and coatings on the major joint surfaces.

*Moderately welded subzone (Tptpv2)
1302.4–1339.0 ft (396.9–408.1 m)*

This subzone of the crystal-poor vitric zone is distinguished with difficulty from the overlying vitrophyre principally by progressively decreased welding (fusing) downward and by the presence of subangular orange pumice fragments. The matrix is glossy, vitric, and slightly more altered (argillized?) in the lower part. The interval contains light-brown, vitric pumice clasts and small, light-gray rhyolitic lithics set in a matrix of distinguishable bubble-wall shards. Vitric, quartz-latite lithics averaging 0.4 to 0.6 inch (10–15 mm) across are common. Fracturing is much reduced

and becomes dominantly subhorizontal downward as the intensity of welding decreases.

*Nonwelded subzone (Tptpv1) 1339.0–1411.3 ft
(408.1–430.2 m)*

Buesch and others (1996) distinguish a nonwelded subzone at the base of the crystal-poor vitric zone as the progressive decrease in welding eventually produces a nonwelded tuff. The contact is distinctly gradational and has been assigned at 1339.0 ft (408.1 m) at the lowermost occurrence of meaningfully flattened pumice. The core from the upper part of the nonwelded subzone in SD-12 contains 15 to 20 percent light-orange-brown pumice fragments that average 0.20 inch (5 mm) in diameter, 1 to 2 percent quartz-latite and rhyolite lithics clasts (0.20 inch diameter), and 2–3 percent phenocrysts in a vitric matrix containing up to 75 percent black shards. Pumice fragments locally contain spherulites. Visible zeolitic alteration is first encountered at a depth of 1381.1 ft (420.9 m) and extends to the base of the subzone at 1411.3 ft (430.2 m). Zeolitic alteration is represented as a porcelaneous micro-recrystallization of the formerly vitric tuff matrix; zeolites also replace pumice clasts. The fraction of hard volcanic lithic fragments increases downward to 10–12 percent between depths of approximately 1390.0 and 1405.7 ft (423.7–428.5 m). The matrix is speckled by 2 percent finely crystalline black spots of presumed iron-manganese oxides (Fe-MnO_x in the log). The rock texture flattens and becomes lithic-poor and pumiceous below 1405.9 ft. The base of the Topopah Spring Tuff was identified at a depth 1411.3 ft (430.2 m).

Pre-Topopah Spring Tuff bedded tuff (Tpbt1)

Rocks identifiable as the pre-Topopah Spring Tuff bedded tuff are absent in this hole.

Calico Hills Formation

**Calico Hills ash-flow unit 4 (Tac4)
1411.3–1475.0 (430.2–449.6 m)**

No paleosol or reworked material is evident above ash-flow deposits of the upper Calico Hills Formation in drill hole USW SD-12. The uppermost ash-flow deposit, identified as ash-flow

unit 4 of Moyer and Geslin (1995; their ash-flow unit 5 appears to be absent) is nonwelded, moderately zeolitized and is pumice- and lithic-rich. The ash-flow tuff contains up to 25 percent pumice clasts up to 40 mm (1.6 inches) in size and about 25 percent mixed-composition lithics down to a depth of 1447.0 ft (441.0 m). Between 1447.0 and 1470.7 ft (441.0–448.3 m), the pumice content decreases to 10–15 percent, the lithic content drops to 7–10 percent and the rock becomes slightly vapor-phase altered. This latter interval may represents a separate flow unit.

A “bedded tuff” subzone extending from 1470.7 to 1475.0 ft (448.3–449.6 m) forms the base of Calico Hills ash-flow unit 4. The bedded tuff is composed of lithic-rich, reworked, clast-supported tuffaceous material that lies over a 0.2-foot (60-cm) thick coarse-grained pumice fall deposit at 1471.6 ft (448.5 m). A small quantity of sand was recovered from a bedded unit that underlies the pumice fall and marks the bottom of unit 4. It is also possible that the recovered sand was derived from the reworked top of the underlying ash-flow unit 3.

Calico Hills ash-flow unit 3 (Tac3)
1475.0–1554.0 ft (449.6–473.7 m)

Ash-flow unit 3 of the Calico Hills Formation is capped by weakly reworked zone that probably represents a paleosol; core recovery was poor through this interval. This unit appears to consist of a pyroclastic-flow deposit that is zeolitically altered and partially clast-supported. The rock contains 20 to 30 percent partially zeolitized pumice clasts, 2 to 3 percent phenocrysts of feldspar, quartz with traces of biotite and sericite, and up to 20 to 40 percent mixed-composition lithic fragments as large as 70 mm (2.75 inches) in size. The lithic fragments are composed principally of red-brown or black devitrified volcanic rock, black vitric and red-orange pumiceous tuff, or large, complex clasts that themselves contain fragments of a variety of other volcanic rock types. The large lithics decrease in abundance at 1505.0 ft (458.7 m). Zeolitization remains fairly constant through most of the unit. A lithic-rich pumice fall encountered at a depth of about 1549.4 ft (472.3 m), and which

exhibits slightly increased zeolitization, forms the base of ash-flow unit 3.

Calico Hills ash-flow unit 2, (Tac2)
1554.0–1600.6 ft (473.7–487.9 m)

Calico Hills ash-flow tuff unit 2 is similar in many respects to the overlying unit 3. The diagnostic lithic-rich fallout deposit separating the two ash-flow units described by Moyer and Geslin (1995) may have been lost in a 6-foot (1.8-m) unrecovered interval beginning at 1551.0 ft (472.7 m). The pumice content of ash-flow unit 2 is 20 to 40 percent and the lithic content is markedly lower at 1–3 percent red-brown and red-orange fragments of varying composition. The matrix is more heavily zeolitized with the intensity of alteration increasing downward. Pumice fragments are generally smaller than 0.8 inch (20 mm) in diameter. The fine, ashy matrix of this unit has been heavily zeolitized to an orange-pink color. A sandy, pumiceous, bedded, basal interval composed of 50 percent pumice and 15 percent small dark lithics was recovered from a depth of 1599.1 to 1600.6 ft (487.4–487.9 m).

Calico Hills ash-flow unit 1, (Tac1)
1600.6–1611.6 ft (487.9–491.2 m).

Ash-flow unit 1 of the Calico Hills Formation is a zeolitized pyroclastic-flow deposit containing 5 to 10 percent pumice clasts, 3 to 5 percent lithics of varying composition and texture, and 5 to 10 percent phenocrysts of feldspar, quartz, and lesser biotite. The preserved, upper ash-flow portion of unit 1 is only 0.9 ft thick. The “bedded tuff” unit that forms the base of unit 1 is approximately 11.0 ft (3.4 m) thick. A 0.5-foot thick pumice fall composed of 60 percent pale yellow pumice and 10 percent small, dark, volcanic lithics forms the top of the bedded tuff. Between 1602.0 and 1607.1 ft is a complex unit consisting of a sandy, clast-supported bedded tuff that grades downward into a sandy ash-flow interval, which in turn grades downward into a coarse-grained basal pumice-fall deposit. The lowest subunit of the bedded sequence, recovered from between 1607.1 and 1611.6 ft (489.8–491.2 m), is a fine-grained, sandy ash-flow tuff that has been zeolitized to an overall pale yellow-green color. The base of the Calico

Hills unit 1 is assigned at the top of a 4.8 inch (12.2 cm) intensely altered, porcelaneous ash bed.

**Calico Hills Formation bedded tuff unit (Tacbt)
1611.6–1641.3 ft (491.2–500.3 m)**

The bedded tuff deposit that underlies the main Calico Hills Formation ash-flow deposits, as defined by Moyer and Geslin (1995), is a moderately to heavily zeolitized sequence of alternating layers of ash-fall, pumice-fall, ash-flow and reworked (bedded) tuffs. The topmost subunit is a 4.8-inch (12.2-cm)-thick, heavily zeolitized, porcelaneous ash-fall bed. At a depth of 1612.0 ft (491.3 m), a medium-grained pumiceous ash-fall deposit contains up to 50 percent small green pumice clasts and 2 to 4 percent small dark lithic fragments. Between depths of 1621.9 and 1623.0 ft (494.3–494.7 m), a fine-grained, sandy, bedded tuff separates the pumiceous ash fall above from a pumiceous ash-flow deposit below. This lower ash-flow tuff contains 35 to 45 percent small green pumice fragments, 10 percent small lithic clasts of varying composition, and 15 percent phenocrysts of quartz, feldspar, and minor biotite. A coarse-grained pumice fall that grades into fine-grained sandy bedded tuff was encountered from 1629.0 to 1631.5 ft (496.5 to 497.3 m). Another medium-grained bedded tuff occurs from 1631.5 to 1640.0 ft (497.3–499.9m). The lowest subunit of the sequence is a sandy, medium-grained bedded tuff that contains constituents that are derived from the underlying tuffaceous sandstone. The intensity of the zeolitic alteration decreases downward toward the base of the overall bedded tuff unit.

**Calico Hills Formation basal sandstone unit
(Tacs) 1641.3–1648.4 ft (500.3–502.4 m)**

The basal unit of the Calico Hills Formation according to work by Moyer and Geslin (1995) is an immature, tuffaceous sandstone with a 1.1-foot (0.34 m) hematite-stained top (a presumed paleosol). The tuffaceous sandstone is yellow-brown, fine- to medium-grained, with 5 percent altered pumice fragments, 2 percent lithic fragments, and 20 to 30 percent quartz and feldspar grains. There is very little altered fine-grained material between the particles and some of the clasts are rimmed by iron and manganese oxides.

Prow Pass Tuff (Crater Flat Group)

**Prow Pass ash-flow unit 4 (Tcp4)
1648.4–1656.6 ft (502.4–504.9 m)**

The Prow Pass Tuff of the Crater Flat Group has been subdivided by Moyer and Geslin (1995) into four units dominated by ash-flow tuffs plus a basal “bedded tuff” unit. Ash-flow unit 4 in SD-12 is a thin, fine-grained, nonwelded, zeolitized ash-flow tuff exhibiting a sandy, possibly reworked texture. The rock contains 4 to 6 percent pale-yellow pumice clasts, 2 percent small lithic fragments in dark compositions and 2 to 5 percent phenocrysts. A highly altered bedded tuff interval containing a wide variety of lithic clasts was encountered from 1650.5 to 1655.0 ft (503.1–504.5 m). The dominant rock type is a coarse-grained pumice-fall deposit containing small lithic chips, including fragments of pumiceous tuff, devitrified volcanic rock, and generally unrecognizable red-orange material. The base of Prow Pass ash-flow unit 4 is a zeolitized, pumiceous ash-flow deposit containing particularly large lithics between 1655.0 and 1656.6 ft (503.1–504.9 m). Constituents of this bed include 40 to 55 percent pale-yellow or pink pumice clasts to 15 mm in diameter, 2 to 4 percent lithic fragments up to 40 mm (1.6 inches) across, and 10 to 13 percent phenocrysts.

**Prow Pass ash-flow unit 3 (Tcp3)
1656.6–1872.1 ft (504.9–570.6 m)**

Prow Pass ash-flow unit 3 is variably welded and exhibits local vapor-phase alteration. The rock consists of 10 to 25 percent altered pumice clasts, 7 to 12 percent phenocrysts of quartz, feldspar, biotite and pyroxene, and 1 to 4 percent lithic fragments of fine-grained red-brown or black volcanic rock or siltstone. The recognizable pumice content decreases in the middle part of the unit. Welding increases below the upper contact at 1656.6 ft (504.9 m) to a maximum intensity of moderately welded between about 1710 and 1715 ft (521.2–522.7 m), and then decreases downward, with the rock becoming nonwelded at a depth of about 1790 ft (545.6 m).

Vapor-phase alteration associated with welding in unit 3 was first encountered at a depth of 1677.6 ft (511.3 m); alteration turns the core

light gray to white in color. Vapor-phase alteration increases in intensity downward to the point that the rock texture is obscured, except for larger pumice clasts and small lithic fragments. Alteration is most intense at about 1745 ft (531.9 m), and vapor-phase alteration decreases below this depth to a minimal level extending from about 1790 to 1855 ft (545.6–(565.9 m). Zeolitic alteration overprints the entire unit 3 welded and vapor-phase altered tuffs. The intensity of zeolite alteration decreases downward from the upper contact to about 1720 ft (524.3 m) as the degree of welding increases. Recognizable zeolitic alteration was again encountered at a depth of 1830 ft (557.8 m) and zeolite intensity increases downward concurrently with the decrease in vapor-phase alteration.

Prow Pass ash-flow Unit 2 (Tcp2)
1872.1–1947.0 ft (570.6–593.5 m)

Prow Pass unit 2 is a zeolitized, nonwelded ash-flow tuff similar to unit 3 but with a higher lithic content. The rock is composed of 10 to 20 percent equigranular, pale-pink, zeolitized, undeformed pumice, 3 to 7 percent lithic fragments of a dense, devitrified volcanic composition or of red siltstone, and 10 to 15 percent phenocrysts including feldspar, quartz, oxybiotite, and pseudomorphs after pyroxene. Zeolitic alteration is relatively intense from the top of the unit to about 1900 ft (579.1 m). Alteration then decreases in intensity downward to a uniform, minimal level below a depth of 1930 ft (588.3 m). Zeolitic alteration in the lower part of unit 2, approximately apple-green in color, affects principally pumice clasts and 35–45 percent of the groundmass.

Prow Pass ash-flow unit 1 (Tcp1)
1947.0–2133.0 ft (593.5–650.1 m)

Ash-flow unit 1 comprises a nonwelded, zeolitically altered unit, containing 10–15 percent phenocrysts and 15 to 25 percent large, subrounded, altered pumice clasts. The pumice fragments are dense and laminated, and they are zeolitically altered to a pale-pink or green-gray color with intensely-zeolitized, green spots; some fragments retain relict froth structure. The rock also contains 5 to 7 percent small, angular, red-brown volcanic or red siltstone lithics that are generally less than 3 mm in size, but which may be as

much as 30 mm (1.2 inches) across. Zeolitic alteration associated with the development of secondary porosity appears to increase downward beginning at 1970–1980 ft (600–605 m) to about 2020–2030 ft (615–620 m), with open spaces occupied by some form of botryoidal recrystallized zeolite. Alteration intensity decreases noticeably from 2105 to 2133 ft (641.7–650.1 m), and the intensity decreases abruptly near the lower contact of this unit with the underlying tuffaceous sandstone. A one-foot thick (0.3-m), coarse-grained, pumice fall marks the base of unit 1; the pumice-fall deposit becomes slightly bedded toward the lower contact at 2133.0 ft (650.1 m).

Prow Pass tuffaceous sandstone unit (Tcpbs)
2133.0–2144.9 ft (650.1–653.8 m)

The lowermost unit of the Prow Pass Tuff is an immature, tuffaceous sandstone (Moyer and Geslin, 1995) that interingers with the overlying ash-flow tuff above through a vertical interval of approximately two ft. The sandstone is composed of an ash-rich matrix containing small clasts consisting of 20 to 30 percent pumice, 8 to 10 percent red siltstone lithics, 5 to 7 percent devitrified volcanic lithics, and 3 to 5 percent crystals of quartz, feldspar, biotite and pyroxene. The sandstone becomes deeply hematite stained and medium red in color below about 2138.0 ft (651.7 m). The base of the sandstone unit was placed at 2144.9 ft (653.8 m)

Bullfrog Tuff (Tcb) 2144.9 ft –TD (2166.3 ft)
(653.8–660.3 m)

Nonwelded ash-flow unit 4

Only 21.4 ft (6.5 m) of the upper Bullfrog Tuff in this hole was encountered in drill hole USW SD-12. The Bullfrog Tuff at this location is a nonwelded, zeolitized unit containing 30 to 40 percent white pumice clasts generally less than 20 mm (1.0 inch) across, 1 to 2 percent small, devitrified, volcanic lithics, and 3 to 5 percent phenocrysts including quartz, feldspar, fresh-looking biotite, and possibly pyroxene or hornblende. This unit has been correlated with the Bullfrog nonwelded ash-flow unit 4 that has been identified by Rautman and Engstrom (1996) in core from drill hole USW SD-7. Black Fe-Mn oxides coat some of the lithic

fragments and phenocrysts. The groundmass has been zeolitized and may be weakly vapor-phase altered; the resulting texture appears somewhat

microgranular. Drilling of the SD-12 borehole was terminated shortly below the upper contact of the Bullfrog Tuff.

Appendix B: Geologic Core Logs

Geologic Core Logs

The geologic core logs in this appendix are reproduced in color at their original full scale of 1:120 (1 inch equals 10 feet). Full-size reproduction means that the log sheets that follow have not been formatted or numbered in the same manner as the remainder of this document, although the page count of this report is continuous and the log-sheet pages are themselves numbered consecutively. Copies of the original log forms may be retrieved from the Yucca Mountain Project records system under data-tracking number SNT02012894001.002.

The log form (figure 1) contains a graphic representation of the actual geology of the core. Bedding within reworked units, clasts representing lithic fragments, lithophysal cavities, fractures, and similar textural features are drawn in a "cartoon," but still highly realistic, fashion. For example, large lithophysal cavities are drawn larger than small cavities, and flattened cavities in the core are represented as more oval features than spherical lithophysae. Near-vertical fracturing is represented by stylized fracture lines nearly parallel to the depth axis of the diagram, as such jointing is nearly parallel to the core axis in an essentially vertical drill hole, such as USW SD-12.

The degree of welding, devitrification, and the intensity of secondary alteration of the core is represented semiquantitatively by several parallel bars of vertically varying width. A blank column represents "no alteration" of the indicated type; a fully shaded column indicates "extremely intense alteration." This style of presentation can be very exact over short core distances (feet to tens of feet) and it allows relatively subtle, small-scale variation in these phenomena to be represented quite precisely. The gradational nature of several lithostratigraphic "contacts" becomes quite obvious in this manner. The representation, however, is not rigorously quantitative, and a 3-mm-wide bar at one depth should not be presumed to represent precisely the same intensity of that phenomenon as a 3-mm-wide bar several hundred feet away. Note that the type of alteration indicated by a particular column may change with depth to conserve space on the

log form; the column headings are kept consistent over broad depth ranges, however.

Engineering and geologic information related to the core itself is also presented on the log sheets. Highly broken or rubblized zones are indicated by a shaded pattern in the fracturing column, and intervals of core loss are indicated by arrows extending through the indicated interval of non-recovery. The geology of these unrecovered intervals has been interpreted through the intervals of core loss where there is reasonable evidence for such an interpretation (for example, down-hole-video imagery or a relatively consistent lithology in a known, thick geologic unit) Large intervals of lost core in geologic units known from outcrop or other drill holes to be highly variable vertically have been left uninterpreted. Note that drilling support staff assigned lost-core intervals by convention to the bottom of the core run, whereas the actual core loss may have occurred at multiple levels during the drilling of a particular run. Quantitative information (varying from 0 to 100) for per-run core recovery and 10-ft-composite, drilling-support Deere RQD values (from tables C-1 and D-2) are presented in columns to the right of the geologic descriptions.

The framework material properties, porosity and bulk density (from table G-1) are presented in similar columnar-graphic form to the right of the core-recovery and RQD information. Saturated hydraulic conductivity information does not present well because the wide (orders-of-magnitude) variability of this framework property requires a logarithmic scale; these values have been omitted from the core log. Saturation values, however, have been included as this information may bear on the identification of geologic controls of perched-water bodies. These graphic representations of materials-property data contain quantitative information. Porosity values are scaled from 0 to 70 percent, bulk density values are scaled from 1.0 to 3.0 g/cm³, and saturation is scaled from 0 to 1. The locations of changes in the porosity and density of core samples clearly indicate that the boundaries between material property units do not correspond exactly to the boundaries of the different formation-level lithostratigraphic units (Tiva Canyon Tuff, Bullfrog Tuff, etc.).

Note: This page and the color log sheet pages that follow are single sided.

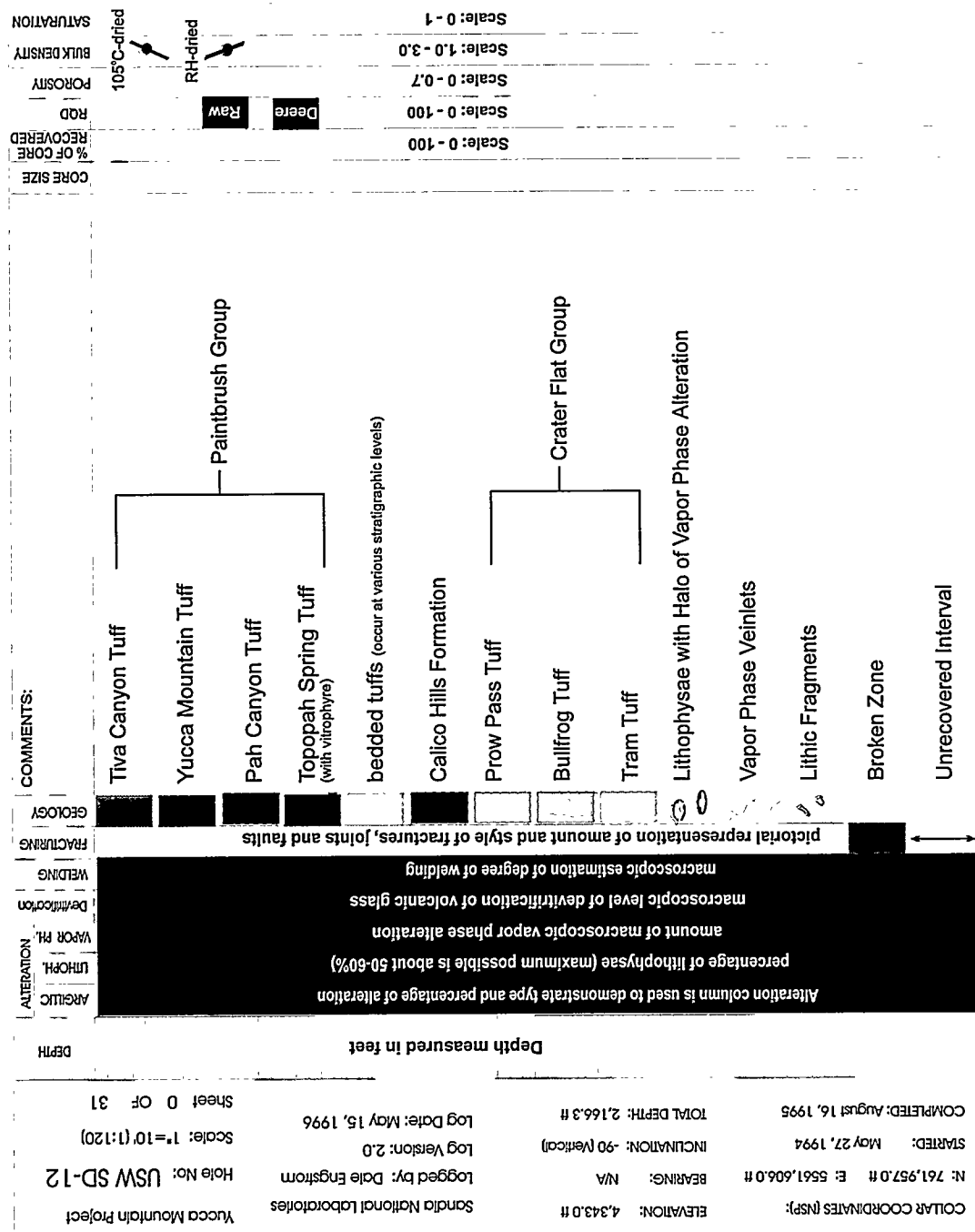


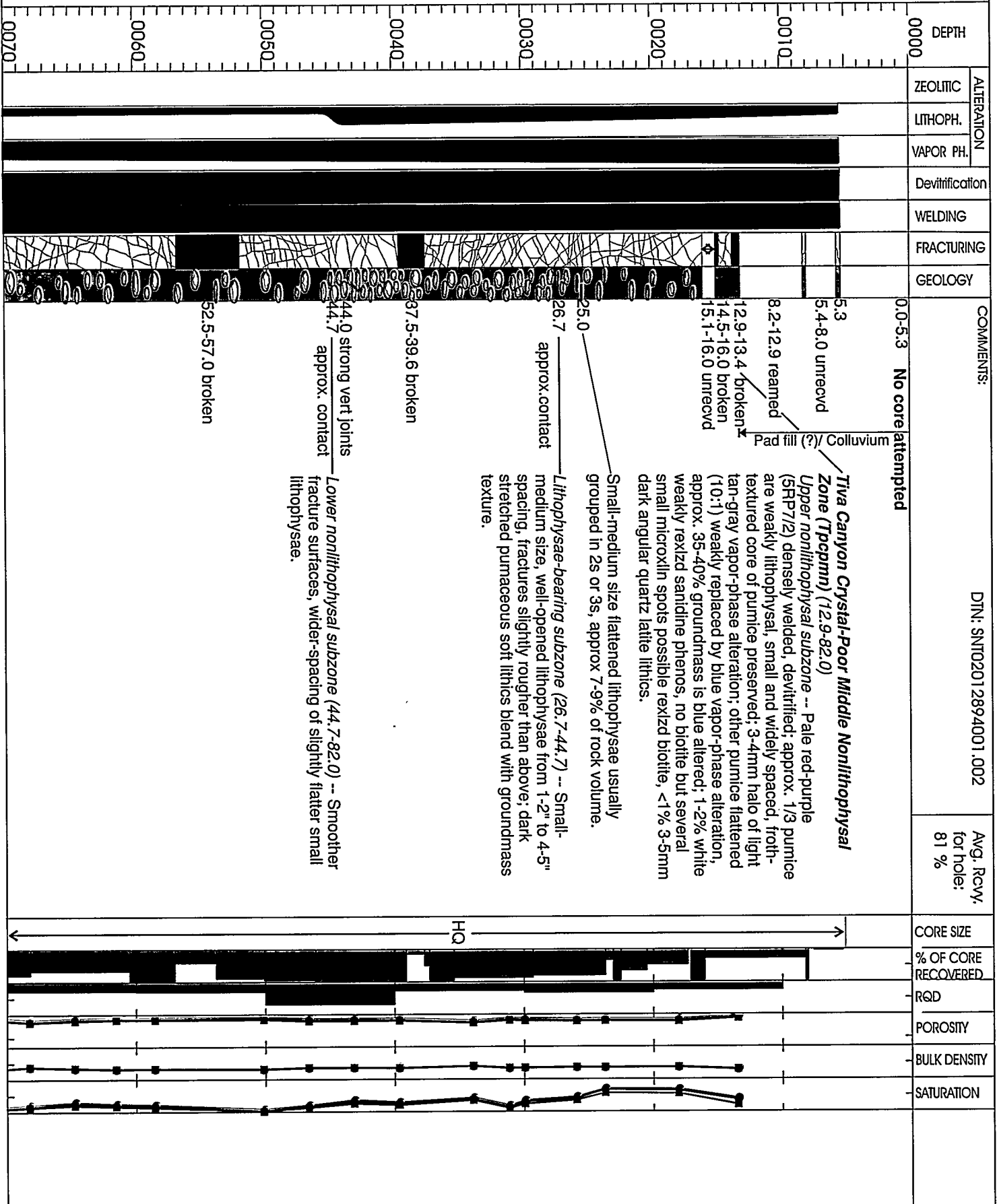
Figure B-1. Example geologic core log form with parallel columns for representing various geologic features and other quantitative and semiquantitative information as a function of depth.

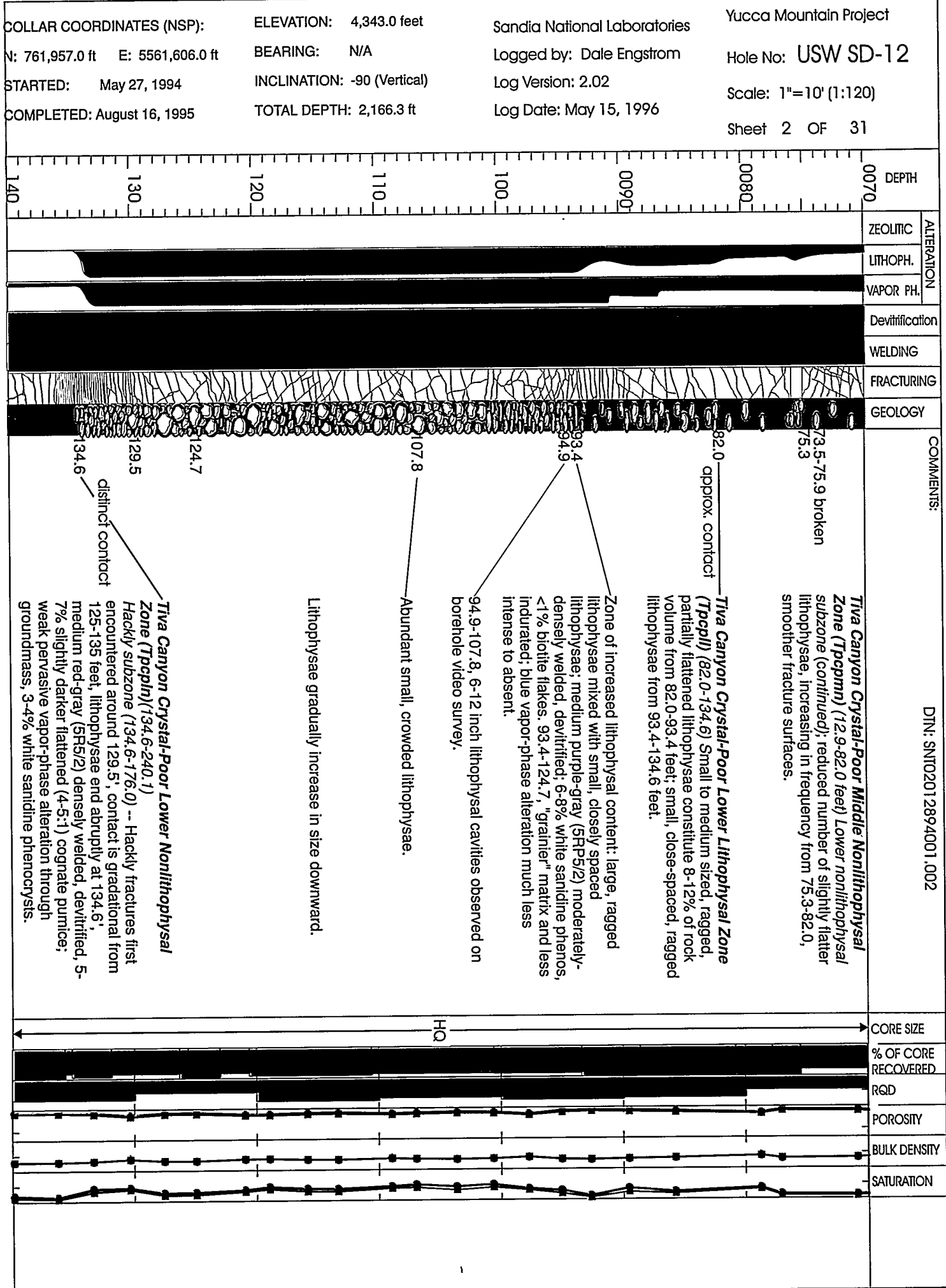
COLLAR COORDINATES (NSP):
N: 761,957.0 ft E: 5561,606.0 ft
STARTED: May 27, 1994
COMPLETED: August 16, 1995

ELEVATION: 4,343.0 ft
BEARING: N/A
INCLINATION: -90 (Vertical)
TOTAL DEPTH: 2,166.3 ft

Sandia National Laboratories
Logged by: Dale Engstrom
Log Version: 2.02
Log Date: May 15, 1996

Yucca Mountain Project
Hole No: USW SD-12
Scale: 1"=10' (1:120)
Sheet 1 OF 31



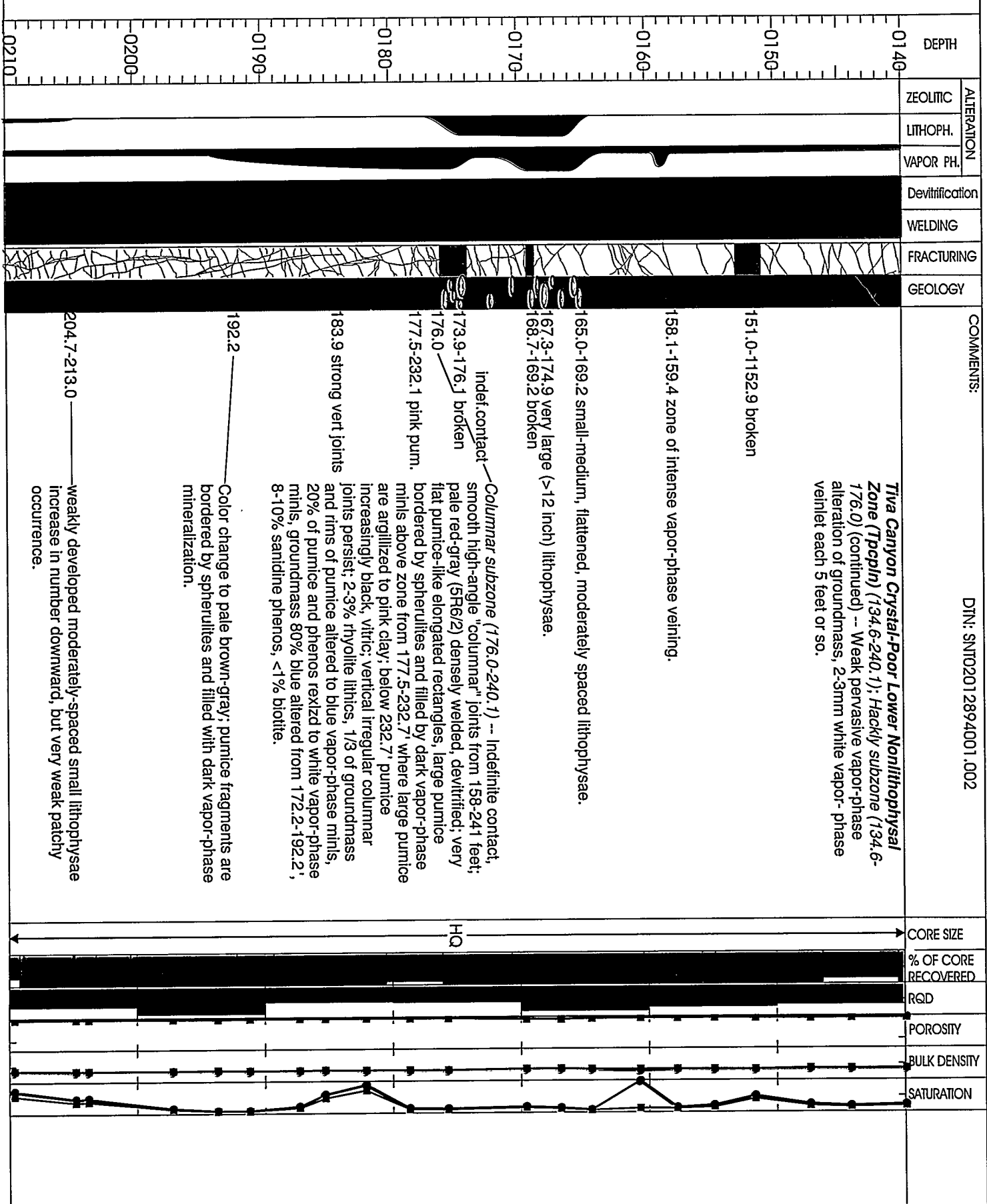


COLLAR COORDINATES (NSP):
N: 761,957.0 ft E: 5561,606.0 ft
STARTED: May 27, 1994
COMPLETED: August 16, 1995

ELEVATION: 4,343.0 feet
BEARING: N/A
INCLINATION: -90 (Vertical)
TOTAL DEPTH: 2,166.3 ft

Sandia National Laboratories
Logged by: Dale Engstrom
Log Version: 2.02
Log Date: May 15, 1996

Yucca Mountain Project
Hole No: USW SD-12
Scale: 1"=10' (1:120)
Sheet 3 OF 31



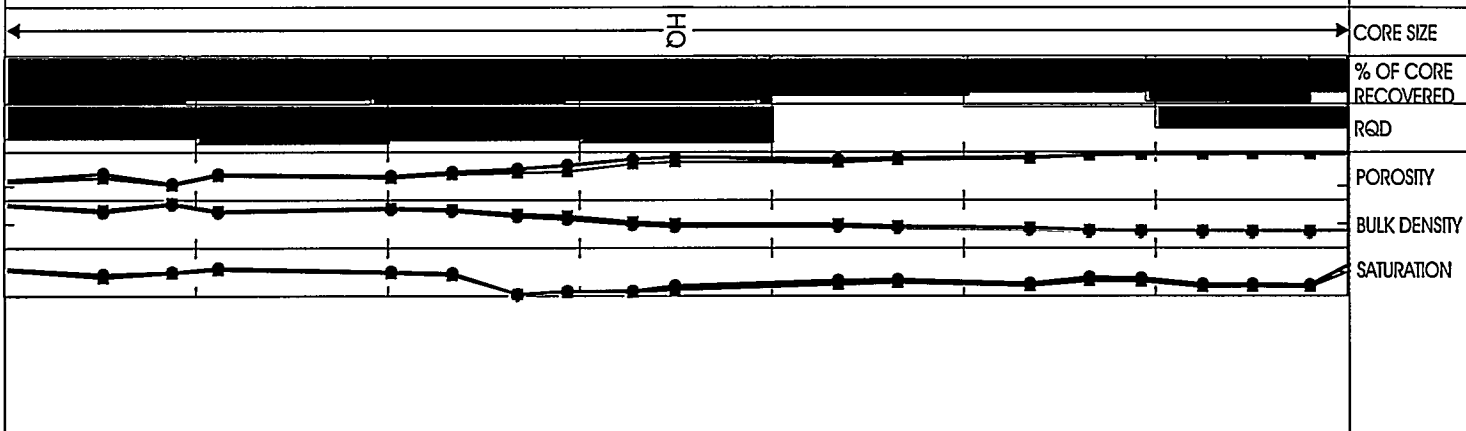
COLLAR COORDINATES (NSP):
N: 761,957.0 ft E: 5561,606.0 ft
STARTED: May 27, 1994
COMPLETED: August 16, 1995

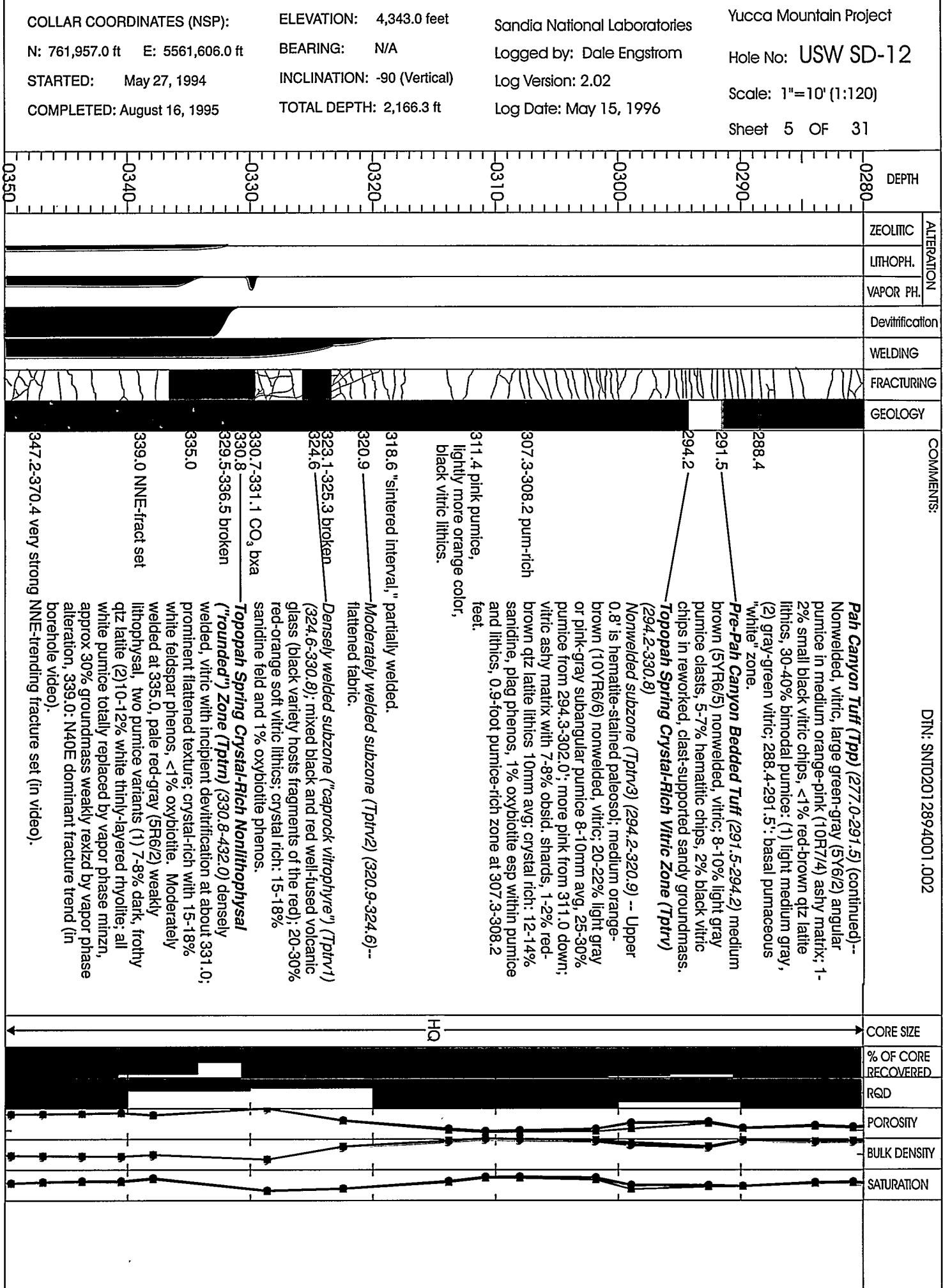
ELEVATION: 4,343.0 ft
BEARING: N/A
INCLINATION: -90 (Vertical)
TOTAL DEPTH: 2,166.3 ft

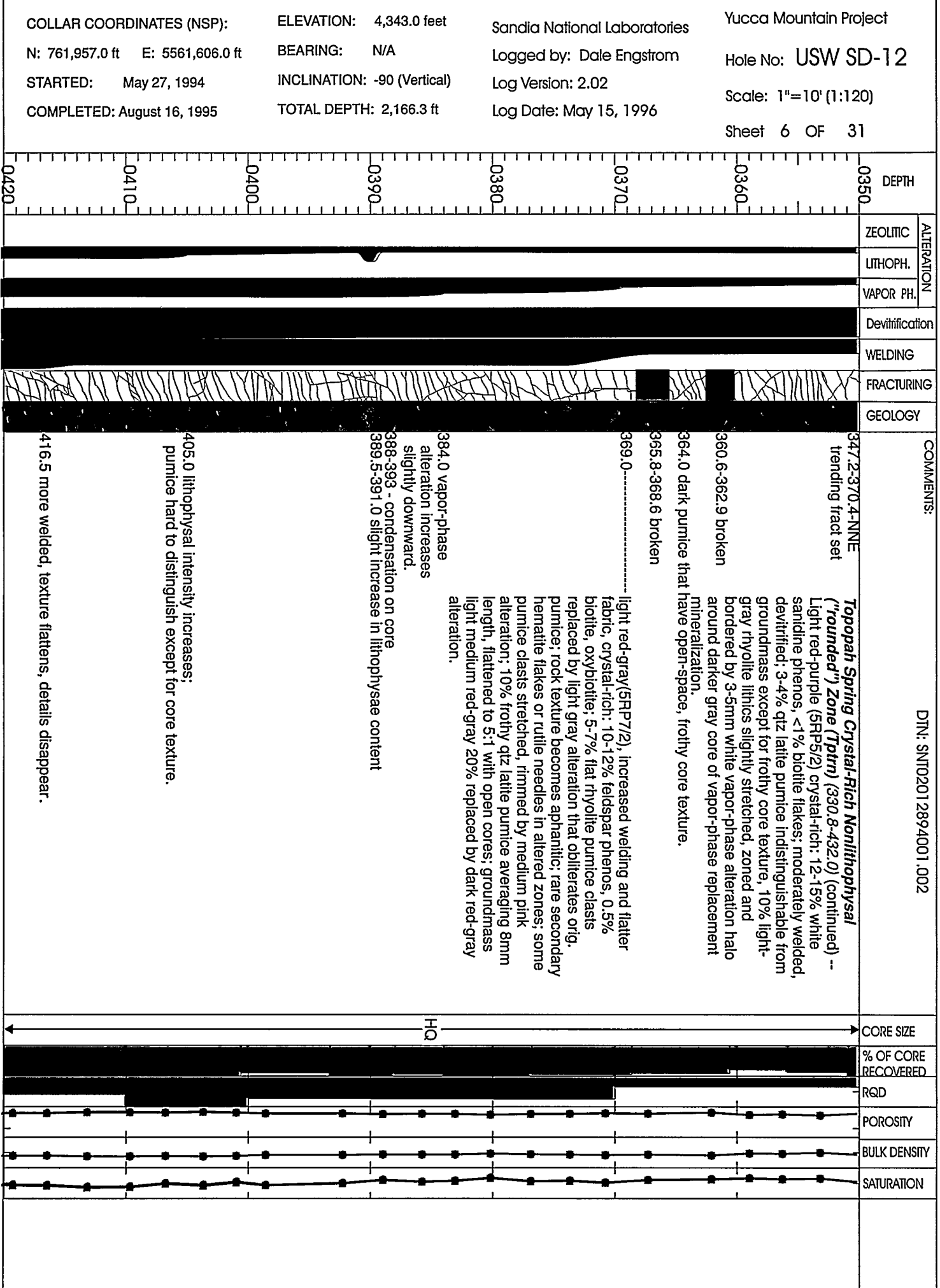
Sandia National Laboratories
Logged by: Dale Engstrom
Log Version: 2.02
Log Date: May 15, 1996

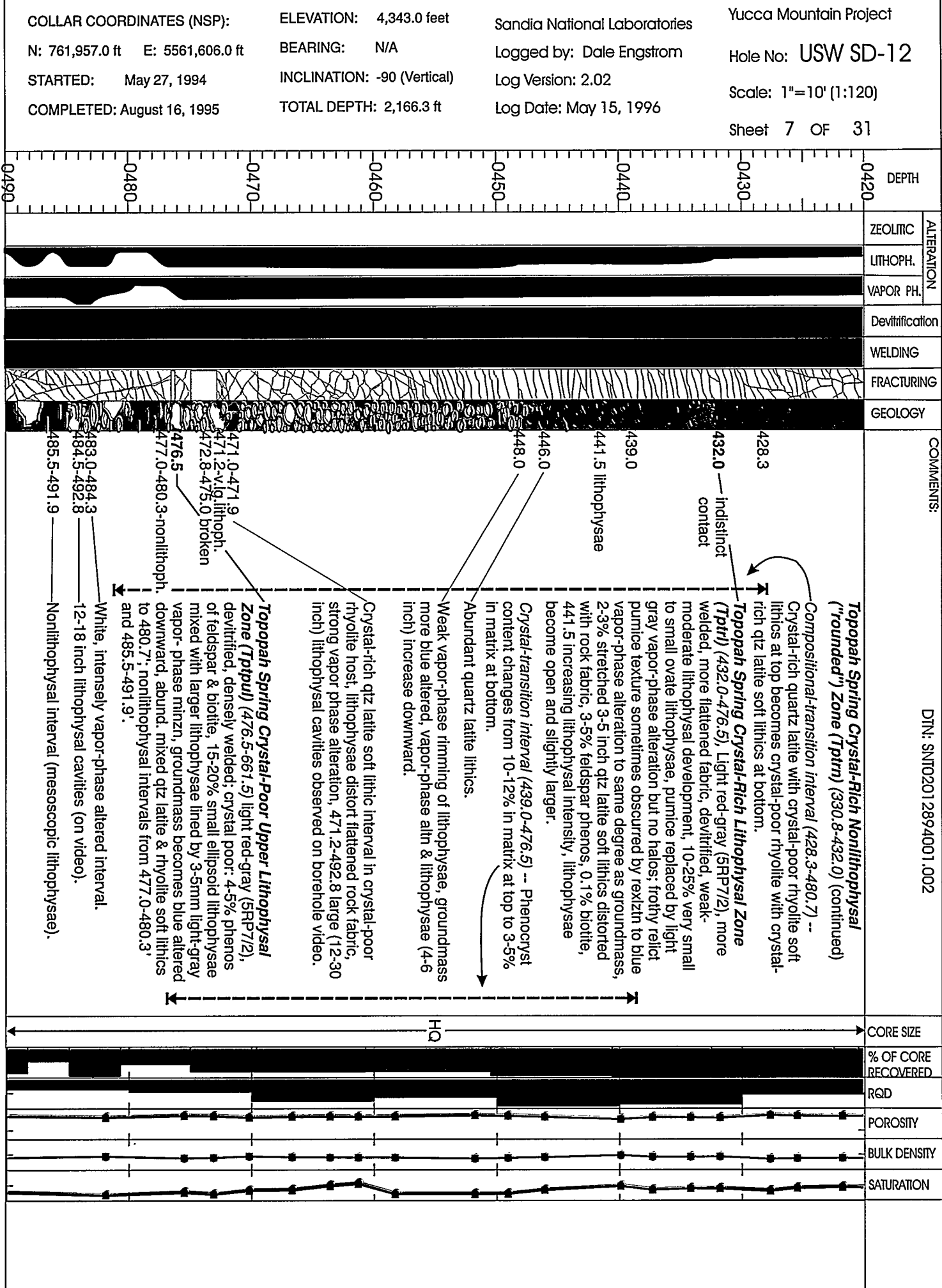
Yucca Mountain Project
Hole No: USW SD-12
Scale: 1"=10' (1:120)
Sheet 4 OF 31

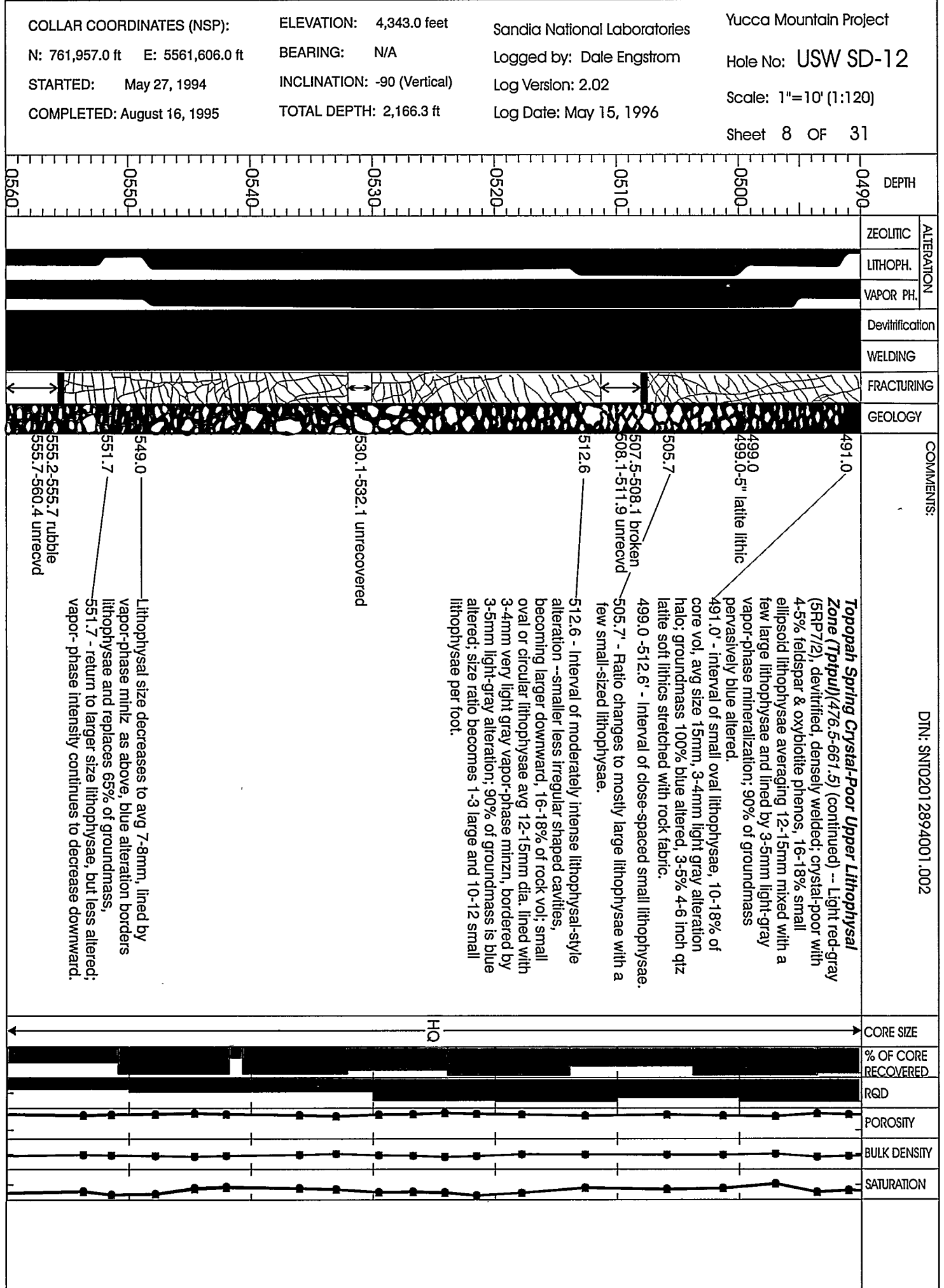
DEPTH	ALTERATION	ZEOLITIC	LITHOPH.	VAPOR PH.	GEOLOGY		COMMENTS:
					Devitrification	WELDING	
0210							
0220							
0230							
0240							
0250							
0260							
0270							
0280							

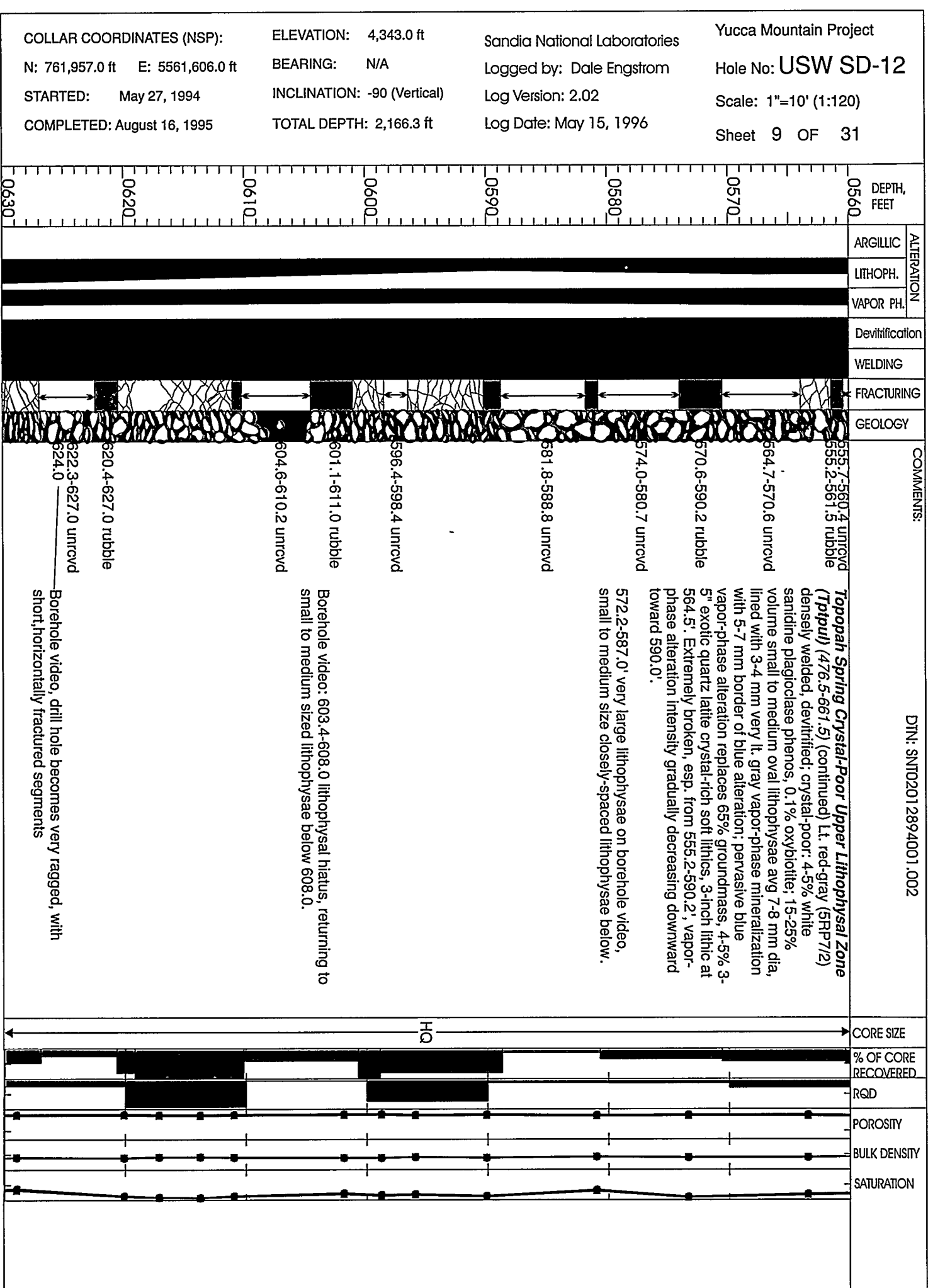


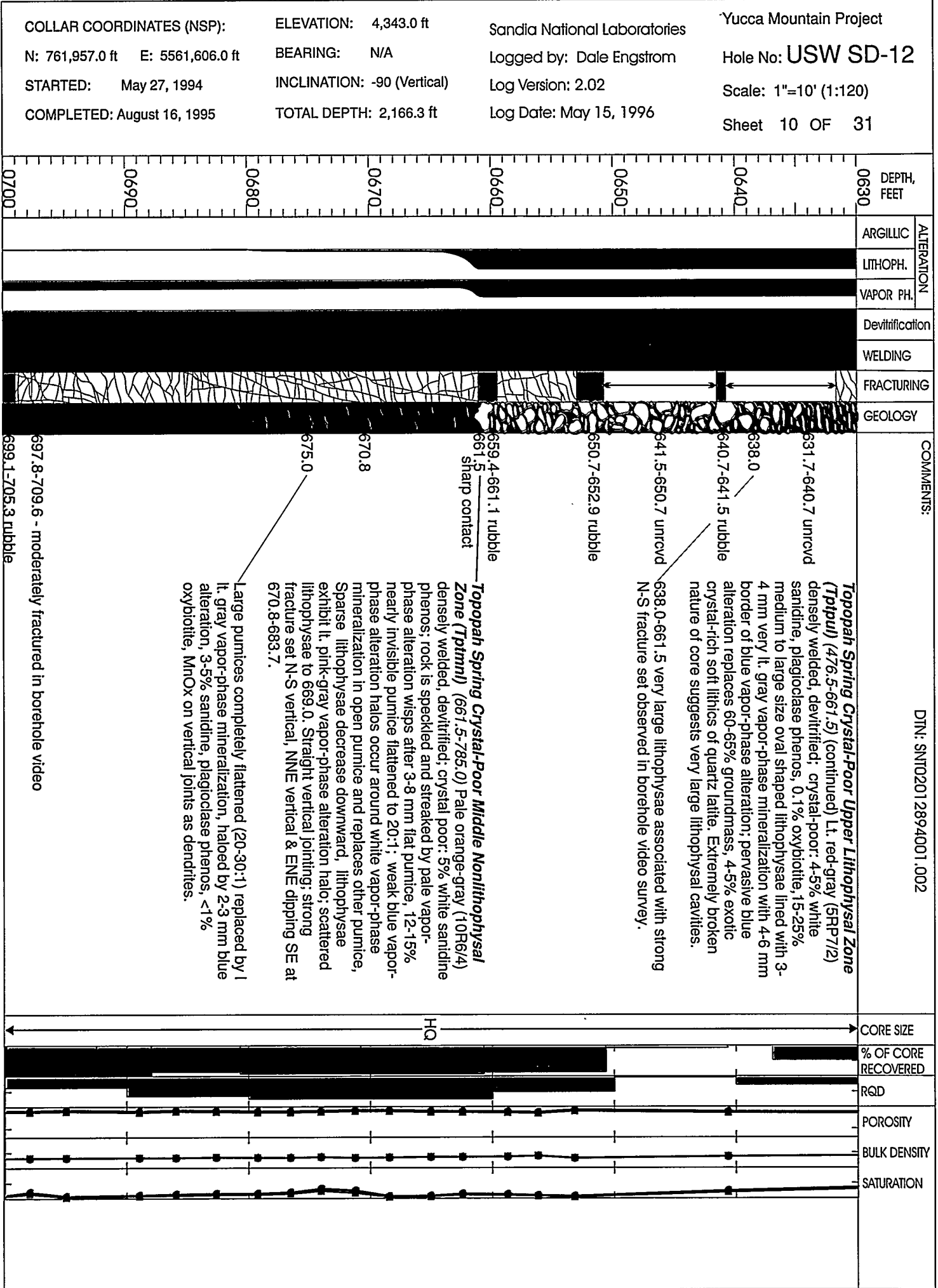












COLLAR COORDINATES (NSP):
N: 761,957.0 ft E: 5561,606.0 ft
STARTED: May 27, 1994
COMPLETED: August 16, 1995

ELEVATION: 4,343.0 ft
BEARING: N/A
INCLINATION: -90 (Vertical)
TOTAL DEPTH: 2,166.3 ft

Sandia National Laboratories
Logged by: Dale Engstrom
Log Version: 2.02
Log Date: May 15, 1996

Yucca Mountain Project
Hole No: **USW SD-12**
Scale: 1"=10' (1:120)
Sheet 11 OF 31

DTN: SNT02012894001.002

DEPTH, FEET	ALTERATION	COMMENTS:		
		ARGILLIC	LITHOPH.	VAPOR PH.
0700	Devitrification			
0710	WELDING			
0720	FRACTURING			
0730	GEOLOGY			
699.1-705.3 rubble	<i>Topopah Spring Crystal-Poor Middle Nonlithophysal Zone (Tpfpul)</i> (661.5-785.0) (continued) Pale orange-gray (10R6/4) densely welded, devitrified; crystal-poor: 3-5% white sardine phenos, <1% oxybiotite; 12-15% of rock is speckled and streaked by 3-8 mm wisps of lt-gray vapor-phase alteration after mm-size nearly invisible pumice flattened to 15-20:1, former large pumice completely flat (30:1) become more sparse downward, replaced by light-gray vapor-phase mineralization, 2-3 mm blue vapor-phase alteration halo; straight vertical joints persist; 704.5: slight increase of vapor-phase alteration of groundmass (grayer); 709.6-723.8: strong fracture set with large voids in borehole video; 723.8: moderately fractured to 773.2,			
704.5				
709.6				
708.8-716.7 broken				
716.7-720.6 unrcvd				
720.6-724.3 broken				
724.3-726.4 unrcvd				
726.4-729.9 broken				
734.5	Increased size and number of alteration speckles and halos; also increase in number of lithics, mostly (80%) small subround cognate rhyolite lithics, flattened and soft; 17% of lithics are exotic crystal-rich, hard quartz latite; 3-4% very small rhyolite hard lithics,			
734.8 - 25mm rhyolite lithic				
738.0	738.0-739.0 slight increase in blue alteration.			
739.9-742.5 rubble				
747.4 - 20mm rhyo.lithic				
747.9-750.0 rubble	Pale red (10R6/2) fine, dense grained, densely welded, devitrified 10-15% speckled by lt. tan-gray vapor-phase alteration streaks nucleated by micropumice and small lithics; below 750 most small pumice weakly blue altered with lt. tan-gray 1-2 mm halo; 3-4% small subround crystal-rich quartz latite hard lithics, 1% very small rhyolite hard lithics, 1% sardine phenos, no biotite seen, severely broken, most natural fractures coated and hardened by vapor-phase SiO ₂ and speckled by 2-3 mm MnO _x spots.			
753.1-755.0 rubble				
756.6-759.8 rubble				
762.0-787.0				
767.8-769.0 rubble	Hematite vapor-phase SiO ₂ veinlets with 2-3 mm lt. gray vapor-phase alteration halo.			

↔ CORE SIZE

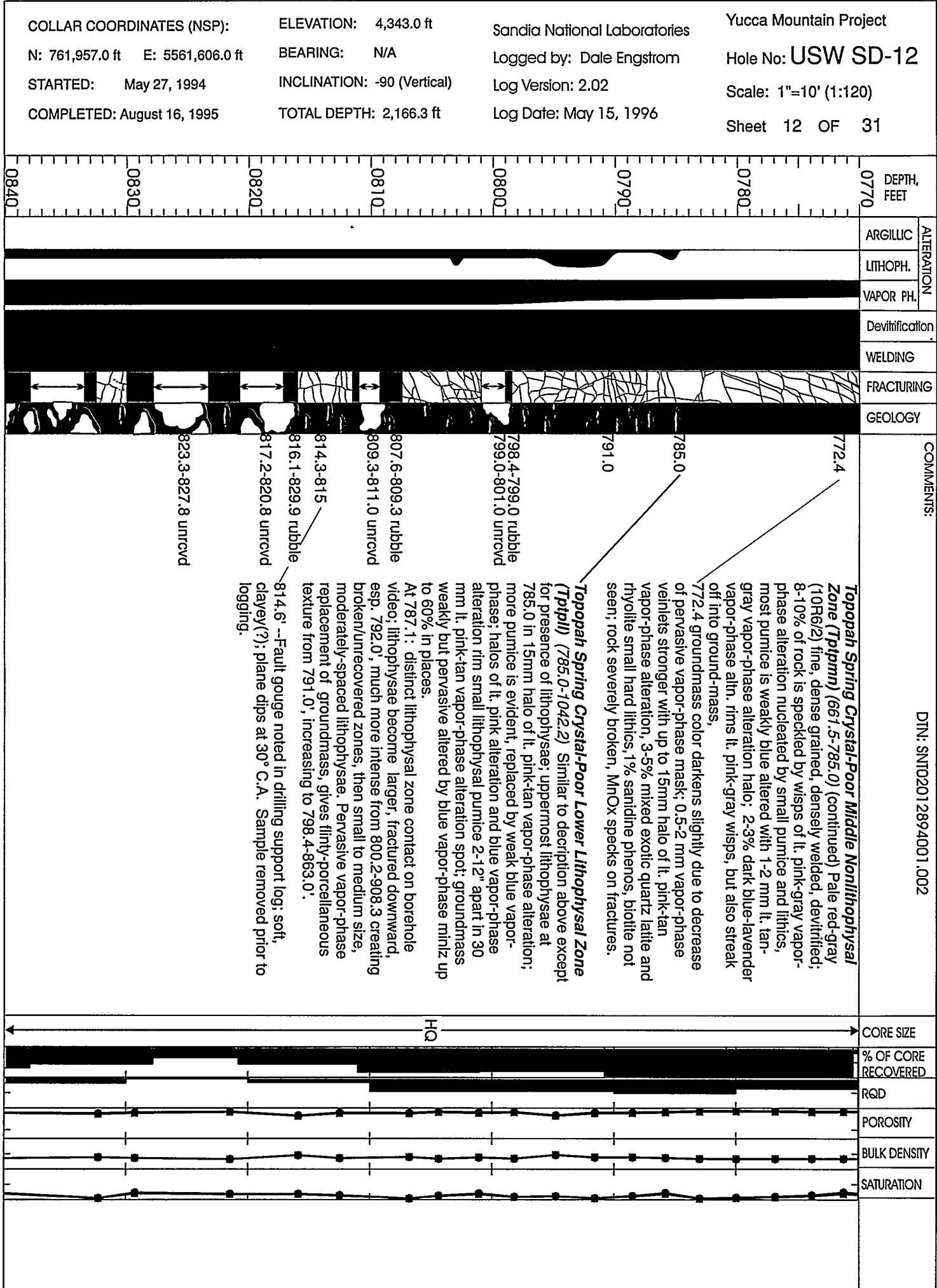
↔ % OF CORE RECOVERED

↔ RQD

↔ POROSITY

↔ BULK DENSITY

↔ SATURATION



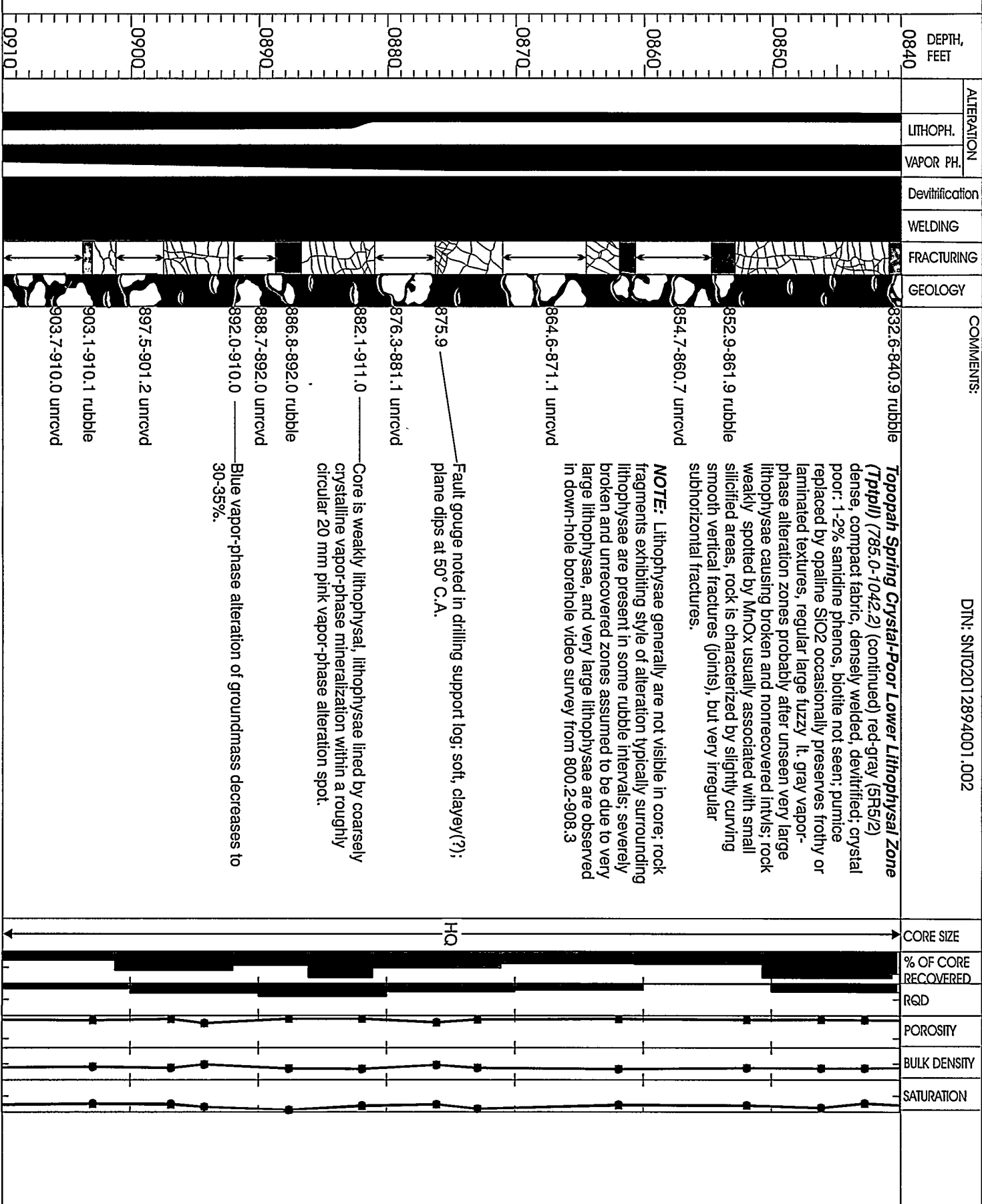
DTN: SNTO201289401.002

COLLAR COORDINATES (NSP):
N: 761,957.0 ft E: 5561,606.0
STARTED: May 27, 1994
COMPLETED: August 16, 1995

ELEVATION: 4,343.0 ft
BEARING: N/A
INCLINATION: -90 (Vertical)
TOTAL DEPTH: 2,166.3 ft

Sandia National Laboratories
Logged by: Dale Engstrom
Log Version: 2.02
Log Date: May 15, 1996

Yucca Mountain Project
Hole No: USW SD-12
Scale: 1"=10' (1:120)
Sheet 13 OF 31

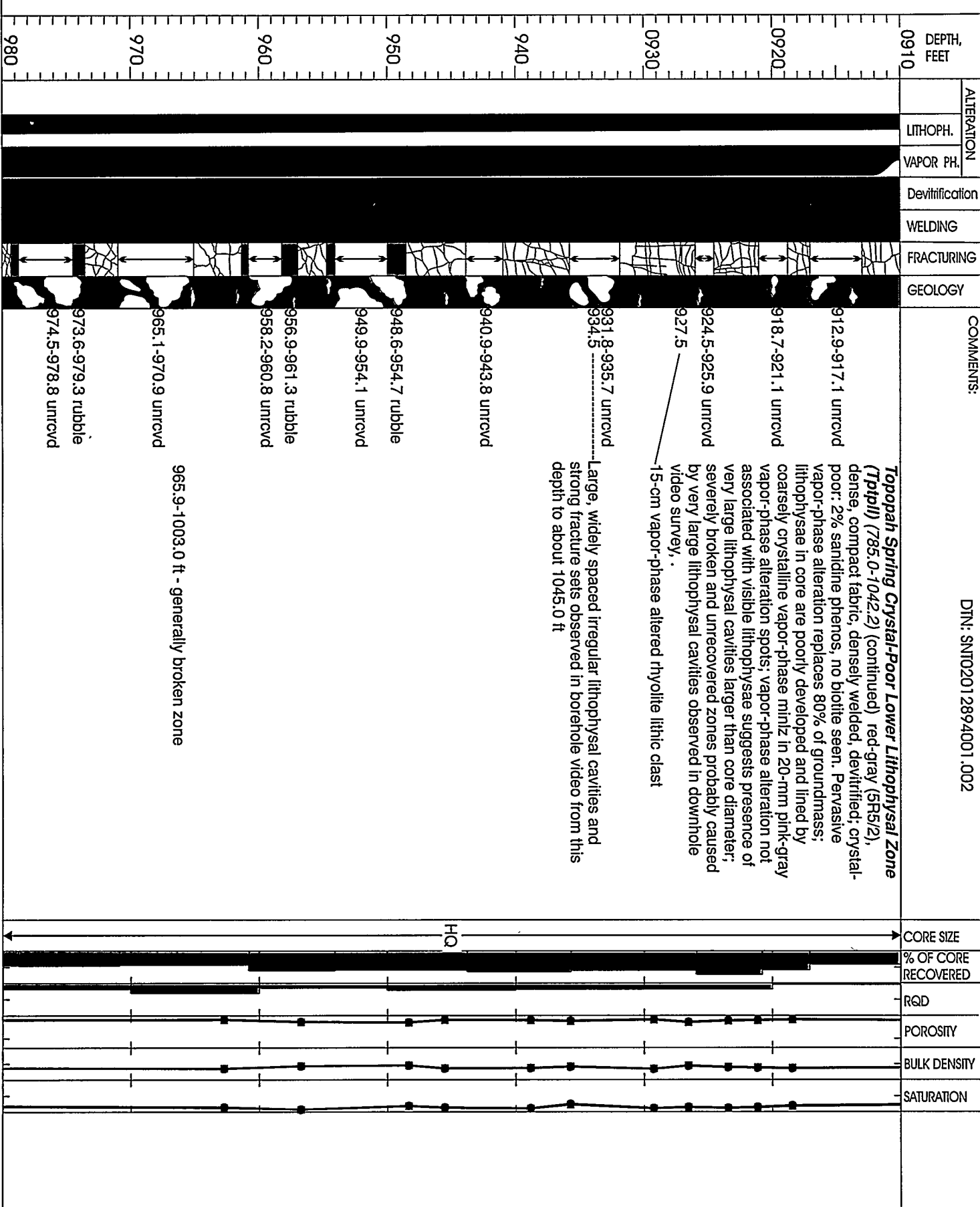


COLLAR COORDINATES (NSP):
N: 761,957.0 ft E: 5561,606.0
STARTED: May 27, 1994
COMPLETED: August 16, 1995

ELEVATION: 4,343.0 ft
BEARING: N/A
INCLINATION: -90 (Vertical)
TOTAL DEPTH: 2,166.3 ft

Sandia National Laboratories
Logged by: Dale Engstrom
Log Version: 2.02
Log Date: May 15, 1996

Yucca Mountain Project
Hole No: USW SD-12
Scale: 1"=10' (1:120)
Show: 14 SE - 21

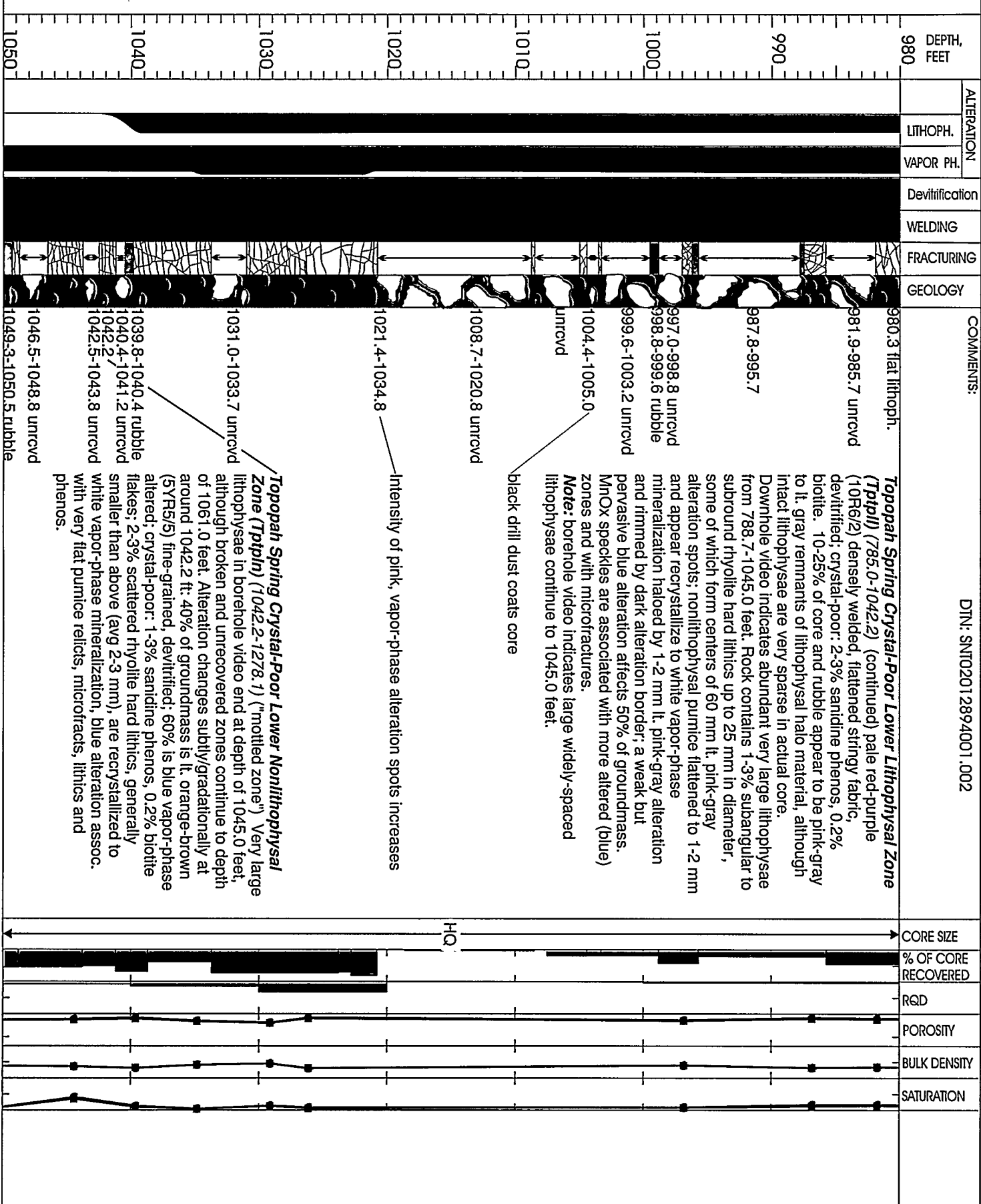


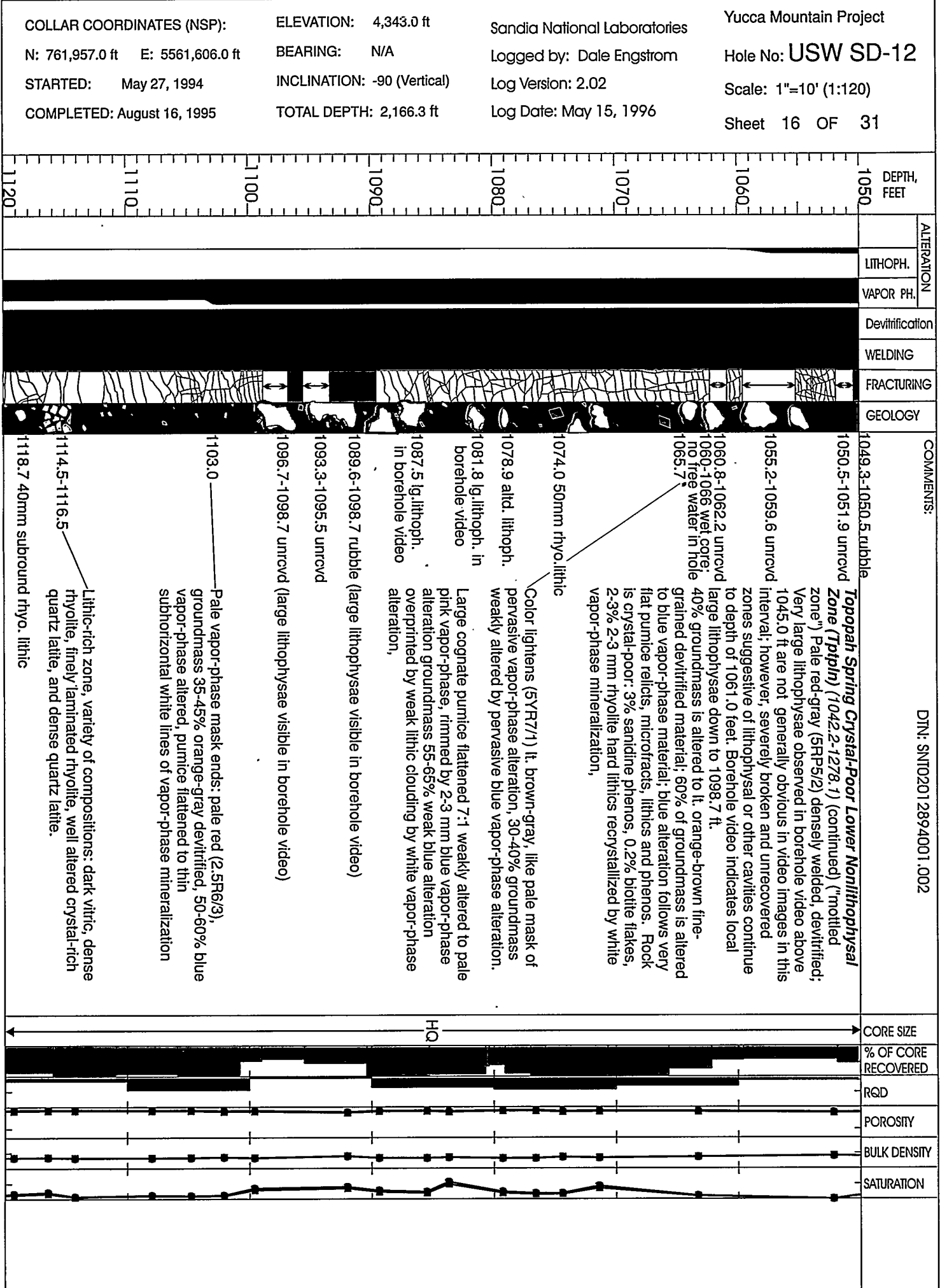
COLLAR COORDINATES (NSP):
N: 761,957.0 ft E: 5561,606.0
STARTED: May 27, 1994
COMPLETED: August 16, 1995

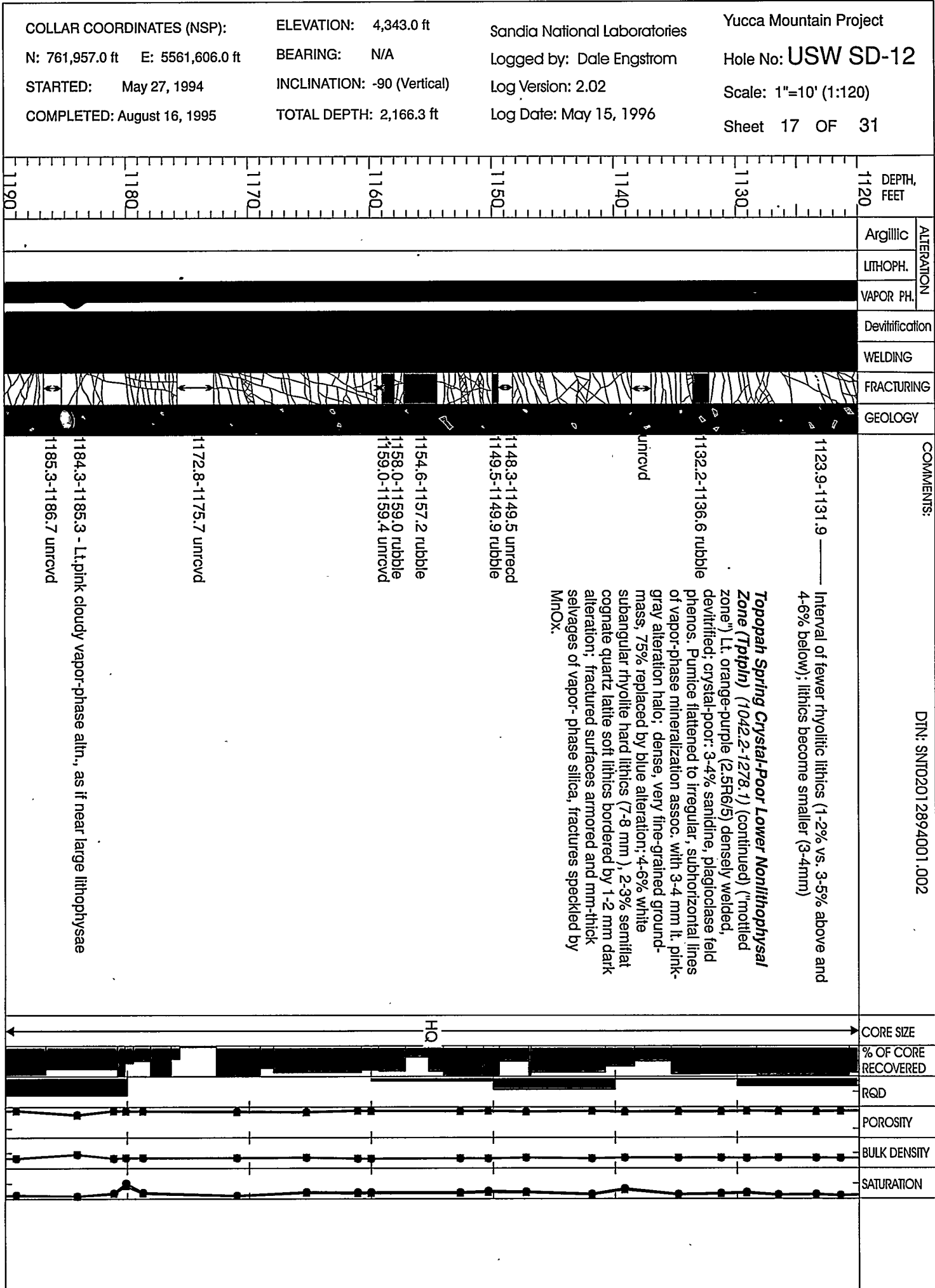
ELEVATION: 4,343.0 ft
BEARING: N/A
INCLINATION: -90 (Vertical)
TOTAL DEPTH: 2,166.3 ft

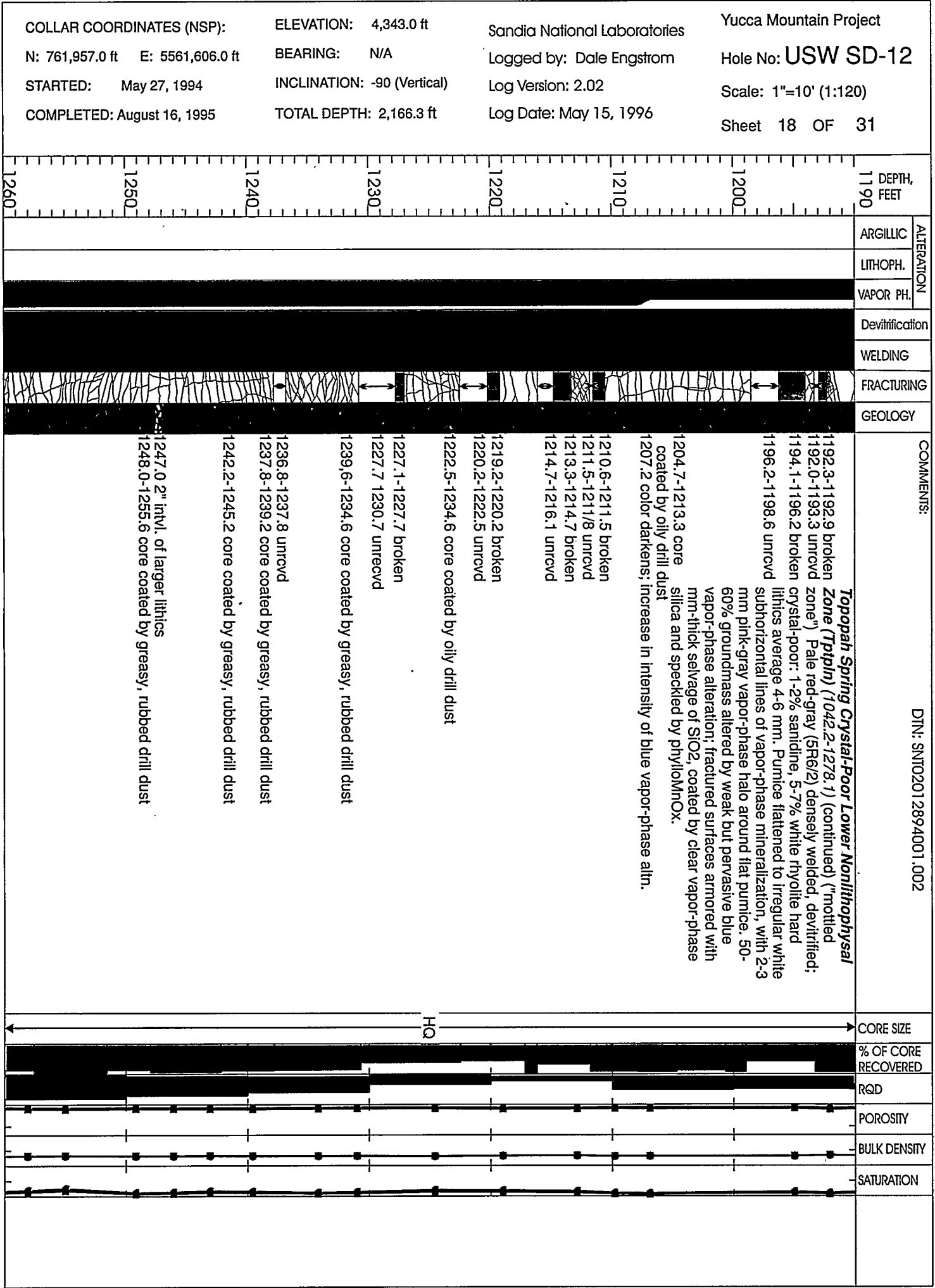
Sandia National Laboratories
Logged by: Dale Engstrom
Log Version: 2.02
Log Date: May 15, 1996

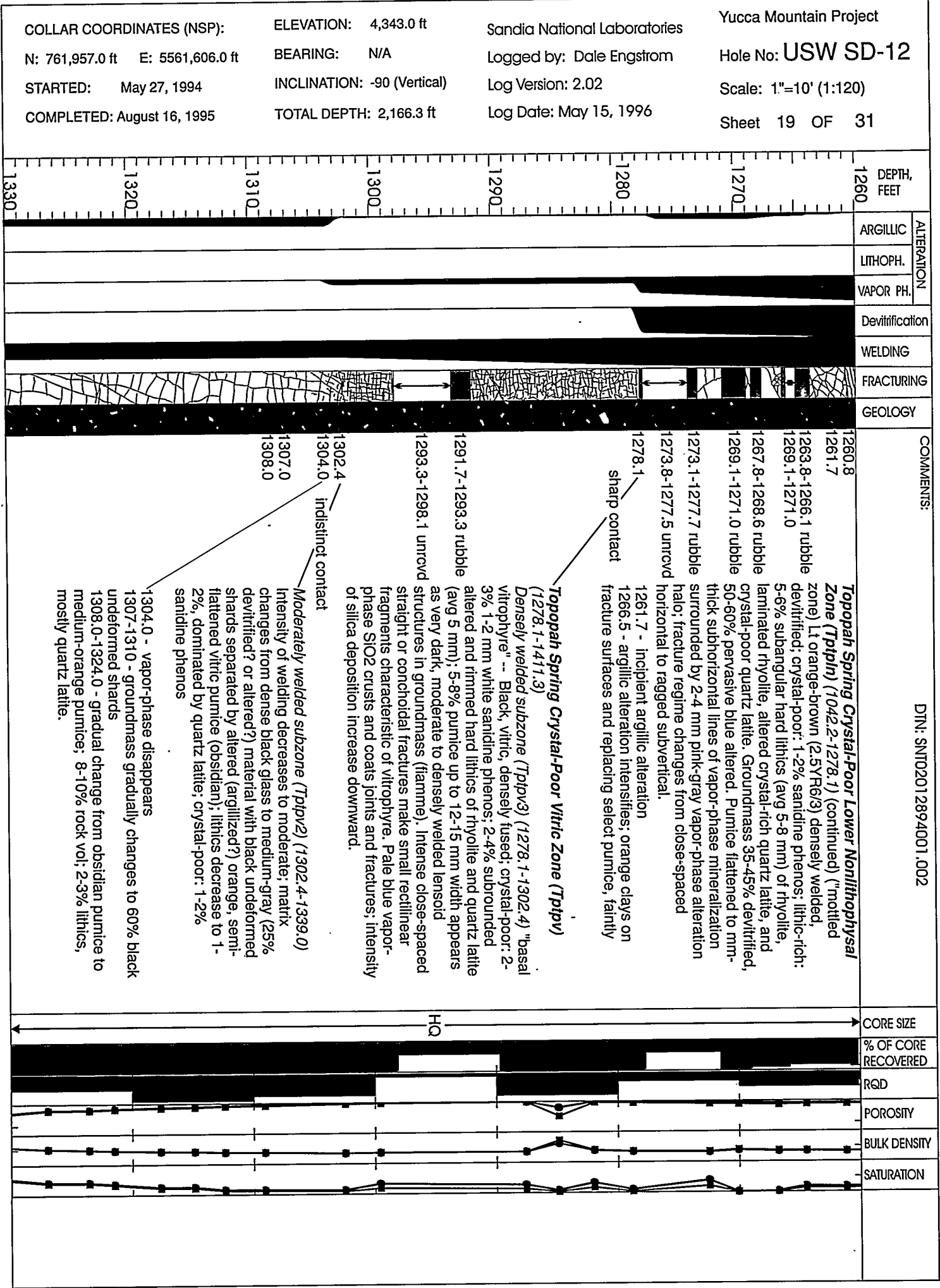
Yucca Mountain Project
Hole No: USW SD-12
Scale: 1"=10' (1:120)
Sheet 15 OF 31

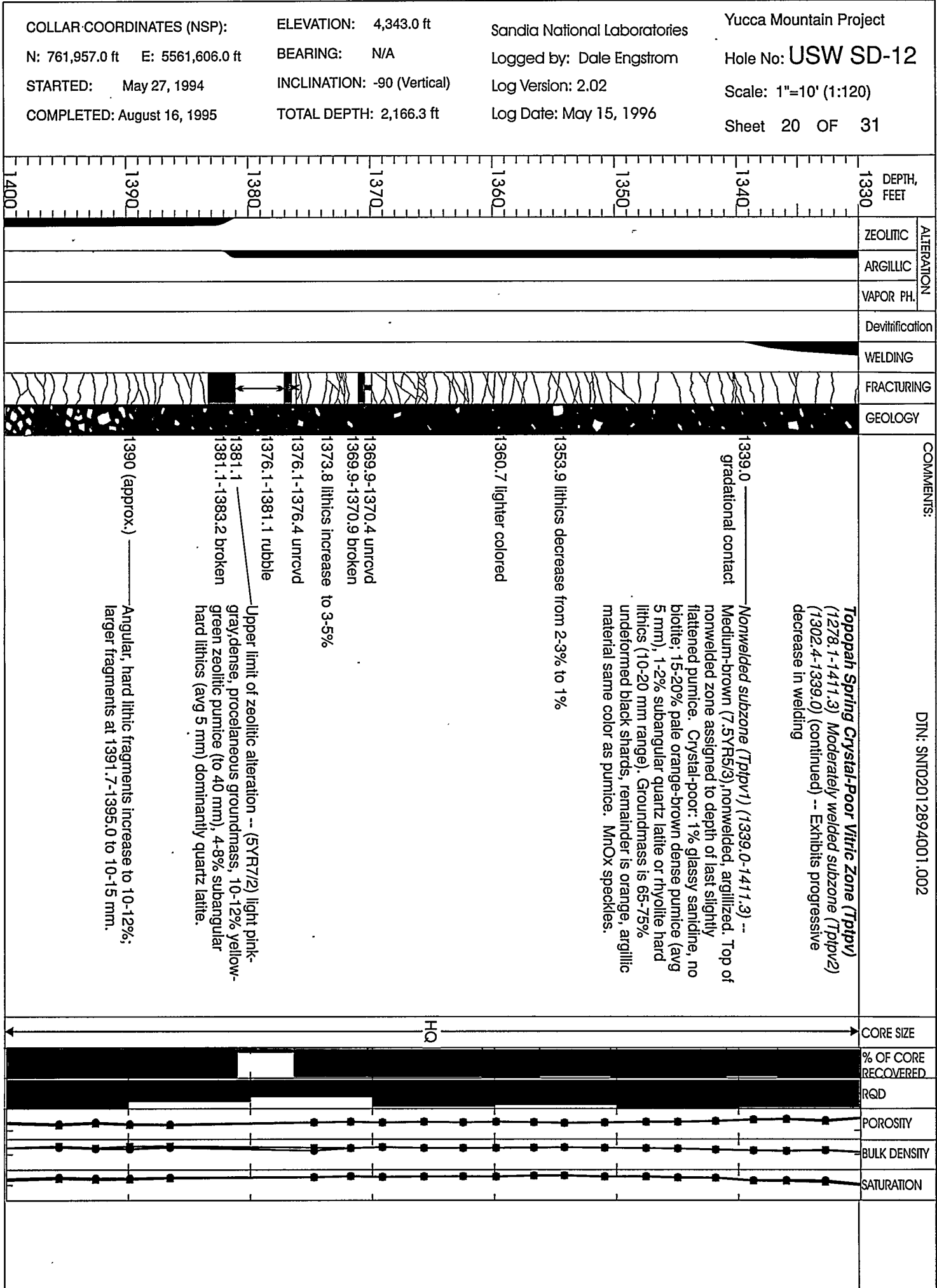












COLLAR COORDINATES (NSP):
N: 761,957.0 ft E: 5561,606.0
STARTED: May 27, 1994
COMPLETED: August 16, 1995

ELEVATION: 4,343.0 ft
BEARING: N/A
INCLINATION: -90 (Vertical)
TOTAL DEPTH: 2,166.3 f

Sandia National Laboratories
Logged by: Dale Engstrom
Log Version: 2.02
Log Date: May 15, 1996

Yucca Mountain Project
Hole No: USW SD-12
Scale: 1"=10' (1:120)
Sheet 21 OF 31

COLLAR COORDINATES (NSP):
N: 761,957.0 ft E: 5561,606.0 ft
STARTED: May 27, 1994
COMPLETED: August 16, 1995

ELEVATION: 4,343.0 ft

BEARING: N/A

INCLINATION: -90 (Vertical)

TOTAL DEPTH: 2,166.3 ft

Sandia National Laboratories

Logged by: Dale Engstrom

Log Version: 2.02

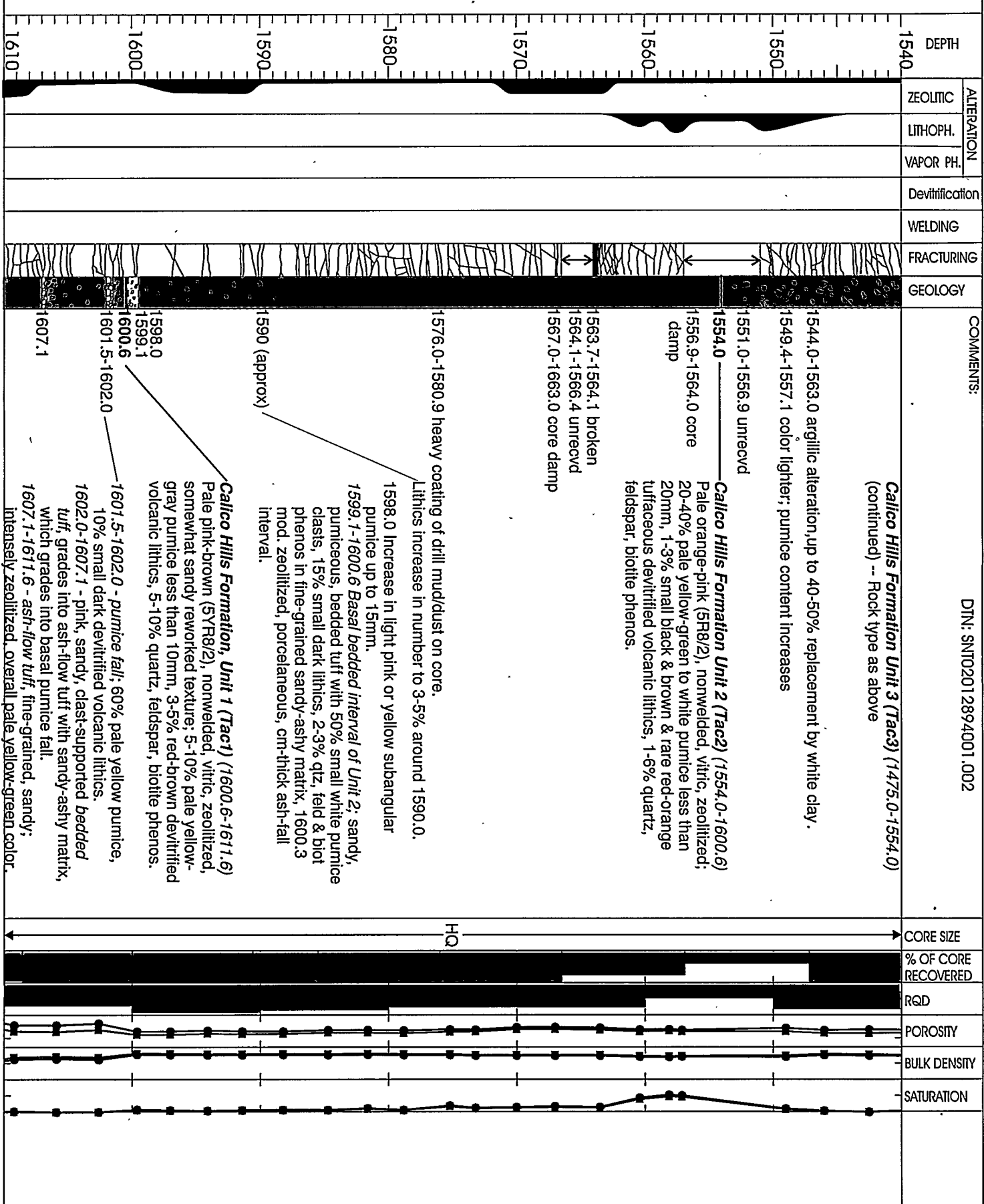
Log Date: May 15, 1996

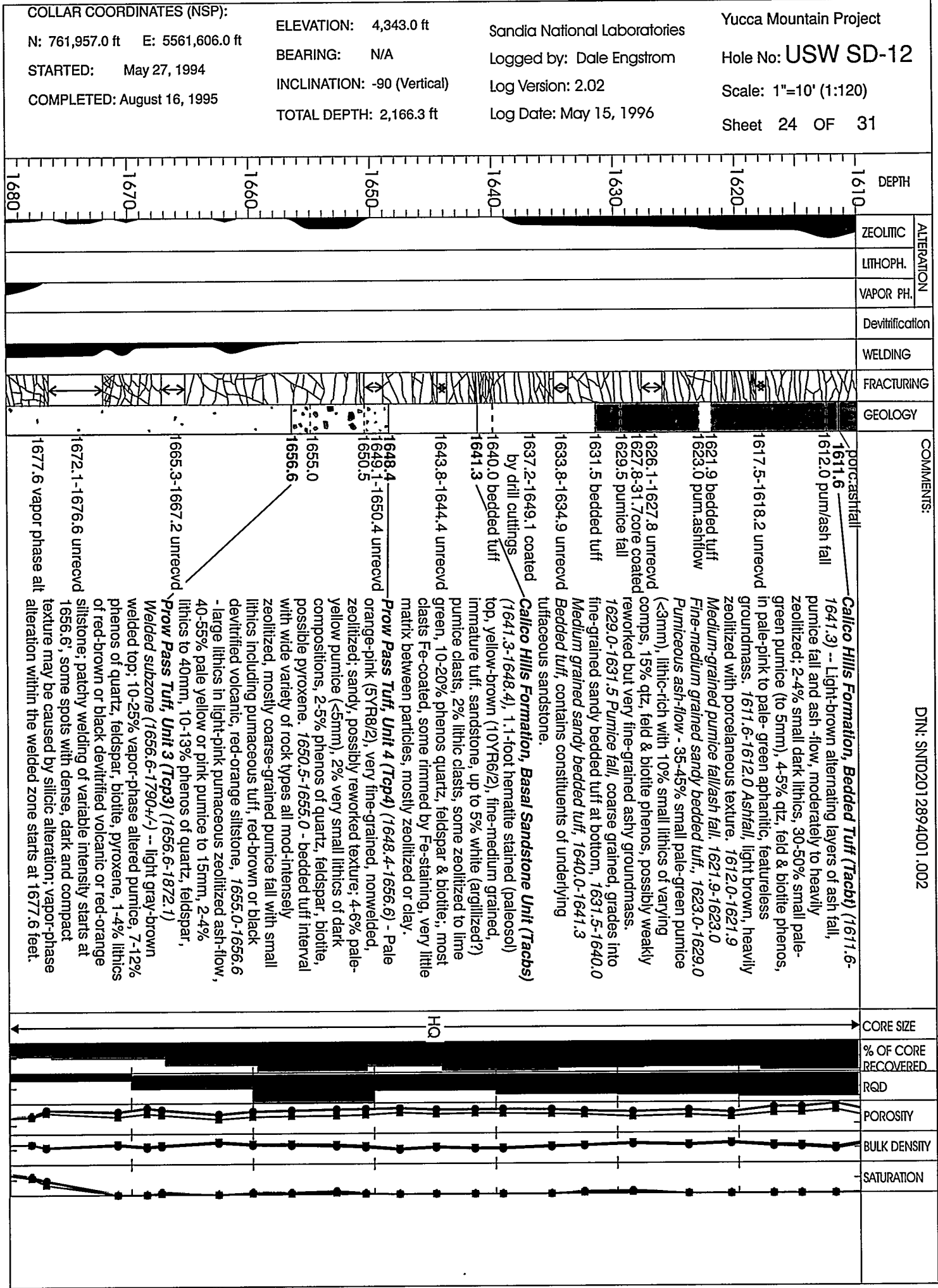
Yucca Mountain Project.

Hole No: USW SD-12

Scale: 1"=10' (1:120)

Sheet 23 OF 31



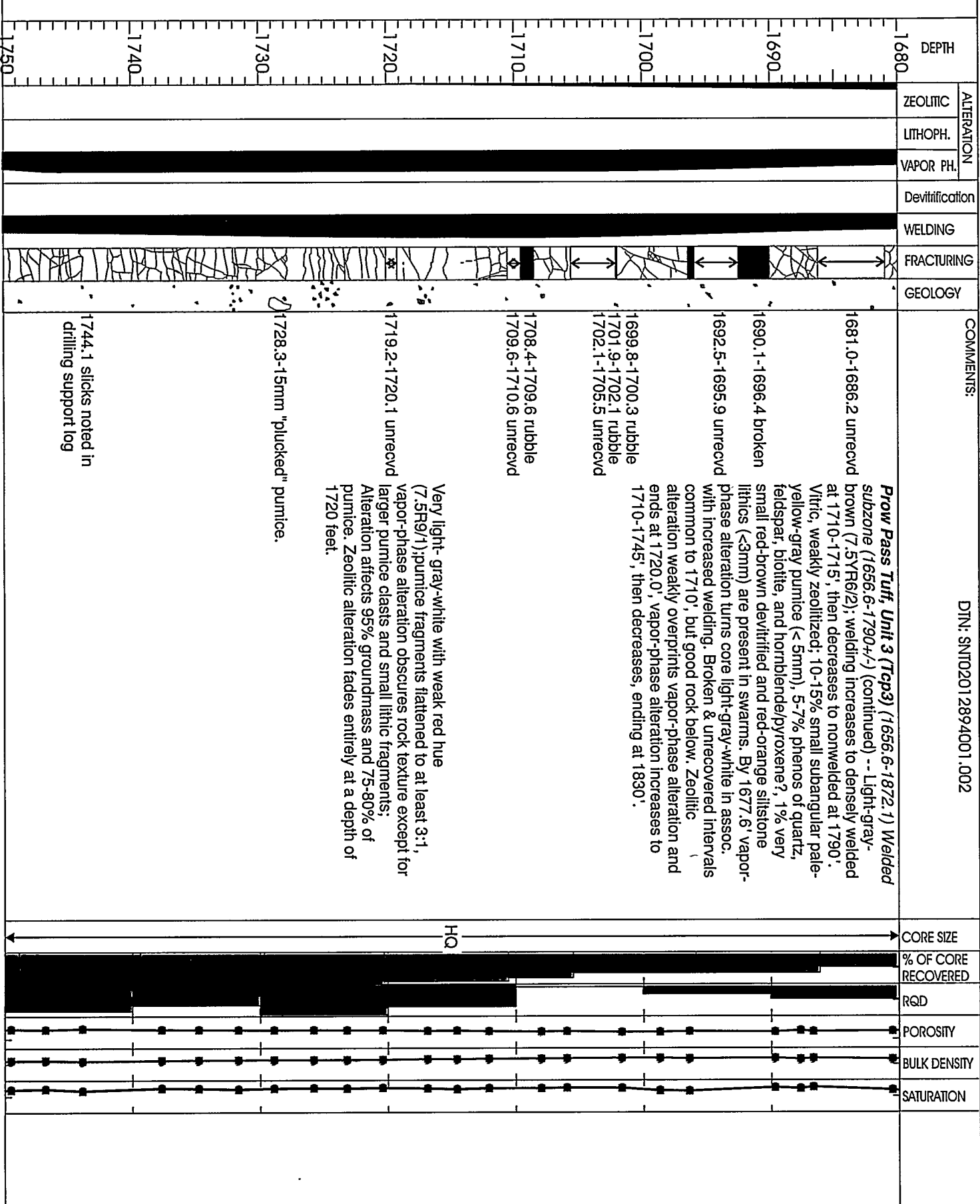


COLLAR COORDINATES (NSP):
N: 761,957.0 ft E: 5561,606.0
STARTED: May 27, 1994
COMPLETED: August 16, 1995

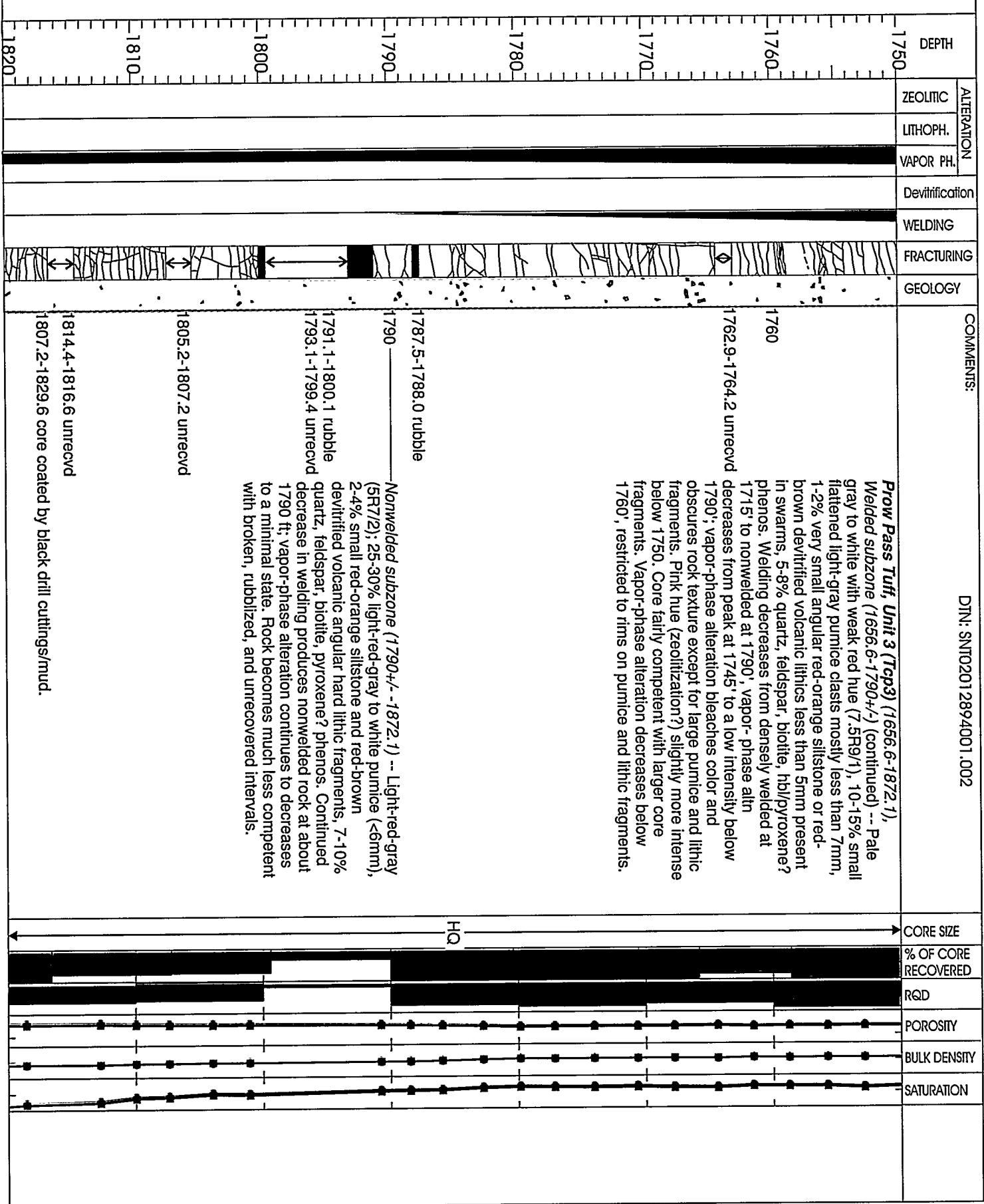
ELEVATION: 4,343.0 ft
BEARING: N/A
INCLINATION: -90 (Vertical)
TOTAL DEPTH: 2,166.3 ft

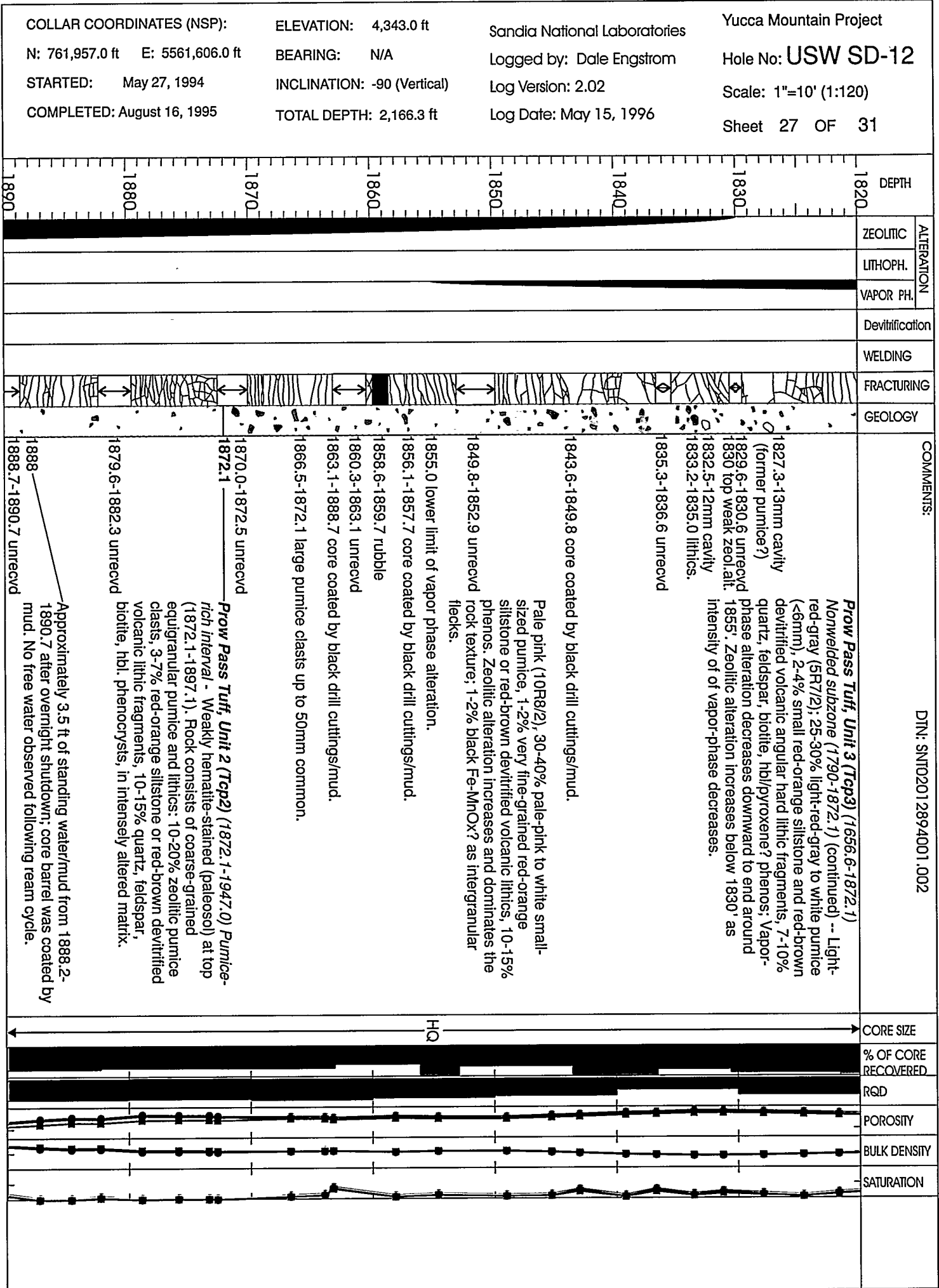
Sandia National Laboratories
Logged by: Dale Engstrom
Log Version: 2.02
Log Date: May 15, 1996

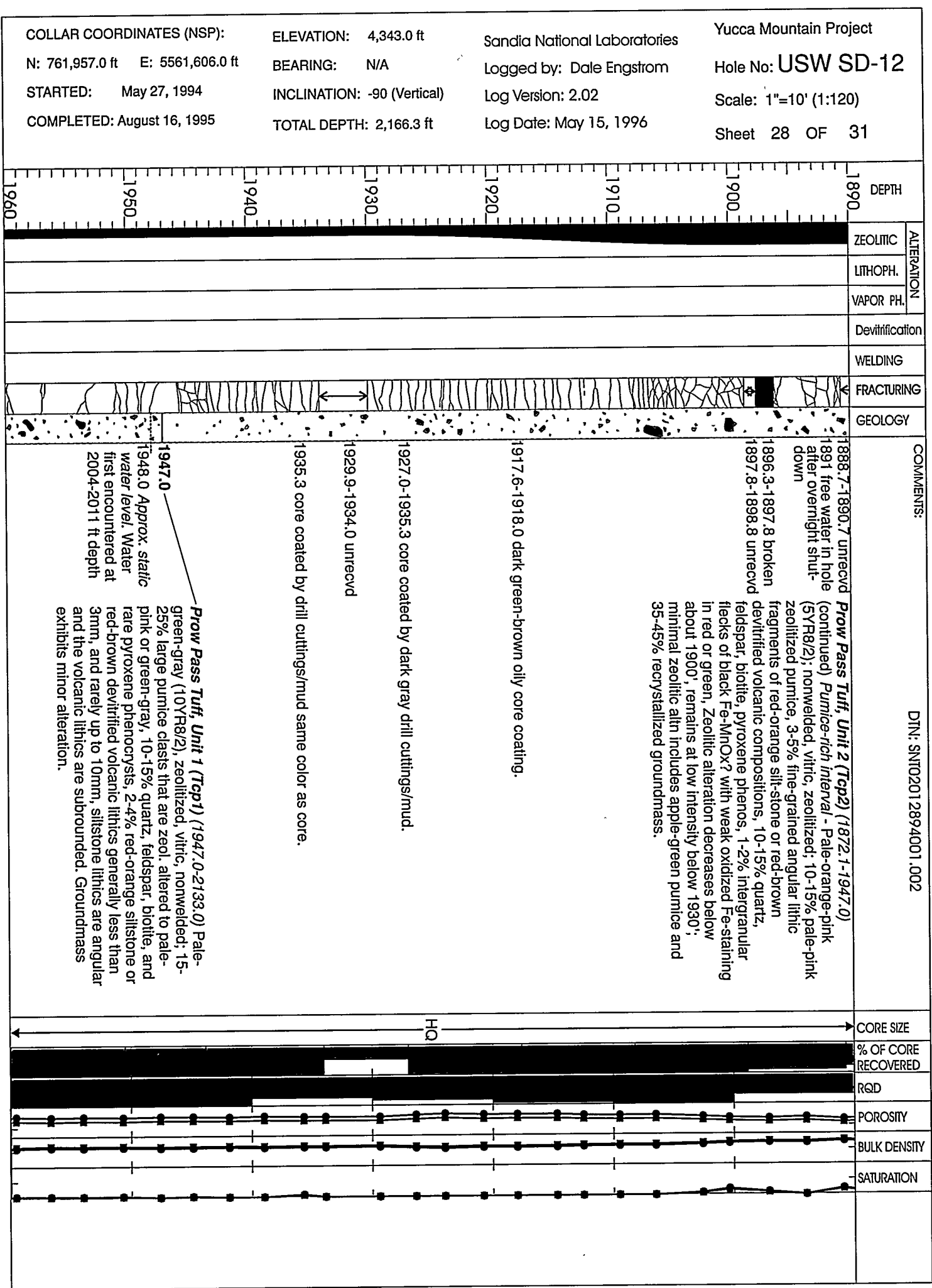
Yucca Mountain Project
Hole No: **USW SD-12**
Scale: 1"=10' (1:120)

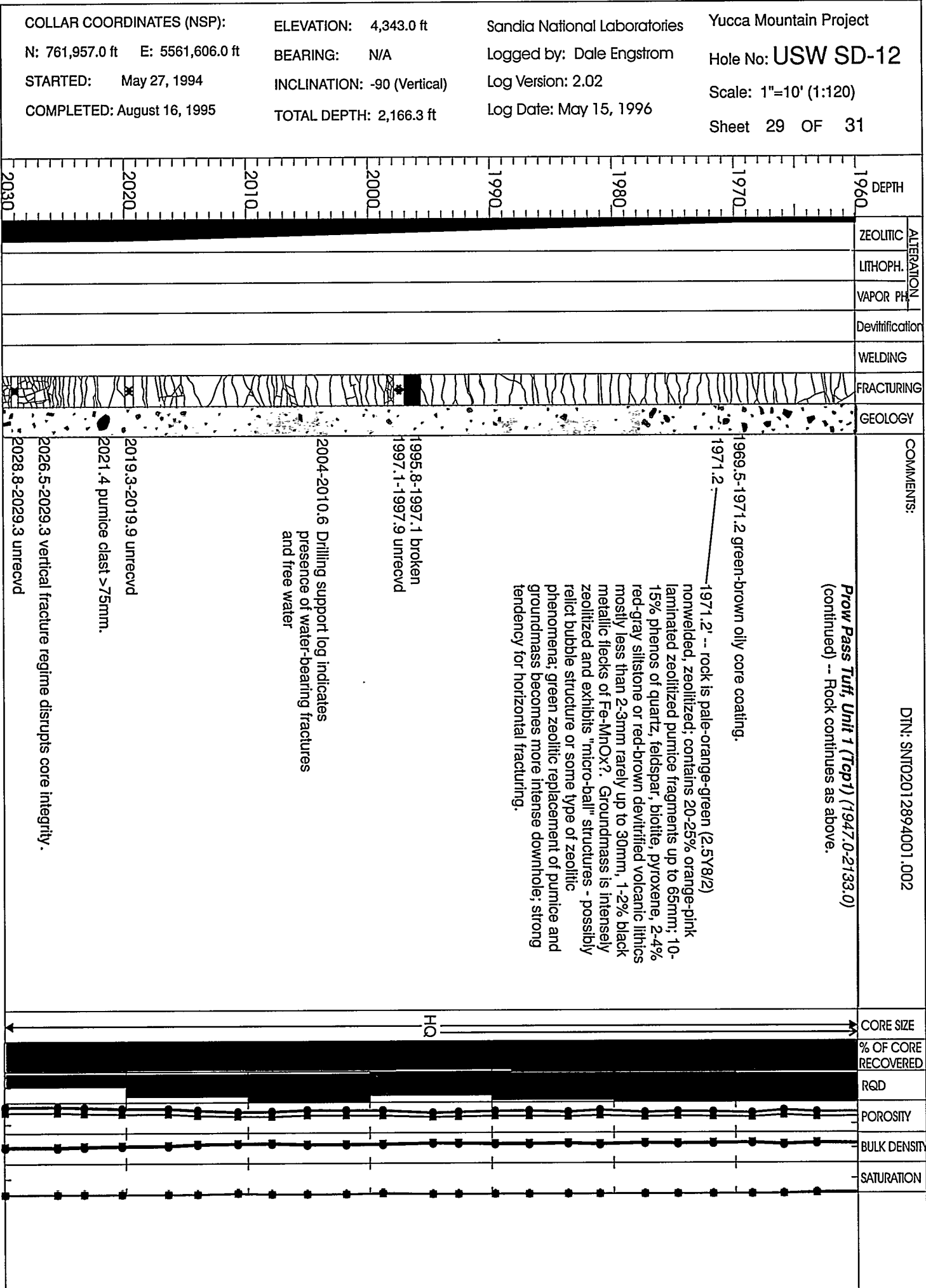


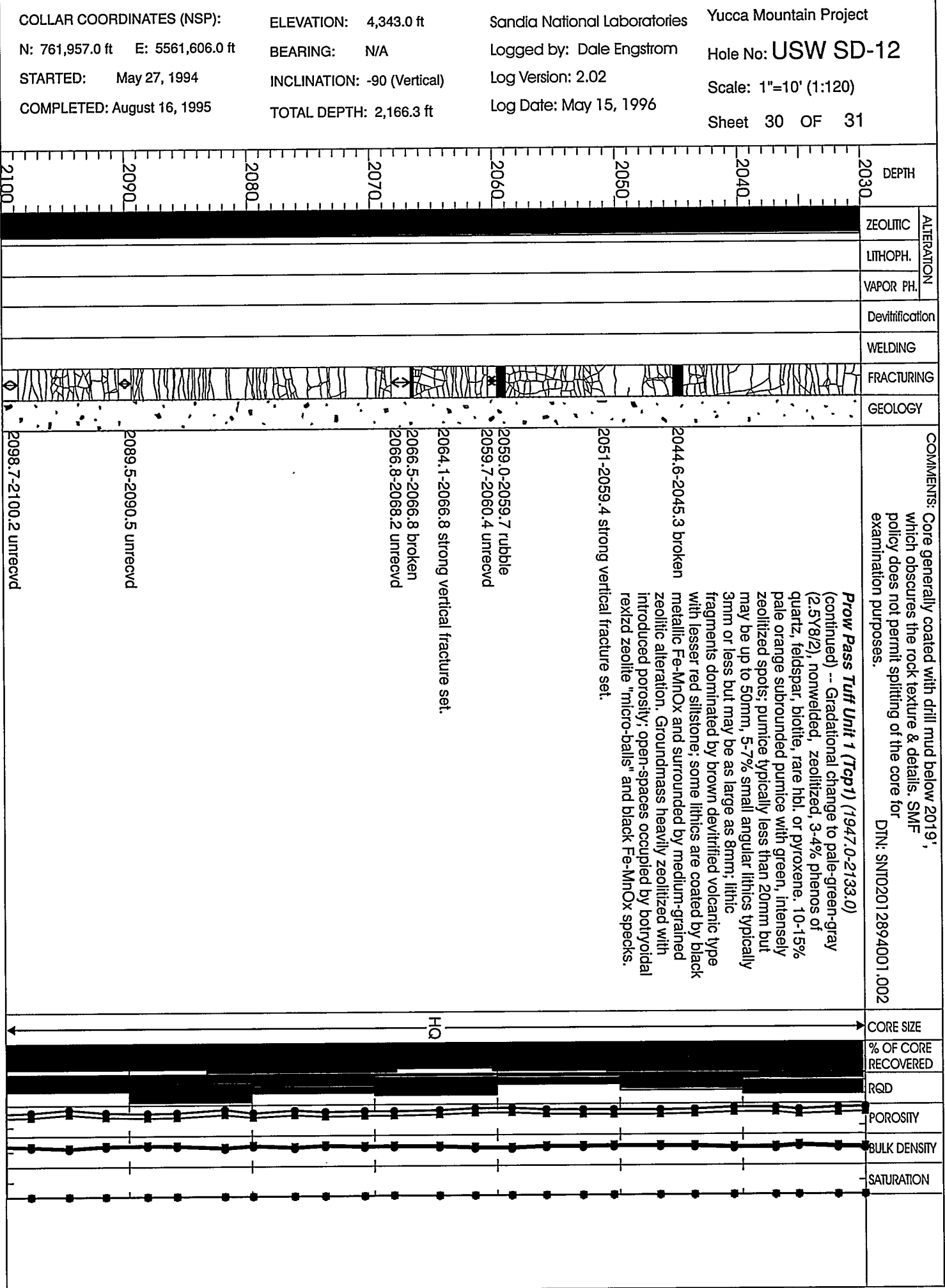
COLLAR COORDINATES (NSP):	ELEVATION: 4,343.0 ft	Sandia National Laboratories	Yucca Mountain Project
N: 761,957.0 ft E: 5561,606.0 ft	BEARING: N/A	Logged by: Dale Engstrom	Hole No: USW SD-12
STARTED: May 27, 1994	INCLINATION: -90 (Vertical)	Log Version: 2.02	Scale: 1"=10' (1:120)
COMPLETED: August 16, 1995	TOTAL DEPTH: 2,166.3 ft	Log Date: May 15, 1996	Sheet 26 of 31









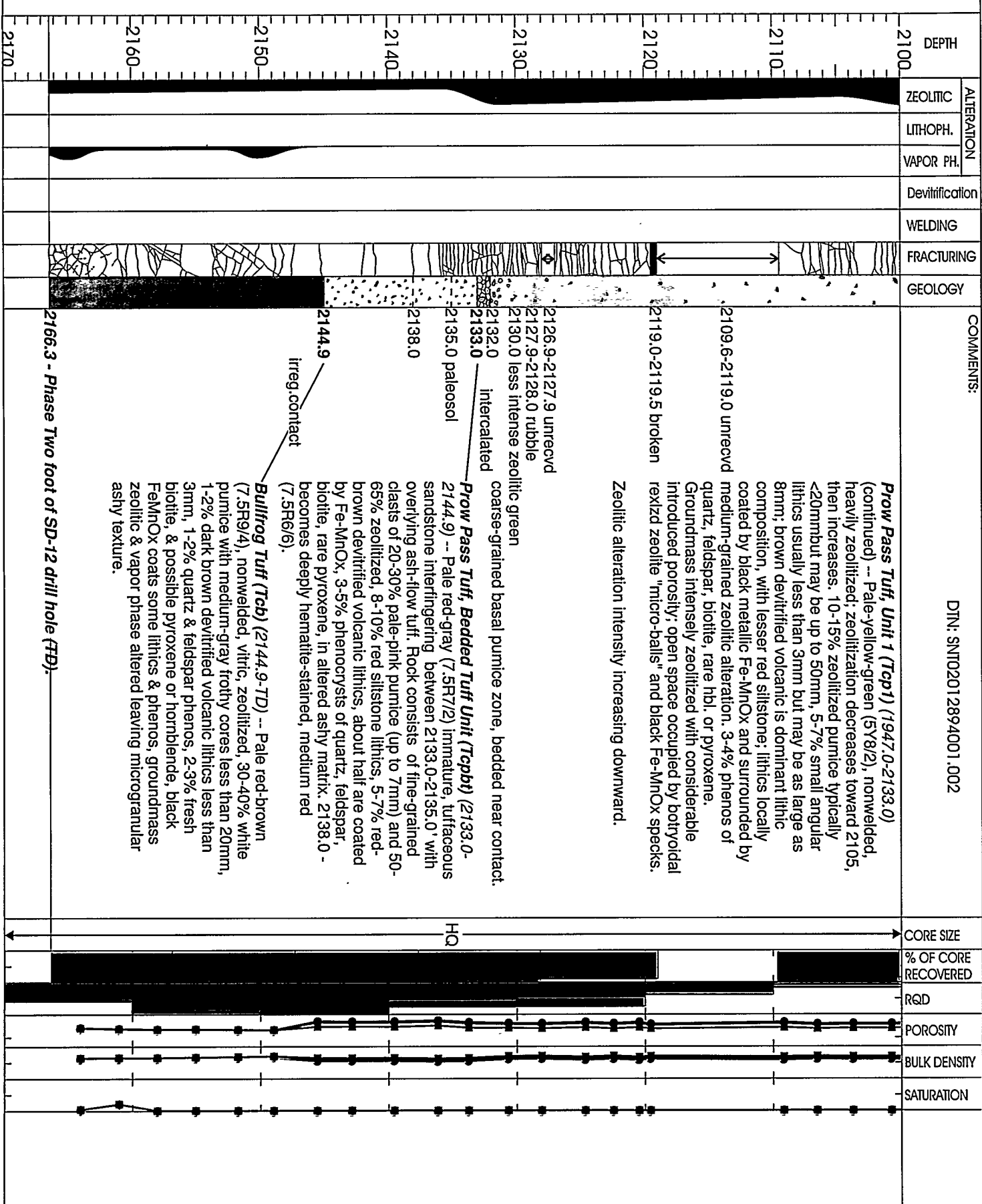


COLLAR COORDINATES (NSP):
N: 761,957.0 ft E: 5561,606.0 f
STARTED: May 27, 1994
COMPLETED: August 16, 1995

ELEVATION: 4,343.0 ft
BEARING: N/A
INCLINATION: -90 (Vertical)
TOTAL DEPTH: 2,166.3 ft

Sandia National Laboratories
Logged by: Dale Engstrom
Log Version: 2.02
Log Date: May 15, 1996

Yucca Mountain Project
Hole No: USW SD-12
Scale: 1"=10' (1:120)
Sheet 31 OF 31



Appendix C: Core Recovery Data

Table C-1: Core Recovery Data for USW SD-12

{Sources (TDIF numbers): 1-TM000000SD12RS.006, 2-TM000000SD12RS.001, 3-TM000000SD12RP.002, 4-TM000000SD12RP.003, 5-TM000000SD12RP.004, 6-TM000000SD12RP.005, 7-TM000000SD12RP.007, 8-TM000000SD12RP.008, 9-TM000000SD12RP.009, 10-TM000000SD12RP.010, 11-TM000000SD12RS.011]

Run Number	Interval Bottom (feet)	Drilled (feet)	Recovered (feet)	Core Recovery (percent)	Source	Run Number	Interval Bottom (feet)	Drilled (feet)	Recovered (feet)	Core Recovery (percent)	Source
0	5.3	--	--	--	1	30	123.0	2.4	2.0	83	1
1	7.6	2.3	0.1	4	1	31	125.6	2.6	2.5	96	1
2	8.0	0.4	0.0	0	1	32	126.3	0.7	0.7	100	1
3	8.2	0.2	0.2	100	1	33	131.9	5.6	4.7	84	1
4	16.0	7.8	2.2	28	1	34	135.1	3.2	3.0	94	1
5	17.1	1.1	1.1	100	1	35	135.7	0.6	0.5	83	1
6	17.3	0.2	0.0	0	1	36	140.5	4.8	4.8	100	1
7	20.5	3.2	1.5	47	1	37	146.4	5.9	4.9	83	1
8	22.5	2.0	1.3	65	1	38	154.8	8.4	8.4	100	1
9	23.1	0.6	0.6	100	1	39	155.7	0.9	0.9	100	1
10	23.7	0.6	0.2	33	1	40	155.8	0.1	0.0	0	1
11	29.3	5.6	4.5	80	1	41	160.4	4.6	4.6	100	1
12	35.4	6.1	5.3	87	1	42	170.7	10.3	9.9	96	1
13	37.3	1.9	1.9	100	1	43	176.1	5.4	5.3	98	1
14	37.7	0.4	0.2	50	1	44	180.5	4.4	3.9	89	1
15	39.1	1.4	0.2	14	1	45	189.3	8.8	8.8	100	1
16	46.1	7.0	6.9	99	1	46	192.2	2.9	2.9	100	1
17	50.1	4.0	3.8	95	1	47	200.5	8.3	8.3	100	1
18	53.8	3.7	3.3	89	1	48	203.2	2.7	2.7	100	1
19	57.0	3.2	1.3	41	1	49	204.9	1.7	1.7	100	1
20	60.5	3.5	3.5	100	1	50	205.0	0.1	0.1	100	1
21	68.2	7.7	5.1	66	1	51	208.8	3.8	3.8	100	1
22	75.5	7.3	5.8	79	1	52	208.9	0.1	0.0	0	1
23	77.8	2.3	2.3	100	1	53	209.2	0.3	0.3	100	1
24	80.8	3.0	3.0	100	1	54	212.0	2.8	2.1	75	1
25	88.6	7.8	7.5	96	1	55	214.5	2.5	2.5	100	1
26	93.4	4.8	4.8	100	1	56	216.3	1.8	1.8	100	1
27	100.6	7.2	6.3	88	1	57	220.5	4.2	4.0	95	1
28	110.6	10.0	8.7	87	1	58	229.8	9.3	7.0	75	1
29	120.6	10.0	9.2	92	1	59	240.1	10.3	8.4	82	1

Table C-1: Core Recovery Data for USW SD-12 (Continued)

Run Number	Interval Bottom (feet)	Drilled (feet)	Recovered (feet)	Core Recovery (percent)	Source	Run Number	Interval Bottom (feet)	Drilled (feet)	Recovered (feet)	Core Recovery (percent)	Source
1	5.3	--	--	--	1	30	123.0	2.4	2.0	83	1
2	7.6	2.3	0.1	4	1	31	125.6	2.6	2.5	96	1
3	8.0	0.4	0.0	0	1	32	126.3	0.7	0.7	100	1
4	8.2	0.2	0.2	100	1	33	131.9	5.6	4.7	84	1
5	16.0	7.8	2.2	28	1	34	135.1	3.2	3.0	94	1
6	17.1	1.1	1.1	100	1	35	135.7	0.6	0.5	83	1
7	17.3	0.2	0.0	0	1	36	140.5	4.8	4.8	100	1
8	20.5	3.2	1.5	47	1	37	146.4	5.9	4.9	83	1
9	22.5	2.0	1.3	65	1	38	154.8	8.4	8.4	100	1
10	23.1	0.6	0.6	100	1	39	155.7	0.9	0.9	100	1
11	23.7	0.6	0.2	33	1	40	155.8	0.1	0.0	0	1
12	29.3	5.6	4.5	80	1	41	160.4	4.6	4.6	100	1
13	35.4	6.1	5.3	87	1	42	170.7	10.3	9.9	96	1
14	37.3	1.9	1.9	100	1	43	176.1	5.4	5.3	98	1
15	37.7	0.4	0.2	50	1	44	180.5	4.4	3.9	89	1
16	39.1	1.4	0.2	14	1	45	189.3	8.8	8.8	100	1
17	46.1	7.0	6.9	99	1	46	192.2	2.9	2.9	100	1
18	50.1	4.0	3.8	95	1	47	200.5	8.3	8.3	100	1
19	53.8	3.7	3.3	89	1	48	203.2	2.7	2.7	100	1
20	57.0	3.2	1.3	41	1	49	204.9	1.7	1.7	100	1
21	60.5	3.5	3.5	100	1	50	205.0	0.1	0.1	100	1
22	68.2	7.7	5.1	66	1	51	208.8	3.8	3.8	100	1
23	75.5	7.3	5.8	79	1	52	208.9	0.1	0.0	0	1
24	77.8	2.3	2.3	100	1	53	209.2	0.3	0.3	100	1
25	80.8	3.0	3.0	100	1	54	212.0	2.8	2.1	75	1
26	88.6	7.8	7.5	96	1	55	214.5	2.5	2.5	100	1
27	93.4	4.8	4.8	100	1	56	216.3	1.8	1.8	100	1
28	100.6	7.2	6.3	88	1	57	220.5	4.2	4.0	95	1
29	110.6	10.0	8.7	87	1	58	229.8	9.3	7.0	75	1
30	120.6	10.0	9.2	92	1	59	240.1	10.3	8.4	82	1

Table C-1: Core Recovery Data for USW SD-12 (Continued)

{Sources (TDIF numbers): 1-TM0000000SD12RS.006, 2-TM0000000SD12RP.001, 3-TM0000000SD12RP.002, 4-TM0000000SD12RP.003, 5-TM0000000SD12RP.004, 6-TM0000000SD12RP.005, 7-TM0000000SD12RP.007, 8-TM0000000SD12RP.008, 9-TM0000000SD12RP.009, 10-TM0000000SD12RP.010, 11-TM0000000SD12RS.011}

Table C-1: Core Recovery Data for USW SD-12 (Continued)

{Sources (TDIF numbers): 1-TM0000000SD12RS.006, 2-TM0000000SD12RS.006, 3-TM0000000SD12RP.002, 4-TM0000000SD12RP.003, 5-TM0000000SD12RP.004, 6-TM0000000SD12RP.005, 7-TM0000000SD12RP.007, 8-TM0000000SD12RP.008, 9-TM0000000SD12RP.009, 10-TM0000000SD12RP.010, 11-TM0000000SD12RS.011}

Run Number	Interval Bottom (feet)	Drilled (feet)	Recovered (feet)	Core Recovery (percent)	Source
60	240.8	0.7	0.7	100	1
61	250.8	10.0	9.2	92	1
62	260.9	10.1	10.1	100	1
63	270.6	9.7	8.8	91	1
64	280.6	10.0	9.9	99	1
65	290.6	10.0	10.0	100	1
66	295.8	5.2	4.6	88	1
67	300.8	5.0	4.7	94	1
68	310.9	10.1	10.1	100	2
69	320.8	9.9	9.9	100	2
70	330.7	9.9	9.7	98	2
71	334.3	3.6	1.8	50	2
72	340.8	6.5	5.7	88	2
73	350.9	10.1	10.1	100	2
74	355.9	5.0	4.3	86	2
75	360.6	4.7	3.7	79	2
76	368.6	8.0	7.2	90	2
77	376.8	8.2	7.7	94	2
78	384.0	7.2	7.2	100	2
79	388.0	4.0	3.7	93	2
80	393.3	5.3	5.3	100	2
81	400.6	7.3	6.5	89	2
82	410.5	9.9	9.9	100	2
83	420.5	10.0	10.0	100	2
84	422.5	2.0	2.0	100	2
85	432.5	10.0	9.9	99	2
86	440.6	8.1	8.0	99	2
87	450.5	9.9	9.3	94	2
88	460.7	10.2	8.2	80	2
89	469.6	8.9	7.2	81	2

Run Number	Interval Bottom (feet)	Drilled (feet)	Recovered (feet)	Core Recovery (percent)	Source
60	240.8	0.7	0.7	100	1
61	250.8	10.0	9.2	92	1
62	260.9	10.1	10.1	100	1
63	270.6	9.7	8.8	91	1
64	280.6	10.0	9.9	99	1
65	290.6	10.0	10.0	100	1
66	295.8	5.2	4.6	88	1
67	300.8	5.0	4.7	94	1
68	310.9	10.1	10.1	100	2
69	320.8	9.9	9.9	100	2
70	330.7	9.9	9.7	98	2
71	334.3	3.6	1.8	50	2
72	340.8	6.5	5.7	88	2
73	350.9	10.1	10.1	100	2
74	355.9	5.0	4.3	86	2
75	360.6	4.7	3.7	79	2
76	368.6	8.0	7.2	90	2
77	376.8	8.2	7.7	94	2
78	384.0	7.2	7.2	100	2
79	388.0	4.0	3.7	93	2
80	393.3	5.3	5.3	100	2
81	400.6	7.3	6.5	89	2
82	410.5	9.9	9.9	100	2
83	420.5	10.0	10.0	100	2
84	422.5	2.0	2.0	100	2
85	432.5	10.0	9.9	99	2
86	440.6	8.1	8.0	99	2
87	450.5	9.9	9.3	94	2
88	460.7	10.2	8.2	80	2
89	469.6	8.9	7.2	81	2

Run Number	Interval Bottom (feet)	Drilled (feet)	Recovered (feet)	Core Recovery (percent)	Source
60	240.8	0.7	0.7	100	1
61	250.8	10.0	9.2	92	1
62	260.9	10.1	10.1	100	1
63	270.6	9.7	8.8	91	1
64	280.6	10.0	9.9	99	1
65	290.6	10.0	10.0	100	1
66	295.8	5.2	4.6	88	1
67	300.8	5.0	4.7	94	1
68	310.9	10.1	10.1	100	2
69	320.8	9.9	9.9	100	2
70	330.7	9.9	9.7	98	2
71	334.3	3.6	1.8	50	2
72	340.8	6.5	5.7	88	2
73	350.9	10.1	10.1	100	2
74	355.9	5.0	4.3	86	2
75	360.6	4.7	3.7	79	2
76	368.6	8.0	7.2	90	2
77	376.8	8.2	7.7	94	2
78	384.0	7.2	7.2	100	2
79	388.0	4.0	3.7	93	2
80	393.3	5.3	5.3	100	2
81	400.6	7.3	6.5	89	2
82	410.5	9.9	9.9	100	2
83	420.5	10.0	10.0	100	2
84	422.5	2.0	2.0	100	2
85	432.5	10.0	9.9	99	2
86	440.6	8.1	8.0	99	2
87	450.5	9.9	9.3	94	2
88	460.7	10.2	8.2	80	2
89	469.6	8.9	7.2	81	2

Run Number	Interval Bottom (feet)	Drilled (feet)	Recovered (feet)	Core Recovery (percent)	Source
60	240.8	0.7	0.7	100	1
61	250.8	10.0	9.2	92	1
62	260.9	10.1	10.1	100	1
63	270.6	9.7	8.8	91	1
64	280.6	10.0	9.9	99	1
65	290.6	10.0	10.0	100	1
66	295.8	5.2	4.6	88	1
67	300.8	5.0	4.7	94	1
68	310.9	10.1	10.1	100	2
69	320.8	9.9	9.9	100	2
70	330.7	9.9	9.7	98	2
71	334.3	3.6	1.8	50	2
72	340.8	6.5	5.7	88	2
73	350.9	10.1	10.1	100	2
74	355.9	5.0	4.3	86	2
75	360.6	4.7	3.7	79	2
76	368.6	8.0	7.2	90	2
77	376.8	8.2	7.7	94	2
78	384.0	7.2	7.2	100	2
79	388.0	4.0	3.7	93	2
80	393.3	5.3	5.3	100	2
81	400.6	7.3	6.5	89	2
82	410.5	9.9	9.9	100	2
83	420.5	10.0	10.0	100	2
84	422.5	2.0	2.0	100	2
85	432.5	10.0	9.9	99	2
86	440.6	8.1	8.0	99	2
87	450.5	9.9	9.3	94	2
88	460.7	10.2	8.2	80	2
89	469.6	8.9	7.2	81	2

Table C-1: Core Recovery Data for USW SD-12 (Continued)

{Sources (TDIF numbers): 1-TM000000SD12RS.006, 2-TM000000SD12RP.001, 3-TM000000SD12RP.002, 4-TM000000SD12RP.003, 5-TM000000SD12RP.004, 6-TM000000SD12RP.005, 7-TM000000SD12RP.007, 8-TM000000SD12RP.008, 9-TM000000SD12RP.009, 10-TM000000SD12RP.010, 11-TM000000SD12RS.011}

Run Number	Interval Bottom (feet)	Drilled (feet)	Recovered (feet)	Core Recovery (percent)	Source
120	699.9	7.4	7.2	97	5
121	700.8	0.9	0.9	100	5
122	703.9	3.1	2.7	87	6
123	709.0	5.1	5.1	100	6
124	711.3	2.3	2.3	100	6
125	720.6	9.3	5.4	58	6
126	726.4	5.8	3.7	64	6
127	729.0	2.6	2.3	88	6
128	732.5	3.5	3.1	89	6
129	733.8	1.3	1.3	100	7
130	742.2	8.4	8.2	98	7
131	743.4	1.2	1.2	100	7
132	750.2	6.8	6.6	97	7
133	753.6	3.4	3.4	100	7
134	758.4	4.8	4.8	100	7
135	760.8	2.4	2.4	100	7
136	768.3	7.5	7.3	97	7
137	769.9	1.6	1.6	100	7
138	770.4	0.5	0.1	20	7
139	772.4	2.0	2.0	100	7
140	780.8	8.4	8.4	100	7
141	790.8	10.0	9.8	98	7
142	801.0	10.2	8.2	80	7
143	811.0	10.0	8.3	83	7
144	820.8	9.8	5.6	57	7
145	827.8	7.0	2.5	36	7
146	837.9	10.1	5.8	57	7
147	840.6	2.7	1.9	70	7
148	850.7	10.1	8.4	83	7
149	860.7	10.0	4.0	40	7

Table C-1: Core Recovery Data for USW SD-12 (Continued)

{Sources (TDIF numbers): 1-TM000000SD12RS.006, 2-TM000000SD12RP.001, 3-TM000000SD12RP.002, 4-TM000000SD12RP.003, 5-TM000000SD12RP.004, 6-TM000000SD12RP.005, 7-TM000000SD12RP.007, 8-TM000000SD12RP.008, 9-TM000000SD12RP.009, 10-TM000000SD12RP.010, 11-TM000000SD12RS.011}

Run Number	Interval Bottom (feet)	Drilled (feet)	Recovered (feet)	Core Recovery (percent)	Source
	Run Number	Interval Bottom (feet)	Drilled (feet)	Recovered (feet)	Core Recovery (percent)
	150	871.1	10.4	3.9	38
	151	881.1	10.0	5.2	52
	152	886.1	5.0	4.1	82
	153	892.0	5.9	2.6	44
	154	901.2	9.2	5.5	60
	155	910.0	8.8	2.5	28
	156	917.1	7.1	2.9	41
	157	920.8	3.7	2.2	59
	158	925.9	5.1	3.7	73
	159	935.7	9.8	5.9	60
	160	943.8	8.1	5.2	64
	161	954.1	10.3	6.1	59
	162	960.8	6.7	4.1	61
	163	970.9	10.1	4.3	43
	164	978.8	7.9	3.6	46
	165	985.7	6.9	3.1	45
	166	995.7	10.0	2.1	21
	167	998.8	3.1	1.3	42
	168	1003.3	4.5	0.8	18
	169	1004.4	1.1	0.2	18
	170	1007.5	3.1	0.6	19
	171	1008.5	1.0	0.0	0
	172	1018.6	10.1	0.2	2
	173	1020.8	2.2	0.0	0
	174	1022.8	2.0	1.6	80
	175	1023.8	1.0	0.7	70
	176	1033.7	9.9	7.2	73
	177	1038.7	5.0	1.9	38
	178	1041.2	2.5	1.7	68
	179	1043.8	2.6	1.3	50

Table C-1: Core Recovery Data for USW SD-12 (Continued)

{Sources (TDIF numbers): 1-TM000000SD12RS.006, 2-TM000000SD12RP.001, 3-TM000000SD12RP.002, 4-TM000000SD12RP.003, 5-TM000000SD12RP.004, 6-TM000000SD12RP.005, 7-TM000000SD12RP.007, 8-TM000000SD12RP.008, 9-TM000000SD12RP.009, 10-TM000000SD12RP.010, 11-TM000000SD12RS.011}

Table C-1: Core Recovery Data for USW SD-12 (Continued)

{Sources (TDIF numbers): 1-TM000000SD12RS.006, 2-TM000000SD12RP.001,

3-TM000000SD12RP.002, 4-TM000000SD12RP.003, 5-TM000000SD12RP.004,

6-TM000000SD12RP.005, 7-TM000000SD12RP.007, 8-TM000000SD12RP.008,

9-TM000000SD12RP.009, 10-TM000000SD12RP.010, 11-TM000000SD12RS.011}

Run Number	Interval Bottom (feet)	Drilled (feet)	Recovered (feet)	Core Recovery (percent)	Source	Run Number	Interval Bottom (feet)	Drilled (feet)	Recovered (feet)	Core Recovery (percent)	Source
180	1048.8	5.0	2.7	54	7	210	1154.1	1.9	1.9	100	7
181	1051.9	3.1	1.7	55	7	211	1155.3	1.2	1.0	83	7
182	1059.6	7.7	3.3	43	7	212	1157.2	1.9	0.7	37	7
183	1062.2	2.6	1.2	46	7	213	1159.4	2.2	1.8	82	7
184	1065.7	3.5	2.6	74	7	214	1160.8	1.4	1.1	79	7
185	1070.7	5.0	4.8	96	7	215	1168.0	7.2	6.3	87	7
186	1075.8	5.1	5.1	100	7	216	1169.1	1.1	0.8	73	7
187	1077.0	1.2	1.2	100	7	217	1172.7	3.6	3.6	100	7
188	1079.1	2.1	1.9	90	7	218	1175.7	3.0	0.1	3	7
189	1080.4	1.3	0.8	62	7	219	1176.4	0.7	0.3	43	7
190	1080.7	0.3	0.2	67	7	220	1178.1	1.7	1.7	100	7
191	1085.3	4.6	4.3	93	7	221	1179.5	1.4	0.7	50	7
192	1090.4	5.1	5.0	98	7	222	1180.2	0.7	0.4	57	7
193	1095.5	5.1	2.9	57	7	223	1180.8	0.6	0.6	100	7
194	1099.0	3.5	1.5	43	7	224	1186.7	5.9	4.5	76	7
195	1100.8	1.8	0.9	50	7	225	1193.3	6.6	6.2	94	7
196	1105.9	5.1	4.9	96	7	226	1199.0	5.7	3.3	58	7
197	1110.9	5.0	4.6	92	7	227	1200.7	1.7	1.6	94	7
198	1116.1	5.2	5.2	100	7	228	1204.7	4.0	3.5	88	7
199	1120.8	4.7	4.1	87	7	229	1207.9	3.2	3.0	94	7
200	1128.4	7.6	7.3	96	7	230	1211.8	3.9	3.6	92	7
201	1133.0	4.6	4.2	91	7	231	1216.2	4.4	3.0	68	7
202	1135.4	2.4	2.2	92	7	232	1217.2	1.0	1.0	100	7
203	1138.4	3.0	1.5	50	7	233	1222.5	5.3	3.0	57	8
204	1140.8	2.4	1.6	67	7	234	1230.7	8.2	5.2	63	8
205	1146.9	6.1	5.3	87	7	235	1237.8	7.1	6.1	86	8
206	1147.1	0.2	0.2	100	7	236	1242.2	4.4	3.9	89	8
207	1149.5	2.4	1.2	50	7	237	1248.0	5.8	5.5	95	8
208	1150.8	1.3	1.3	100	7	238	1251.6	3.6	3.1	86	8
209	1152.2	1.4	1.4	100	7	239	1257.6	6.0	5.8	97	8

Table C-1: Core Recovery Data for USW SD-12 (Continued)

{ Sources (TDIF numbers): 1-TM000000SD12RS.006, 2-TM000000SD12RP.001, 3-TM000000SD12RP.002, 4-TM000000SD12RP.003, 5-TM000000SD12RP.004, 6-TM000000SD12RP.005, 7-TM000000SD12RP.007, 8-TM000000SD12RP.008, 9-TM000000SD12RP.009, 10-TM000000SD12RP.010, 11-TM000000SD12RS.011]

Run Number	Interval Bottom (feet)	Drilled (feet)	Recovered (feet)	Core Recovery (percent)	Source
240	1260.8	3.2	2.8	87	8
241	1265.8	5.0	4.1	82	8
242	1268.9	3.1	2.8	90	8
243	1270.4	1.5	1.5	100	8
244	1271.1	0.7	0.7	100	8
245	1271.5	0.4	0.4	100	8
246	1277.7	6.2	2.5	40	8
247	1280.8	3.1	3.1	100	8
248	1289.7	8.9	8.9	100	8
249	1298.1	8.4	3.6	43	8
250	1301.0	2.9	2.9	100	8
251	1310.6	9.6	9.6	100	8
252	1316.7	6.1	6.1	100	8
253	1321.0	4.3	4.3	100	8
254	1327.1	6.1	6.1	100	8
255	1336.8	9.7	9.7	100	8
256	1341.0	4.2	3.9	93	8
257	1350.5	9.5	9.5	100	8
258	1356.3	5.8	5.4	93	8
259	1361.0	4.7	4.6	98	8
260	1370.4	9.4	8.9	95	8
261	1376.4	6.0	5.7	95	8
262	1381.1	4.7	0.7	15	8
263	1390.5	9.4	9.3	99	8
264	1395.5	5.0	4.8	96	8
265	1401.1	5.6	5.6	100	8
266	1411.2	10.1	7.7	76	9
267	1420.9	9.7	9.7	100	9
268	1430.2	9.3	9.3	100	9
269	1435.3	5.1	5.1	100	9

Table C-1: Core Recovery Data for USW SD-12 (Continued)

{ Sources (TDIF numbers): 1-TM000000SD12RS.006, 2-TM000000SD12RP.001, 3-TM000000SD12RP.002, 4-TM000000SD12RP.003, 5-TM000000SD12RP.004, 6-TM000000SD12RP.005, 7-TM000000SD12RP.007, 8-TM000000SD12RP.008, 9-TM000000SD12RP.009, 10-TM000000SD12RP.010, 11-TM000000SD12RS.011]

Run Number	Interval Bottom (feet)	Drilled (feet)	Recovered (feet)	Core Recovery (percent)	Source	Run Number	Interval Bottom (feet)	Drilled (feet)	Recovered (feet)	Core Recovery (percent)	Source
270						271	1453.1	8.1	8.1	100	10
						272	1462.9	9.8	9.8	100	10
						273	1468.2	5.3	5.0	94	10
						274	1477.8	9.6	4.8	50	10
						275	1487.5	9.7	9.7	100	10
						276	1492.6	5.1	5.1	100	10
						277	1501.4	8.8	8.8	100	10
						278	1510.8	9.4	9.4	100	10
						279	1520.8	10.0	10.0	100	10
						280	1528.3	7.5	7.5	100	10
						281	1537.7	9.4	9.4	100	10
						282	1547.2	9.5	9.2	97	10
						283	1556.9	9.7	3.8	39	10
						284	1566.5	9.6	7.2	75	10
						285	1576.0	9.5	9.3	98	10
						286	1585.5	9.5	9.2	97	10
						287	1590.6	5.1	5.0	98	10
						288	1600.0	9.4	9.4	100	10
						289	1608.6	8.6	8.3	97	10
						290	1618.2	9.6	8.9	93	10
						291	1627.8	9.6	7.9	82	10
						292	1634.9	7.1	6.0	85	10
						293	1644.4	9.5	8.9	94	10
						294	1650.6	6.2	4.9	79	10
						295	1659.6	9.0	9.0	100	10
						296	1667.2	7.6	5.7	75	10
						297	1676.6	9.4	4.9	52	10
						298	1686.2	9.6	4.4	46	10
						299	1695.9	9.7	6.3	65	10

Table C-1: Core Recovery Data for USW SD-12 (Continued)

{ Sources (TDIF numbers): 1-TM0000000SD12RS.006, 2-TM0000000SD12RP.001, 3-TM0000000SD12RP.002, 4-TM0000000SD12RP.003, 5-TM0000000SD12RP.004, 6-TM0000000SD12RP.005, 7-TM0000000SD12RP.007, 8-TM0000000SD12RP.008, 9-TM0000000SD12RP.009, 10-TM0000000SD12RP.010, 11-TM0000000SD12RS.011]

Table C-1: Core Recovery Data for USW SD-12 (Continued)

{ Sources (TDIF numbers): 1-TM0000000SD12RS.006, 2-TM0000000SD12RP.001, 3-TM0000000SD12RP.002, 4-TM0000000SD12RP.003, 5-TM0000000SD12RP.004, 6-TM0000000SD12RP.005, 7-TM0000000SD12RP.007, 8-TM0000000SD12RP.008, 9-TM0000000SD12RP.009, 10-TM0000000SD12RP.010, 11-TM0000000SD12RS.011]

Run Number	Interval Bottom (feet)	Drilled (feet)	Recovered (feet)	Core Recovery (percent)	Source
300	1705.5	9.6	6.2	65	10
301	1710.6	5.1	4.1	80	10
302	1720.3	9.7	8.8	91	10
303	1729.7	9.4	9.4	100	10
304	1739.4	9.7	9.7	100	10
305	1748.9	9.5	9.5	100	10
306	1758.6	9.7	9.5	98	10
307	1765.8	7.2	5.9	82	10
308	1770.6	4.8	4.8	100	10
309	1780.4	9.8	9.8	100	10
310	1790.0	9.6	9.6	100	10
311	1799.4	9.4	3.1	33	10
312	1807.2	7.8	5.8	74	10
313	1816.6	9.4	7.2	77	10
314	1821.6	5.0	5.0	100	10
315	1830.6	9.0	8.0	89	10
316	1836.6	6.0	4.7	78	10
317	1843.6	7.0	6.9	99	10
318	1852.9	9.3	6.2	67	10
319	1856.1	3.2	3.1	97	10
320	1863.1	7.0	4.2	60	11
321	1872.5	9.4	6.9	73	11
322	1882.3	9.8	7.1	72	11
323	1890.7	8.4	6.4	76	11
324	1898.8	8.1	7.1	88	11
325	1908.2	9.4	9.4	100	11
326	1917.6	9.4	9.4	100	11
327	1927.0	9.4	9.3	99	11
328	1934.0	7.0	3.3	47	11
329	1943.8	9.8	9.8	100	11

Table C-1: Core Recovery Data for USW SD-12 (Continued)

{ Sources (TDIF numbers): 1-TM0000000SD12RS.006, 2-TM0000000SD12RP.001, 3-TM0000000SD12RP.002, 4-TM0000000SD12RP.003, 5-TM0000000SD12RP.004, 6-TM0000000SD12RP.005, 7-TM0000000SD12RP.007, 8-TM0000000SD12RP.008, 9-TM0000000SD12RP.009, 10-TM0000000SD12RP.010, 11-TM0000000SD12RS.011]

Table C-1: Core Recovery Data for USW SD-12 (Continued)

{ Sources (TDIF numbers): 1-TM0000000SD12RS.006, 2-TM0000000SD12RP.001, 3-TM0000000SD12RP.002, 4-TM0000000SD12RP.003, 5-TM0000000SD12RP.004, 6-TM0000000SD12RP.005, 7-TM0000000SD12RP.007, 8-TM0000000SD12RP.008, 9-TM0000000SD12RP.009, 10-TM0000000SD12RP.010, 11-TM0000000SD12RS.011]

(This page intentionally left blank.)

Appendix D: Rock Quality Designation (RQD) Data

Table D-1: Core-Run RQD Data for USW SD-12
 {Source: DTN/TN0005SD12SUPER.002. Raw piece lengths not measured separately prior to core run no. 186.]

Run No.	Interval Bottom (feet)	Drilled (feet)	Raw Length (feet) ¹	Raw RQD	Adj. Length (feet)	RQD	Page No.
0	5.3	--	--	--	--	--	
1	7.60	2.30	--	0.00	0	1	
2	8.00	0.40	--	0.00	0	1	
3	8.20	0.20	--	0.00	0	1	
4	16.00	3.10	--	1.10	35	1	
5	17.10	1.10	--	1.10	100	2	
6	17.30	0.20	--	0.00	0	2	
7	20.50	3.20	--	0.40	13	2	
8	22.50	2.00	--	0.40	20	3	
9	23.10	0.60	--	0.50	83	3	
10	23.70	0.60	--	0.00	0	3	
11	29.30	5.60	--	2.12	38	4	
12	35.40	6.10	--	2.00	33	5	
13	37.30	1.90	--	0.35	18	6	
14	37.70	0.40	--	0.00	0	7	
15	39.10	1.40	--	0.00	0	7	
16	46.10	7.00	--	4.80	69	7	
17	50.10	4.00	--	2.80	70	8	
18	53.80	3.70	--	0.90	24	10	
19	57.00	3.20	--	0.00	0	11	
20	60.50	3.50	--	2.40	69	11	
21	68.20	7.70	--	2.30	30	12	
22	75.50	7.30	--	0.60	8	13	
23	77.80	2.30	--	1.90	83	14	
24	80.80	3.00	--	2.90	97	15	
25	88.60	7.80	--	5.00	64	15	
26	93.40	4.80	--	4.00	83	17	
27	100.60	7.20	--	4.99	69	17	
28	110.60	10.00	--	6.60	66	19	
29	120.60	10.00	--	7.60	76	20	
30	123.00	2.40	--	1.50	62	22	
31	125.60	2.60	--	0.80	31	22	

Table D-1: Core-Run RQD Data for USW SD-12 (Continued)
 {Source: DTN/TN0005SD12SUPER.002. Raw piece lengths not measured separately prior to core run no. 186.]

Run No.	Interval Bottom (feet)	Drilled (feet)	Raw Length (feet) ¹	Raw RQD	Page No.	Run No.	Interval Bottom (feet)	Drilled (feet)	Raw Length (feet) ¹	Raw RQD	Adj. Length (feet)	RQD	Page No.
32	126.30	--	0.70	--		--	--	--	--	--	0.00	0	23
33	131.90	--	5.60	--		--	--	--	--	--	2.75	49	23
34	135.10	--	3.20	--		--	--	--	--	--	1.25	39	24
35	135.70	--	0.60	--		--	--	--	--	--	0.50	83	25
36	140.50	--	4.80	--		--	--	--	--	--	4.70	98	25
37	146.40	--	5.90	--		--	--	--	--	--	3.20	54	26
38	154.80	--	8.40	--		--	--	--	--	--	6.25	74	27
39	155.70	--	0.90	--		--	--	--	--	--	1.90	211	28
40	155.80	--	0.10	--		--	--	--	--	--	0.00	0	28
41	160.40	--	4.60	--		--	--	--	--	--	1.80	39	28
42	170.70	--	10.30	--		--	--	--	--	--	8.60	83	28
43	176.10	--	5.40	--		--	--	--	--	--	2.20	41	29
44	180.50	--	4.40	--		--	--	--	--	--	2.91	66	30
45	189.30	--	8.80	--		--	--	--	--	--	3.76	43	30
46	192.20	--	2.90	--		--	--	--	--	--	4.60	159	31
47	200.50	--	8.30	--		--	--	--	--	--	5.60	67	32
48	203.20	--	2.70	--		--	--	--	--	--	2.50	66	33
49	204.90	--	1.70	--		--	--	--	--	--	0.43	16	33
50	205.00	--	0.10	--		--	--	--	--	--	2.78	164	33
51	208.80	--	3.80	--		--	--	--	--	--	0.00	0	36
52	208.90	--	0.10	--		--	--	--	--	--	0.00	0	34
53	209.20	--	0.30	--		--	--	--	--	--	1.60	57	34
54	212.00	--	2.80	--		--	--	--	--	--	0.40	4	36
55	214.50	--	2.50	--		--	--	--	--	--	0.70	28	34
56	216.30	--	1.80	--		--	--	--	--	--	1.90	106	35
57	220.50	--	4.20	--		--	--	--	--	--	1.40	33	35
58	229.80	--	9.30	--		--	--	--	--	--	0.40	4	36
59	240.10	--	10.30	--		--	--	--	--	--	1.30	13	38
60	240.80	--	0.70	--		--	--	--	--	--	0.00	0	39
61	250.80	--	10.00	--		--	--	--	--	--	8.70	87	39
62	260.90	--	10.10	--		--	--	--	--	--	7.50	74	40
63	270.60	--	9.70	--		--	--	--	--	--	8.00	82	41

Table D-1: Core-Run RQD Data for USW SD-12 (Continued)
 {Source: DTN TN000SD12SUPER.002. Raw piece lengths not measured separately prior to core run no. 186]

Table D-1: Core-Run RQD Data for USW SD-12 (Continued)
 {Source: DTN TN000SD12SUPER.002. Raw piece lengths not measured separately prior to core run no. 186]

Run No.	Interval Bottom (feet)	Drilled (feet)	Raw Length (feet) ¹	Raw RQD	Adj. Length (feet)	RQD	Page No.
64	280.60	10.00	--	--	7.10	71	42
65	290.60	10.00	--	--	9.85	99	42
66	295.80	5.20	--	--	3.40	65	43
67	300.80	5.00	--	--	4.70	94	44
68	310.90	10.10	--	--	10.04	99	44
69	320.80	9.90	--	--	9.90	100	44
70	330.70	9.90	--	--	2.69	27	44
71	334.30	3.60	--	--	0.00	0	46
72	340.80	6.50	--	--	4.60	71	47
73	350.90	10.10	--	--	10.27	102	48
74	355.90	5.00	--	--	0.40	8	48
75	360.60	4.70	--	--	2.55	54	49
76	368.60	8.00	--	--	2.30	29	50
77	376.80	8.20	--	--	5.10	62	51
78	384.00	7.20	--	--	7.30	101	52
79	388.00	4.00	--	--	2.00	50	53
80	393.30	5.30	--	--	3.60	68	55
81	400.60	7.30	--	--	5.50	75	56
82	410.50	9.90	--	--	9.80	99	57
83	420.50	10.00	--	--	5.80	58	58
84	422.50	2.00	--	--	0.00	0	59
85	432.50	10.00	--	--	6.80	68	60
86	440.60	8.10	--	--	7.50	93	61
87	450.50	9.90	--	--	9.10	92	62
88	460.70	10.20	--	--	6.40	63	63
89	469.60	8.90	--	--	6.90	78	64
90	475.00	5.40	--	--	3.85	71	66
91	480.70	5.70	--	--	1.15	20	67
92	484.90	4.20	--	--	1.63	39	68
93	488.30	3.40	--	--	0.90	26	69
94	493.60	5.30	--	--	3.40	64	69
95	503.80	10.20	--	--	8.80	86	70

Table D-1: Core-Run RQD Data for USW SD-12 (Continued)
 {Source: DTN TN000SD12SUPER.002. Raw piece lengths not measured separately prior to core run no. 186]

Run No.	Interval Bottom (feet)	Drilled (feet)	Raw Length (feet) ¹	Raw RQD	Adj. Length (feet)	RQD	Page No.
96			513.90	10.10	--	--	52
			523.90	10.00	--	--	71
			532.10	8.20	--	--	72
			540.70	8.60	--	--	73
			541.80	1.10	--	--	74
			550.90	9.10	--	--	75
			560.40	9.50	--	--	75
			570.60	10.20	--	--	75
			580.70	10.10	--	--	78
			588.80	8.10	--	--	78
			598.90	10.10	--	--	78
			600.70	1.80	--	--	13
			610.20	9.50	--	--	78
			619.20	9.00	--	--	79
			620.70	1.50	--	--	79
			627.00	6.30	--	--	80
			637.00	10.00	--	--	80
			640.70	3.70	--	--	82
			650.70	10.00	--	--	10
			660.70	10.00	--	--	82
			670.80	10.10	--	--	41
			680.70	9.90	--	--	83
			688.00	7.30	--	--	5
			699.90	7.40	--	--	84
			700.80	0.90	--	--	0
			703.90	3.10	--	--	93
			709.00	5.10	--	--	93
			711.30	2.30	--	--	42
			720.60	9.30	--	--	93
			726.40	5.80	--	--	93
			729.00	2.60	--	--	93
			729.00	2.60	--	--	93

Table D-1: Core-Run RQD Data for USW SD-12 (Continued)
 (Source: DTN TN000SD12SUPER.002. Raw piece lengths not measured separately prior to core run no. 186]

Table D-1: Core-Run RQD Data for USW SD-12 (Continued)
 (Source: DTN TN000SD12SUPER.002. Raw piece lengths not measured separately prior to core run no. 186]

Run No.	Interval Bottom (feet)	Drilled (feet)	Raw Length (feet) ¹	Raw RQD	Adj. Length (feet)	RQD	Page No.
128	732.50	3.50	--	0	0.00	0	100
129	733.80	1.30	--	0.70	0.70	54	101
130	742.20	8.40	--	3.70	44	101	162
131	743.40	1.20	--	0.00	0	103	163
132	750.20	6.80	--	1.40	21	103	164
133	753.60	3.40	--	2.70	79	104	165
134	758.40	4.80	--	0.00	0	105	166
135	760.80	2.40	--	0.00	0	105	167
136	768.30	7.50	--	0.00	0	106	168
137	769.90	1.60	--	0.00	0	108	169
138	770.40	0.50	--	0.00	0	109	170
139	772.40	2.00	--	0.00	0	109	171
140	780.80	8.40	--	4.13	49	109	172
141	790.80	10.00	--	5.18	52	110	173
142	801.00	10.20	--	4.50	44	112	174
143	811.00	10.00	--	4.63	46	113	175
144	820.80	9.80	--	1.40	14	115	176
145	827.80	7.00	--	0.00	0	117	177
146	837.90	10.10	--	2.00	20	117	178
147	840.60	2.70	--	0.40	15	119	179
148	850.70	10.10	--	2.80	28	119	180
149	860.70	10.00	--	0.00	0	121	181
150	871.10	10.40	--	2.30	22	122	182
151	881.10	10.00	--	2.60	26	123	183
152	886.10	5.00	--	3.80	76	124	184
153	892.00	5.90	--	0.00	0	125	185
154	901.20	9.20	--	3.60	39	126	186
155	910.00	8.80	--	1.20	14	127	187
156	917.10	7.10	--	0.40	6	127	188
157	920.80	3.70	--	0.00	0	128	189
158	925.90	5.10	--	1.33	26	128	190
159	935.70	9.80	--	1.11	11	129	191

Run No.	Interval Bottom (feet)	Drilled (feet)	Raw Length (feet) ¹	Raw RQD	Adj. Length (feet)	RQD	Page No.
160			943.80	8.10	--	--	29
			954.10	10.30	--	--	2.32
			960.80	6.70	--	--	1.80
			970.90	10.10	--	--	0.90
			978.80	7.90	--	--	3.25
			985.70	6.90	--	--	1.60
			995.70	10.00	--	--	2.0
			1003.30	4.50	--	--	0
			1004.40	1.10	--	--	0
			1007.50	3.10	--	--	0.50
			1008.50	1.00	--	--	0
			1018.60	10.10	--	--	0
			1020.80	2.20	--	--	0
			1022.80	2.00	--	--	0
			1023.80	1.00	--	--	0
			1033.70	9.90	--	--	0.67
			1038.70	5.00	--	--	0.69
			1041.20	2.50	--	--	0.70
			1043.80	2.60	--	--	0.70
			1062.20	2.60	--	--	0.70
			1065.70	3.50	--	--	0.70
			1070.70	5.00	--	--	0.70
			1075.80	5.10	--	--	0.70
			1080.70	0.30	--	--	0.70
			1080.40	1.30	--	--	0.70
			1085.30	4.60	--	--	0.70
			1085.30	4.60	--	--	0.70

Table D-1: Core-Run RQD Data for USW SD-12 (Continued)
 {Source: DTN TN0005SD12SUPER.002. Raw piece lengths not measured separately prior to core run no. 186 }

Table D-1: Core-Run RQD Data for USW SD-12 (Continued)
 {Source: DTN TN0005SD12SUPER.002. Raw piece lengths not measured separately prior to core run no. 186]

Run No.	Interval Bottom (feet)	Drilled (feet)	Raw Length (feet) ¹	Raw RQD	Adj. Length (feet)	RQD	Page No.
192	1090.40	5.10	0.00	0	2.73	54	150
193	1095.50	5.10	0.00	0	0.00	0	152
194	1099.00	3.50	0.00	0	0.00	0	153
195	1100.80	1.80	0.36	20	0.71	39	153
196	1105.90	5.10	1.60	31	2.06	40	154
197	1110.90	5.00	2.53	51	2.54	51	155
198	1116.10	5.20	4.81 [†]	8 [‡]	0.40 [†]	8 [‡]	156
199	1120.80	4.70	3.94 [†]	19 [‡]	0.90 [†]	19 [‡]	156
200	1128.40	7.60	1.20	16	2.50	33	157
201	1133.00	4.60	0.00	0	1.40	30	159
202	1135.40	2.40	0.00	0	0.00	0	160
203	1138.40	3.00	0.00	0	0.00	0	161
204	1140.80	2.40	0.00	0	0.00	0	162
205	1146.90	6.10	3.40	56	3.40	56	163
206	1147.10	0.20	0.00	0	0.00	0	164
207	1149.50	2.40	0.00	0	0.77	32	164
208	1150.80	1.30	0.00	0	0.44	34	164
209	1152.20	1.40	0.00	0	0.40	29	165
210	1154.10	1.90	0.81	43	0.81	43	165
211	1155.30	1.20	0.00	0	0.00	0	166
212	1157.20	1.90	0.00	0	0.00	0	166
213	1159.40	2.20	0.00	0	0.00	0	167
214	1160.80	1.40	0.00	0	0.00	0	168
215	1168.00	7.20	0.00	0	0.00	0	168
216	1169.10	1.10	0.00	0	0.00	0	170
217	1172.70	3.60	0.00	0	0.00	0	170
218	1175.70	3.00	0.00	0	0.00	0	171
219	1176.40	0.70	0.00	0	0.00	0	172
220	1178.10	1.70	0.00	0	0.00	0	172
221	1179.50	1.40	0.00	0	0.00	0	173
222	1180.20	0.70	0.00	0	0.00	0	173
223	1180.80	0.60	0.00	0	0.00	0	173

Table D-1: Core-Run RQD Data for USW SD-12 (Continued)
 {Source: DTN TN0005SD12SUPER.002. Raw piece lengths not measured separately prior to core run no. 186]

Table D-1: Core-Run RQD Data for USW SD-12 (Continued)
 {Source: DTN TN0005SD12SUPER.002. Raw piece lengths not measured separately prior to core run no. 186 }

Table D-1: Core-Run RQD Data for USW SD-12 (Continued)
 {Source: DTN/TN000SD12SUPER.002. Raw piece lengths not measured separately
 prior to core run no. 186]

Table D-1: Core-Run RQD Data for USW SD-12 (Continued)
 {Source: DTN/TN000SD12SUPER.002. Raw piece lengths not measured separately
 prior to core run no. 186]

Run No.	Interval Bottom (feet)	Drilled (feet)	Raw Length (feet) ¹	Raw RQD	Adj. Length (feet)	RQD	Page No.
256	1341.00	4.20	4.20	100	4.23	101	199
257	1350.50	9.50	8.18	86	9.40	99	199
258	1356.30	5.80	3.41	59	5.20	90	200
259	1361.00	4.70	2.05	44	3.82	81	201
260	1370.40	9.40	5.28	56	8.90	95	201
261	1376.40	6.00	4.11	69	5.70	95	203
262	1378.10	1.70	0.00	0	0.00	0	203
263	1390.50	9.40	6.45	69	8.05	86	204
264	1395.50	5.00	4.30	86	4.80	96	205
265	1401.10	5.60	5.65	101	5.65	101	205
266	1411.20	10.10	5.93	59	6.90	68	206
267	1420.90	9.70	5.92	61	9.30	96	207
268	1430.20	9.30	9.30	100	9.80	105	208
269	1435.30	5.10	4.61	90	5.00	98	209
270	1445.00	9.70	1.59	16	9.68	100	210
271	1453.10	8.10	4.49	55	8.24	102	212
272	1462.90	9.80	7.90	81	9.80	100	213
273	1468.20	5.30	3.33	63	4.40	83	214
274	1477.80	9.60	2.16	23	3.43	36	215
275	1487.10	9.30	8.60	92	9.12	98	216
276	1492.60	5.10	5.00	98	5.00	98	217
277	1501.40	8.80	8.80	100	8.80	100	217
278	1510.80	9.40	9.42	100	9.67	103	217
279	1520.80	10.00	9.19	92	9.24	92	218
280	1528.30	7.50	7.45	99	7.45	99	219
281	1537.70	9.40	9.63	102	9.63	102	220
282	1547.20	9.50	3.88	41	9.31	98	220
283	1556.90	9.70	0.00	0	3.45	36	221
284	1566.50	9.60	0.00	0	6.97	73	222
285	1576.00	9.50	5.54	58	7.60	80	222
285	1585.50	9.50	3.90	41	6.20	65	223
286	1590.60	5.10	3.97	78	5.50	108	224

Run No.	Interval Bottom (feet)	Drilled (feet)	Raw Length (feet) ¹	Raw RQD	Adj. Length (feet)	Raw RQD	Adj. Length (feet)	Page No.
288	1600.00		9.40		8.43	90	8.43	90
289	1608.60		8.60		3.61	42	5.80	67
290	1618.20		9.60		0.33	3	7.90	82
291	1627.80		9.60		2.28	24	7.30	76
292	1634.90		7.10		0.78	11	5.00	70
293	1644.40		9.50		1.20	13	6.90	73
294	1650.60		6.20		1.80	29	3.00	48
295	1659.60		9.00		7.76	86	9.26	103
296	1667.20		7.60		1.80	24	5.10	67
297	1676.60		9.40		0.00	0	1.25	13
298	1686.20		9.60		0.00	0	4.40	46
299	1695.90		9.70		0.00	0	4.60	47
300	1705.50		9.60		0.00	0	0.60	6
301	1710.60		5.10		0.00	0	0.68	13
302	1720.30		9.70		7.10	73	7.10	73
303	1729.70		9.40		7.02	75	9.04	96
304	1739.40		9.70		3.68	38	6.30	65
305	1748.90		9.50		1.10	12	7.90	83
306	1758.60		9.70		6.00	62	9.00	93
307	1765.80		7.20		2.10	29	4.30	60
308	1770.60		4.80		1.70	35	4.45	93
309	1780.40		9.80		6.50	66	8.01	82
310	1790.00		9.60		6.65	69	7.35	77
311	1799.40		10.40		1.21	12	1.72	17
312	1807.20		7.80		0.00	0	4.47	57
313	1816.60		9.40		1.00	11	6.16	66
314	1821.60		5.00		1.19	24	3.19	64
315	1830.60		9.00		2.76	31	5.57	62
316	1836.60		6.00		2.05	34	2.10	35
317	1843.60		7.00		4.30†	61	4.13†	59
318	1852.90		9.30		1.02	11	6.20	67
319	1856.10		3.20		0.75	23	2.90	91

Table D-1: Core-Run RQD Data for USW SD-12 (Continued)
 {Source: DTN TN0005SD12SUPR.002. Raw piece lengths not measured separately prior to core run no. 186.]

Run No.	Interval Bottom (feet)	Drilled (feet)	Raw Length (feet) ¹	Raw RQD	Adj. Length (feet)	RQD	Page No.
320	1863.10	7.00	0.38	5	3.81	54	252
321	1872.50	9.40	2.73	29	8.00	85	252
322	1882.30	9.80	0.00	0	6.80	69	254
323	1890.70	8.40	1.10	13	6.40	76	254
324	1898.80	8.10	4.60	57	5.20	64	255
325	1908.20	9.40	6.53	69	9.32	99	256
326	1917.60	9.40	4.52	48	8.67	92	257
327	1927.00	9.40	0.00	0	9.30	99	258
328	1934.00	7.00	0.00	0	2.90	41	258
328	1943.80	9.80	0.00	0	9.30	95	258
330	1950.50	6.70	3.93	59	6.60	99	259
331	1960.10	9.60	9.28	97	9.50	99	259
332	1969.50	9.40	3.47	37	9.30	99	260
333	1979.00	9.50	0.00	0	9.40	99	261
334	1988.40	9.40	0.00	0	9.10	97	261
335	1997.90	9.50	0.00	0	6.80	72	261
336	2004.00	6.10	0.84	14	5.80	95	262
337	2010.60	6.60	1.39	21	6.70	102	263
338	2019.90	9.30	6.60	71	7.40	80	264
339	2029.30	9.40	1.47	16	4.30	46	264
340	2038.70	9.40	2.33	25	7.17	76	266
341	2045.30	6.60	1.20	18	1.40	21	268
342	2051.10	5.80	5.69	98	5.69	98	269
343	2060.40	9.30	0.49	5	2.66	29	269
344	2068.20	7.80	0.51	7	5.94	76	271
345	2077.80	9.60	3.60	37	4.80	50	272
346	2083.70	5.90	3.66	62	6.11	104	273
347	2090.50	6.80	0.94	14	5.70	84	273
348	2100.20	9.70	2.52	26	5.26	54	273
349	2109.60	9.40	0.70	7	1.36	14	274
350	2119.00	9.40	2.75	29	3.30	35	275
351	2128.20	9.20	4.47	49	7.01	76	275

¹ Unconventional treatment of healed natural fractures in the drill core by drilling support staff allows the derivation of raw piece lengths that are greater than adjusted piece lengths. Typically, this logical inconsistency produces only single-digit difference in the raw vs. the adjusted RQD values. Thus, we have allowed the piece lengths reported by the Yucca Mountain Project drilling support group to stand in most cases.

² The difference in RQD values produced by the unconventional treatment of healed natural fractures for these intervals is excessive, both in absolute terms and in comparison with surrounding values. The adjusted RQD values have been substituted both in the table and in graphics and computations throughout this report.

Table D-2: RQD Values by 10-foot Intervals

[-- Raw RQD piece lengths were not recorded by drilling support staff prior to core run 186 (approximately 1070.0 ft). Study 8.3.1.14.2 did not record either raw or enhanced piece lengths below a depth of 1530 ft. Sources: "Drilling Support" values computed from table D-1; "Study 8.3.1.14.2"-TDIF No. SNF29041993002.071]

Table D-2: RQD Values by 10-foot Intervals (Continued)

[-- Raw RQD piece lengths were not recorded by drilling support staff prior to core run 186 (approximately 1070.0 ft). Study 8.3.1.14.2 did not record either raw or enhanced piece lengths below a depth of 1530 ft. Sources: "Drilling Support" values computed from table D-1; "Study 8.3.1.14.2"-TDIF No. SNF29041993002.071]

Interval Bottom (feet)	Drilling Support			Study 8.3.1.14.2			Drilling Support			Study 8.3.1.14.2		
	Raw RQD	Adj. RQD	Raw RQD	Raw RQD	Enhanced RQD	Raw RQD	Raw RQD	Adj. RQD	Raw RQD	Raw RQD	Enhanced RQD	
10.0	--	0	--	--	--	310.0	--	99	94	96	96	
20.0	--	25	--	--	--	320.0	--	100	97	100	100	
30.0	--	33	27	39	330.0	--	33	41	50	50	50	
40.0	--	27	31	52	340.0	--	42	42	45	45	45	
50.0	--	69	46	61	350.0	--	99	69	83	83	83	
60.0	--	30	20	37	360.0	--	35	9	33	33	33	
70.0	--	28	17	33	370.0	--	35	24	28	28	28	
80.0	--	45	31	52	380.0	--	75	66	77	77	77	
90.0	--	69	48	71	390.0	--	74	5	72	72	72	
100.0	--	74	44	78	400.0	--	73	64	88	88	88	
110.0	--	66	26	60	410.0	--	98	80	96	96	96	
120.0	--	75	22	78	420.0	--	60	48	74	74	74	
130.0	--	46	16	63	430.0	--	54	59	75	75	75	
140.0	--	69	46	81	440.0	--	86	47	82	82	82	
150.0	--	64	73	84	450.0	--	92	79	93	93	93	
160.0	--	71	37	46	460.0	--	64	53	64	64	64	
170.0	--	82	62	75	470.0	--	76	28	54	54	54	
180.0	--	54	50	67	480.0	--	46	12	29	29	29	
190.0	--	52	61	66	490.0	--	38	14	51	51	51	
200.0	--	88	44	49	500.0	--	78	59	63	63	63	
210.0	--	65	55	72	510.0	--	65	50	57	57	57	
220.0	--	50	16	30	520.0	--	78	59	81	81	81	
230.0	--	6	12	16	530.0	--	75	50	76	76	76	
240.0	--	0	0	15	540.0	--	46	26	37	37	37	
250.0	--	80	42	51	550.0	--	47	27	59	59	59	
260.0	--	75	83	95	560.0	--	38	14	26	26	26	
270.0	--	82	87	97	570.0	--	29	20	29	29	29	
280.0	--	72	80	88	580.0	--	14	5	13	13	13	
290.0	--	97	90	97	590.0	--	13	0	4	4	4	
300.0	--	79	68	86	600.0	--	74	34	66	66	66	

Table D-2: RQD Values by 10-foot Intervals (Continued)

[-- Raw RQD piece lengths were not recorded by drilling support staff prior to core run 186 (approximately 1070.0 ft). Study 8.3.1.14.2 did not record either raw or enhanced piece lengths below a depth of 1530 ft. Sources: "Drilling Support" values computed from table D-1; "Study 8.3.1.14.2"; "TDIF No. SNF29041993002.071]"

Table D-2: RQD Values by 10-foot Intervals (Continued)

[-- Raw RQD piece lengths were not recorded by drilling support staff prior to core run 186 (approximately 1070.0 ft). Study 8.3.1.14.2 did not record either raw or enhanced piece lengths below a depth of 1530 ft. Sources: "Drilling Support" values computed from table D-1; "Study 8.3.1.14.2"; "TDIF No. SNF29041993002.071]"

Interval Bottom (feet)	Drilling Support			Study 8.3.1.14.2			Interval Bottom (feet)	Drilling Support			Study 8.3.1.14.2		
	Raw RQD	Adj. RQD	Enhanced RQD	Raw RQD	Adj. RQD	Enhanced RQD		Raw RQD	Adj. RQD	Enhanced RQD	Raw RQD	Adj. RQD	Enhanced RQD
610.0	--	7	.7	7	.7	.7	910.0	--	17	0	0	0	0
620.0	--	93	65	90	5	32	920.0	--	4	5	10	10	10
630.0	--	24	5	14	5	14	930.0	--	18	5	26	26	26
640.0	--	28	5	0	0	5	940.0	--	19	12	25	25	25
650.0	--	4	4	40	40	59	950.0	--	22	8	20	20	20
660.0	--	51	40	75	75	75	960.0	--	15	4	11	11	11
670.0	--	75	41	25	25	25	970.0	--	31	23	29	29	29
680.0	--	74	11	25	25	25	980.0	--	19	7	17	17	17
690.0	--	65	28	38	38	38	990.0	--	2	0	4	4	4
700.0	--	37	25	42	42	42	1000.0	--	3	0	0	0	0
710.0	--	24	20	33	33	33	1010.0	--	0	0	0	0	0
720.0	--	15	0	0	0	0	1020.0	--	0	0	0	0	0
730.0	--	5	4	21	21	21	1030.0	--	32	30	48	48	48
740.0	--	34	41	59	59	59	1040.0	--	15	0	5	5	5
750.0	--	23	24	25	25	25	1050.0	--	8	4	4	4	4
760.0	--	27	42	42	42	42	1060.0	--	12	0	6	6	6
770.0	--	0	0	14	14	14	1070.0	--	31	7	13	13	13
780.0	--	37	33	40	40	40	1080.0	0	43	23	25	25	25
790.0	--	52	46	89	89	89	1090.0	0	36	22	22	22	22
800.0	--	45	8	40	40	40	1100.0	2	6	4	4	4	4
810.0	--	46	8	39	39	39	1110.0	38	45	38	50	50	50
820.0	--	17	4	15	15	15	1120.0	16	16	16	65	65	65
830.0	--	5	5	11	11	11	1130.0	14	31	29	53	53	53
840.0	--	19	0	15	15	15	1140.0	0	9	7	16	16	16
850.0	--	27	5	11	11	11	1150.0	34	43	30	39	39	39
860.0	--	2	0	11	11	11	1160.0	8	15	3	8	8	8
870.0	--	21	0	12	12	12	1170.0	0	0	3	9	9	9
880.0	--	26	17	42	42	42	1180.0	0	0	7	7	7	7
890.0	--	41	18	23	23	23	1190.0	27	62	27	44	44	44
900.0	--	31	0	21	21	21	1200.0	32	49	9	22	22	22

Table D-2: RQD Values by 10-foot Intervals (Continued)

[-- Raw RQD piece lengths were not recorded by drilling support staff prior to core run 186 (approximately 1070.0 ft). Study 8.3.1.14.2 did not record either raw or enhanced piece lengths below a depth of 1530 ft. Sources: "Drilling Support" values computed from table D-1; "Study 8.3.1.14.2"-TDIF No. SNF29041993002.071]

Interval Bottom (feet)	Drilling Support			Study 8.3.1.14.2		
	Raw RQD	Adj. RQD	Raw RQD	Raw RQD	Adj. RQD	Raw RQD
1210.0	21	51	30	44	1510.0	100
1220.0	15	23	8	13	1520.0	93
1230.0	5	34	3	3	1530.0	99
1240.0	19	60	13	18	1540.0	88
1250.0	6	71	4	8	1550.0	29
1260.0	3	81	4	5	1560.0	0
1270.0	34	53	14	18	1570.0	20
1280.0	23	34	23	24	1580.0	51
1290.0	78	78	61	61	1590.0	58
1300.0	14	16	10	14	1600.0	89
1310.0	67	76	82	87	1610.0	37
1320.0	80	91	84	87	1620.0	7
1330.0	48	54	52	64	1630.0	21
1340.0	87	95	93	95	1640.0	12
1350.0	87	99	87	96	1650.0	22
1360.0	55	87	48	95	1660.0	80
1370.0	55	93	57	86	1670.0	17
1380.0	43	61	42	55	1680.0	0
1390.0	61	76	60	74	1690.0	0
1400.0	92	98	93	97	1700.0	0
1410.0	63	72	67	80	1710.0	0
1420.0	61	93	54	89	1720.0	69
1430.0	96	105	95	100	1730.0	74
1440.0	56	99	--	--	1740.0	36
1450.0	36	101	--	--	1750.0	17
1460.0	73	101	--	--	1760.0	57
1470.0	61	79	--	--	1770.0	32
1480.0	38	49	--	--	1780.0	64
1490.0	90	94	--	--	1790.0	69
1500.0	99	99	--	--	1800.0	11

Table D-2: RQD Values by 10-foot Intervals (Continued)

[-- Raw RQD piece lengths were not recorded by drilling support staff prior to core run 186 (approximately 1070.0 ft). Study 8.3.1.14.2 did not record either raw or enhanced piece lengths below a depth of 1530 ft. Sources: "Drilling Support" values computed from table D-1; "Study 8.3.1.14.2"-TDIF No. SNF29041993002.071]

Study 8.3.1.14.2

Interval	Bottom (feet)	Raw RQD	Adj. RQD	Raw RQD	Adj. RQD	Raw RQD

Table D-2: RQD Values by 10-foot Intervals (Continued)

[-- Raw RQD piece lengths were not recorded by drilling support staff prior to core run 186 (approximately 1070.0 ft). Study 8.3.1.14.2 did not record either raw or enhanced piece lengths below a depth of 1530 ft. Sources: "Drilling Support" values computed from table D-1; "Study 8.3.1.14.2"-TDIF No. SNF29041993002.071]

Table D-2: RQD Values by 10-foot Intervals (Continued)
 [-- Raw RQD piece lengths were not recorded by drilling support staff prior to core run 186 (approximately 1070.0 ft). Study 8.3.1.14.2 did not record either raw or enhanced piece lengths below a depth of 1530 ft. Sources: "Drilling Support" values computed from table D-1; "Study 8.3.1.14.2"-TDIF No. SNF29041993002.071]

Interval Bottom (feet)	Drilling Support			Study 8.3.1.14.2			Study 8.3.1.14.2
	Raw RQD	Adj. RQD	Raw RQD	Enhanced RQD	Raw RQD	Adj. RQD	
1810.0	3	60	--	--	2110.0	9	16
1820.0	15	65	--	--	2120.0	31	--
1830.0	30	62	--	--	2130.0	47	--
1840.0	43	45	--	--	2140.0	54	--
1850.0	29	64	--	--	2150.0	96	--
1860.0	13	70	--	--	2160.0	83	--
1870.0	22	76	--	--	2170.0	50	--
1880.0	7	73	--	--			
1890.0	10	75	--	--			
1900.0	55	69	--	--			
1910.0	66	98	--	--			
1920.0	37	94	--	--			
1930.0	0	82	--	--			
1940.0	0	74	--	--			
1950.0	36	97	--	--			
1960.0	95	99	--	--			
1970.0	36	99	--	--			
1980.0	0	99	--	--			
1990.0	0	93	--	--			
2000.0	3	77	--	--			
2010.0	18	99	--	--			
2020.0	67	81	--	--			
2030.0	16	48	--	--			
2040.0	24	69	--	--			
2050.0	56	57	--	--			
2060.0	15	36	--	--			
2070.0	12	70	--	--			
2080.0	43	62	--	--			
2090.0	32	91	--	--			
2100.0	25	56	--	--			

(This page intentionally left blank.)

Appendix E: Lithophysal Cavity Data

Table E-1: Measured Lithophysal Cavity Abundances for 10-foot Composite Intervals
[< – less than; NM – not meaningful. Source: DTN No. SNF29041193002.071]

Table E-1: Measured Lithophysal Cavity Abundances for 10-foot Composite Intervals (Continued)
[< – less than; NM – not meaningful. Source: DTN No. SNF29041193002.071]

Depth to Base of Interval (feet)	Estimated Cavities (percent)	Lost Core (feet)	Rubble (feet)	Depth to Base of Interval (feet)	Estimated Cavities (percent)	Lost Core (feet)	Rubble (feet)
30	2	2.7	1.3	340	<1	2.1	3.2
40	3	2.2	1.3	350	1	0.4	0.0
50	2	0.2	0.6	360	<1	1.1	1.3
60	<1	2.3	2.3	370	<1	1.4	2.2
70	2	2.6	1.5	380	1	0.0	0.1
80	2	1.5	1.1	390	1	0.3	1.2
90	2	0.3	0.9	400	1	0.4	0.0
100	5	0.4	0.8	410	1	0.4	0.0
110	5	1.3	1.7	420	2	0.0	0.6
120	10	0.8	0.6	430	3	0.0	0.6
130	5	1.1	2.3	440	5	0.2	0.5
140	2	0.9	0.6	450	10	0.1	0.4
150	<1	0.0	0.4	460	10	1.8	1.4
160	<1	0.1	2.0	470	10	2.4	0.5
170	2	0.0	0.7	480	6	2.9	2.5
180	<1	0.5	1.7	490	4	1.7	2.2
190	<1	0.5	0.1	500	11	0.8	0.9
200	<1	0.0	0.0	510	18	2.7	1.3
210	<1	0.2	0.0	520	18	1.9	0.0
220	<1	0.4	0.4	530	12	0.6	0.7
230	<1	2.5	2.5	540	10	2.3	1.1
240	<1	1.8	0.2	550	6	1.6	1.1
250	<1	0.9	3.1	560	11	5.2	1.0
260	<1	0.0	0.2	570	15	5.7	1.1
270	0	0.3	0.0	580	10	6.6	1.9
280	0	0.6	0.3	590	10	7.7	1.6
290	0	0.1	0.0	600	12	2.0	1.1
300	0	0.6	0.8	610	10	5.4	2.4
310	0	0.3	0.1	620	12	0.5	0.5
320	0	0.0	0.0	630	8	5.0	1.5
330	0	0.1	0.0	640	7	8.3	0.1

Table E-1: Measured Lithophysal Cavity Abundances for 10-foot Composite Intervals (Continued)
[< – less than; NM – not meaningful. Source: DTN No. SNF29041193002.071]

Depth to Base of Interval (feet)	Estimated Cavities (percent)	Lost Core (feet)	Rubble (feet)	Depth to Base of Interval (feet)	Estimated Cavities (percent)	Lost Core (feet)	Rubble (feet)
650	NM	9.2	0.3	960	1	5.9	1.8
660	14	1.3	1.5	970	<1	5.7	1.0
670	<1	0.7	1.5	980	<1	5.2	2.0
680	<1	0.7	0.4	990	<1	6.0	2.7
690	<1	1.7	1.8	1000	<1	7.9	2.1
700	<1	0.2	1.4	1010	<1	9.0	0.4
710	<1	0.4	5.1	1020	NM	10.0	0.0
720	<1	3.3	4.3	1030	<1	1.5	0.6
730	<1	3.0	3.8	1040	<1	5.8	2.2
740	<1	0.4	1.0	1050	<1	4.4	2.6
750	<1	0.2	0.9	1060	<1	5.8	2.7
760	<1	0.2	4.9	1070	<1	2.3	3.3
770	<1	0.2	2.7	1080	<1	0.7	1.8
780	<1	0.4	0.5	1090	<1	0.8	1.6
790	<1	0.0	0.2	1100	<1	4.4	4.0
800	<1	1.2	1.6	1110	<1	1.0	1.6
810	<1	1.7	0.4	1120	<1	0.5	0.1
820	<1	3.8	2.1	1130	<1	0.8	0.2
830	<1	5.3	2.7	1140	<1	2.1	1.8
840	<1	4.5	2.1	1150	<1	2.8	2.3
850	<1	1.6	1.3	1160	<1	1.8	3.8
860	<1	6.0	1.5	1170	<1	1.5	3.4
870	<1	6.1	2.1	1180	<1	4.2	1.5
880	<1	4.8	0.6	1190	<1	1.5	0.9
890	<1	3.3	2.9	1200	<1	2.8	1.8
900	<1	4.5	1.9	1210	<1	0.7	2.1
910	<1	7.5	1.9	1220	<1	1.7	3.1
920	<1	4.9	3.0	1230	<1	4.6	2.7
930	<1	2.2	2.5	1240	<1	1.3	1.3
940	<1	3.9	1.1	1250	<1	0.8	0.4
950	<1	3.0	2.2	1260	<1	0.7	1.3

Table E-1: Measured Lithophysal Cavity Abundances for 10-foot Composite Intervals (Continued)
[< – less than; NM – not meaningful. Source: DTN No. SNF29041193002.071]

Depth to Base of Interval (feet)	Estimated Cavities (percent)	Lost Core (feet)	Rubble (feet)	Depth to Base of Interval (feet)	Estimated Cavities (percent)	Lost Core (feet)	Rubble (feet)
650	NM	9.2	0.3	960	1	5.9	1.8
660	14	1.3	1.5	970	<1	5.7	1.0
670	<1	0.7	1.5	980	<1	5.2	2.0
680	<1	0.7	0.4	990	<1	6.0	2.7
690	<1	1.7	1.8	1000	<1	7.9	2.1
700	<1	0.2	1.4	1010	<1	9.0	0.4
710	<1	0.4	5.1	1020	NM	10.0	0.0
720	<1	3.3	4.3	1030	<1	1.5	0.6
730	<1	3.0	3.8	1040	<1	5.8	2.2
740	<1	0.4	1.0	1050	<1	4.4	2.6
750	<1	0.2	0.9	1060	<1	5.8	2.7
760	<1	0.2	4.9	1070	<1	2.3	3.3
770	<1	0.2	2.7	1080	<1	0.7	1.8
780	<1	0.4	0.5	1090	<1	0.8	1.6
790	<1	0.0	0.2	1100	<1	4.4	4.0
800	<1	1.2	1.6	1110	<1	1.0	1.6
810	<1	1.7	0.4	1120	<1	0.5	0.1
820	<1	3.8	2.1	1130	<1	0.8	0.2
830	<1	5.3	2.7	1140	<1	2.1	1.8
840	<1	4.5	2.1	1150	<1	2.8	2.3
850	<1	1.6	1.3	1160	<1	1.8	3.8
860	<1	6.0	1.5	1170	<1	1.5	3.4
870	<1	6.1	2.1	1180	<1	4.2	1.5
880	<1	4.8	0.6	1190	<1	1.5	0.9
890	<1	3.3	2.9	1200	<1	2.8	1.8
900	<1	4.5	1.9	1210	<1	0.7	2.1
910	<1	7.5	1.9	1220	<1	1.7	3.1
920	<1	4.9	3.0	1230	<1	4.6	2.7
930	<1	2.2	2.5	1240	<1	1.3	1.3
940	<1	3.9	1.1	1250	<1	0.8	0.4
950	<1	3.0	2.2	1260	<1	0.7	1.3

Table E-1: Measured Lithophysal Cavity Abundances for 10-foot Composite Intervals (Continued)
 [$<$ – less than; NM – not meaningful. Source: DTN No. SNF29041193002.071]

Depth to Base of Interval (feet)	Estimated Cavities (percent)	Lost Core (feet)	Rubble (feet)
1270	<1	1.6	1.7
1280	<1	3.7	2.6
1290	<1	0.0	0.0
1300	<1	4.8	1.7
1310	<1	0.0	0.0
1320	0	0.0	0.0
1330	0	0.3	0.0
1340	0	0.0	0.0
1350	0	0.0	0.3
1360	0	0.4	0.1
1370	0	0.2	0.8
1380	0	3.2	1.1
1390	0	1.1	1.1
1400	0	0.3	0.0
1410	0	1.9	0.1
1420	0	0.5	0.4
1430	0	0.0	0.0

Appendix F: Fracture Information

Table F-1: Measured Fracture Data for 10-foot Composite Intervals

[N=natural, I=indeterminate, C=coring-induced, V=vug or void; dip classes are 10-degree intervals ending with the indicated value. Minlzd.= mineralized. Source: TDIF SNF29041993002.071]

Depth to Base of Interval (feet)	Type of Fracture				Dip of Fracture (degrees)									Clean	Minlzd.
	N	I	C	V	10	20	30	40	50	60	70	80	90		
30	8	7	16	--	8	2	1	--	--	1	--	2	1	15	8
40	1	5	22	--	1	--	1	--	2	--	--	1	1	6	1
50	3	16	18	--	8	--	3	2	1	--	2	--	3	19	3
60	4	1	13	--	--	1	1	--	--	1	--	1	1	5	3
70	7	3	21	--	2	1	--	--	--	--	3	1	3	10	7
80	3	5	16	--	3	1	1	--	--	1	--	--	2	8	3
90	5	--	25	--	1	--	--	--	--	2	--	--	2	5	5
100	3	7	21	--	4	--	2	--	--	--	--	2	2	10	3
110	1	6	29	--	1	--	--	--	--	--	--	1	5	7	1
120	1	--	28	--	--	--	--	--	--	--	--	--	1	1	1
130	2	--	32	--	2	--	--	--	--	--	--	--	--	2	2
140	4	--	24	--	1	--	--	--	--	2	1	--	--	4	3
150	12	--	13	--	1	3	1	1	1	3	2	--	--	12	12
160	10	1	6	--	1	1	1	--	--	1	2	--	5	11	10
170	3	5	11	1	4	--	--	--	1	1	1	--	1	8	3
180	4	3	15	--	2	--	1	2	1	--	--	--	1	7	4
190	14	2	3	--	9	3	--	--	--	1	1	--	2	16	14
200	8	5	8	2	6	2	--	--	--	1	1	--	3	13	6
210	11	4	15	--	4	--	2	--	4	--	1	1	3	15	6
220	5	3	10	--	2	--	--	--	1	--	1	--	4	8	5
230	5	2	15	--	1	--	--	--	1	--	--	1	4	7	4
240	1	2	31	--	1	--	--	--	1	--	--	--	1	3	1
250	8	3	10	--	4	--	2	--	1	2	1	--	1	11	8
260	4	4	8	--	4	1	--	--	1	--	--	1	1	8	5
270	3	--	11	--	--	--	--	--	--	--	2	1	--	3	2
280	1	1	6	--	--	--	--	--	--	--	2	--	--	2	1
290	--	2	8	--	--	--	--	--	--	1	1	--	--	2	0
300	--	--	22	--	--	--	--	--	--	--	--	--	--	0	0
310	--	--	6	--	--	--	--	--	--	--	--	--	--	0	0
320	--	--	4	--	--	--	--	--	--	--	--	--	--	0	0
330	12	6	15	--	7	1	2	1	1	1	2	--	3	18	10
340	9	--	9	--	6	--	--	--	--	1	2	--	--	9	7
350	2	3	5	--	1	--	1	--	--	1	--	1	1	5	1
360	3	15	24	--	4	--	2	1	--	1	2	4	4	18	1
370	2	3	13	--	--	--	--	--	2	--	--	--	3	5	2
380	1	4	18	--	--	--	--	--	--	--	1	2	2	5	1
390	--	5	36	--	1	--	--	--	--	--	--	1	3	5	1
400	1	2	22	--	--	--	--	--	--	--	--	2	1	3	0
410	1	--	15	--	--	--	--	--	--	--	1	--	--	1	1
420	5	1	21	1	--	--	--	--	--	--	--	3	3	6	0
430	3	--	17	--	--	--	--	--	--	1	1	--	1	3	1
440	--	3	30	1	--	--	--	--	--	--	--	1	2	3	0
450	--	--	22	--	--	--	--	--	--	--	--	--	--	0	0
460	--	1	13	--	--	--	--	--	--	1	--	--	--	1	0
470	3	1	23	1	--	--	--	--	--	--	2	1	1	4	0
480	1	6	21	--	1	--	1	--	--	1	1	--	3	7	0
490	2	5	20	2	2	1	--	1	1	--	--	--	2	7	1

Table F-1: Measured Fracture Data for 10-foot Composite Intervals (Continued)

[N=natural, I=indeterminate, C=coring-induced, V=vug or void; dip classes are 10-degree intervals ending with the indicated value. Minlzd.= mineralized. Source: TDIF SNF29041993002.071]

Depth to Base of Interval (feet)	Type of Fracture				Dip of Fracture (degrees)										Clean	Minlzd.
	N	I	C	V	10	20	30	40	50	60	70	80	90			
500	3	5	14	1	1	1	--	--	3	--	1	--	2	8	3	3
510	1	--	11	2	--	--	--	--	--	--	1	--	--	1	1	1
520	--	--	13	--	--	--	--	--	--	--	--	--	--	0	0	0
530	1	--	28	--	--	--	--	--	--	--	--	--	1	1	0	0
540	4	2	14	--	3	--	--	--	--	--	--	--	3	6	1	1
550	3	5	22	1	1	--	--	1	--	--	1	5	--	8	2	2
560	--	5	14	--	1	--	--	--	--	--	2	2	--	5	0	0
570	--	--	13	--	--	--	--	--	--	--	--	--	--	0	0	0
580	--	--	8	--	--	--	--	--	--	--	--	--	--	0	0	0
590	--	--	5	--	--	--	--	--	--	--	--	--	--	0	0	0
600	--	1	21	--	1	--	--	--	--	--	--	--	--	1	0	0
610	2	--	10	--	--	--	--	--	--	--	--	--	2	2	0	0
620	--	--	21	--	--	--	--	--	--	--	--	--	--	0	0	0
630	--	--	18	--	--	--	--	--	--	--	--	--	--	0	0	0
640	--	--	7	--	--	--	--	--	--	--	--	--	--	0	0	0
650	--	--	5	--	--	--	--	--	--	--	--	--	--	0	0	0
660	4	--	23	--	--	--	--	--	1	--	--	2	1	4	0	0
670	6	1	21	--	--	1	--	--	2	--	--	2	2	7	5	5
680	9	9	15	--	7	--	--	--	1	--	2	1	7	18	11	11
690	3	2	19	--	--	1	1	--	--	1	--	--	2	5	3	3
700	27	4	9	--	12	6	1	--	1	2	4	1	4	31	27	27
710	4	3	12	--	--	1	1	--	1	1	--	2	1	7	4	4
720	7	3	8	--	4	2	--	--	--	--	1	1	2	10	7	7
730	5	2	14	--	--	--	1	--	--	--	1	2	3	7	5	5
740	4	12	11	--	2	2	2	1	--	1	3	1	4	16	4	4
750	--	39	5	--	--	33	--	--	--	--	--	--	6	39	0	0
760	--	8	5	--	3	3	--	--	1	--	--	--	1	8	0	0
770	16	10	12	--	7	4	1	--	--	1	--	3	10	26	16	16
780	9	13	9	--	4	1	--	--	3	3	5	3	3	22	9	9
790	5	8	14	--	4	1	2	--	--	1	2	2	1	13	5	5
800	3	5	20	1	1	--	--	--	--	--	--	--	7	8	3	3
810	4	9	24	--	4	1	--	--	--	1	1	1	5	13	5	5
820	7	4	10	--	3	1	--	--	--	--	1	3	3	11	6	6
830	--	6	7	--	--	--	2	--	1	--	1	2	--	6	0	0
840	3	3	6	--	1	1	--	--	--	--	--	1	3	6	2	2
850	7	4	17	--	1	--	--	--	--	--	--	1	9	11	4	4
860	--	5	8	--	--	1	--	--	--	1	--	--	3	5	0	0
870	1	2	8	--	--	--	--	1	--	--	--	1	1	3	1	1
880	1	6	11	--	1	--	1	1	--	1	2	1	--	7	2	2
890	1	2	12	1	--	--	--	--	--	1	--	--	2	3	1	1
900	2	6	18	--	1	--	--	--	--	3	1	--	3	8	1	1
910	2	2	2	--	--	--	--	--	--	1	--	--	1	2	0	0
920	1	1	15	--	--	--	--	--	--	--	--	--	2	2	1	1
930	6	7	14	1	1	2	--	--	1	2	2	5	--	13	6	6
940	4	5	8	--	4	--	--	1	--	--	2	2	--	9	4	4
950	6	6	12	--	5	--	2	--	1	--	--	1	3	12	6	6
960	5	3	5	1	1	4	--	1	--	--	--	1	1	8	5	5

Table F-1: Measured Fracture Data for 10-foot Composite Intervals (Continued)

[N=natural, I=indeterminate, C=coring-induced, V=vug or void; dip classes are 10-degree intervals ending with the indicated value. Minlzd.= mineralized. Source: TDIF SNF29041993002.071]

Depth to Base of Interval (feet)	Type of Fracture				Dip of Fracture (degrees)										Clean	Minlzd.
	N	I	C	V	10	20	30	40	50	60	70	80	90			
970	2	2	4	1	--	--	1	--	--	1	1	1	--	4	2	
980	3	7	7	--	3	1	--	--	1	2	2	1	10	2		
990	3	2	4	--	2	1	--	--	--	--	--	1	1	5	3	
1000	--	--	--	--	--	--	--	--	--	--	--	--	--	0	0	
1010	--	3	--	--	2	--	--	--	--	--	--	--	1	3	0	
1020	--	--	--	--	--	--	--	--	--	--	--	--	--	0	0	
1030	11	17	7	--	16	--	1	1	1	--	1	6	2	28	8	
1040	4	8	6	--	5	1	3	--	--	1	1	--	1	12	1	
1050	27	8	2	--	26	3	1	--	1	1	3	--	--	35	29	
1060	--	9	4	--	6	--	1	--	--	--	--	--	2	9	0	
1070	9	14	6	--	11	--	2	--	--	2	2	--	6	23	9	
1080	23	12	4	1	22	2	3	--	1	--	1	4	2	35	20	
1090	25	12	2	1	23	8	--	1	2	--	1	--	2	37	24	
1100	7	5	--	--	7	3	--	--	--	--	1	1	--	12	7	
1110	14	11	3	--	11	5	2	1	1	--	--	1	4	25	15	
1120	15	2	4	1	12	3	--	--	--	--	--	--	2	17	15	
1130	18	4	5	--	7	4	1	1	3	1	--	1	4	22	18	
1140	31	10	1	--	32	2	--	2	--	--	2	1	2	41	28	
1150	9	3	6	--	8	3	--	--	--	--	--	1	--	12	9	
1160	24	6	13	--	16	2	--	--	5	1	--	--	6	30	22	
1170	18	9	3	--	9	6	1	--	--	--	1	2	8	27	18	
1180	22	6	4	--	13	2	3	2	3	--	--	--	5	28	20	
1190	20	7	10	--	16	3	--	1	2	--	1	2	2	27	19	
1200	15	5	6	--	10	2	3	--	1	--	--	1	3	20	14	
1210	16	10	10	--	14	2	3	--	--	--	--	4	3	26	11	
1220	13	16	4	1	21	2	--	--	--	1	--	3	2	29	11	
1230	4	8	2	--	9	1	--	--	--	--	--	--	2	12	2	
1240	14	13	7	2	22	--	--	--	--	--	--	--	5	27	13	
1250	5	37	1	2	40	--	1	1	--	--	--	--	--	42	6	
1260	6	42	--	--	44	1	1	1	--	--	--	--	1	48	5	
1270	11	25	1	1	27	2	1	--	--	2	--	2	2	36	8	
1280	3	10	2	1	11	--	1	--	--	--	--	--	1	13	3	
1290	17	13	2	--	17	1	--	1	--	--	6	1	4	30	24	
1300	4	7	4	--	6	1	--	--	--	--	--	2	2	11	3	
1310	3	2	10	--	1	1	--	--	--	--	1	1	1	5	2	
1320	1	--	4	--	--	--	--	--	--	--	--	--	1	1	1	
1330	2	5	9	--	--	--	--	--	--	1	3	1	2	7	0	
1340	--	8	3	--	7	--	1	--	--	--	--	--	--	8	0	
1350	--	1	15	--	1	--	--	--	--	--	--	--	--	1	0	
1360	--	--	26	--	--	--	--	--	--	--	--	--	--	0	0	
1370	--	2	26	--	--	--	1	1	--	--	--	--	--	2	0	
1380	--	--	16	--	--	--	--	--	--	--	--	--	--	0	0	
1390	--	3	15	--	--	1	2	--	--	--	--	--	--	3	0	
1400	--	--	11	--	--	--	--	--	--	--	--	--	--	0	0	
1410	--	--	14	--	--	--	--	--	--	--	--	--	--	0	0	
1420	--	--	25	--	--	--	--	--	--	--	--	--	--	0	0	
1430	--	--	10	--	--	--	--	--	--	--	--	--	--	0	0	

Appendix G: Laboratory Material Properties

Table G-1: Laboratory Material Properties and Water Contents Measured on Core Samples from Drill Hole USW SD-12

[Measurements reported by L.E. Flint, U.S. Geological Survey Hydrologic Research Facility; DTN No. GS950308312231.002. J. Curtis and C. Vidano, analysts]

Depth (feet)	Depth (m)	Relative Humidity Oven-Dried					105°C Oven-Dried				
		Dry Bulk Density (g/cm ³)	Porosity (cm ³ /cm ³)	Particle Density (g/cm ³)	Vol. Water Content (cm ³ /cm ³)	Relative Satn.	Dry Bulk Density (g/cm ³)	Porosity (cm ³ /cm ³)	Particle Density (g/cm ³)	Vol. Water Content (cm ³ /cm ³)	Relative Satn.
13.4	4.08	2.34	0.035	2.42	0.021	0.605	2.31	0.057	2.45	0.044	0.759
18.0	5.49	2.20	0.107	2.47	0.034	0.323	2.19	0.124	2.50	0.051	0.415
23.7	7.22	2.22	0.101	2.47	0.031	0.303	2.20	0.117	2.50	0.046	0.395
25.9	7.89	2.21	0.107	2.48	0.059	0.553	2.20	0.123	2.50	0.075	0.612
29.9	9.11	2.24	0.092	2.47	0.061	0.663	2.22	0.114	2.51	0.083	0.729
31.1	9.48	2.26	0.084	2.46	0.069	0.824	2.24	0.103	2.49	0.088	0.857
33.9	10.33	2.13	0.141	2.48	0.082	0.581	2.12	0.154	2.50	0.095	0.616
39.6	12.07	2.25	0.091	2.47	0.065	0.714	2.23	0.108	2.50	0.082	0.759
43.1	13.14	2.23	0.095	2.47	0.062	0.647	2.21	0.117	2.50	0.083	0.713
46.6	14.20	2.23	0.099	2.47	0.079	0.804	2.21	0.119	2.50	0.100	0.838
50.1	15.27	2.32	0.056	2.45	0.052	0.934	2.29	0.083	2.50	0.079	0.956
58.5	17.83	2.28	0.074	2.47	0.058	0.791	2.27	0.092	2.50	0.077	0.833
61.5	18.75	2.30	0.076	2.49	0.058	0.767	2.28	0.089	2.51	0.072	0.802
64.7	19.72	2.25	0.088	2.47	0.063	0.707	2.23	0.110	2.51	0.084	0.765
68.2	20.79	2.17	0.134	2.50	0.109	0.814	2.16	0.141	2.51	0.116	0.824
71.0	21.64	2.30	0.069	2.47	0.060	0.868	2.28	0.090	2.51	0.081	0.899
77.2	23.53	2.33	0.059	2.48	0.050	0.841	2.31	0.078	2.51	0.069	0.879
78.9	24.05	2.16	0.132	2.49	0.083	0.630	2.15	0.142	2.50	0.093	0.655
85.9	26.18	2.27	0.084	2.48	0.062	0.745	2.25	0.103	2.51	0.082	0.793
89.7	27.34	2.32	0.060	2.47	0.038	0.631	2.29	0.083	2.50	0.061	0.733
92.8	28.29	2.35	0.045	2.47	0.039	0.870	2.33	0.068	2.50	0.062	0.913
95.2	29.02	2.32	0.064	2.48	0.044	0.690	2.30	0.087	2.52	0.068	0.773
97.9	29.84	2.17	0.139	2.52	0.087	0.628	2.16	0.149	2.54	0.097	0.653
100.8	30.72	2.26	0.090	2.49	0.044	0.488	2.25	0.105	2.51	0.059	0.562
103.8	31.64	2.29	0.080	2.49	0.044	0.555	2.28	0.099	2.53	0.063	0.640
107.1	32.64	2.25	0.097	2.49	0.047	0.483	2.24	0.113	2.52	0.063	0.557
109.1	33.25	2.21	0.112	2.49	0.060	0.533	2.20	0.124	2.51	0.072	0.580
113.5	34.59	2.28	0.083	2.49	0.051	0.610	2.26	0.100	2.52	0.068	0.677
116.0	35.36	2.27	0.089	2.49	0.053	0.597	2.25	0.109	2.52	0.073	0.670
119.1	36.30	2.21	0.112	2.49	0.060	0.539	2.20	0.128	2.52	0.076	0.595
121.1	36.91	2.22	0.113	2.50	0.072	0.633	2.21	0.125	2.52	0.083	0.666
125.1	38.13	2.32	0.073	2.50	0.051	0.701	2.30	0.091	2.53	0.069	0.761
127.7	38.92	2.31	0.074	2.49	0.053	0.716	2.29	0.093	2.53	0.072	0.774
130.5	39.78	2.19	0.131	2.52	0.072	0.551	2.18	0.140	2.54	0.081	0.580
133.5	40.69	2.31	0.070	2.49	0.040	0.573	2.30	0.086	2.51	0.056	0.655
136.4	41.57	2.36	0.050	2.49	0.042	0.849	2.35	0.063	2.51	0.056	0.881
140.0	42.67	2.35	0.052	2.48	0.041	0.792	2.34	0.066	2.50	0.056	0.838
144.3	43.98	2.35	0.050	2.48	0.042	0.837	2.34	0.067	2.50	0.059	0.878
147.5	44.96	2.34	0.055	2.47	0.043	0.778	2.32	0.073	2.50	0.061	0.834
151.8	46.27	2.39	0.054	2.53	0.028	0.522	2.38	0.067	2.55	0.041	0.609
155.0	47.24	2.38	0.038	2.47	0.031	0.811	2.36	0.057	2.50	0.050	0.873
157.9	48.13	2.37	0.045	2.48	0.039	0.873	2.35	0.063	2.51	0.057	0.909
160.8	49.01	2.43	0.048	2.48	0.018	0.042	2.35	0.060	2.50	0.054	0.903
164.6	50.17	2.36	0.047	2.47	0.044	0.941	2.34	0.066	2.50	0.063	0.958

Table G-1: Laboratory Material Properties and Water Contents Measured on Core Samples from Drill Hole USW SD-12 (Continued)

[Measurements reported by L.E. Flint, U.S. Geological Survey Hydrologic Research Facility; DTN No. GS950308312231.002. J. Curtis and C. Vidano, analysts]

Depth (feet)	Depth (m)	Relative Humidity Oven-Dried					105°C Oven-Dried				
		Dry Bulk Density (g/cm ³)	Porosity (cm ³ /cm ³)	Particle Density (g/cm ³)	Vol. Water Content (cm ³ /cm ³)	Relative Satn.	Dry Bulk Density (g/cm ³)	Porosity (cm ³ /cm ³)	Particle Density (g/cm ³)	Vol. Water Content (cm ³ /cm ³)	Relative Satn.
167.0	50.90	2.32	0.065	2.49	0.057	0.872	2.31	0.084	2.52	0.075	0.900
169.7	51.72	2.33	0.061	2.48	0.051	0.836	2.31	0.078	2.51	0.068	0.871
175.8	53.58	2.38	0.038	2.48	0.034	0.886	2.37	0.054	2.50	0.049	0.919
178.8	54.50	2.38	0.038	2.48	0.033	0.870	2.37	0.055	2.50	0.050	0.911
182.2	55.53	2.38	0.042	2.48	0.006	0.132	2.37	0.053	2.50	0.017	0.315
185.4	56.51	2.36	0.041	2.46	0.018	0.432	2.35	0.052	2.48	0.028	0.546
187.4	57.12	2.38	0.036	2.47	0.029	0.798	2.37	0.049	2.49	0.042	0.851
191.3	58.31	2.38	0.037	2.47	0.034	0.932	2.37	0.051	2.50	0.048	0.951
193.8	59.07	2.36	0.045	2.47	0.042	0.933	2.34	0.060	2.49	0.057	0.950
197.3	60.14	2.37	0.042	2.48	0.036	0.854	2.36	0.054	2.50	0.048	0.887
203.9	62.15	2.38	0.041	2.48	0.022	0.531	2.36	0.053	2.49	0.034	0.639
204.9	62.45	2.38	0.040	2.48	0.022	0.545	2.37	0.053	2.50	0.035	0.657
209.7	63.92	2.34	0.044	2.45	0.013	0.295	2.33	0.057	2.47	0.026	0.455
212.1	64.65	2.36	0.041	2.46	0.033	0.799	2.35	0.054	2.48	0.046	0.846
215.1	65.56	2.36	0.039	2.46	0.031	0.782	2.35	0.053	2.48	0.044	0.838
217.7	66.35	2.35	0.041	2.46	0.032	0.782	2.34	0.058	2.48	0.049	0.844
220.9	67.33	2.34	0.045	2.45	0.030	0.656	2.33	0.057	2.47	0.041	0.727
223.6	68.15	2.33	0.055	2.46	0.035	0.634	2.31	0.072	2.49	0.052	0.718
226.7	69.10	2.23	0.084	2.44	0.064	0.761	2.20	0.114	2.49	0.094	0.824
233.6	71.20	2.17	0.105	2.42	0.071	0.682	2.14	0.133	2.47	0.099	0.749
236.7	72.15	2.11	0.120	2.40	0.084	0.698	2.06	0.171	2.48	0.135	0.789
245.2	74.74	2.12	0.086	2.32	0.070	0.810	2.04	0.160	2.43	0.144	0.898
247.4	75.41	2.04	0.120	2.31	0.111	0.923	1.97	0.188	2.42	0.179	0.951
250.8	76.44	1.82	0.205	2.28	0.190	0.927	1.72	0.305	2.47	0.290	0.951
253.4	77.24	1.70	0.261	2.30	0.259	0.991	1.64	0.321	2.41	0.319	0.992
256.8	78.27	1.47	0.308	2.13	0.169	0.547	1.43	0.344	2.19	0.205	0.595
260.0	79.25	1.40	0.366	2.21	0.189	0.515	1.37	0.395	2.27	0.217	0.550
269.0	81.99	1.53	0.334	2.30	0.145	0.433	1.50	0.363	2.36	0.174	0.479
271.4	82.72	1.20	0.477	2.29	0.249	0.522	1.17	0.501	2.35	0.273	0.545
275.0	83.82	1.52	0.327	2.26	0.185	0.566	1.45	0.395	2.40	0.253	0.640
280.9	85.62	1.20	0.438	2.14	0.185	0.422	1.17	0.471	2.21	0.218	0.463
284.0	86.56	1.24	0.405	2.09	0.179	0.441	1.21	0.438	2.16	0.211	0.483
289.9	88.36	1.16	0.470	2.20	0.267	0.567	1.14	0.489	2.24	0.285	0.583
292.7	89.21	1.59	0.323	2.35	0.174	0.539	1.55	0.368	2.45	0.219	0.595
299.0	91.14	1.43	0.348	2.19	0.186	0.535	1.28	0.494	2.53	0.333	0.673
301.9	92.02	1.18	0.491	2.32	0.143	0.292	1.12	0.553	2.51	0.206	0.372
308.1	93.91	1.11	0.526	2.35	0.138	0.264	1.07	0.565	2.47	0.178	0.315
310.9	94.76	1.07	0.541	2.33	0.145	0.268	1.03	0.574	2.43	0.178	0.311
313.9	95.68	1.21	0.488	2.37	0.198	0.406	1.17	0.528	2.48	0.238	0.451
322.5	98.30	1.58	0.298	2.25	0.193	0.648	1.56	0.312	2.27	0.208	0.665
328.7	100.19	2.41	0.030	2.49	0.021	0.716	2.41	0.032	2.49	0.024	0.739
338.0	103.02	2.11	0.174	2.55	0.054	0.310	2.10	0.185	2.58	0.065	0.351
340.6	103.81	2.22	0.127	2.55	0.052	0.404	2.21	0.137	2.57	0.061	0.446
343.8	104.79	2.21	0.144	2.58	0.059	0.405	2.20	0.153	2.59	0.067	0.437

Table G-1: Laboratory Material Properties and Water Contents Measured on Core Samples from Drill Hole USW SD-12 (Continued)

[Measurements reported by L.E. Flint, U.S. Geological Survey Hydrologic Research Facility; DTN No. GS950308312231.002. J. Curtis and C. Vidano, analysts]

Depth (feet)	Depth (m)	Relative Humidity Oven-Dried					105°C Oven-Dried				
		Dry Bulk Density (g/cm ³)	Porosity (cm ³ /cm ³)	Particle Density (g/cm ³)	Vol. Water Content (cm ³ /cm ³)	Relative Satn.	Dry Bulk Density (g/cm ³)	Porosity (cm ³ /cm ³)	Particle Density (g/cm ³)	Vol. Water Content (cm ³ /cm ³)	Relative Satn.
347.0	105.77	2.19	0.152	2.58	0.067	0.437	2.18	0.158	2.59	0.072	0.457
349.6	106.56	2.16	0.158	2.57	0.075	0.476	2.16	0.162	2.57	0.079	0.489
353.0	107.59	2.03	0.206	2.56	0.073	0.354	2.03	0.209	2.56	0.076	0.363
356.1	108.54	2.10	0.180	2.56	0.067	0.373	2.10	0.184	2.57	0.071	0.387
358.8	109.36	2.07	0.192	2.56	0.066	0.344	2.07	0.196	2.57	0.070	0.359
361.9	110.31	2.20	0.139	2.56	0.052	0.373	2.20	0.144	2.57	0.057	0.395
367.1	111.89	2.15	0.162	2.57	0.065	0.399	2.15	0.167	2.58	0.069	0.416
370.6	112.96	2.18	0.153	2.57	0.074	0.482	2.17	0.158	2.58	0.078	0.496
373.5	113.84	2.14	0.164	2.56	0.069	0.420	2.14	0.169	2.57	0.074	0.438
376.7	114.82	2.12	0.167	2.54	0.073	0.436	2.11	0.171	2.55	0.077	0.450
380.0	115.82	2.07	0.185	2.54	0.060	0.325	2.07	0.189	2.55	0.065	0.341
382.9	116.71	2.13	0.163	2.54	0.068	0.419	2.12	0.168	2.55	0.073	0.436
385.6	117.53	2.14	0.162	2.55	0.072	0.449	2.13	0.165	2.55	0.076	0.461
388.8	118.51	2.12	0.166	2.54	0.065	0.390	2.12	0.171	2.55	0.070	0.407
392.1	119.51	2.15	0.153	2.54	0.075	0.494	2.15	0.158	2.55	0.080	0.509
398.4	121.43	2.15	0.152	2.54	0.085	0.559	2.15	0.156	2.54	0.089	0.572
400.8	122.16	2.21	0.130	2.54	0.058	0.451	2.20	0.137	2.55	0.066	0.481
403.5	122.99	2.24	0.114	2.53	0.063	0.551	2.23	0.123	2.54	0.072	0.585
406.6	123.93	2.21	0.127	2.53	0.063	0.496	2.20	0.134	2.55	0.070	0.523
409.5	124.82	2.23	0.119	2.53	0.072	0.604	2.23	0.127	2.55	0.080	0.629
413.0	125.88	2.23	0.120	2.53	0.075	0.619	2.22	0.128	2.55	0.082	0.642
416.3	126.89	2.18	0.139	2.53	0.077	0.558	2.17	0.146	2.55	0.084	0.578
419.1	127.74	2.19	0.137	2.54	0.074	0.541	2.18	0.145	2.55	0.082	0.565
421.7	128.53	2.16	0.143	2.52	0.074	0.516	2.15	0.149	2.53	0.080	0.537
425.4	129.66	2.18	0.136	2.53	0.074	0.544	2.17	0.145	2.54	0.083	0.572
427.6	130.33	2.22	0.121	2.53	0.076	0.632	2.21	0.131	2.54	0.087	0.662
431.7	131.58	2.07	0.181	2.53	0.102	0.561	2.06	0.190	2.54	0.110	0.581
434.1	132.31	2.08	0.174	2.52	0.098	0.564	2.08	0.179	2.53	0.103	0.575
437.2	133.26	2.09	0.170	2.51	0.103	0.605	2.08	0.178	2.53	0.111	0.622
439.8	134.05	1.98	0.213	2.51	0.103	0.483	1.97	0.220	2.53	0.110	0.499
446.0	135.94	2.11	0.161	2.51	0.098	0.609	2.10	0.170	2.53	0.107	0.630
449.0	136.86	2.16	0.138	2.51	0.102	0.733	2.15	0.150	2.53	0.113	0.753
451.7	137.68	2.20	0.121	2.50	0.089	0.737	2.19	0.135	2.53	0.103	0.764
458.2	139.66	2.13	0.150	2.50	0.111	0.740	2.12	0.163	2.53	0.125	0.762
461.2	140.57	2.12	0.154	2.51	0.061	0.394	2.11	0.164	2.53	0.070	0.429
463.5	141.27	2.12	0.151	2.50	0.070	0.463	2.11	0.163	2.52	0.082	0.503
466.6	142.22	2.10	0.154	2.49	0.093	0.602	2.09	0.167	2.51	0.106	0.633
470.1	143.29	2.05	0.171	2.47	0.107	0.625	2.04	0.184	2.50	0.120	0.651
473.0	144.17	2.14	0.140	2.49	0.104	0.748	2.13	0.153	2.51	0.118	0.771
475.4	144.90	2.16	0.130	2.49	0.088	0.680	2.15	0.145	2.51	0.104	0.713
481.8	146.85	2.05	0.169	2.47	0.132	0.781	2.04	0.183	2.50	0.146	0.798
491.0	149.66	2.14	0.137	2.48	0.092	0.669	2.12	0.153	2.50	0.108	0.705
493.6	150.45	2.20	0.114	2.48	0.083	0.734	2.18	0.130	2.51	0.100	0.767
497.0	151.49	2.00	0.180	2.44	0.082	0.456	1.99	0.193	2.46	0.095	0.492

Table G-1: Laboratory Material Properties and Water Contents Measured on Core Samples from Drill Hole USW SD-12 (Continued)

[Measurements reported by L.E. Flint, U.S. Geological Survey Hydrologic Research Facility; DTN No. GS950308312231.002. J. Curtis and C. Vidano, analysts]

Depth (feet)	Depth (m)	Relative Humidity Oven-Dried					105°C Oven-Dried				
		Dry Bulk Density (g/cm ³)	Porosity (cm ³ /cm ³)	Particle Density (g/cm ³)	Vol. Water Content (cm ³ /cm ³)	Relative Satn.	Dry Bulk Density (g/cm ³)	Porosity (cm ³ /cm ³)	Particle Density (g/cm ³)	Vol. Water Content (cm ³ /cm ³)	Relative Satn.
501.3	152.80	2.07	0.167	2.48	0.101	0.608	2.05	0.182	2.51	0.117	0.641
505.9	154.20	2.06	0.144	2.41	0.092	0.640	2.05	0.161	2.44	0.109	0.678
512.6	156.24	2.06	0.169	2.48	0.101	0.597	2.04	0.185	2.50	0.116	0.630
517.8	157.83	2.04	0.143	2.38	0.111	0.772	2.02	0.157	2.40	0.124	0.792
521.5	158.95	2.16	0.126	2.47	0.108	0.858	2.14	0.143	2.50	0.125	0.875
524.1	159.75	2.21	0.103	2.47	0.078	0.754	2.19	0.124	2.50	0.098	0.794
526.7	160.54	2.13	0.133	2.46	0.098	0.731	2.12	0.153	2.50	0.117	0.766
529.5	161.39	2.10	0.144	2.46	0.108	0.749	2.09	0.162	2.49	0.126	0.777
533.0	162.46	2.01	0.183	2.46	0.119	0.653	1.99	0.200	2.49	0.137	0.683
536.0	163.37	2.08	0.159	2.47	0.098	0.617	2.06	0.174	2.50	0.113	0.651
542.0	165.20	2.14	0.135	2.47	0.077	0.573	2.12	0.153	2.50	0.095	0.623
544.6	165.99	2.19	0.115	2.47	0.070	0.609	2.17	0.134	2.50	0.089	0.665
547.8	166.97	2.14	0.131	2.46	0.105	0.805	2.12	0.152	2.50	0.127	0.832
551.4	168.07	2.11	0.140	2.45	0.116	0.828	2.08	0.164	2.49	0.140	0.853
553.7	168.77	2.07	0.159	2.45	0.114	0.716	2.04	0.182	2.50	0.137	0.752
563.5	171.75	2.17	0.122	2.47	0.098	0.798	2.15	0.146	2.51	0.121	0.831
573.4	174.77	2.18	0.123	2.48	0.110	0.894	2.16	0.144	2.52	0.131	0.909
581.0	177.09	2.14	0.134	2.47	0.089	0.660	2.12	0.152	2.50	0.106	0.700
590.1	179.86	2.20	0.116	2.49	0.100	0.860	2.18	0.136	2.52	0.119	0.881
596.0	181.66	2.16	0.124	2.46	0.099	0.800	2.14	0.147	2.50	0.122	0.832
598.8	182.51	2.21	0.107	2.47	0.088	0.826	2.19	0.129	2.51	0.110	0.856
601.9	183.46	2.21	0.110	2.48	0.085	0.770	2.19	0.132	2.52	0.106	0.807
611.0	186.23	2.18	0.122	2.49	0.106	0.868	2.17	0.139	2.52	0.123	0.885
613.8	187.09	2.16	0.134	2.49	0.124	0.925	2.14	0.152	2.52	0.142	0.934
617.2	188.12	2.16	0.128	2.48	0.116	0.911	2.14	0.145	2.51	0.134	0.922
620.1	189.01	2.21	0.116	2.50	0.100	0.864	2.19	0.135	2.53	0.119	0.883
629.0	191.72	2.18	0.120	2.48	0.075	0.626	2.16	0.139	2.51	0.094	0.675
640.7	195.29	2.23	0.108	2.50	0.081	0.748	2.22	0.126	2.54	0.099	0.785
653.3	199.13	2.34	0.061	2.50	0.057	0.921	2.32	0.088	2.54	0.084	0.945
656.3	200.04	2.19	0.122	2.49	0.109	0.898	2.17	0.139	2.52	0.126	0.911
658.8	200.80	2.24	0.104	2.50	0.089	0.861	2.22	0.122	2.53	0.107	0.881
662.5	201.93	2.26	0.096	2.50	0.080	0.841	2.24	0.113	2.53	0.098	0.866
665.1	202.72	2.26	0.091	2.48	0.083	0.909	2.24	0.111	2.52	0.103	0.925
668.5	203.76	2.30	0.069	2.46	0.063	0.922	2.27	0.091	2.50	0.085	0.941
671.3	204.61	2.31	0.065	2.47	0.047	0.734	2.29	0.087	2.51	0.070	0.802
674.1	205.47	2.26	0.084	2.47	0.057	0.672	2.24	0.106	2.51	0.078	0.739
676.6	206.23	2.30	0.096	2.55	0.076	0.794	2.28	0.116	2.58	0.096	0.829
679.3	207.05	2.29	0.097	2.54	0.080	0.830	2.27	0.116	2.57	0.100	0.859
682.7	208.09	2.28	0.079	2.47	0.066	0.833	2.26	0.100	2.51	0.087	0.867
686.0	209.09	2.30	0.070	2.48	0.060	0.854	2.28	0.092	2.51	0.082	0.889
689.0	210.01	2.30	0.094	2.54	0.083	0.887	2.28	0.114	2.57	0.103	0.907
695.0	211.84	2.31	0.064	2.46	0.058	0.918	2.28	0.090	2.50	0.084	0.942
698.0	212.75	2.31	0.082	2.52	0.064	0.781	2.29	0.103	2.56	0.085	0.824
700.8	213.60	2.32	0.077	2.51	0.071	0.924	2.29	0.099	2.54	0.093	0.940

Table G-1: Laboratory Material Properties and Water Contents Measured on Core Samples from Drill Hole USW SD-12 (Continued)

[Measurements reported by L.E. Flint, U.S. Geological Survey Hydrologic Research Facility; DTN No. GS950308312231.002. J. Curtis and C. Vidano, analysts]

Depth (feet)	Depth (m)	Relative Humidity Oven-Dried					105°C Oven-Dried				
		Dry Bulk Density (g/cm ³)	Porosity (cm ³ /cm ³)	Particle Density (g/cm ³)	Vol. Water Content (cm ³ /cm ³)	Relative Satn.	Dry Bulk Density (g/cm ³)	Porosity (cm ³ /cm ³)	Particle Density (g/cm ³)	Vol. Water Content (cm ³ /cm ³)	Relative Satn.
703.9	214.55	2.31	0.078	2.51	0.064	0.818	2.29	0.099	2.54	0.084	0.855
706.8	215.43	2.29	0.077	2.48	0.069	0.892	2.27	0.101	2.52	0.093	0.918
709.9	216.38	2.24	0.096	2.48	0.069	0.724	2.23	0.114	2.51	0.087	0.768
713.0	217.32	2.28	0.093	2.52	0.079	0.846	2.26	0.110	2.54	0.096	0.869
716.2	218.30	2.27	0.092	2.50	0.079	0.862	2.25	0.111	2.53	0.098	0.885
728.4	222.02	2.27	0.081	2.47	0.063	0.777	2.24	0.104	2.50	0.086	0.826
731.0	222.81	2.25	0.090	2.48	0.067	0.737	2.24	0.110	2.51	0.086	0.783
733.8	223.66	2.24	0.092	2.47	0.075	0.812	2.22	0.113	2.51	0.096	0.847
736.9	224.61	2.25	0.086	2.46	0.075	0.881	2.23	0.111	2.51	0.101	0.908
739.9	225.52	2.25	0.085	2.46	0.064	0.747	2.23	0.110	2.51	0.089	0.804
743.4	226.59	2.25	0.087	2.47	0.072	0.822	2.23	0.109	2.51	0.094	0.858
746.0	227.38	2.25	0.091	2.48	0.075	0.828	2.23	0.112	2.51	0.096	0.860
749.0	228.30	2.27	0.088	2.49	0.072	0.816	2.25	0.110	2.52	0.094	0.853
755.0	230.12	2.25	0.085	2.46	0.062	0.728	2.23	0.108	2.50	0.084	0.784
757.9	231.01	2.27	0.096	2.51	0.074	0.778	2.25	0.114	2.54	0.093	0.814
761.1	231.98	2.30	0.086	2.51	0.072	0.844	2.28	0.105	2.55	0.092	0.873
763.8	232.81	2.30	0.071	2.47	0.059	0.836	2.28	0.092	2.51	0.080	0.873
767.4	233.90	2.31	0.067	2.47	0.057	0.852	2.29	0.088	2.51	0.078	0.887
771.2	235.06	2.32	0.064	2.47	0.048	0.753	2.30	0.084	2.51	0.068	0.813
773.8	235.85	2.32	0.073	2.50	0.062	0.849	2.30	0.092	2.53	0.081	0.881
776.8	236.77	2.32	0.057	2.46	0.051	0.898	2.30	0.080	2.50	0.074	0.928
780.0	237.74	2.33	0.055	2.47	0.051	0.930	2.31	0.078	2.50	0.074	0.950
783.0	238.66	2.33	0.057	2.47	0.055	0.956	2.30	0.079	2.50	0.077	0.968
785.8	239.51	2.27	0.082	2.47	0.064	0.779	2.25	0.101	2.50	0.083	0.820
788.5	240.33	2.23	0.097	2.47	0.086	0.880	2.21	0.116	2.50	0.105	0.899
791.6	241.28	2.23	0.098	2.48	0.093	0.952	2.21	0.121	2.52	0.116	0.961
794.8	242.26	2.07	0.166	2.49	0.148	0.889	2.06	0.178	2.51	0.159	0.897
798.2	243.29	2.31	0.087	2.53	0.079	0.907	2.30	0.102	2.56	0.094	0.921
801.1	244.18	2.24	0.097	2.48	0.078	0.800	2.22	0.115	2.51	0.096	0.832
804.4	245.18	2.33	0.080	2.53	0.069	0.868	2.31	0.096	2.55	0.085	0.890
806.8	245.91	2.22	0.112	2.49	0.108	0.962	2.20	0.127	2.52	0.123	0.967
812.5	247.65	2.28	0.105	2.55	0.090	0.858	2.27	0.120	2.58	0.106	0.876
815.9	248.69	2.09	0.172	2.52	0.140	0.814	2.08	0.182	2.54	0.150	0.824
821.5	250.39	2.34	0.084	2.56	0.068	0.813	2.34	0.091	2.57	0.076	0.829
829.3	252.77	2.28	0.099	2.53	0.076	0.768	2.26	0.115	2.55	0.092	0.801
832.3	253.69	2.22	0.123	2.54	0.117	0.954	2.21	0.137	2.56	0.132	0.959
842.7	256.85	2.31	0.104	2.58	0.077	0.738	2.30	0.114	2.59	0.087	0.762
846.1	257.89	2.32	0.094	2.56	0.083	0.882	2.31	0.108	2.58	0.097	0.897
851.9	259.66	2.30	0.097	2.55	0.078	0.806	2.29	0.112	2.57	0.093	0.832
861.9	262.71	2.37	0.077	2.56	0.061	0.786	2.35	0.093	2.59	0.076	0.822
872.9	266.06	2.29	0.090	2.52	0.083	0.917	2.28	0.106	2.55	0.099	0.929
876.1	267.04	2.11	0.157	2.50	0.122	0.778	2.10	0.170	2.53	0.135	0.795
881.9	268.80	2.36	0.073	2.54	0.060	0.812	2.34	0.092	2.58	0.078	0.851
887.6	270.54	2.33	0.075	2.52	0.071	0.954	2.31	0.092	2.55	0.089	0.963

Table G-1: Laboratory Material Properties and Water Contents Measured on Core Samples from Drill Hole USW SD-12 (Continued)

[Measurements reported by L.E. Flint, U.S. Geological Survey Hydrologic Research Facility; DTN No. GS950308312231.002. J. Curtis and C. Vidano, analysts]

Depth (feet)	Depth (m)	Relative Humidity Oven-Dried					105°C Oven-Dried				
		Dry Bulk Density (g/cm ³)	Porosity (cm ³ /cm ³)	Particle Density (g/cm ³)	Vol. Water Content (cm ³ /cm ³)	Relative Satn.	Dry Bulk Density (g/cm ³)	Porosity (cm ³ /cm ³)	Particle Density (g/cm ³)	Vol. Water Content (cm ³ /cm ³)	Relative Satn.
894.2	272.55	2.08	0.174	2.51	0.150	0.863	2.06	0.185	2.53	0.161	0.871
896.8	273.34	2.29	0.079	2.49	0.060	0.758	2.27	0.096	2.52	0.077	0.800
902.9	275.20	2.22	0.109	2.50	0.082	0.748	2.21	0.125	2.52	0.098	0.780
918.4	279.93	2.30	0.085	2.51	0.069	0.810	2.28	0.102	2.54	0.086	0.843
921.1	280.75	2.27	0.099	2.52	0.085	0.858	2.25	0.115	2.54	0.101	0.878
923.4	281.45	2.23	0.109	2.51	0.097	0.888	2.22	0.124	2.53	0.111	0.901
926.5	282.40	2.14	0.143	2.50	0.123	0.860	2.13	0.158	2.53	0.138	0.873
929.2	283.22	2.34	0.086	2.56	0.076	0.892	2.33	0.101	2.59	0.092	0.908
935.7	285.20	2.20	0.117	2.50	0.089	0.763	2.19	0.134	2.52	0.106	0.793
938.8	286.15	2.30	0.100	2.55	0.090	0.899	2.28	0.116	2.58	0.106	0.913
945.5	288.19	2.31	0.093	2.55	0.081	0.871	2.29	0.108	2.57	0.096	0.889
948.3	289.04	2.13	0.148	2.50	0.122	0.821	2.12	0.160	2.52	0.133	0.834
956.7	291.60	2.16	0.138	2.51	0.129	0.936	2.15	0.149	2.53	0.140	0.941
962.7	293.43	2.33	0.086	2.55	0.075	0.862	2.31	0.102	2.57	0.090	0.883
981.7	299.22	2.28	0.092	2.51	0.075	0.819	2.27	0.106	2.53	0.089	0.843
986.8	300.78	2.33	0.078	2.52	0.064	0.823	2.31	0.095	2.55	0.081	0.854
996.8	303.82	2.17	0.131	2.50	0.117	0.898	2.16	0.140	2.51	0.126	0.905
1026.1	312.76	2.35	0.072	2.53	0.065	0.908	2.34	0.089	2.56	0.083	0.926
1029.1	313.67	2.06	0.180	2.52	0.152	0.846	2.06	0.188	2.53	0.160	0.852
1034.8	315.41	2.14	0.142	2.50	0.134	0.943	2.13	0.152	2.52	0.144	0.947
1039.6	316.87	2.33	0.074	2.52	0.063	0.857	2.32	0.091	2.55	0.080	0.883
1044.4	318.33	2.24	0.102	2.49	0.059	0.582	2.22	0.115	2.51	0.072	0.629
1052.2	320.71	2.19	0.119	2.48	0.119	0.998	2.18	0.132	2.51	0.132	0.999
1063.3	324.09	2.27	0.096	2.51	0.086	0.898	2.26	0.112	2.54	0.102	0.912
1071.4	326.56	2.33	0.087	2.55	0.051	0.580	2.31	0.105	2.58	0.069	0.651
1074.4	327.48	2.28	0.100	2.53	0.082	0.818	2.26	0.117	2.56	0.099	0.845
1076.6	328.15	2.36	0.074	2.55	0.061	0.819	2.34	0.093	2.58	0.080	0.855
1079.3	328.97	2.36	0.076	2.55	0.058	0.768	2.34	0.093	2.58	0.076	0.811
1083.7	330.31	2.30	0.100	2.56	0.044	0.444	2.29	0.115	2.58	0.060	0.520
1085.5	330.86	2.34	0.082	2.55	0.063	0.772	2.32	0.098	2.58	0.080	0.811
1089.4	332.05	2.33	0.088	2.56	0.064	0.727	2.31	0.106	2.59	0.082	0.773
1092.0	332.84	2.22	0.119	2.52	0.073	0.608	2.20	0.136	2.55	0.090	0.657
1099.6	335.16	2.34	0.086	2.56	0.057	0.659	2.32	0.104	2.59	0.075	0.717
1102.1	335.92	2.29	0.092	2.52	0.081	0.886	2.27	0.110	2.55	0.099	0.904
1104.8	336.74	2.33	0.074	2.51	0.067	0.901	2.31	0.092	2.54	0.084	0.920
1108.0	337.72	2.34	0.074	2.53	0.066	0.887	2.32	0.092	2.56	0.083	0.908
1114.3	339.64	2.34	0.067	2.50	0.062	0.929	2.32	0.085	2.53	0.080	0.944
1116.5	340.31	2.30	0.066	2.46	0.052	0.788	2.28	0.085	2.49	0.071	0.835
1119.3	341.16	2.31	0.072	2.49	0.060	0.839	2.30	0.090	2.52	0.078	0.872
1121.5	341.83	2.32	0.074	2.51	0.065	0.869	2.30	0.092	2.54	0.083	0.894
1123.5	342.44	2.31	0.087	2.53	0.072	0.836	2.29	0.104	2.56	0.090	0.863
1126.6	343.39	2.30	0.082	2.50	0.069	0.848	2.28	0.098	2.53	0.086	0.874
1129.2	344.18	2.32	0.074	2.51	0.057	0.770	2.30	0.092	2.54	0.075	0.816
1131.3	344.82	2.30	0.086	2.51	0.069	0.802	2.28	0.104	2.54	0.087	0.836

Table G-1: Laboratory Material Properties and Water Contents Measured on Core Samples from Drill Hole USW SD-12 (Continued)

[Measurements reported by L.E. Flint, U.S. Geological Survey Hydrologic Research Facility; DTN No. GS950308312231.002. J. Curtis and C. Vidano, analysts]

Depth (feet)	Depth (m)	Relative Humidity Oven-Dried					105°C Oven-Dried				
		Dry Bulk Density (g/cm ³)	Porosity (cm ³ /cm ³)	Particle Density (g/cm ³)	Vol. Water Content (cm ³ /cm ³)	Relative Satn.	Dry Bulk Density (g/cm ³)	Porosity (cm ³ /cm ³)	Particle Density (g/cm ³)	Vol. Water Content (cm ³ /cm ³)	Relative Satn.
1134.8	345.89	2.31	0.087	2.53	0.072	0.834	2.29	0.106	2.56	0.091	0.864
1139.2	347.23	2.29	0.091	2.52	0.059	0.652	2.28	0.107	2.55	0.075	0.702
1141.9	348.05	2.34	0.077	2.54	0.064	0.826	2.33	0.094	2.57	0.081	0.858
1147.3	349.70	2.29	0.091	2.52	0.068	0.750	2.27	0.109	2.55	0.086	0.792
1150.4	350.64	2.34	0.072	2.52	0.053	0.730	2.32	0.089	2.55	0.069	0.782
1152.7	351.34	2.33	0.081	2.53	0.063	0.776	2.31	0.097	2.56	0.079	0.814
1160.0	353.57	2.35	0.072	2.54	0.056	0.770	2.34	0.091	2.57	0.074	0.816
1161.1	353.90	2.35	0.069	2.52	0.053	0.775	2.33	0.087	2.55	0.071	0.822
1165.3	355.18	2.28	0.101	2.54	0.077	0.765	2.26	0.120	2.57	0.096	0.803
1171.0	356.92	2.31	0.091	2.54	0.081	0.883	2.29	0.112	2.58	0.101	0.904
1178.7	359.27	2.31	0.079	2.51	0.061	0.780	2.29	0.097	2.54	0.080	0.822
1180.1	359.69	2.31	0.077	2.50	0.037	0.478	2.29	0.095	2.53	0.055	0.579
1181.1	360.00	2.34	0.074	2.52	0.059	0.802	2.32	0.091	2.55	0.076	0.839
1184.1	360.91	2.08	0.168	2.50	0.152	0.903	2.07	0.187	2.54	0.171	0.913
1189.1	362.44	2.34	0.067	2.50	0.058	0.862	2.32	0.086	2.54	0.077	0.892
1192.1	363.35	2.30	0.081	2.51	0.074	0.908	2.28	0.099	2.54	0.092	0.924
1195.0	364.24	2.35	0.060	2.50	0.052	0.865	2.34	0.076	2.53	0.068	0.894
1206.9	367.86	2.36	0.065	2.52	0.060	0.913	2.34	0.083	2.55	0.078	0.931
1209.8	368.75	2.36	0.064	2.52	0.058	0.900	2.35	0.081	2.55	0.075	0.921
1212.9	369.69	2.32	0.073	2.51	0.062	0.844	2.31	0.089	2.53	0.078	0.872
1219.0	371.55	2.34	0.074	2.52	0.061	0.818	2.32	0.091	2.55	0.077	0.851
1224.6	373.26	2.35	0.063	2.51	0.050	0.802	2.34	0.079	2.54	0.066	0.842
1231.0	375.21	2.34	0.062	2.49	0.053	0.861	2.32	0.081	2.52	0.072	0.893
1234.2	376.18	2.34	0.067	2.51	0.059	0.886	2.32	0.086	2.54	0.079	0.912
1239.6	377.83	2.34	0.075	2.53	0.064	0.849	2.32	0.094	2.56	0.083	0.880
1243.1	378.90	2.32	0.071	2.50	0.059	0.833	2.30	0.090	2.53	0.078	0.868
1246.1	379.81	2.34	0.070	2.51	0.061	0.869	2.32	0.089	2.54	0.080	0.897
1249.2	380.76	2.34	0.066	2.50	0.059	0.891	2.32	0.086	2.54	0.078	0.915
1255.0	382.52	2.31	0.076	2.50	0.057	0.750	2.29	0.095	2.54	0.076	0.800
1258.1	383.47	2.33	0.067	2.50	0.054	0.804	2.31	0.086	2.53	0.073	0.848
1261.2	384.41	2.35	0.055	2.49	0.046	0.844	2.33	0.076	2.52	0.067	0.887
1264.5	385.42	2.33	0.060	2.48	0.050	0.828	2.31	0.080	2.51	0.070	0.870
1266.8	386.12	2.33	0.055	2.47	0.054	0.992	2.30	0.094	2.53	0.093	0.995
1270.1	387.13	2.26	0.043	2.36	0.046	1.065	2.22	0.080	2.41	0.083	1.035
1272.5	387.86	2.38	0.035	2.46	0.022	0.618	2.34	0.068	2.51	0.055	0.804
1278.8	389.78	2.33	0.014	2.36	0.012	0.911	2.30	0.041	2.40	0.040	0.971
1282.0	390.75	2.23	0.014	2.26	0.009	0.684	2.22	0.026	2.28	0.022	0.836
1284.9	391.64	1.76	0.145	2.06	0.134	0.925	1.57	0.340	2.37	0.329	0.968
1287.6	392.46	2.30	0.007	2.32	0.005	0.738	2.30	0.014	2.33	0.012	0.864
1299.6	396.12	2.30	0.011	2.33	0.008	0.673	2.29	0.020	2.34	0.016	0.819
1302.5	397.00	2.32	0.022	2.37	0.019	0.873	2.31	0.031	2.39	0.028	0.909
1309.1	399.01	2.25	0.049	2.37	0.042	0.854	2.24	0.063	2.39	0.056	0.887
1312.4	400.02	2.23	0.058	2.37	0.050	0.852	2.22	0.070	2.39	0.061	0.876
1314.9	400.78	2.18	0.083	2.37	0.063	0.754	2.17	0.095	2.39	0.074	0.784

Table G-1: Laboratory Material Properties and Water Contents Measured on Core Samples from Drill Hole USW SD-12 (Continued)

[Measurements reported by L.E. Flint, U.S. Geological Survey Hydrologic Research Facility; DTN No. GS950308312231.002. J. Curtis and C. Vidano, analysts]

Depth (feet)	Depth (m)	Relative Humidity Oven-Dried					105°C Oven-Dried				
		Dry Bulk Density (g/cm ³)	Porosity (cm ³ /cm ³)	Particle Density (g/cm ³)	Vol. Water Content (cm ³ /cm ³)	Relative Satn.	Dry Bulk Density (g/cm ³)	Porosity (cm ³ /cm ³)	Particle Density (g/cm ³)	Vol. Water Content (cm ³ /cm ³)	Relative Satn.
1317.7	401.63	2.15	0.091	2.37	0.069	0.756	2.14	0.104	2.39	0.082	0.786
1321.5	402.79	2.09	0.118	2.37	0.077	0.648	2.08	0.128	2.39	0.087	0.675
1323.6	403.43	2.04	0.140	2.37	0.083	0.593	2.03	0.150	2.38	0.093	0.620
1327.0	404.47	1.97	0.143	2.30	0.084	0.585	1.96	0.152	2.31	0.093	0.610
1332.9	406.27	1.73	0.265	2.35	0.093	0.350	1.71	0.288	2.40	0.117	0.404
1336.1	407.24	1.77	0.234	2.31	0.080	0.343	1.76	0.245	2.33	0.091	0.371
1338.8	408.07	1.74	0.248	2.31	0.086	0.347	1.73	0.254	2.32	0.092	0.363
1341.9	409.01	1.68	0.281	2.34	0.073	0.259	1.68	0.286	2.35	0.078	0.271
1345.0	409.96	1.62	0.300	2.31	0.075	0.249	1.61	0.305	2.32	0.080	0.261
1347.6	410.75	1.59	0.302	2.28	0.065	0.216	1.59	0.306	2.29	0.070	0.227
1351.0	411.78	1.57	0.315	2.29	0.069	0.219	1.56	0.318	2.29	0.073	0.228
1354.3	412.79	1.53	0.323	2.26	0.059	0.182	1.53	0.326	2.27	0.062	0.190
1356.8	413.55	1.55	0.309	2.25	0.058	0.188	1.55	0.312	2.26	0.061	0.195
1359.9	414.50	1.57	0.300	2.24	0.065	0.218	1.57	0.302	2.24	0.068	0.224
1362.6	415.32	1.57	0.311	2.28	0.066	0.211	1.57	0.313	2.28	0.067	0.215
1365.8	416.30	1.57	0.298	2.24	0.063	0.213	1.57	0.300	2.25	0.066	0.219
1369.2	417.33	1.51	0.316	2.21	0.073	0.231	1.51	0.319	2.22	0.076	0.238
1371.8	418.12	1.58	0.299	2.25	0.062	0.206	1.58	0.301	2.26	0.064	0.213
1374.8	419.04	1.75	0.312	2.26	0.074	0.237	1.55	0.314	2.27	0.076	0.243
1386.6	422.64	1.55	0.366	2.29	0.094	0.258	1.44	0.376	2.31	0.104	0.277
1389.9	423.64	1.65	0.359	2.29	0.103	0.286	1.45	0.372	2.31	0.116	0.312
1392.7	424.49	1.62	0.321	2.34	0.091	0.285	1.57	0.338	2.37	0.108	0.320
1395.7	425.41	1.54	0.360	2.29	0.093	0.258	1.45	0.379	2.33	0.112	0.295
1402.2	427.39	1.58	0.306	2.36	0.102	0.333	1.62	0.324	2.39	0.120	0.370
1404.3	428.03	1.70	0.349	2.32	0.105	0.300	1.49	0.373	2.37	0.129	0.345
1407.7	429.07	1.67	0.362	2.32	0.109	0.301	1.46	0.382	2.36	0.129	0.338
1410.6	429.95	1.63	0.336	2.38	0.092	0.274	1.56	0.358	2.43	0.114	0.318
1415.8	431.54	1.65	0.359	2.28	0.077	0.213	1.45	0.368	2.30	0.085	0.232
1419.3	432.60	1.63	0.323	2.25	0.072	0.223	1.51	0.337	2.27	0.086	0.255
1423.0	433.73	1.63	0.335	2.27	0.077	0.231	1.50	0.347	2.29	0.090	0.258
1429.1	435.59	1.64	0.349	2.29	0.087	0.249	1.48	0.358	2.30	0.096	0.268
1432.0	436.47	1.57	0.358	2.28	0.083	0.233	1.45	0.368	2.30	0.094	0.255
1437.9	438.27	1.41	0.382	2.28	0.085	0.222	1.40	0.394	2.31	0.097	0.246
1440.0	438.91	1.50	0.340	2.26	0.102	0.302	1.46	0.370	2.33	0.133	0.360
1440.8	439.16	1.46	0.335	2.20	0.095	0.283	1.45	0.346	2.22	0.106	0.306
1447.0	441.05	1.49	0.284	2.08	0.115	0.403	1.45	0.317	2.13	0.148	0.465
1450.2	442.02	1.51	0.279	2.09	0.094	0.339	1.48	0.304	2.13	0.120	0.394
1452.7	442.78	1.48	0.343	2.25	0.106	0.310	1.44	0.380	2.33	0.144	0.378
1456.6	443.97	1.50	0.331	2.25	0.120	0.363	1.40	0.433	2.47	0.222	0.513
1458.9	444.67	1.40	0.376	2.25	0.110	0.293	1.38	0.404	2.31	0.139	0.343
1462.1	445.65	1.43	0.359	2.23	0.106	0.297	1.40	0.390	2.30	0.137	0.352
1465.6	446.71	1.44	0.344	2.20	0.120	0.349	1.41	0.376	2.26	0.152	0.404
1468.8	447.69	1.42	0.360	2.22	0.111	0.308	1.38	0.397	2.30	0.148	0.372
1470.7	448.27	1.60	0.325	2.37	0.122	0.374	1.56	0.360	2.44	0.156	0.435

Table G-1: Laboratory Material Properties and Water Contents Measured on Core Samples from Drill Hole USW SD-12 (Continued)

[Measurements reported by L.E. Flint, U.S. Geological Survey Hydrologic Research Facility; DTN No. GS950308312231.002.
J. Curtis and C. Vidano, analysts]

Depth (feet)	Depth (m)	Relative Humidity Oven-Dried					105°C Oven-Dried				
		Dry Bulk Density (g/cm ³)	Porosity (cm ³ /cm ³)	Particle Density (g/cm ³)	Vol. Water Content (cm ³ /cm ³)	Relative Satn.	Dry Bulk Density (g/cm ³)	Porosity (cm ³ /cm ³)	Particle Density (g/cm ³)	Vol. Water Content (cm ³ /cm ³)	Relative Satn.
1478.3	450.59	1.67	0.291	2.36	0.091	0.312	1.65	0.309	2.39	0.109	0.353
1479.5	450.95	1.59	0.314	2.32	0.108	0.343	1.56	0.346	2.38	0.140	0.404
1482.5	451.87	1.47	0.359	2.29	0.134	0.373	1.44	0.383	2.34	0.159	0.414
1485.6	452.81	1.57	0.267	2.14	0.174	0.652	1.54	0.303	2.20	0.211	0.694
1488.6	453.73	1.50	0.250	2.00	0.203	0.811	1.46	0.285	2.05	0.238	0.835
1491.4	454.58	1.51	0.254	2.03	0.203	0.801	1.47	0.293	2.08	0.243	0.828
1494.7	455.58	1.50	0.230	1.95	0.207	0.901	1.46	0.270	2.00	0.247	0.915
1497.6	456.47	1.52	0.252	2.03	0.228	0.906	1.48	0.289	2.09	0.265	0.918
1500.6	457.38	1.43	0.295	2.03	0.236	0.801	1.40	0.326	2.08	0.268	0.820
1504.0	458.42	1.41	0.361	2.21	0.301	0.835	1.40	0.379	2.25	0.319	0.843
1507.0	459.33	1.48	0.336	2.23	0.332	0.990	1.44	0.378	2.32	0.375	0.991
1509.8	460.19	1.50	0.333	2.24	0.329	0.990	1.45	0.374	2.32	0.371	0.991
1513.0	461.16	1.49	0.335	2.25	0.330	0.984	1.45	0.381	2.34	0.376	0.986
1515.7	461.99	1.47	0.324	2.18	0.328	1.012	1.43	0.366	2.26	0.370	1.011
1519.1	463.02	1.51	0.304	2.17	0.303	0.994	1.46	0.355	2.26	0.353	0.995
1522.2	463.97	1.48	0.308	2.14	0.295	0.958	1.43	0.355	2.22	0.342	0.963
1524.5	464.67	1.47	0.260	1.99	0.276	1.060	1.43	0.307	2.06	0.322	1.051
1528.2	465.80	1.52	0.308	2.19	0.287	0.933	1.45	0.372	2.31	0.351	0.945
1531.0	466.65	1.45	0.340	2.20	0.317	0.933	1.40	0.389	2.30	0.367	0.942
1534.4	467.69	1.53	0.309	2.21	0.299	0.967	1.47	0.367	2.32	0.357	0.973
1537.2	468.54	1.48	0.333	2.22	0.322	0.964	1.42	0.394	2.34	0.382	0.970
1539.8	469.33	1.53	0.318	2.25	0.305	0.959	1.47	0.380	2.37	0.367	0.966
1542.5	470.15	1.52	0.312	2.21	0.314	1.005	1.44	0.390	2.36	0.391	1.004
1546.0	471.22	1.48	0.327	2.20	0.317	0.971	1.42	0.388	2.32	0.379	0.976
1549.0	472.14	1.59	0.280	2.21	0.254	0.907	1.52	0.352	2.34	0.326	0.926
1557.1	474.60	1.57	0.321	2.31	0.158	0.493	1.54	0.351	2.37	0.188	0.536
1558.1	474.91	1.59	0.304	2.29	0.145	0.475	1.56	0.338	2.36	0.178	0.527
1560.4	475.61	1.58	0.310	2.29	0.174	0.560	1.54	0.351	2.37	0.215	0.612
1563.5	476.55	1.52	0.272	2.08	0.231	0.852	1.47	0.318	2.16	0.278	0.874
1567.0	477.62	1.51	0.257	2.03	0.213	0.828	1.47	0.304	2.10	0.260	0.854
1570.0	478.54	1.51	0.260	2.04	0.222	0.852	1.46	0.304	2.10	0.265	0.873
1573.2	479.51	1.51	0.313	2.19	0.273	0.873	1.46	0.354	2.27	0.315	0.888
1575.2	480.12	1.47	0.307	2.12	0.248	0.807	1.42	0.357	2.20	0.298	0.834
1578.8	481.22	1.47	0.330	2.19	0.310	0.939	1.41	0.384	2.30	0.364	0.948
1581.6	482.07	1.45	0.318	2.12	0.283	0.892	1.39	0.376	2.23	0.342	0.909
1584.7	483.02	1.47	0.320	2.16	0.301	0.940	1.41	0.378	2.27	0.359	0.949
1588.2	484.08	1.45	0.347	2.22	0.324	0.933	1.40	0.403	2.34	0.379	0.943
1591.4	485.06	1.47	0.348	2.25	0.329	0.945	1.41	0.404	2.37	0.385	0.953
1594.1	485.88	1.47	0.333	2.21	0.321	0.963	1.41	0.395	2.33	0.382	0.969
1597.0	486.77	1.45	0.348	2.23	0.330	0.948	1.39	0.415	2.37	0.397	0.957
1599.6	487.56	1.44	0.352	2.22	0.326	0.927	1.37	0.418	2.35	0.392	0.939
1602.6	488.47	1.76	0.175	2.13	0.196	1.115	1.62	0.315	2.36	0.335	1.064
1605.9	489.48	1.71	0.215	2.18	0.219	1.020	1.57	0.356	2.44	0.360	1.012
1609.2	490.48	1.73	0.213	2.20	0.208	0.977	1.60	0.344	2.44	0.339	0.986

Table G-1: Laboratory Material Properties and Water Contents Measured on Core Samples from Drill Hole USW SD-12 (Continued)

[Measurements reported by L.E. Flint, U.S. Geological Survey Hydrologic Research Facility; DTN No. GS950308312231.002. J. Curtis and C. Vidano, analysts]

Depth (feet)	Depth (m)	Relative Humidity Oven-Dried					105°C Oven-Dried				
		Dry Bulk Density (g/cm ³)	Porosity (cm ³ /cm ³)	Particle Density (g/cm ³)	Vol. Water Content (cm ³ /cm ³)	Relative Satn.	Dry Bulk Density (g/cm ³)	Porosity (cm ³ /cm ³)	Particle Density (g/cm ³)	Vol. Water Content (cm ³ /cm ³)	Relative Satn.
1612.0	491.34	2.09	0.042	2.18	0.043	1.030	1.95	0.181	2.38	0.182	1.007
1614.8	492.19	1.94	0.118	2.20	0.122	1.034	1.81	0.243	2.39	0.247	1.017
1617.1	492.89	1.91	0.117	2.16	0.118	1.010	1.78	0.248	2.37	0.249	1.005
1620.6	493.96	1.72	0.237	2.25	0.242	1.020	1.62	0.335	2.43	0.339	1.014
1624.1	495.03	1.84	0.187	2.26	0.197	1.056	1.74	0.289	2.44	0.299	1.036
1628.7	496.43	1.75	0.223	2.25	0.206	0.924	1.65	0.329	2.45	0.312	0.949
1632.7	497.65	1.86	0.202	2.33	0.191	0.947	1.79	0.276	2.47	0.265	0.961
1635.4	498.47	1.92	0.165	2.30	0.169	1.025	1.83	0.261	2.47	0.266	1.016
1639.4	499.69	2.04	0.159	2.43	0.191	1.200	1.95	0.249	2.60	0.281	1.128
1641.7	500.39	2.03	0.164	2.44	0.194	1.180	1.96	0.242	2.58	0.272	1.122
1644.9	501.37	1.96	0.167	2.35	0.167	0.997	1.87	0.260	2.52	0.260	0.998
1647.9	502.28	2.09	0.132	2.41	0.152	1.148	2.00	0.226	2.58	0.246	1.087
1650.7	503.13	1.94	0.146	2.27	0.143	0.982	1.81	0.275	2.49	0.272	0.990
1653.1	503.86	1.85	0.159	2.20	0.145	0.916	1.71	0.292	2.42	0.279	0.954
1656.8	504.99	1.79	0.181	2.19	0.174	0.961	1.67	0.302	2.39	0.295	0.977
1660.0	505.97	1.78	0.200	2.23	0.189	0.948	1.67	0.316	2.43	0.305	0.967
1662.8	506.82	1.63	0.269	2.23	0.274	1.018	1.53	0.372	2.43	0.377	1.013
1667.5	508.25	1.84	0.163	2.20	0.154	0.941	1.74	0.268	2.38	0.259	0.964
1668.7	508.62	1.93	0.119	2.18	0.119	1.000	1.81	0.236	2.37	0.236	1.000
1671.1	509.35	1.77	0.207	2.23	0.235	1.133	1.66	0.310	2.41	0.338	1.089
1677.0	511.15	1.91	0.166	2.30	0.093	0.558	1.86	0.219	2.38	0.146	0.665
1678.2	511.52	1.69	0.301	2.41	0.128	0.424	1.67	0.314	2.44	0.141	0.448
1680.5	512.22	1.70	0.327	2.53	0.100	0.305	1.69	0.335	2.55	0.108	0.323
1686.7	514.11	1.65	0.339	2.49	0.074	0.218	1.64	0.346	2.51	0.081	0.234
1687.7	514.41	1.71	0.315	2.50	0.083	0.263	1.70	0.323	2.52	0.091	0.281
1689.7	515.02	1.64	0.345	2.51	0.081	0.235	1.64	0.353	2.53	0.088	0.251
1696.4	517.06	1.68	0.334	2.52	0.114	0.341	1.67	0.344	2.54	0.124	0.360
1698.7	517.76	1.65	0.348	2.52	0.113	0.325	1.64	0.358	2.55	0.123	0.344
1701.7	518.68	1.64	0.352	2.53	0.088	0.250	1.63	0.360	2.55	0.096	0.268
1706.0	519.99	1.67	0.335	2.51	0.081	0.240	1.66	0.344	2.53	0.089	0.259
1708.0	520.60	1.68	0.342	2.56	0.088	0.257	1.67	0.350	2.57	0.096	0.273
1712.1	521.85	1.70	0.334	2.55	0.086	0.258	1.69	0.344	2.57	0.096	0.278
1714.6	522.61	1.72	0.321	2.54	0.092	0.287	1.71	0.331	2.56	0.103	0.310
1716.9	523.31	1.72	0.326	2.55	0.086	0.264	1.71	0.334	2.57	0.094	0.282
1720.4	524.38	1.76	0.311	2.55	0.076	0.246	1.75	0.320	2.57	0.086	0.268
1723.2	525.23	1.76	0.312	2.56	0.082	0.264	1.75	0.321	2.58	0.092	0.285
1725.8	526.02	1.76	0.307	2.55	0.077	0.252	1.75	0.317	2.57	0.087	0.276
1728.9	526.97	1.76	0.310	2.55	0.082	0.264	1.75	0.320	2.58	0.092	0.287
1731.7	527.82	1.77	0.306	2.56	0.088	0.289	1.76	0.317	2.58	0.099	0.312
1734.8	528.77	1.78	0.301	2.55	0.080	0.266	1.77	0.311	2.57	0.090	0.290
1737.7	529.65	1.80	0.298	2.56	0.076	0.255	1.79	0.308	2.58	0.086	0.280
1743.9	531.54	1.85	0.278	2.56	0.093	0.334	1.84	0.289	2.58	0.104	0.359
1746.8	532.42	1.79	0.299	2.56	0.083	0.279	1.78	0.308	2.58	0.093	0.302
1749.5	533.25	1.81	0.288	2.54	0.086	0.297	1.80	0.301	2.57	0.099	0.327

Table G-1: Laboratory Material Properties and Water Contents Measured on Core Samples from Drill Hole USW SD-12 (Continued)

[Measurements reported by L.E. Flint, U.S. Geological Survey Hydrologic Research Facility; DTN No. GS950308312231.002. J. Curtis and C. Vidano, analysts]

Depth (feet)	Depth (m)	Relative Humidity Oven-Dried					105°C Oven-Dried				
		Dry Bulk Density (g/cm ³)	Porosity (cm ³ /cm ³)	Particle Density (g/cm ³)	Vol. Water Content (cm ³ /cm ³)	Relative Satn.	Dry Bulk Density (g/cm ³)	Porosity (cm ³ /cm ³)	Particle Density (g/cm ³)	Vol. Water Content (cm ³ /cm ³)	Relative Satn.
1752.9	534.28	1.83	0.283	2.55	0.097	0.343	1.82	0.297	2.58	0.110	0.372
1755.8	535.17	1.81	0.291	2.56	0.086	0.297	1.80	0.303	2.58	0.098	0.324
1758.8	536.08	1.83	0.286	2.56	0.084	0.293	1.82	0.296	2.58	0.094	0.318
1761.6	536.94	1.80	0.295	2.55	0.084	0.285	1.79	0.307	2.58	0.096	0.312
1764.4	537.79	1.85	0.273	2.55	0.090	0.330	1.84	0.287	2.58	0.104	0.362
1767.8	538.83	1.83	0.282	2.54	0.090	0.318	1.81	0.295	2.57	0.103	0.349
1770.7	539.71	1.83	0.282	2.54	0.082	0.290	1.81	0.296	2.58	0.096	0.324
1774.1	540.75	1.83	0.280	2.54	0.086	0.308	1.82	0.292	2.57	0.099	0.337
1777.2	541.69	1.83	0.281	2.55	0.084	0.297	1.82	0.292	2.57	0.094	0.323
1779.9	542.51	1.82	0.285	2.54	0.082	0.287	1.81	0.294	2.57	0.091	0.310
1782.8	543.40	1.86	0.266	2.54	0.084	0.314	1.86	0.275	2.56	0.093	0.337
1786.0	544.37	1.92	0.247	2.55	0.093	0.378	1.91	0.255	2.57	0.102	0.399
1788.5	545.13	1.96	0.237	2.57	0.092	0.389	1.95	0.246	2.59	0.101	0.412
1790.8	545.84	1.97	0.228	2.55	0.090	0.395	1.96	0.239	2.57	0.101	0.422
1801.1	548.98	2.00	0.215	2.55	0.105	0.489	1.99	0.228	2.57	0.118	0.519
1804.0	549.86	2.00	0.214	2.54	0.100	0.468	1.98	0.229	2.57	0.115	0.503
1807.4	550.90	2.02	0.209	2.55	0.116	0.556	2.00	0.222	2.58	0.129	0.582
1810.0	551.69	2.03	0.200	2.54	0.116	0.580	2.02	0.216	2.57	0.132	0.611
1812.8	552.54	2.08	0.183	2.54	0.130	0.710	2.06	0.201	2.58	0.147	0.734
1818.6	554.31	2.06	0.191	2.54	0.147	0.769	2.04	0.204	2.57	0.160	0.784
1821.8	555.28	2.09	0.172	2.52	0.143	0.835	2.07	0.193	2.56	0.164	0.853
1824.7	556.17	2.14	0.144	2.50	0.135	0.932	2.11	0.173	2.55	0.163	0.943
1828.0	557.17	2.18	0.130	2.51	0.114	0.872	2.16	0.153	2.55	0.136	0.891
1831.3	558.18	2.20	0.113	2.48	0.090	0.799	2.18	0.141	2.53	0.119	0.840
1833.7	558.91	2.20	0.110	2.48	0.098	0.889	2.17	0.144	2.53	0.132	0.915
1836.8	559.86	2.15	0.137	2.49	0.100	0.727	2.12	0.163	2.54	0.125	0.770
1839.3	560.62	2.12	0.146	2.48	0.136	0.931	2.09	0.180	2.54	0.170	0.944
1843.1	561.78	2.01	0.189	2.48	0.137	0.727	1.98	0.217	2.53	0.165	0.762
1845.4	562.48	1.94	0.206	2.45	0.184	0.894	1.91	0.235	2.50	0.213	0.907
1849.1	563.61	1.88	0.241	2.47	0.220	0.914	1.86	0.262	2.51	0.241	0.921
1854.7	565.31	1.87	0.235	2.45	0.204	0.868	1.85	0.257	2.49	0.226	0.880
1858.2	566.38	1.93	0.218	2.47	0.202	0.924	1.90	0.246	2.52	0.230	0.933
1863.3	567.93	1.85	0.256	2.48	0.164	0.642	1.83	0.275	2.52	0.183	0.666
1864.0	568.15	1.86	0.237	2.44	0.206	0.866	1.84	0.256	2.48	0.224	0.876
1866.8	569.00	1.86	0.235	2.43	0.215	0.915	1.85	0.252	2.47	0.232	0.921
1872.8	570.83	1.91	0.223	2.45	0.247	1.107	1.84	0.289	2.59	0.313	1.082
1873.5	571.04	1.88	0.201	2.36	0.199	0.991	1.80	0.280	2.50	0.278	0.994
1876.0	571.80	1.87	0.198	2.33	0.195	0.985	1.78	0.280	2.48	0.277	0.989
1879.0	572.72	1.87	0.187	2.30	0.199	1.063	1.77	0.284	2.48	0.295	1.042
1882.4	573.76	1.70	0.258	2.28	0.243	0.941	1.61	0.344	2.45	0.329	0.956
1884.8	574.49	1.71	0.249	2.27	0.261	1.046	1.62	0.340	2.45	0.352	1.034
1887.4	575.28	1.63	0.285	2.28	0.297	1.040	1.53	0.379	2.47	0.391	1.030
1890.9	576.35	1.46	0.354	2.26	0.282	0.796	1.39	0.426	2.42	0.354	0.831
1894.0	577.29	1.57	0.303	2.25	0.310	1.024	1.48	0.389	2.42	0.396	1.019

Table G-1: Laboratory Material Properties and Water Contents Measured on Core Samples from Drill Hole USW SD-12 (Continued)

[Measurements reported by L.E. Flint, U.S. Geological Survey Hydrologic Research Facility; DTN No. GS950308312231.002. J. Curtis and C. Vidano, analysts]

Depth (feet)	Depth (m)	Relative Humidity Oven-Dried					105°C Oven-Dried				
		Dry Bulk Density (g/cm ³)	Porosity (cm ³ /cm ³)	Particle Density (g/cm ³)	Vol. Water Content (cm ³ /cm ³)	Relative Satn.	Dry Bulk Density (g/cm ³)	Porosity (cm ³ /cm ³)	Particle Density (g/cm ³)	Vol. Water Content (cm ³ /cm ³)	Relative Satn.
1897.1	578.24	1.54	0.329	2.30	0.300	0.912	1.47	0.406	2.47	0.377	0.929
1900.4	579.24	1.58	0.310	2.29	0.250	0.806	1.50	0.385	2.44	0.325	0.844
1902.6	579.91	1.66	0.283	2.31	0.263	0.930	1.57	0.366	2.48	0.346	0.946
1906.5	581.10	1.73	0.239	2.27	0.240	1.004	1.64	0.332	2.45	0.333	1.003
1909.5	582.02	1.72	0.245	2.28	0.245	0.999	1.64	0.333	2.45	0.333	0.999
1912.5	582.93	1.74	0.237	2.28	0.245	1.032	1.65	0.326	2.45	0.334	1.023
1914.7	583.60	1.78	0.211	2.26	0.213	1.007	1.68	0.310	2.44	0.311	1.005
1918.0	584.61	1.80	0.213	2.28	0.228	1.071	1.71	0.304	2.45	0.319	1.050
1920.8	585.46	1.78	0.211	2.26	0.219	1.039	1.68	0.311	2.44	0.319	1.027
1924.0	586.44	1.83	0.190	2.26	0.195	1.023	1.73	0.288	2.44	0.293	1.015
1926.4	587.17	1.79	0.210	2.27	0.219	1.040	1.69	0.306	2.44	0.314	1.027
1929.4	588.08	1.71	0.250	2.28	0.268	1.071	1.62	0.338	2.45	0.355	1.053
1933.9	589.45	1.73	0.246	2.30	0.259	1.050	1.65	0.333	2.47	0.345	1.037
1935.7	590.00	1.72	0.246	2.28	0.228	0.927	1.63	0.333	2.45	0.316	0.946
1939.0	591.01	1.74	0.228	2.26	0.260	1.139	1.65	0.323	2.44	0.355	1.098
1941.9	591.89	1.72	0.248	2.28	0.283	1.141	1.63	0.335	2.45	0.370	1.104
1944.9	592.81	1.74	0.234	2.27	0.229	0.979	1.64	0.329	2.45	0.324	0.985
1947.6	593.63	1.75	0.230	2.27	0.235	1.025	1.66	0.324	2.45	0.330	1.018
1950.7	594.57	1.71	0.245	2.27	0.237	0.968	1.62	0.339	2.45	0.331	0.977
1954.0	595.58	1.72	0.234	2.25	0.227	0.972	1.63	0.330	2.43	0.323	0.980
1956.7	596.40	1.70	0.241	2.24	0.233	0.968	1.60	0.339	2.43	0.331	0.977
1959.6	597.29	1.74	0.223	2.25	0.214	0.959	1.64	0.323	2.43	0.314	0.972
1963.4	598.44	1.72	0.229	2.23	0.221	0.964	1.62	0.333	2.42	0.325	0.975
1966.1	599.27	1.81	0.190	2.23	0.189	0.996	1.71	0.292	2.41	0.291	0.997
1968.7	600.06	1.70	0.251	2.27	0.254	1.013	1.61	0.340	2.45	0.343	1.010
1971.9	601.04	1.73	0.225	2.23	0.226	1.004	1.63	0.328	2.42	0.329	1.003
1974.8	601.92	1.75	0.218	2.24	0.219	1.002	1.66	0.316	2.42	0.316	1.001
1977.5	602.74	1.72	0.236	2.25	0.245	1.039	1.62	0.330	2.42	0.339	1.028
1981.2	603.87	1.80	0.185	2.20	0.197	1.065	1.68	0.300	2.40	0.312	1.040
1983.8	604.66	1.73	0.227	2.24	0.232	1.020	1.64	0.324	2.42	0.329	1.014
1987.0	605.64	1.77	0.199	2.21	0.209	1.051	1.66	0.314	2.42	0.324	1.032
1989.8	606.49	1.77	0.206	2.22	0.214	1.041	1.66	0.311	2.41	0.319	1.027
1992.8	607.41	1.72	0.228	2.23	0.241	1.054	1.63	0.321	2.40	0.333	1.038
1994.9	608.05	1.70	0.245	2.26	0.256	1.047	1.62	0.333	2.42	0.345	1.035
1999.0	609.30	1.79	0.188	2.20	0.183	0.972	1.68	0.298	2.39	0.292	0.982
2002.0	610.21	1.80	0.190	2.22	0.191	1.006	1.69	0.292	2.39	0.294	1.004
2005.2	611.18	1.80	0.185	2.21	0.221	1.198	1.70	0.291	2.39	0.327	1.126
2008.1	612.07	1.73	0.218	2.21	0.242	1.107	1.63	0.318	2.39	0.341	1.074
2010.9	612.92	1.74	0.224	2.24	0.217	0.965	1.65	0.313	2.40	0.305	0.975
2014.2	613.93	1.78	0.187	2.19	0.190	1.014	1.68	0.293	2.37	0.295	1.009
2016.6	614.66	1.88	0.146	2.20	0.148	1.014	1.77	0.257	2.38	0.259	1.008
2020.4	615.82	1.89	0.144	2.21	0.149	1.034	1.78	0.255	2.39	0.260	1.019
2023.5	616.76	1.93	0.119	2.19	0.123	1.034	1.81	0.239	2.38	0.243	1.017
2025.7	617.43	1.98	0.099	2.20	0.108	1.093	1.86	0.219	2.38	0.228	1.042

Table G-1: Laboratory Material Properties and Water Contents Measured on Core Samples from Drill Hole USW SD-12 (Continued)

[Measurements reported by L.E. Flint, U.S. Geological Survey Hydrologic Research Facility; DTN No. GS950308312231.002.
J. Curtis and C. Vidano, analysts]

Depth (feet)	Depth (m)	Relative Humidity Oven-Dried					105°C Oven-Dried				
		Dry Bulk Density (g/cm ³)	Porosity (cm ³ /cm ³)	Particle Density (g/cm ³)	Vol. Water Content (cm ³ /cm ³)	Relative Satn.	Dry Bulk Density (g/cm ³)	Porosity (cm ³ /cm ³)	Particle Density (g/cm ³)	Vol. Water Content (cm ³ /cm ³)	Relative Satn.
2030.0	618.74	1.97	0.101	2.19	0.107	1.054	1.84	0.224	2.38	0.229	1.025
2032.2	619.41	1.94	0.111	2.18	0.119	1.071	1.81	0.239	2.38	0.247	1.033
2035.4	620.39	1.82	0.158	2.17	0.174	1.097	1.71	0.272	2.35	0.288	1.057
2037.3	620.97	1.94	0.110	2.19	0.114	1.030	1.83	0.224	2.36	0.228	1.015
2040.7	622.01	1.95	0.105	2.18	0.117	1.118	1.84	0.221	2.36	0.234	1.056
2043.9	622.98	1.86	0.146	2.19	0.160	1.095	1.76	0.252	2.35	0.266	1.055
2046.7	623.83	1.84	0.160	2.20	0.175	1.093	1.74	0.267	2.37	0.281	1.056
2050.5	624.99	1.85	0.152	2.18	0.153	1.009	1.73	0.267	2.36	0.268	1.005
2053.0	625.75	1.87	0.151	2.20	0.163	1.079	1.76	0.262	2.38	0.274	1.046
2056.0	626.67	1.87	0.147	2.19	0.167	1.139	1.76	0.254	2.36	0.275	1.080
2058.8	627.52	1.96	0.109	2.20	0.148	1.360	1.85	0.220	2.37	0.259	1.179
2061.8	628.44	1.93	0.114	2.18	0.150	1.312	1.82	0.223	2.34	0.258	1.160
2064.7	629.32	1.84	0.152	2.17	0.173	1.137	1.73	0.258	2.34	0.278	1.081
2068.4	630.45	1.81	0.169	2.18	0.167	0.986	1.70	0.276	2.35	0.273	0.992
2070.8	631.18	1.84	0.164	2.20	0.167	1.012	1.73	0.277	2.39	0.279	1.007
2074.0	632.16	1.77	0.181	2.16	0.194	1.070	1.66	0.290	2.34	0.302	1.044
2076.5	632.92	1.88	0.141	2.18	0.149	1.057	1.76	0.253	2.36	0.261	1.032
2079.9	633.95	1.76	0.199	2.20	0.213	1.071	1.66	0.305	2.38	0.319	1.046
2082.2	634.65	1.90	0.119	2.16	0.122	1.020	1.78	0.239	2.34	0.242	1.010
2086.1	635.84	1.76	0.193	2.19	0.202	1.045	1.66	0.300	2.37	0.309	1.029
2088.5	636.57	1.74	0.203	2.18	0.216	1.066	1.63	0.306	2.36	0.319	1.043
2091.9	637.61	1.77	0.185	2.17	0.196	1.056	1.66	0.293	2.35	0.304	1.035
2094.9	638.53	1.92	0.110	2.16	0.117	1.062	1.80	0.226	2.33	0.233	1.030
2098.0	639.47	1.81	0.180	2.20	0.191	1.063	1.70	0.289	2.39	0.300	1.039
2100.7	640.29	1.74	0.202	2.18	0.210	1.036	1.63	0.307	2.36	0.314	1.024
2103.7	641.21	1.75	0.204	2.20	0.205	1.004	1.65	0.304	2.37	0.305	1.003
2106.5	642.06	1.73	0.212	2.19	0.218	1.028	1.62	0.318	2.38	0.324	1.019
2109.1	642.85	1.78	0.175	2.16	0.184	1.054	1.66	0.293	2.35	0.302	1.032
2119.5	646.02	1.73	0.216	2.20	0.217	1.006	1.62	0.319	2.38	0.320	1.004
2120.4	646.30	1.80	0.171	2.17	0.172	1.007	1.68	0.291	2.37	0.292	1.004
2122.4	646.91	1.72	0.200	2.15	0.201	1.007	1.61	0.314	2.34	0.316	1.004
2124.6	647.58	1.78	0.172	2.15	0.176	1.021	1.67	0.290	2.34	0.293	1.012
2128.0	648.61	1.72	0.201	2.15	0.205	1.022	1.60	0.312	2.33	0.317	1.014
2130.6	649.41	1.73	0.193	2.14	0.194	1.001	1.62	0.302	2.32	0.302	1.001
2133.7	650.35	1.86	0.178	2.26	0.197	1.107	1.74	0.298	2.47	0.317	1.064
2136.1	651.08	1.89	0.136	2.18	0.145	1.069	1.77	0.250	2.37	0.260	1.037
2139.5	652.12	1.84	0.158	2.19	0.168	1.060	1.72	0.275	2.38	0.284	1.035
2142.8	653.13	1.85	0.160	2.20	0.175	1.093	1.74	0.269	2.38	0.284	1.056
2145.5	653.95	1.85	0.153	2.18	0.159	1.042	1.73	0.273	2.38	0.280	1.024
2148.9	654.98	1.63	0.343	2.47	0.359	1.049	1.62	0.347	2.48	0.363	1.048
2151.7	655.84	1.67	0.336	2.51	0.338	1.004	1.66	0.341	2.52	0.343	1.004
2155.0	656.84	1.69	0.326	2.51	0.338	1.035	1.69	0.331	2.52	0.342	1.034
2158.0	657.76	1.72	0.328	2.56	0.331	1.010	1.71	0.334	2.57	0.337	1.009
2161.0	658.67	1.72	0.314	2.51	0.250	0.796	1.72	0.319	2.52	0.255	0.800
2164.0	659.59	1.74	0.295	2.47	0.285	0.966	1.73	0.300	2.48	0.290	0.966

Table G-2: Porosity and Saturated Hydraulic Conductivity Values Measured on Core Samples from Drill Hole USW SD-12

[Measurements reported by L.E. Flint, U.S. Geological Survey Hydrologic Research Facility, DTN No. GS950308312231.002. Ksat –saturated hydraulic conductivity; nf – no flow.]

Depth (feet)	Depth (m)	Porosity (cm ³ /cm ³)	Ksat (m/sec)
262.5	80.01	0.383	5.70E-07
265.4	80.89	0.529	1.80E-10
286.4	87.29	0.483	8.60E-07
304.9	92.93	0.518	1.50E-06
317.0	96.62	0.501	1.13E-06
443.0	135.03	0.157	1.13E-10
1067.3	325.31	0.044	9.11E-11
1252.0	381.61	0.076	nf
1305.6	397.95	0.072	nf
1329.9	405.35	0.189	4.13E-09
1413.3	430.77	0.367	1.90E-06
1426.1	434.68	0.317	5.20E-07
1435.1	437.42	0.295	4.30E-07
1740.7	530.57	0.284	1.50E-07
1853.0	564.79	0.240	6.50E-11

(This page intentionally left blank.)

**Yucca Mountain Site Characterization Project
SAND96-1368 Distribution List**

1	D. A. Dreyfus (RW-1) Director OCRWM US Department of Energy 1000 Independence Avenue SW Washington, DC 20585	1	Director, Public Affairs Office c/o Technical Information Resource Center DOE Nevada Operations Office US Department of Energy P.O. Box 98518 Las Vegas, NV 89193-8518
1	L. H. Barrett (RW-2) Acting Deputy Director OCRWM US Department of Energy 1000 Independence Avenue SW Washington, DC 20585	10	Technical Information Officer DOE Nevada Operations Office US Department of Energy P.O. Box 98518 Las Vegas, NV 89193-8518
1	S. Rousso (RW-40) Office of Storage and Transportation OCRWM US Department of Energy 1000 Independence Avenue SW Washington, DC 20585	1	J. R. Dyer, Deputy Project Manager Yucca Mountain Site Characterization Office US Department of Energy P.O. Box 98608 -- MS 523 Las Vegas, NV 89193-88608
1	R. A. Milner (RW-30) Office of Program Management and Integration OCRWM US Department of Energy 1000 Independence Avenue SW Washington, DC 20585	5	M.C. Tynan U.S. Department of Energy P. O. Box 98608; MS-523 Las Vegas, NV 87193-8608
1	D. R. Elle, Director Environmental Protection Division DOE Nevada Field Office US Department of Energy P.O. Box 98518 Las Vegas, NV 89193-8518	1	Repository Licensing & Quality Assurance Project Directorate Division of Waste Management, MS T7J-9 US NRC Washington, DC 20555
1	T. Wood (RW-14) Contract Management Division OCRWM US Department of Energy 1000 Independence Avenue SW Washington, DC 20585	1	Senior Project Manager for Yucca Mountain Repository Project Branch Division of Waste Management, MS T7J-9 US NRC Washington, DC 20555
5	Victoria F. Reich, Librarian Nuclear Waste Technical Review Board 1100 Wilson Blvd., Suite 910 Arlington, VA 22209	5	NRC Document Control Desk Division of Waste Management, MS T7J-9 US NRC Washington, DC 20555
5	Wesley Barnes, Project Manager Yucca Mountain Site Characterization Office US Department of Energy P.O. Box 98608--MS 523 Las Vegas, NV 89193-8608	1	Chad Glenn NRC Site Representative 301 E Stewart Avenue, Room 203 Las Vegas, NV 89101
1	Steve Hanauer (RW-2) OCRWM U. S. Department of Energy 1000 Independence Ave. Washington, DC 20585	5	Center for Nuclear Waste Regulatory Analyses Southwest Research Institute 6220 Culebra Road Drawer 28510 San Antonio, TX 78284
		1	Robert L. Strickler Vice President & General Manager TRW Environmental Safety Systems, Inc. 2650 Park Tower Dr. Vienna, VA 22180

5	L. D. Foust Technical Project Officer for YMP TRW Environmental Safety Systems 101 Convention Center Drive; Suite P-110 Las Vegas, NV 89109	3	John Fordham, Deputy Director Water Resources Center Desert Research Institute P.O. Box 60220 Reno, NV 89506
5	M. C. Brady Laboratory Lead for YMP M&O/Sandia National Laboratories 1261 Town Center Drive Bldg. 4, Room 421A Las Vegas, NV 89134	1	The Honorable Jim Regan, Chairman Churchill County Board of Commissioners 10 W. Williams Avenue Fallon, NV 89406
5	J. A. Canepa Laboratory Lead for YMP EES-13, Mail Stop J521 M&O/Los Alamos National Laboratory P.O. Box 1663 Los Alamos, NM 87545	3	R. R. Loux, Executive Director Agency for Nuclear Projects State of Nevada Evergreen Center, Suite 252 1802 N. Carson Street Carson City, NV 89710
5	W. L. Clarke Laboratory Lead for YMP M&O/ Lawrence Livermore Nat'l Lab P.O. Box 808 (L-51) Livermore, CA 94550	1	Brad R. Mettam Inyo County Yucca Mountain Repository Assessment Office P. O. Drawer L Independence, CA 93526
5	G. S. Bodvarsson Head, Nuclear Waste Department Lawrence Berkeley National Laboratory 1 Cyclotron Road, MS 50E Berkeley, CA 94720	1	Vernon E. Poe Office of Nuclear Projects Mineral County P.O. Box 1600 Hawthorne, NV 89415
5	Robert W. Craig Acting Technical Project Officer/YMP US Geological Survey 101 Convention Center Drive, Suite P-110 Las Vegas, NV 89109	1	Les W. Bradshaw, Program Manager Nye County Nuclear Waste Repository Project Office P.O. Box 1767 Tonopah, NV 89049
3	Jim Krulik, Geology Manager US Bureau of Reclamation Code D-8322 P.O. Box 25007 Denver, CO 80225-0007	1	Florindo Mariani White Pine County Coordinator P. O. Box 135 Ely, NV 89301
1	M. D. Voegele Deputy of Technical Operations M&O/SAIC 101 Convention Center Drive Suite P-110 Las Vegas, NV 89109	1	Tammy Manzini Lander County Yucca Mountain Information Officer P.O. Box 10 Austin, NV 89310
2	A. T. Tamura Science and Technology Division OSTI US Department of Energy P.O. Box 62 Oak Ridge, TN 37831	1	Jason Pitts, Manager Lincoln County Nuclear Waste Program P. O. Box 158 Pioche, NV 89043
1	P. J. Weeden, Acting Director Nuclear Radiation Assessment Div. US EPA Environmental Monitoring Sys. Lab P.O. Box 93478 Las Vegas, NV 89193-3478	1	Dennis Bechtel, Coordinator Nuclear Waste Division Clark County Dept. of Comprehensive Planning P.O. Box 55171 Las Vegas, NV 89155-1751
		1	Juanita D. Hoffman Nuclear Waste Repository Oversight Program Esmeralda County P.O. Box 490 Goldfield, NV 89013

1	Sandy Green Yucca Mountain Information Office Eureka County P.O. Box 714 Eureka, NV 89316	20	B. T. Brady Records Specialist US Geological Survey MS 421 P.O. Box 25046 Denver, CO 80225
1	Economic Development Dept. City of Las Vegas 400 E. Stewart Avenue Las Vegas, NV 89101	2	A. L. Flint U. S. Geological Survey MS 721 P. O. Box 327 Mercury, NV 89023
1	Community Planning & Development City of North Las Vegas P.O. Box 4086 North Las Vegas, NV 89030	1	L. E. Flint US Geological Survey; MS-509 101 Convention Center Drive Las Vegas, NV 89109
2	Librarian YMP Research & Study Center 101 Convention Center Drive, Suite P-110 Las Vegas, NV 89109	1	P. H. Nelson U.S. Geological Survey P. O. Box 25046; MS-425 Denver, CO 80225
1	Library Acquisitions Argonne National Laboratory Building 203, Room CE-111 9700 S. Cass Avenue Argonne, IL 60439	3	W. C. Day U.S. Geological Survey P. O. Box 25046; MS-425 Denver, CO 80225
1	Glenn Van Roekel Manager, City of Caliente P.O. Box 158 Caliente, NV 89008	2	J. W. Whitney U.S. Geological Survey P. O. Box 25046; MS-425 Denver, CO 80225
1	Mark Bandurraga Lawrence Berkeley National Laboratory 1 Cyclotron Road, MS 50E Berkeley, CA 94720	2	R. W. Spengler US Geological Survey P.O. Box 25046; MS-425 Denver, CO 80225
3	D. T. Vaniman EES-13, Mail Stop J521 M&O/Los Alamos National Laboratory P.O. Box 1663 Los Alamos, NM 87545	2	D. C. Buesch US Geological Survey; MS-509 101 Convention Center Drive Las Vegas, NV 89109
5	J. S. Stuckless, Chief Geologic Studies Program Yucca Mountain Project Branch US Geological Survey P.O. Box 25046; MS 425 Denver, CO 80225	3	L.E. "bud" Thompson CWRMS M&O; MS-423 101 Convention Center Drive Las Vegas, NV 89109
5	Michael P. Chornack US Geological Survey; P.O. Box 25046; MS-425 Denver, CO 80225	2	Kal Bhattacharyya CWRMS M&O; MS-423 101 Convention Center Drive Las Vegas, NV 89109
5	Daniel C. Gillies US Geological Survey; P.O. Box 25046; MS-425 Denver, CO 80225	3	Robert Elayer CWRMS M&O; MS-423 101 Convention Center Drive Las Vegas, NV 89109 Las Vegas, NV 89109
5	Richard R. Luckey US Geological Survey; P.O. Box 25046; MS-425 Denver, CO 80225	2	Robb Clayton CWRMS M&O; MS-423 101 Convention Center Drive Las Vegas, NV 89109

1	R. C. Quittmeyer CWRMS M&O; MS-423 101 Convention Center Drive Las Vegas, NV 89109	MS	2	1330	B. Pierson, 6811 100/WBS123274/SAND95-2080/NQ
			20	1330	WMT Library, 6752
			5	1324	C.A. Rautman, 6115
3	Chris Lewis YMP Sample Management Facility CWRMS M&O; MS-719 101 Convention Center Drive Las Vegas, NV 89109		1	1324	S.A. McKenna, 6115
			1	1324	W.P. Zelinski, 6115
			1	1325	N.S. Brodsky, 6852
			1	1325	R.E. Finley, 6852
			1	1326	H.A. Dockery, 6851
1	Dale A. Engstrom Spectra Research Institute 2201 Buena Vista, SE; Ste. 300 Albuquerque, NM 87106		1	1326	S.J. Altman, 6851
			1	1326	B.W. Arnold, 6851
			1	1326	R.W. Barnard, 6851
			1	1326	G.E. Barr, 6851
			1	1326	N.D. Francis
			1	1326	J.H. Gauthier
			1	1326	M.L. Wilson
			1	1325	L.S. Costin, 6852
			5	1399	C. Lum, 6853
			1	9018	Central Technical Files, 8523-2
			5	0899	Technical Library, 4414
			2	0619	Review and Approval Desk, 12630
					For DOE/OSTI